# 4-E (Energy, Exergy, Ecological and Economic) analyses of Chemical-Looping Combustion based Coal Fired Power Plants for $CO_2$ Capture and Utilization

Submitted in partial fulfillment of the requirements

for the award of the degree of

**DOCTOR OF PHILOSOPHY**

**in**

**CHEMICAL ENGINEERING**

by

**Mr. SURYWANSHI GAJANAN DATTARAO**
(Roll No. 716040)

Supervisor
**Dr. Venkata Suresh Patnaikuni**
Associate Professor

**Department of Chemical Engineering**

**National Institute of Technology Warangal**

Warangal-506004, Telangana, India

January – 2021

**Dedicated**

**to**

**My parents**

# *DECLARATION*

This is to certify that the work presented in the thesis entitled "***4-E (Energy, Exergy, Ecological and Economic) analyses of Chemical-Looping Combustion based Coal Fired Power Plants for*** $CO_2$ ***Capture and Utilization***" is a bonafide work done by me under the supervision of ***Dr. Venkata Suresh Patnaikuni*** and was not submitted elsewhere for award of any degree.

I declare that this written submission represents my ideas in my own words and where others' ideas or words have been included, I have adequately cited and referenced the original source. I also declare that I have adhered to all principles of academic honesty and integrity and have not misrepresented or fabricated or falsified any idea/data/fact/source in my submission. I understand that any violation of the above will be a cause for disciplinary action by the Institute and can also evoke penal action from the sources which have thus not been properly cited or from whom proper permission has not been taken when needed.

Surywanshi Gajanan Dattarao
(716040)

# *THESIS APPROVAL SHEET*

# *CERTIFICATE*

**NATIONAL INSTITUTE OF TECHNOLOGY- WARANGAL**
**Warangal – 506004, Telangana, INDIA.**

This is to certify that the thesis entitled "***4-E (Energy, Exergy, Ecological and Economic) analyses of Chemical-Looping Combustion based Coal Fired Power Plants for*** $CO_2$ ***Capture and Utilization***" being submitted by ***Mr. SURYWANSHI GAJANAN DATTARAO (Roll No.716040)*** for the award of the degree of Doctor of Philosophy (Ph.D.) in Chemical Engineering to the National Institute of Technology, Warangal, India is a record of the bonafide research work carried out by him under my supervision. The thesis has fulfilled the requirements according to the regulations of this Institute and in my opinion has reached the standards for submission. The results embodied in the thesis have not been submitted to any other University or Institute for the award of any degree or diploma.

**Date:** 04-06-2021

**Dr. Patnaikuni Venkata Suresh**
Associate Professor
Supervisor
Department of Chemical Engineering,
National Institute of Technology, Warangal

# *ACKNOWLEDGEMENT*

I take this opportunity to express my sincere gratitude to my respected supervisor ***Dr. Venkata Suresh Patnaikuni***, Associate Professor, Department of Chemical Engineering, National Institute of Technology (NIT), Warangal, India for giving me an opportunity to pursue doctoral thesis work under his esteemed supervision. His outstanding guidance, constant support, patience, motivation and immense knowledge extremely helped me in all the time of research and writing of this thesis. I could not have imagined having a better advisor and mentor for my PhD study. This work was not possible without inspiration of my M. Tech. Supervisors ***Prof. R. C. Sastry***, Former Professor, Department of Chemical Engineering, NIT Warangal. He inspired me during my post-graduation studies and accelerated my passion of pursuing higher studies with greater impact. He is my constant source of the inspiration throughout my life.

I wish to sincerely thank university authorities, ***Prof. N.V. Ramana Rao***, Director, NIT Warangal and other top officials who gave me an opportunity to carry out research work. I also sincerely thank ***Prof. Shirish H. Sonawane***, Head, Chemical Engineering Department, NIT Warangal for his continuous support towards carrying out research work and for providing necessary facilities in the department.

I wish to express my sincere and whole hearted thanks and gratitude to my doctoral scrutiny committee (DSC) members***, Prof. A. Sarat Babu***, Department of Chemical Engineering*,* ***Dr. S. Vidyasagar,*** Associate Professor, Department of Chemical Engineering*,* ***Dr. D. Jaya Krishna,*** Associate Professor Department of Mechanical Engineering, NIT Warangal for their kind help, encouragement and valuable suggestions for successful completion of research work. I would like to express heart-felt thanks to former DSC member ***Prof. Y. Pydi Setty***, Department of Chemical Engineering, NIT Warangal for his suggestions, support and encouragement. I also sincerely thank Visiting Faculty ***Dr. P. M. Satya Sai***, Department of Chemical Engineering, NIT Warangal for his encouragement and guiding me in the paper and thesis writing.

I wish to express my profound thanks to the entire Faculty, Scholars, Non-teaching staff and all others in the Chemical Engineering Department and in the Institute who directly and indirectly helped me during the course of my research work at NIT Warangal.

I wish to express sincere thanks to my beloved friends and lab mates *Dr. Abdulla Sheikh, Mr. B. Basant Kumar Pillai, Mr. Shailesh Sikarwar, Mr. Bidesh Kirtania* and *Ms. Snigdha Saha* for their constant encouragement and help acquired during my research period at NITW.

I am very much thankful to all my special Marathi Mandal and fellow research scholars specially, to *Dr. Uday Bagle, Dr. Prashant Suryawanshi, Dr. Abhay Lingayat, Dr. Vinay Rangari, Mr. Harshal Patil, Mr. Roshan Bodile, Mr. Ganesh Gawale, Mr. Avinash Borgaonkar, Mr. Swapnil Adsul, Mr. Kishor Ingle, Mr. Upendra Maurya, Mr. Vikas Hakke, Mrs. Vividha Landge, Mrs. Shital Potdar, Mr. Sandip Khobragade, Mr. Rahul Gaikwad* and *Mrs. Anita Zade* for their constant support and encouragement throughout my research work.

I take this opportunity to sincerely acknowledge the ***Science and Engineering Research Board (SERB), Government of India*** for providing the financial assistance in the form of stipend.

Last but not the least; I would like to express my profound gratitude to my family members: my father ***Mr. Dattarao Suryawanshi***, my mother ***Mrs. Aruna Suryawanshi***, my brother ***Mr. Prem Suryawanshi***, my wife ***Dr. Sujata Suryawanshi*** and other members of my family for their support and continuous encouragement throughout my years of study and through process of researching and writing this thesis.

**Surywanshi Gajanan Dattarao**

# *Abstract*

Carbon dioxide emissions into the atmosphere are accelerated due to increased demand for energy. Coal-fired power plants (CFPPs) are still the major sources of power generation in many countries and have become the major sources of anthropogenic carbon dioxide emissions. Chemical looping combustion (CLC) is one of the most promising "next generation" carbon dioxide capture technologies that captures almost all $CO_2$ emitted from the plant. Despite having the capability to capture 100% $CO_2$, the major concerns such as the permanent and efficient sequestration, safety of geological, ocean and mineral storages still persist. Hence, in addition to $CO_2$ capture, the utilization of the captured $CO_2$ is a much more important task to realize negative $CO_2$ emissions and to produce the valuable products.

Basically, there are two approaches of CLC technology – two-reactor system for power generation alone and three-reactor system for co-generation of power and hydrogen. In two-reactor CLC process, the air and fuel reactors are interconnected in a loop. Oxygen ($O_2$) from air reactor is transported to the fuel reactor using solid oxygen carrier particles. Thus, the fuel is combusted without mixing with air, thereby resulting in a mixture of steam and $CO_2$ as the combustion products, from which, $CO_2$ is recovered by condensing steam. The reduced oxygen carrier particles are oxidised back to its original state in the air reactor in presence of air. In three-reactor CLC process, a third reactor called steam reactor, is introduced in between the air and fuel reactors. The oxygen carrier is first partially reduced in the fuel reactor in the presence of fuel. This partially reduced oxygen carrier is then completely reduced in the steam reactor using steam and completely oxidised in the air reactor with the presence of air. The gaseous streams leaving the fuel and steam reactors, after condensing steam, results in pure carbon dioxide and hydrogen, respectively.

In the present study, steady-state simulations of the CLC based power plants and carbon dioxide utilization (CDU) plants are carried out using aspenONE v10.0. A detailed parametric analysis of two- and three-reactor CLC systems in the power plant is conducted to identify the scope for further improvement of the overall performance of the plant. The present simulation work is carried out systematically and encompasses four categories: (i) Simulation of two-reactor CLC based subcritical, supercritical and ultra-supercritical CFPPs, (ii) Simulation of two-reactor CLC based CFPP for different oxygen carriers, (iii) Simulation of three-reactor CLC based CFPP for power and hydrogen co-generation and (iv) Simulation of three-reactor CLC based plant coupled with different CDU plants. The overall performance of all the power plant cases are analysed based on energy, exergy, ecological and economic (4-E) analyses. The first objective of the thesis is formulated as to check the feasibility of CLC based CFPP for three steam generation technologies and overall performance is compared based on 4-E analyses. This plant is then considered to check the feasibility of CLC based CFPP for different oxygen carriers such as iron oxide, copper oxide and bimetallic oxide (10% copper oxide in iron oxide) supported on aluminium oxide in the second objective of thesis. In the third objective, the oxygen carrier with better overall performance is considered for three-reactor CLC system to generate power and hydrogen together. In the fourth part of thesis, the CLC plant with hydrogen generation is coupled with CDU plants to produce the valuable product from $CO_2$ and $H_2$ as reactants. In this study, four case studies of CDU plants have been considered, which are formic acid, methane, methanol and dimethyl ether synthesis.

The 4-E analyses revealed that, the two-reactor CLC based supercritical and ultra-supercritical power plants are energetically, exergetically, environmentally, and economically favoured plants for power generation compared to the other variants with levelised cost of electricity (LCOE) of 89.05 and 87.83 €/MWh, respectively. The 4-E analyses also revealed that, the two-reactor CLC based supercritical CFPP with bimetallic oxygen carrier (LCOE: 91.95 €/MWh) is a preferable option as compared to iron oxide (LCOE: 89.05 €/MWh) and copper oxide (LCOE: 98.25 €/MWh) alone. Further, a three-reactor CLC based power plant configuration is energetically, exergetically, environmentally and economically feasible compared to the two-reactor CLC based power plant configuration. The CLC based plant with 50% hydrogen and 50% power co-generation has the levelised cost of 1.94 €/kg of hydrogen, which is in the marginal range reported in literature. Finally, the 4-E and life cycle analyses of three-reactor CLC plant coupled with CDU plant revealed that, the formic acid synthesis is the most favourable option with 100% $CO_2$ utilization efficiency. The levelised cost of product (LOCP) values of CLC based plant with formic acid, methane, methanol and DME are found to be 0.0416, 0.5433, 0.1930 and 0.2914 €/kg of product, with payback periods of 1.47, 1.50, 1.49 and 1.44 years, respectively.

This study demonstrates the superiority of chemical looping combustion based coal fired power plant for $CO_2$ capture coupled with the carbon dioxide utilization plant over the conventional plant. The outcome of this study can provide the basis for potential improvement of CLC plant integrated with CDU plant performance based on 4-E&L analyses.

# *Table of Content*

# *List of Figures*

# *List of Tables*

# *Nomenclature*

| | |
|---|---|
| ASU | air separation unit |
| CCS | carbon capture and sequestration |
| CCR | carbonation-calcination reaction |
| CCU | carbon capture and utilisation |
| CDU | carbon dioxide utilisation |
| CFPP | coal-fired power plant |
| CLAS | chemical looping air separation |
| CLC | chemical looping combustion |
| CLG | chemical looping gasification |
| CLOU | chemical looping oxygen uncoupling |
| CLR | chemical looping reforming |
| CLRG | chemical looping reforming of glycerol |
| DCC | direct contact cooler |
| DME | dimethyl ether |
| FA | formic acid |
| FWH | feed water heater |
| GHG | greenhouse gas |
| HP | high pressure |
| HPFWH | high pressure feed water heater |
| HPT | high pressure turbine |
| HRSG | heat recovery steam generation |
| IEA | international energy agency |
| IGCC | integrated gasification combined cycle |
| iG-CLC | integrated gasification chemical looping combustion |
| IP | intermediate pressure |
| IPT | intermediate pressure turbine |
| LCA | life cycle analysis |
| LCOE | levelised cost of electricity |
| LCOP | levelised cost of product |
| LP | low pressure |

| | |
|---|---|
| LPFWH | low pressure feed water heater |
| LPT | low pressure turbine |
| MCFC | molten carbonate fuel cell |
| MEA | monoethanolamine |
| NETL | National Energy Technology Laboratory |
| NRTL | non-random two-liquid model |
| PCC | post-combustion capture |
| PFEC | primary fossil energy consumption |
| PR-BM | Peng Robinson and Boston Mathias |
| RKS | Redlich Kwong Soave |
| SCL | syngas chemical looping |
| SubC | subcritical |
| TGA | thermogravimetric analysis |

### ***Greek symbols***

| | |
|---|---|
| $\varepsilon$ | exergy efficiency, % |
| C | carbon |
| Ex | molar exergy, kJ/kmol |
| H | molar enthalpy, kJ/kmol |
| H | hydrogen |
| $h_{fg}$ | latent heat of vaporization, kJ/kg |
| HHV | higher heating value, MJ/kg |
| LHV | lower heating value, MJ/kg |
| M | molar flow rate |
| n | number of components |
| N | nitrogen |
| O | oxygen |
| R | universal gas constant, kJ/kmol K |
| S | specific molar entropy, kJ/kmol K |
| S | sulfur |
| T | temperature, K |
| w | moisture content, % |
| x | mole fraction |
| $\eta$ | energy efficiency, % |

### *Subscripts*

| | |
|---|---|
| ch | chemical |
| d | destruction |
| i | $i^{h}$ component |
| o | at standard state or the environment condition |
| ph | physical |

# Chapter 1

# Introduction

# Chapter 1

# *Introduction*

The present chapter discusses on the real world problems of climate change and its causes briefly, followed by the scope of this research in the context of developing clean energy from coal through chemical looping combustion technology. This chapter starts with the motivation and background, technical challenges of chemical looping combustion system, carbon dioxide utilization to produce valuable products and the overview of comprehensive energy, exergy, ecological, economic and life cycle analyses. This chapter concludes with the organization of the thesis work.

## 1.1 Motivation

Global warming by greenhouse gases (GHG) has become a major concern worldwide due to its adverse effect on climate change. With the growing energy demand, fossil fuel consumption has increased and this is leading to enormous carbon dioxide ($CO_2$) emissions. Countries such as China, United States of America and the European Union are the leading $CO_2$ emitters in the world, while the developing countries like India also contribute to a significant amount of global $CO_2$ emissions. Figure 1.1 shows the share of global $CO_2$ emissions by different countries from fossil fuels during the year 2010 to 2018 [1,2]. India ranks 4th after China, United States and the European Union with 7.26% share of global $CO_2$ emissions during the year 2018. In the recent years, notable decrease in global share of $CO_2$ emissions can be observed in case of United States and European Union due to good $CO_2$ management. In case of China, Russia and Japan, the share of emissions is stable, whereas it is on the increase for India due to increased power production. For countries like India, the problem of $CO_2$ emission is more critical as 55% of electricity is generated from coal [3] as on November 2020 because of its vast coal resources, amounting to 8.3% of global reserves [4] To meet the global commitments on emissions, India is planning for a judicial mix of coal, renewables and nuclear. The low calorific value (or high-ash content) in Indian coal reduces the net efficiency of the power plant as compared to low ash content (or high calorific value) coals [5]. One way of increasing net plant efficiency is by adapting advanced power plant technologies such as - supercritical (SupC) and ultra-supercritical (Ultra-SupC) plants. Further, the integration of the upcoming chemical looping combustion (CLC) technology with these advanced plants can reduce the energy penalty associated with carbon dioxide capture.

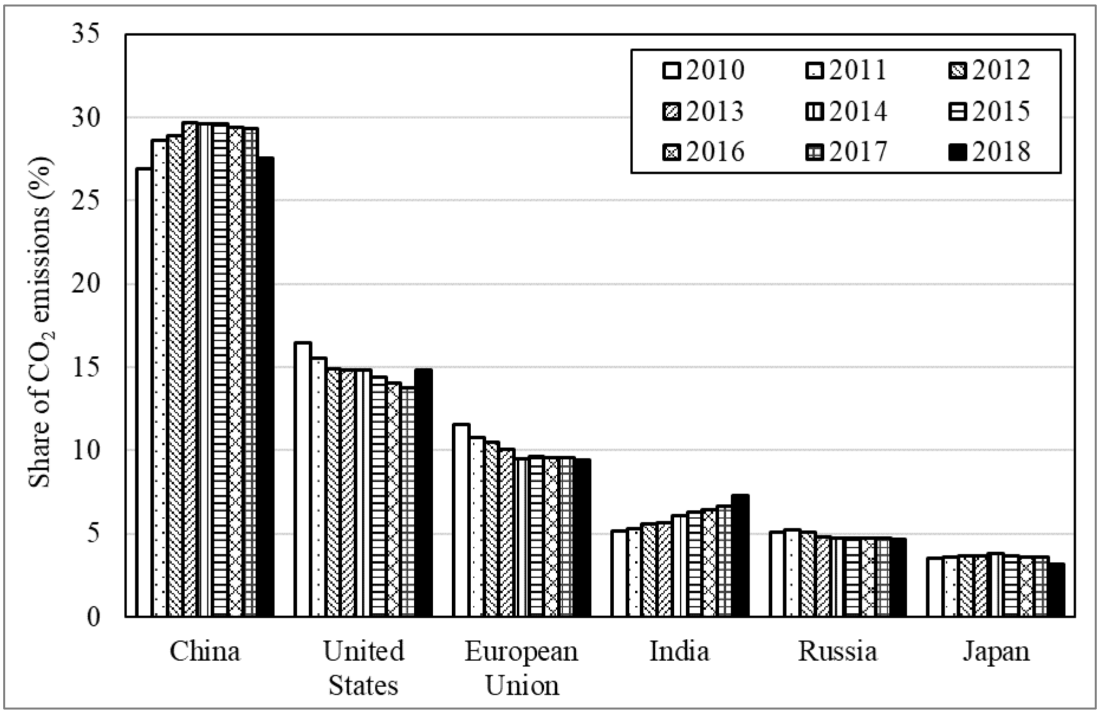

Figure 1.1. Share of global $CO_2$ emission by different countries during 2010-2018.

## 1.2 Conventional coal-fired power plants

A conventional coal fired power plant (CFPP) produces electricity by combusting coal in the presence of air. The heat recovered from the hot flue gas from the combustion is used to generate high pressure and temperature steam in the steam generator. The steam is passed through the series of steam turbines, which spins the electrical generator to generate the electricity. The steam from the steam turbines is cooled to condense steam in to water and recycled back to the steam generator. So, the key units / blocks in a conventional CFPP without $CO_2$ capture are coal processing (crushing, sizing & drying), combustor, heat recovery steam generation (HRSG), feed water heaters (FWHs), condenser and steam turbine units. These conventional CFPPs are highly complex and custom designed on a large-scale continuous operation to run the plant continuously throughout the year. Such plants provide most of the electrical energy used in many countries. Most conventional CFPPs built in 1980s and 1990 generates about 500 MW of electrical power, while many modern power plants generated about 1000 MW of electrical power [6].

Coal-fired power plants are mainly classified in to three categories based on the steam generation in the power plant, such as – subcritical, supercritical and ultra-supercritical. These steam configurations are classified based on the steam temperatures and pressures in heat recovery steam generation (HRSG) unit. The details of these three steam configurations for conventional coal fired power plants (CFPPs) were given by Suresh at al. [5] and are discussed in *Chapter 3*.

## 1.3 Carbon capture and storage

The concept of $CO_2$ capture and storage (CCS) includes the capturing $CO_2$, separation from other gases and storing it in reservoirs. This is an old and promising concept to stop the release of extreme anthropogenic carbon dioxide into the atmosphere. This can inhibit its contribution in the GHG effect to some extent. The CCS of $CO_2$ allows the fossil fuels to be used without affecting the climate. The steps involved in the CCS includes capture, transportation and storage of carbon dioxide. Presently this is being used in various parts of world because of its efficacy in reducing the impact of released $CO_2$ on climate change while decelerating the rise in atmospheric $CO_2$ [7].

## 1.4 Carbon capture technologies

There are both natural and human sources of carbon dioxide emissions. Natural sources include decomposition, ocean release and respiration. Human sources come from activities like cement production, deforestation as well as the burning of fossil fuels like coal, oil and natural gas. Greenhouse gases trap heat and make the planet warmer. Human activities are responsible for most of the increase in greenhouse gases in the atmosphere over the last 150 years. $CO_2$ is one of the main greenhouse gases that causes global warming, leading to a global detrimental impact on the environment, economy, and society as a whole. Carbon capture is regarded as an important and effective approach for reducing $CO_2$ emissions.

Technologies related to $CO_2$ capture could be classified into three main categories of approach: pre-combustion, oxy-combustion, and post-combustion. Though these technologies result in attractive $CO_2$ reduction, they are associated with huge energy penalty. The post-combustion capture technology directly removes the $CO_2$ from the flue gas after the combustion process. In the pre-combustion capture, the $CO_2$ is removed in the fuel conversion process before the combustion of fuel. The oxy-combustion capture process utilizes the pure oxygen instead of air and generates the concentrated $CO_2$ gas stream.

Some alternative $CO_2$ capture technologies are: $CO_2$ permeable membranes, Molten Carbonate Fuel Cells (MCFC), high-pressure solvent absorption from high-pressure exhaust gas from pressurized combustion/power generation, high-pressure solvent absorption supported by exhaust gas compression, supersonic flow driven $CO_2$ deposition, etc. A wide variety of separation methods can be applied (most of them use the post- and pre-combustion approaches), including gas-phase separation, absorption in a solvent (amines, potassium carbonate, ammonia, sodium hydroxide, etc.), adsorption on a sorbent (molecular sieve, molecular basket, and activated carbon adsorption, adsorption on lithium components, etc.), and membrane as well as hybrid processes such as a combination of chemical absorption and membrane. In addition, other separation methods have been developed. Chemical looping combustion (CLC) and hydrate-based separation are two main methods. CLC is also known as unmixed combustion because there is indirect contact between fuel and air in this method. An oxygen carrier (metal oxides such as $Fe_2O_3$, NiO, CuO, and $Mn_2O_3$) provides oxygen for combustion. This process has one reactor for air and another one for fuel, and the oxygen carrier circulates between two reactors. Another method is hydrate-based separation, in which the hydrates formed by high-pressure injection of the gas stream force $CO_2$ into water. After that, the hydrate is separated and dissociated by releasing $CO_2$.

### 1.4.1 Post-combustion capture

Figure 1.2(a) shows the schematic flow diagram of post-combustion $CO_2$ capture technique. In this process, the coal is combusted in presence of air and power is generated. The $CO_2$ from the flue gas stream is separated to obtain the concentrated $CO_2$ stream. This $CO_2$ is then compressed, transported and stored/sequestrated. Since, the post-combustion capture process captures $CO_2$ after the combustion, the technique can be readily retrofitted in the existing power plants.

The typical coal based power plant process generates the $CO_2$ containing flue gas stream at the ambient pressure. The $CO_2$ separation from this type of technique include low temperature adsorbents, physical/chemical absorption solvents, high temperature sorbents, ionic liquids, $CO_2$ separation membranes, molecular filtration, etc. – based systems [8]. Several post-combustion capture technologies have been deployed commercially and/or under pilot demonstration, such as – carbonation – calcination reaction (CCR) systems, chilled ammonia and monoethanolamine (MEA).

## 1.4.2 Pre-combustion capture

In the pre-combustion capture process (Figure 1.2(b)), the coal first reacts with the pure oxygen (which is taken from the air separation unit (ASU)) in the presence of steam and produces the syngas (composed of CO and $H_2$). The CO in the syngas is then converted into $CO_2$ and $H_2$ through the water gas shift reaction.

$$CO + H_2O \rightarrow CO_2 + H_2 \tag{1.3}$$

Hence, the exit gas stream contains the concentrated $CO_2$. The $CO_2$ and $H_2S$ from this stream can be separated using physical absorption – based processes (Selexol, Rectisol, etc.) or the chemical absorption – based processes (methyldiethanolamine, MEA, etc.), resulting in concentrated hydrogen. This hydrogen is used in the combined cycle power generation systems to generate the electricity.

## 1.4.3 Oxy-combustion capture

The oxy-combustion capture approach was first proposed by Horn and Steinberg in 1982 [8]. Figure 1.2(c) shows the oxy-combustion capture process. In this capture process, the coal is combusted with the oxygen (purity ~ 95%) instead of air. A fraction of flue gas stream is recycled back to the combustor to maintain the temperature. Unlike post-combustion capture technique, the $CO_2$ is not diluted by nitrogen in the flue gas stream of oxy-combustion technique. The flue gas stream is comprised of mainly $CO_2$ and steam.

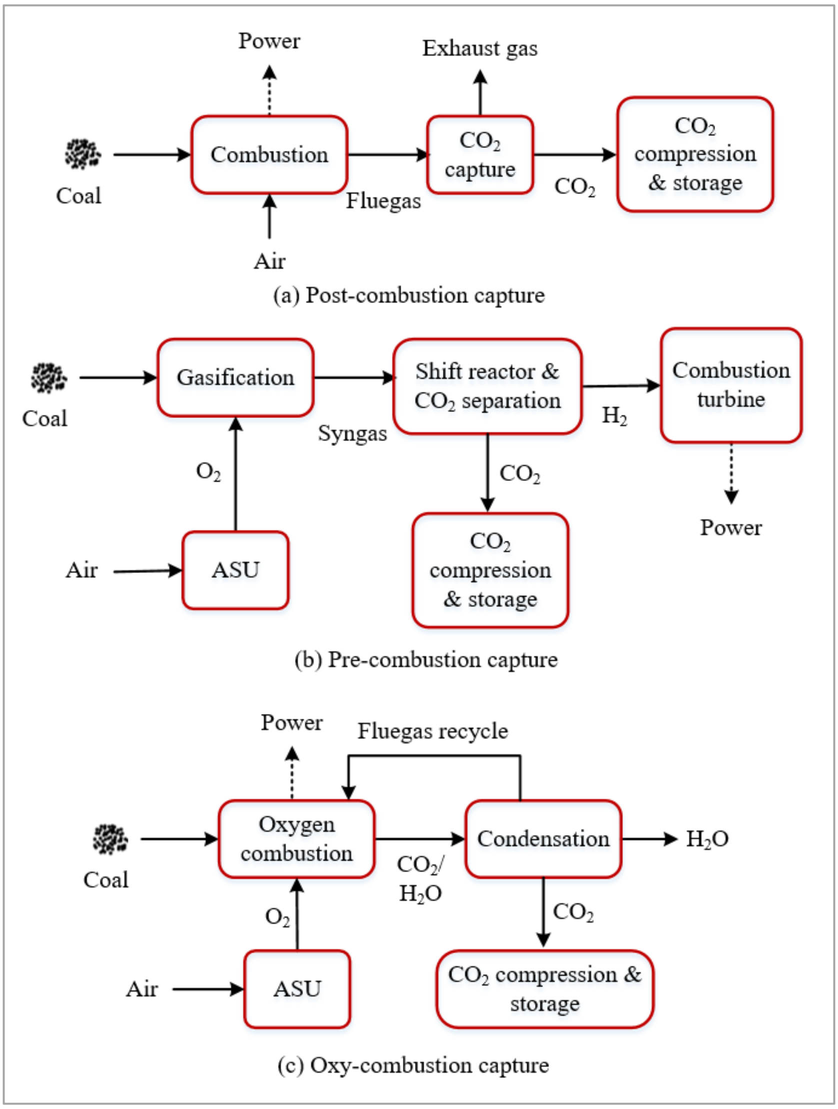

Figure 1.2. Flow diagram of $CO_2$ capture technologies (a) post-combustion, (b) pre-combustion and (c) oxy-combustion techniques.

### 1.4.4 Chemical looping combustion

The three $CO_2$ capture technologies mentioned earlier result in attractive $CO_2$ reduction, but they are associated with huge energy penalty. The post-combustion capture for the conventional coal-based power plant results in around 7-10% energy penalty for 85% $CO_2$ capture efficiency [9]. The pre-combustion and oxy-combustion $CO_2$ capture for the conventional integrated gasification combined cycle (IGCC) plant results in around 7% and 9% energy penalty for the $CO_2$ capture efficiency of 94.80% and 100%, respectively [10].

The CLC process shares the advantages of both oxy-combustion and pre-combustion capture techniques as the fuel is converted / oxidized to $CO_2$ and steam in fuel reactor by the oxygen supplied in the form of metal oxide/oxygen carrier particles rather than direct air. For the past few decades, research on combustion of gaseous, liquid and solid fuels using CLC technology is on high demand [8]. Because of the huge coal reserves and low price of the fuel, more research needs to be focused on co-generation of power and $H_2$ using CLC based coal fired power plants. Basically, there are two approaches of CLC technology- two reactor system for power generation alone and three reactor system for co-generation of power and hydrogen [8]. The block diagram of these two approaches is shown in Figure 1.3. In the first approach (Figure 1.3a), the coal and oxygen carrier are directly fed to the fuel reactor, where fuel is combusted and oxygen carrier is reduced. The reduced oxygen carrier is then re-oxidised in the air reactor in the presence of air. The exit streams from the fuel and air reactors are $CO_2$-rich and $N_2$-rich, respectively. Any oxygen carrying metal oxide such as oxides of copper, iron, manganese, magnesium, etc. can be used in the two reactor CLC system. In the second approach (Figure 1.3b), a third reactor called steam reactor, is introduced in between the air and fuel reactors. Usually, $Fe_2O_3$ is used as the metal oxide for the three reactor CLC system due to its different reducing states (i.e. FeO, Fe and $Fe_3O_4$) [11]. $Fe_2O_3$ is first reduced to FeO/Fe in the fuel reactor in the presence of fuel and $CO_2$/steam as fluidising agent. This reduced oxygen carrier is partially oxidized to $Fe_3O_4$/FeO in the steam reactor using steam and completely oxidized to $Fe_2O_3$ in air reactor in the presence of air. Similar to the two reactor CLC system, the air reactor re-oxidises the completely reduced oxygen carriers in presence of air. The gaseous streams leaving the fuel and steam reactors, after condensing steam, results in pure carbon dioxide and hydrogen, respectively. In addition to easy separation of $CO_2$ from steam, CLC technology has the advantages of eliminating nitrous oxide ($NO_x$) emissions and efficient control of the other air pollutants [12].

The first approach is used for the case of only power generation and second approach is used for both $H_2$ and power generation together. This study is focused on both two and three reactor CLC systems.

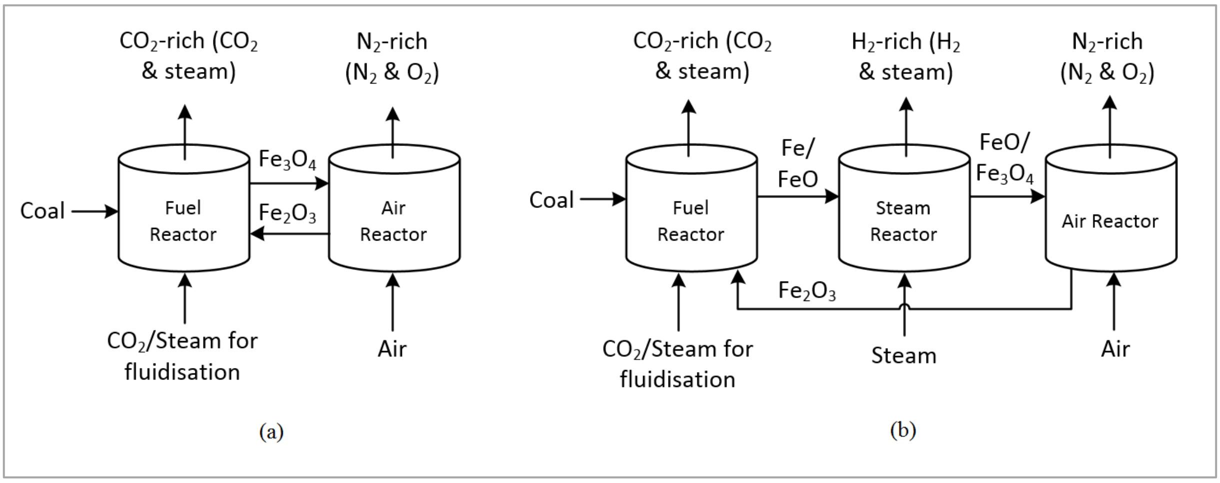

Figure 1.3. Simplified block diagram of CLC for (a) two reactor and (b) three reactor systems.

## 1.5 Technical challenges of CLC with solid fuels

For the past few decades, research on combustion of gaseous, liquid and solid fuels using CLC technology is on high demand [8] and significant development of CLC using solid fuels is available in the literature [13]. However, the critical issues challenging the coal based power plants integrated with the CLC technology need to be adopted. These issues include char reaction enhancement, oxygen carrier particle reactivity, solid conversion, fate of the pollutants and ash, etc.

Different solid fuels from various coals and pet-coke have been widely used in the CLC applications. In the recent years, a significant progress has been found in the utilization of solid fuels in CLC systems from the chemical kinetics to the pilot scale continuous operations.

When the solid fuels (such as coal) are heated, a certain part of calorific value is held in releasing the volatiles in the fuel. These volatiles are responsible for the formation of tars and also causes the problem in the down-stream equipment. The CLC operations in a smaller pilot plants indicates that the active metal oxide particles are excellent at destroying the most hydrocarbon species. However, some volatiles escaping the fuel reactor cannot be prevented when the low cost natural ores are used as oxygen carriers.

The present CLC operations using coal as solid fuel in some pilot-scale CLC plants in the worldwide indicates a big challenge that char gasification rate in the fuel reactor need to be accelerated to reach complete conversion of fuel. Generally, the solid circulation between the fuel reactor and air reactor is high, while the gasification of char in the fuel reactor is a slow process and hence the limiting step in the CLC process of coal. This phenomenon causes high concentrations of unreacted char in the fuel reactor. Therefore, a part of char particles enter the air reactor resulting the combustion of char with oxygen or oxygen carrier in the air reactor and $CO_2$ is formed, which cannot be captured by simple condensation and separation method.

## 1.6 Carbon capture and utilization

Despite having the 100% $CO_2$ capability of the technologies such as CLC, the major concerns such as the permanent and efficient sequestration, safety of geological, ocean and mineral storages still persist [8,14]. The carbon capture and utilization (CCU) is one of the novel climate mitigation technique. In CCU, the carbon dioxide emissions are captured from the sources (power plants) and reused to produce the valuable product. Nowadays, CCU has gained much attention towards reducing $CO_2$ release to curtail GHG emissions. $CO_2$ has been already used in various sectors and processes as shown in Table 1.1.

Currently, there is a surge in the research interest of carbon capture and utilization technologies. In this carbon capture and utilization, the $CO_2$ can be utilised for the synthesis of various products such as: urea, methanol, formaldehyde, formic acid, di-methyl carbonate, etc. [15–17]. Demirel et al. [18] discussed conversion of captured carbon to methanol, formic acid, dimethyl carbonate, and other products in the hydrothermal processes. Further, their review analysed major CLC technologies for carbon capture and conversion to select an appropriate clean energy technology.

Table 1.1 $CO_2$ utilization in various sectors [16].

| Sector | Process/product | Potential |
|---|---|---|
| Food | Refrigeration | Medium |
| | Beverage Carbonation | |
| | Wine production | |
| | Coffee Decaffeination | |
| | Food preservation | |
| | Food processing | |
| | Food packaging | |
| | Horticulture (greenhouses) | |
| | Dry Ice Production | |

|  |  |  |
|---|---|---|
| Chemical and oil | Chemicals and Fuels (methane, Methanol, fertilisers, CO, etc. and derivatives) | High |
|  | Enhanced Gas Recovery |  |
|  | Enhanced Oil Recovery |  |
|  | Urea production |  |
|  | Enhanced Coal bed Methane Recovery |  |
|  | Polymer Processing |  |
|  | Stimulation/Fracturing of oil and gas |  |
| Power | Heat pumps and working medium in other carbon dioxide cycles | Low-Medium |
| Mineralisation | $CO_2$ concrete curing | Medium |
|  | Baking soda |  |
|  | Ca and Mg carbonate for use in cement |  |
|  | Bauxite residue treatment (red mud) |  |
| Pharmaceutical | Chemical synthesis | Low |
|  | Inerting |  |
|  | Product transportation |  |
|  | Supercritical Fluid Extraction |  |
| Energy crops | Algae cultivation | Medium |
| Steel | Chilling medium | Low |
|  | Injection to metal casting |  |
|  | Hardening sand cores and moulds |  |
|  | Bottom stirring agent in basic oxygen furnace |  |
| Pulp and paper | pH reduction during Washing | Low |
| Other | Refrigerant gas | Low |
|  | Electronics (in printed circuit manufacture) |  |
|  | Welding (shield gas) |  |
|  | Pneumatics (working medium in hand tools and equipment) |  |
|  | Flavors, Fragnaces |  |
|  | Fire extinguishers, fire suspension |  |
|  | Aerosol can Propelant |  |
|  | Blanket Products |  |

| | |
|---|---|
| | Soda ash production for glass industry |
| | Inert gas |
| | Water treatment |
| | Dry gas cleaning |

## 1.7 4-E (energy, exergy, ecological and economic) and life cycle analyses

The performance evaluation of the thermal power plants plays a major role. Figure 1.4 shows one way of comparing performances of the plants. At present, most of the researchers are designing the power plants using first law of thermodynamics (or energy analysis). Sometimes this energy balance is not enough to find the system imperfections. The energetic losses taking place in the individual units can be determined by the exergy analysis [19]. Thus, exergetic assessment becomes a powerful tool in the power sector to measure the quality of energy and it helps to solve complex thermodynamic problems efficiently. In addition to energy and exergy analyses, evaluation of ecological assessment is also essential to assess the environmental impact. Further, life cycle analysis helps to assess the GHG emissions and primary fossil energy consumption (PFEC) by defining the stages and boundaries of the overall system. Moreover, assessment of economic parameters can be useful for comparing the levelized cost of product (LOCP) among different plant configurations as well as with the literature costs. At a viewpoint of these evaluations, a comprehensive energy, exergy, ecological and economic (4-E) analyses is required for a sustainable assessment of any new power plant configuration before setting up the real plant. This has been carried out in this study for the various configurations proposed for chemical looping combustion based power plants for $CO_2$ capture and utilization. These analyses are explained in brief as given below:

### 1.7.1 Energy analysis

The concept of energy was initially introduced by Newton when he hypothesized about potential and kinetic energies. However, the emergence of energy was not adopted until the middle of the 19th century [20]. Energy analysis is the conventional method of assessing the way energy is used in various operations involving the physical and/or chemical processing of materials and conversion of energy. This usually entails performing energy balances, which are based on the first law of thermodynamics, and evaluating energy efficiencies. However, an energy balance provides no information on the degradation of energy or resources during a process and does not quantify the usefulness or quality of the various energy and material streams flowing through a system and exiting as products and wastes. Energy analysis gives the efficiency of energy utilization, but does not provide information about source of the losses, whereas exergy analysis provides the location of actual losses. Thus, these analyses are complementary in nature and hence are equally important. Energy efficiency based on thermodynamic analysis does not provide all the necessary insights into the performance of the system.

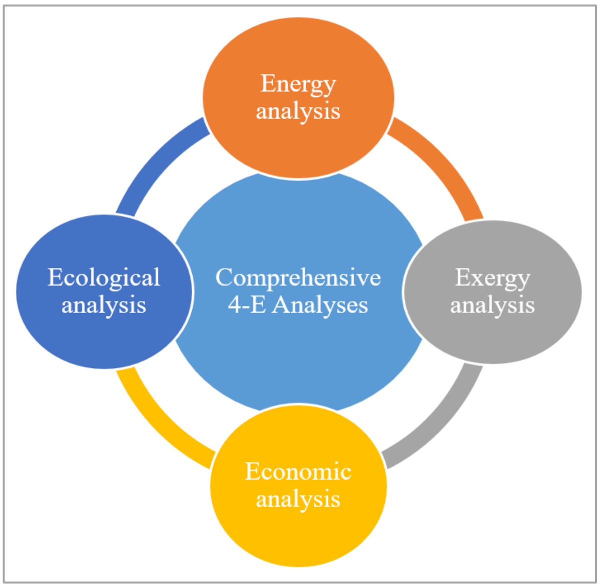

Figure 1.4. 4-E analyses.

### 1.7.2 Exergy analysis

Thermodynamics plays an important role to perform the energy and exergy analysis of the industrial process. Energy is the term that depends on the parameters of matter/energy flow and is independent of the environmental parameters. On the contrary, exergy is the term that depends on the environmental parameters. Technically, exergy is the maximum work output that a system can produce when it comes in equilibrium with the reference environment [21]. Thus, exergy analysis also plays an important role in evaluating the real performance of power plant by identifying the energy and exergy loss. The exergy analysis coupled with energy analysis has been recommended and used by several researchers [19,22]. While locating the source of energy losses, exergy analysis also indicates potential for improvement of the system to reduce the losses.

The exergy analysis is applied to identify the process irreversibilities and to determine their effect on the individual as well as overall process efficiencies. It also allows assessing the impact of exergy loss quantitatively in terms of the environment, energy utilization, and economic performance [23]. The exergy analysis also provides the location of highest energy losses in the system by performing the exergy destruction in individual sections [24].

### 1.7.3 Ecological analysis

Although the thermodynamic analysis, by way of estimating energy and exergy efficiencies is important, it cannot be the only criterion for the estimation of the plants integrated with $CO_2$ installations, as the main purpose of carbon capture process is to reduce $CO_2$ emissions from the flue gas into the atmosphere [25]. The environmental impact of electricity generation became more critical due to increase of electricity consumption worldwide. Hence, evaluation of ecological parameters (usually in terms of $CO_2$ capture efficiency, annual $CO_2$ emission rate per unit fuel, annual $CO_2$ emissions, etc.) plays an important role.

### 1.7.4 Economic analysis

Despite conducting thermodynamic and ecological analyses, the economic analysis of a process/industry needs to be assessed for a complete and comprehensive evaluation. This analysis aims to evaluate how effectively the economy of a power plant is operating. In this report, the capital cost and operation & maintenance (O&M) cost of the power plants are estimated and compared. The economic assessment is given in the National Energy Technology Laboratory (NETL) guidelines of techno-economic analysis for thermal power plants [26]. This method of assessment has different steps as – estimations of total capital cost (including equipment and installation costs), estimation of fixed O&M costs, and variable O&M costs [27]. However, the magnitudes of costs are not exact as the costs associated with the minor equipment of the plant are usually not considered [28] and also because of the uncertainties in the values of equipment cost data, uncertainties in the values of oxygen carriers/fuel/raw material prices which are market dependent and uncertainties in the value of the capacity factor. Nevertheless, the obtained results can be used to study the economic feasibility of modern power plant technologies against conventional technologies. In addition, to compare the environmental impact of different technologies on an equal footing, a cost should be assigned to the environmental benefit/degradation in the analysis.

### 1.7.5 Life cycle analysis

A key role of CCS technology is to reduce carbon dioxide emissions from anthropogenic sources into the atmosphere. The thermal power plant processes associated with CCS require the construction of infrastructure (such as pipelines), installation of facilities (such as compressors, scrubbers, etc.), additional chemicals (such as amines, solvents, hydroxides, etc.) waste solid and waste water disposal, etc. Energy is also required for the manufacturing, transportation, installation and operation of these facilities, hence, results in GHG emissions. Therefore, it is important to carry out LCA analysis to determine the performance of overall system including CCS/CCU technology in addition to 4-E analyses. The LCA method can systematically assess the environmental impact by identifying the flow of material and energy in a process [29]. In this study, LCA is conducted to assess the GHG emissions and PFEC of the total system which contains power plant by defining the stages and boundaries of the system and functional units of the system. The boundary of LCA involves – coal mining & washing, coal transportation, power plant, product compression, product transportation stages. The cradle-to-grave analysis of LCA is given by Li et al. [29]. The primary energy input to the system contains coal, natural gas, electricity, gasoline, steam etc. and the GHG emissions from the system include $N_2O$, $CO_2$ and $CH_4$. These individual GHG emissions from each stage can be estimated as the sum of possible GHG emissions (direct emissions and indirect emissions) from the suitable energy sources used in that stage. Indirect emissions indicate the emissions from the upstream stages and the direct emissions refer to the exhaust gas stream from the combustion process and the process energy use.

## 1.8 Organization of thesis

The present thesis is comprised of 9 chapters from the general background of the work to the outcome from the study and recommendations. The structure of this thesis is shown in Figure 1.5. A brief overview these chapters is given below:

**Chapter 1:** This chapter discusses the importance and motivation of the research work carried out in this thesis. It gives the general overview of chemical looping combustion system and the technical challenges of chemical looping combustion with solid fuels. It also provides the importance of carbon capture, storage and utilization. Further, the performance evaluation of any plant based on energy, exergy, ecological and economic analyses is discussed.

**Chapter 2:** A comprehensive literature review on the carbon capture technologies, CLC for various steam generation technologies, CLC with different oxygen carriers, CLC with hydrogen generation systems, $CO_2$ utilization technology and performance evaluation is presented in this chapter. This chapter concludes by highlighting some gaps in the literature and formulating the objectives and scope of the study, which have guided the definition and conduct of the present research work.

**Chapter 3:** This chapter discusses the tools and methodology used in the flowsheet modelling and simulation of the processes studied in this thesis. The assumptions, Aspen plus units/blocks and operating conditions used for developing the Aspen plus flowsheet models are discussed. It also discusses the key parameters based on the energy, exergy, ecological, economic and life cycle analyses for evaluating the performance of each case.

**Chapter 4:** This chapter provides a detailed description of CLC based power plants with various steam generation technologies (i.e. subcritical, supercritical and ultra-supercritical). It discusses the detailed results including performance evaluation using energy, exergy, ecological and economic analyses results obtained as part of the *Objective I.*

**Chapter 5:** The best suitable CLC based plant configuration obtained from *Chapter 4* is further considered in this chapter to test different oxygen carriers such as $Fe_2O_3$, CuO and mixture of $Fe_2O_3$ and CuO oxygen carriers. The overall performance of these plant cases is compared based on the energy, exergy, ecological and economic analyses. The work performed in this chapter covers the *objective II*.

**Chapter 6:** The best suitable plant configuration and oxygen carrier obtained from the *Chapters 4* and *5*, respectively, are selected to develop the CLC based coal fired power plant for power and hydrogen co-generation. This plant was considered in this chapter for a flexible electric power and hydrogen co-generation. The performance of these cases was compared based on the energy, exergy, ecological and economic analyses covering the *Objective III*.

**Chapter 7:** This chapter discusses the utilization of $CO_2$ to produce valuable product. The hydrogen and carbon dioxide obtained from the *Chapter 6* are used to produce the methane, methanol, dimethyl amine and formic acid products. Life cycle analysis based on GHG emissions and primary fossil energy consumption of overall system is discussed in this chapter. As part of *Objective IV*, The overall performance of all these plants is evaluated and compared based on the 4-E (energy, exergy, ecological and economic) and life cycle analyses.

**Chapter 8:** This chapter provides the overall conclusions obtained from this work. This chapter also includes the potential scope for future work to extend the current study.

At the end, the outcome from the thesis in the form of list of publications in the SCI indexed journals and conferences is presented.

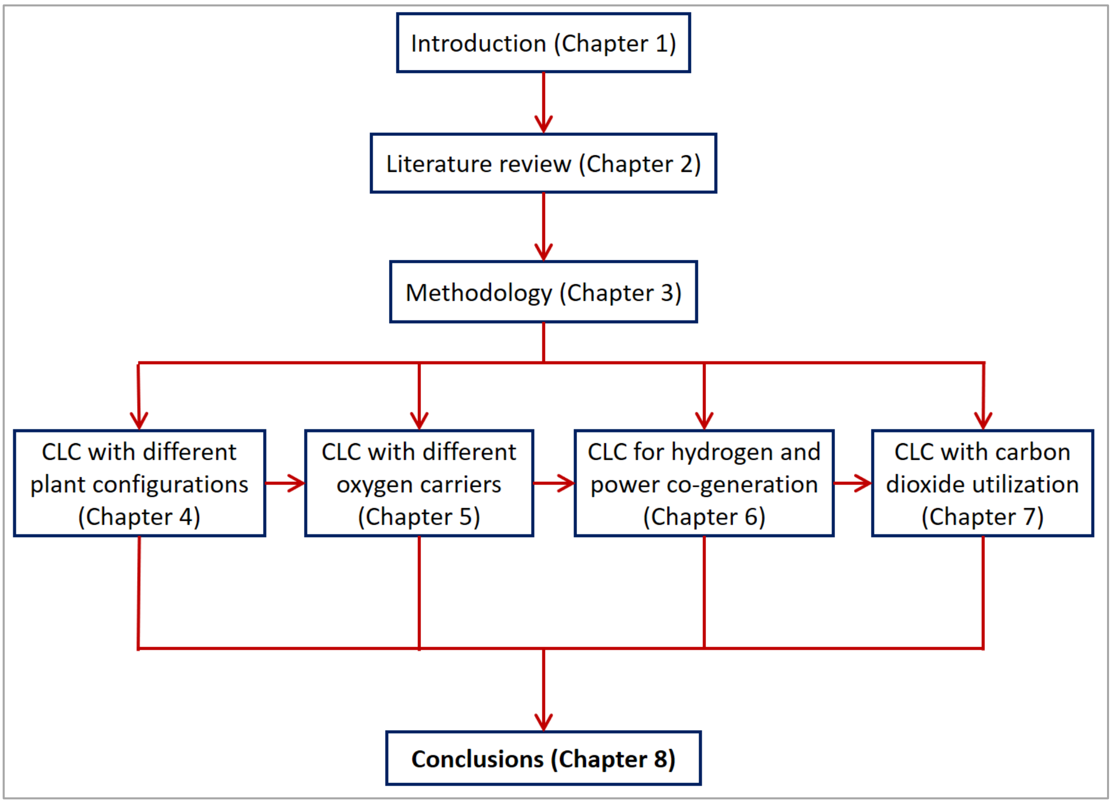

Figure 1.5. Thesis structure.

# Chapter 2

# Literature Review

# Chapter 2

# *Literature Review*

---

This chapter makes an extensive review of the existing literature relevant to the present work. It starts with a discussion on different carbon capture technologies and their applications, advantages and disadvantages. A brief review on chemical looping combustion for power generation alone and power with hydrogen generation is presented. This chapter also include literature on selection of oxygen carrier and power plant configuration in CLC based power plant. This chapter conclude with gaps identified from the literature review and followed by the objectives and scope of the present work.

---

## 2.1 Background

Coal is the world's most potential and widely distributed fossil fuel, with nearly thousand billion tonnes of global proven reserves [30]. Around 40% of world's electricity is generated from the coal based power plants and the figures are much high in many countries, to cite a few – 93% for South Africa, 92% for Poland, 79% for China, 69% for India and 49% for United States [31]. It is estimated that the global energy demand will rise by 30% by 2040 [32]. With the rapid development of global economy, the growing world's energy demand is likely to ensure that the coal remains a key feedstock for the power generation in the future [31,33]. However, the exorbitant consumption of fossil fuels may cause the severe energy crisis and environmental problems, in particular, the global warming [34,35]. Therefore, it is a challenge for the researchers to produce the electricity and/or energy resource from fossil fuels without harming the environment.

In a 900 MW CFPP with conventional carbon capture technology, about 5 million tonnes of carbon dioxide emitted into the atmosphere per year, which means $CO_2$ capture and sequestration could reduce 9 to 16 billion tonnes of $CO_2$ release per annum worldwide [36]. The IEA estimated that to achieve a 50% reduction in $CO_2$ emissions worldwide by 2050, conventional CCS technology would need to contribute to nearly 20% of emission reductions constituting every industrial sector. Moreover, the cost of tackling with carbon dioxide emissions without carbon capture technology could be 70% higher than with carbon technology [37]. However, the fuel consumption is increased by 25–40% and cost of energy generation is increased by 21–91% [38]. Thus, applying these conventional technologies to the existing plants could become more expensive. This concludes, the conventional CCS technologies reduces energy efficiency with increased cost of electricity, even though they reduce $CO_2$ emissions [36]. Hence, there was an urge to develop advanced low cost $CO_2$ capture technology during past few years. The aim was to develop the most promising technology that can produce clean energy with lower energy cost. One process, which evolved with a viable solution, was the CLC process.

## 2.2 Carbon capture technologies

Use of clean energy as an alternative of fossil fuels is an effective strategy to reduce $CO_2$ emission. $CO_2$ capture and storage (CCS) is an attractive countermeasure in contradiction of global warming. The carbon dioxide emission from flue gas of coal-based power plant can be reduced by three conventional strategies such as – pre-combustion, post-combustion and oxy-combustion depending upon plant configuration [39,40]. In recent years, combining two or more standalone carbon dioxide capture technologies (also named as hybrid technology) has attracted more attention due to the potentially low energy requirement and high carbon capture efficiency [41]. Though these technologies result in attractive $CO_2$ reduction, they are associated with huge energy penalty.

In pre-combustion technology, fuel is de-carbonized before combustion process, whereas in post-combustion technology, $CO_2$ is captured from the flue gas after combustion. In oxy-fuel technology, pure oxygen is supplied for combustion. A summary of the literature on different capture technologies used in power plant with the corresponding net energy efficiency and $CO_2$ capture efficiency are given in Table 2.1. All three technologies have undergone a great sort of development. Among three conventional capture technologies, post-combustion capture has been widely used in gaseous as well as solid fuel based power plants as it can be directly applied and the method is matured. There are several options for post-combustion $CO_2$ capture technology, such as adsorption processes [42–44], MEA-based chemical solvent processes [45], temperature swing adsorption processes [46,47] and multi-stage membrane processes [44,48]. The MEA solvent based absorption process has been widely used $CO_2$ post-combustion due to its better absorption effect and large treatment capacity. Moreover, it can also be operated at low $CO_2$ concentration and atmospheric pressure.

The post-combustion capture for the conventional coal-based power plant results in around 7-10% energy penalty for 85% $CO_2$ capture efficiency [9]. The pre-combustion and oxy-combustion $CO_2$ capture for the conventional integrated gasification combined cycle (IGCC) plant results in around 7% and 9% energy penalty for the $CO_2$ capture efficiency of 94.80% and 100%, respectively [49]. Thus, a $CO_2$ capture technology that has lower energy penalty will become a more viable option than these technologies. In this context, chemical looping combustion is very attractive, as it captures around 100% $CO_2$ emitted from the power plant at a lower energy penalty as compared to other conventional $CO_2$ capture technologies [13]. In addition to easy separation of $CO_2$ from steam, CLC technology has the advantages of eliminating nitrous oxide ($NO_x$) emissions and efficient control of the other air pollutants [12]. Mukherjee et al. [49] carried out a comparative analysis of IGCC-CLC and coal-direct chemical looping (CDCL) plant with the conventional IGCC power plant. The results revealed that the CLC based power plants capture 100% $CO_2$ emitted from the plant as compared to the pre-combustion and oxy-combustion plant. For the past few decades, research on combustion of gaseous, liquid and solid fuels using CLC technology is on high demand [8] and significant development of CLC using solid fuels is available in the literature [13].

Table 2.1 Summary of different simulation studies on carbon capture technologies in literature.

| Plant type | Fuel type | Capture technology used | Net energy efficiency (%) | $CO_2$ capture efficiency (%) | Description/Highlights | Source |
|---|---|---|---|---|---|---|
| IGCC plant | Coal | Pre-combustion | 43.0-46.63 | - | Energy balances and costs of making $H_2$ and co-product electricity from coal with $CO_2$ capture and storage were examined. | [50] |
| IGCC plant | Coal | Pre-combustion | 37.10 | 90.00 | Simulated IGCC with pre-combustion capture via membranes and identified boundary limits of membrane technology through economic evaluations. Cost of electricity for optimum water–gas-shift-membrane-reactor was obtained as 57 €/MWh. | [51] |
| IGCC plant | Coal | Pre-combustion | 35.60 | 91.00 | The techno-economic characteristics of four different capture technologies (physical absorption, water gas shift reactor membranes and two CLC cycles), which were built upon a conventional reference case were studied using the chemical process simulation package "ECLIPSE". The power plant characteristics of the IGCC/$CO_2$ using the physical absorption was found to bear more resemblance to the reference case than the other technologies. | [52] |
| IGCC plant | Coal | Pre-combustion | 45.10 | 99.00 | Proposed high pressure IGCC with membrane reactor which enabled direct $CO_2$ condensation and also found that combining IGCC and oxy-fuel was technically challenging but energetically favourable. All | [53] |

| | | | | | | |
|---|---|---|---|---|---|---|
| | | | | | selected IGCC concepts were able to realize $CO_2$ capture rates up to 99%. | |
| IGCC plant | Coal | Pre-combustion | 36.42 | 90.00 | The efficiency of a black coal IGCC process with solvent absorption $CO_2$ capture was analyzed. Three different solvents: mono diethanolamine, Selexol and hot potassium carbonate were compared on a common basis. 2% point efficiency improvement could be achieved by preheating air using high grade heat from the gasifier. | [54] |
| IGCC plant | Coal | Pre-combustion | 37.11 | 90.79 | Energy efficient direct coal chemical looping for hydrogen and power co-generation was analyzed based on the evaluation of mass and energy integration aspects. Shown energy vectors in poly-generation as promising way to increase plant flexibility. | [55] |
| IGCC plant | Coal | Pre-combustion | 38.37 | 86.95 | Assessed the performance of IGCC power plants with $CO_2$ capture based on air-blown gasification. The results showed competitive performance of the assessed plants in terms of efficiency and specific emissions with respect to more conventional IGCC systems based on oxygen-blown gasification. | [56] |
| IGCC plant | Coal | Pre-combustion | 36.44 | 91.56 | Pre-combustion IGCC with $CO_2$ capture by chemical & calcium looping technologies was studied. Technical evaluations of IGCC power plants with & without $CO_2$ capture were carried out along with environmental impact assessment using life cycle analysis methodology. | [57] |

|  |  |  |  |  |  |  |
|---|---|---|---|---|---|---|
| CFPP | Coal | Post-combustion | 32.45 | 90.00 | Retrofit scheme of system integration with selected solid sorbents were studied. Reported efficiency penalty increment as 1.4% per 1.0GJ/t$CO_2$ consumption and as 0.67% per 10°C regeneration temperature. Solid amine sorbents performed the best with the lowest penalty of 9.59%. | [58] |
| CFB plant | Coal | Post-combustion | 36.00 | 90.00 | Conducted dynamic modeling and simulation of entire CFPP-PCC process. Interactions between CFPP/PCC systems were taken into account. Three operating modes were proposed for the CFPP-PCC unit. | [59] |
| CFPP | Coal | Post-combustion | 29.04 to 38.54 | 70.00 to 90.00 | Resilience concept and evaluation studies concerning energy systems were reviewed. A resilience index measure was proposed for solar-assisted CCS energy systems. The solar hybrid CCS power plant showed the highest resilience level. | [60] |
| CFPP | Coal | Post-combustion | 28.00 | 90.00 | Thermodynamic cycle analysis was established for $CO_2$ chemisorption technology. A 4-Step $CO_2$ chemisorption cycle was demonstrated in the isothermal diagram. Second law efficiency of an ideal isothermal cycle ranged from 22.81% to 32.99%. | [61] |
| CFPP | Coal | Post-combustion | 26.55 to 33.65 | 90.00 | Solar-assisted post-combustion CCS processes were analysed trough a life cycle approach, combing life cycle GHG assessment and life cycle cost analysis. Solar-assisted repowering has considerable advantage in both GHG mitigation potential and cost aspect. | [62] |
| CFPP | Coal | Post-combustion | 26.50 to 30.60 | 90.00 | Process integration for the integrated design of $CO_2$ capture with power plants was studied using system-wide energy analysis for minimizing | [63] |

| | | | | | | |
|---|---|---|---|---|---|---|
| | | | | | power generation penalty. Case study for demonstrating the applicability of process integration method. | |
| NGCC | Natural gas | Post-combustion | 48.13 to 50.97 | 90.00 to 95.00 | Used non-linear programming optimization model for simultaneous optimization of the design and operating conditions of NGCC and $CO_2$ capture processes. $CO_2$ avoided cost was minimized for a given $CO_2$ capture and electric power generation. Detailed comparison between optimal and sub-optimal solutions was shown. | [64] |
| NGCC | Natural gas | Post-combustion | 49.16 | 90.00 | Dynamic model of NGCC power plant was developed. Commercial-scale MEA-based $CO_2$ capture plant was integrated with NGCC power plant. | [65] |
| CFB plant | Coal, sawdust, lignite | Oxy-combustion | 20.21 to 28.59 | ~97.00 | An oxy-fuel combustion system with CFB firing different fuels was studied System performance including energy and exergy efficiency were evaluated. | [66] |
| Pressurised fluidised bed | Coal | Oxy-combustion | 36.64 to 36.83 | ~100.00 | Pressurized fluidized bed oxy-fuel combustion power plant was analysed. Plant net power efficiency after optimization was 36.83% (LHV). | [67] |
| Oxy-CLAS | Coal | Oxy-combustion | 31.49 to 36.35 | 94.34 to 97.18 | Chemical looping air separation (CLAS) shows better energy and economic behaviour. Mixture of recycled flue gas and steam was used to achieve targeted oxygen content. Oxy-CCLAS shows 4.80% points higher net efficiency than Oxy-CASU. The cost of electricity of Oxy-CCLAS was 7.92 $/(MWh) lower than that of Oxy-CASU. | [68] |

| | | | | | | |
|---|---|---|---|---|---|---|
| Solar-driven coal gasification | Coal | Oxy-combustion | 46.10 to 48.00 | ~100.00 | Analysed the utilization of both coal resources and solar energy, a novel oxy-combustion supercritical $CO_2$ power cycle with solar-driven coal gasification integration. The solar to electricity efficiency was found as high as 23.3%. | [69] |
| CLC-SEMR | Methane | CLC | 71.07 to 71.46 | 93.63 to 97.47 | Studied the thermodynamic analysis of CLC-SESMR with different inert supports. Maximum plant efficiency of 71.46% was obtained with 30% SiC/$Al_2O_3$ inerts and 71.45% was obtained with 40% $MgAl_2O_4$ inerts. | [70] |
| IGCC-CLC | Coal | CLC | 35.90 to 46.80 | ~100.00 | Conducted power plant simulation studies for indirect and in-situ gasification CLC including economic analysis and comparison of LCOE. Assessed the effect of ash content of coal on performance of power plants. | [71] |
| iG-CLC | Coal | CLC | 39.00 | 89.00 | Thermodynamic performances of iG-CLC power plants with different coal feedstock were assessed. Environmental assessments of iG-CLC power plants were included. Comparisons between iG-CLC plants and other commercialized coal-feed plants were also included. | [72] |
| CDCL | Coal | CLC | 67.40 to 76.00 | ~100 | A novel, chemical looping based coal-to-hydrogen scheme was proposed. The redox process used a CuO promoted iron oxide for $H_2$ production and $CO_2$ capture. The CuO promoted iron oxide exhibited excellent reactivity for coal conversion. CuO promotion led to simpler energy integration and higher efficiency. | [73] |

| | | | | | | |
|---|---|---|---|---|---|---|
| iG-CLC | Coal | CLC | 58.20 | ~100.00 | An ex-situ coal gasification CLC integrated with combined cooling, heating and power process was presented. This novel process maintained a maximum energy efficiency of 60.34%. The fossil energy saving ratio of this process was optimized to be 27.20%. | [74] |

Table 2.2 Performance comparison of CLC based power plants using solid fuel in the literature (Simulation studies).

| Plant type | Coal, MW (HHV/ LHV) | Coal ash content, % | Plant capacity, MW | Hydrogen production, MW | Oxygen carrier | Net energy efficiency, % | $CO_2$ capture efficiency, % | Performance evaluation basis | Description/Highlights | Source |
|---|---|---|---|---|---|---|---|---|---|---|
| CDCL | 27.11 (HHV) | 9.70 | 1000.00 | 701-861 | $Fe_2O_3$-CuO | 67.40 to 76.00 | ~100 | Energy analysis | A novel, CLC based coal-to-hydrogen scheme was proposed. The redox process used CuO promoted iron oxide for $H_2$ production and $CO_2$ capture. The CuO promoted iron oxide exhibited excellent reactivity for coal conversion. CuO promotion led to simpler energy integration and higher efficiency. | [73] |
| CDCL | 27.11 (HHV) | 9.70 | 1.00 | 0.7136 to 0.7720 | $Fe_2O_3$ | 71.36 to 77.20 | 99.00 | Energy analysis | ASPEN Plus reactor simulation models based on both thermodynamic equilibrium limitations and kinetic | [75] |

| | | | | | | | | | | |
|---|---|---|---|---|---|---|---|---|---|---|
| | | | | | | | | | limitations were developed to analyse individual CDCL reactors. Thermal efficiency of 78% (HHV) was obtained with >90% $CO_2$ capture efficiency. | |
| IGCC-CLC | 27.11 (HHV) | 9.70 | 1663.71 | - | NiO | 31.50 | 100.00 | Energy analysis<br>Economic analysis | It was aimed to optimise the performance of a coal-based IGCC plant with double-stage Selexol absorption cycle and Ni-based CLC process technologies through intensive process simulation, heat integration and economic analysis. The CLC technology offered near-zero carbon emissions with higher plant efficiency and lower LCOE. | [76] |
| iG-CLC | 27.14 (HHV) | 9.70 | 100.00 | - | $MoO_3$ | 39.38 | 96.83 | Energy analysis<br>Exergy analysis | A novel Mo-based gaseous oxide assisted looping coal gasification was designed. The plant net power efficiency reached 39.38% (LHV) with a 36.32% exergy efficiency. 351.03 g·kW/h energy saving and 25.87 | [77] |

| | | | | | | | | | | |
|---|---|---|---|---|---|---|---|---|---|---|
| | | | | | | | | | g.$CO_2$·kW/h emission reduction were reported. | |
| CDCL | 26.81 (LHV) | 10.00 | 26.80 | 11.62-13.07 | $Fe_2O_3$ | 59.98 | 100.00 | Energy analysis | A compact fluidized bed composed of two fuel reactors was proposed for complete conversion of fuel gases in fuel reactor. The electricity and hydrogen efficiencies were 14.46% and 36.93% with $CO_2$ capture efficiency of 89.62% and $CO_2$ emission of 238.9 g/kWh. | [78] |
| CLC-SOFC/GT | 25.88 (HHV) | 10.91 | 25.88 | 0 to 6.59 | $Fe_2O_3$ | 37.33 to 56.92 | ~100 | Energy analysis<br>Exergy analysis | A conceptual zero emission tri-generation plant was developed. The plant energy and exergy efficiencies were 56.9% and 45.05%, respectively. | [79] |
| CDCL | 30.53 (HHV) | 10.91 | 1126.50 | - | $Fe_2O_3$ | 39.70 | 100.00 | Energy analysis<br>Exergy analysis | Model-based analysis of coal power plants with/without $CO_2$ capture was performed. CLC plant showed higher energy efficiency than pre- and oxy-fuel combustion technologies. CDCLC process was found to be as efficient as a conventional IGCC process. | [80] |

| | | | | | | | | | | |
|---|---|---|---|---|---|---|---|---|---|---|
| iG-CLC | 30.53 (HHV) | 10.91 | 3.05 | - | NiO | 58.20 | ~100.00 | Energy analysis<br>Exergy analysis | An ex-situ coal gasification CLC integrated with combined cooling, heating and power process was presented. This novel process maintained a maximum energy efficiency of 60.34%. The fossil energy saving ratio of this process was optimized to be 27.20%. | [74] |
| IGCC-CLC | 29.40 (HHV) | 11.00 | 646.80 | 274.68 | $Fe_2O_3$ | 60.42 | 82.64 | Energy analysis | Four designs of three chemical processing units by the integrated intermittent chemical-looping air separation (Design 1), the chemical-looping hydrogen generation (CLHG), and the methanol synthesis loop (MSL) were integrated to retrofit the integrated gasification combined cycle (IGCC) system configuration. Design 4 provided a flexible energy storage allocation to increase ESR by 51.21%. | [81] |

| | | | | | | | | | | |
|---|---|---|---|---|---|---|---|---|---|---|
| CDCL | 28.70 (HHV)<br>27.80 (LHV) | 14.19 | 1055.67 | 0-200 | $Fe_2O_3$ | 42.01 to 49.88 | 99.81 | Energy analysis | Evaluated energy efficient direct coal chemical looping for hydrogen and power co-generation. | [55] |
| IGCC-CLC | 27.80 (LHV) | 14.19 | 236.80 | - | NiO | 53.19 | 99.97 | Energy analysis<br>Ecological analysis<br>Economic analysis | Showed that biomass and coal co-feed feedstock benefited synthetic natural gas production. Integration of chemical looping combustion for polygeneration paid no energy penalty for carbon capture. The energy efficiency of this process was 53.19% with zero-carbon emissions. | [82] |
| iG-CLC | 16.25 (LHV) | 25.20 | 162.50 | - | $Fe_2O_3$/ $TiO_2$ | 39.00<br>40.54 | 88.90<br>90.63 | Energy analysis | The thermodynamic performances of steam and $CO_2$-gasified iG-CLC process were examined. Approximately 3.9% of net power efficiency was increased in $CO_2$-based iG-CLC power plant, compared with steam-based plant. $CO_2$ capture efficiency got elevated in $CO_2$-gasified iG-CLC process. | [83] |

| | | | | | | | | | | |
|---|---|---|---|---|---|---|---|---|---|---|
| iG-CLC | 16.25 (LHV)<br>21.88 (LHV)<br>26.45 (LHV) | 28.80<br>31.80<br>14.90 | 162.50<br>218.80<br>264.35 | - | $FeTiO_3$ | 39.00<br>46.00<br>44.00 | 89.05<br>88.07<br>88.36 | Energy analysis<br>Ecological analysis | Thermodynamic performances of iG-CLC power plants with different coal feedstock were assessed. Environmental assessments of iG-CLC power plants were included. Comparisons between iG-CLC plants and other commercialized coal-feed plants were also included. | [72] |
| IGCC-CLC | 22.30 (HHV)<br>31.90 (HHV) | 30.00<br>9.00 | 150.31<br>149.41 | - | $Fe_2O_3$ / NiO | 35.90 to 46.80 | ~100.00 | Energy analysis<br>Economic analysis | Presented power plant simulation studies for indirect and in-situ gasification based CLC. Assessed the effect of ash content of coal on performance of power plants. | [71] |
| IGCC-CLC | 16.72 (HHV) | 45.25 | 500 | - | NiO | 40.20 | 99.97 | Energy analysis<br>Exergy analysis | Analysis of Indian coal based combined cycle power plant with carbon capture was presented through Aspen Plus simulation of pre-combustion capture and chemical looping combustion. Conducted parametric study of gasification and combustion on overall plant efficiency. | [24] |

## 2.3 Chemical looping combustion

Though the journey of this CLC technology started back in the year 1954 when a patent named ‘production of pure $CO_2$’ was presented by Lewis and Gilliland [84], the CLC concept was forgotten for long time and there was discontinuity in the CLC research until 1980. In the first half of 1980s, Richter and Knoche proposed a fuel oxidation reaction that involves two intermediate reactions with metal oxides like CuO, NiO or CdO as an oxygen carrier [85]. The coinage of the term was done in second half of 1980s by Ishida et al. [86]. Later in the mid of 1990s, Ishida and Jin [87,88] proposed CLC technology for carbon capture using iron and nickel based oxygen carriers. Since then, the process of CLC has gained momentum and has gone leaps and bounds forward. During last 10-15 years, an extensive research of CLC process including reactor system, type of oxygen carrier and type of fuel used have been developed. Many funded research projects and programs came up to the extensive research of CLC technology and its development to establish in a commercial level [89]. In India, a research on CLC has also been initiated at Council of Scientific and Industrial Research (CSIR) laboratories (CSIR-CMERI, CSIR-CIMFR, CSIR-IICT and CSIR-NEERI) [36]. The main objective of these projects is to develop naturally occurring ores and synthetic/hybrid oxygen carriers to test their performance in CLC reactors. The increase in cost of electricity of a CLC based power plant compared to the conventional coal fired power plant without $CO_2$ capture unit was only about 12-22% [89], which is much less than conventional CCS technologies. Hence, CLC technology is found to be more viable option to reduce GHG emissions compared to the conventional technologies to the countries with high electricity consumption.

To date, many researchers have worked theoretically and experimentally on the CLC based power plants. Table 2.2 shows the compilation of different works on performance evaluation of CLC based power plants available in the literature based on method of evaluation, oxygen carrier used, coal type and plant type. It can be observed that most of the studies on performance evaluation of CLC in coal based power plants are with low ash coals and the method of evaluation is either energy analysis or both energy and exergy analyses.

## 2.4 Oxygen carriers for CLC

The oxygen carrier is one of the most significant component of chemical looping combustion system that determines the progress and fate as a carbon capture technology [90–92]. In past few years, most of the works on the CLC is focused on the development of oxygen carriers and their performance evaluation [13,91,93–99]. The selection of oxygen carriers should ideally accomplish the following characteristics:

- It should have sufficient oxygen carrying capacity.
- It should have favourable thermodynamics while converting fuel in to $CO_2$ and steam in the fuel reactor of CLC.
- It should be economically feasible.
- It should be environmental friendly and easily available.
- It should be highly reactive for reduction and oxidation reactions.
- It should have good fluidization properties.
- It should have low carbon deposition to avoid $CO_2$ release in the air reactor while oxidation of oxygen carrier particles.
- It should have multiple reduction-oxidation cycle capability.

First two characteristics are mainly dependent on the red-ox system. The cost and environmental characteristics depends on the type of metal oxide used. The quality of other all characteristics need to be determined experimentally for each metal oxides.

The pure metal oxide particles do not fulfil all the above characteristics and the reaction rates decrease in a few red-ox cycles [8,13]. This shows that there is need of support to these metal oxide particles. A porous support to the metal oxide particle provides higher surface area for the reactions, a binder is used to increase the mechanical strength and attrition resistance [8]. Besides reactivity, the cost of oxygen carrier in CLC system plays a major role, especially in the power sector. Cost of oxygen carrier is sum of several factors including cost of metal oxide, cost of inert/support used and cost associated with preparation of oxygen carrier.

Initially, researchers focused on developing oxygen carriers for gaseous fuels. Due to availability of large quantity of solid fuels (such as coal) in many countries, researchers started developing oxygen carriers for solid fuels to enhance the properties of oxygen carriers [100–102]. The metal oxides are generally supported on the inert materials like $TiO_2$, $Al_2O_3$, $SiO_2$ or

$ZrO_2$, which do not take part in reaction, act as porous support and assist in enhancing the rate of reaction by providing more surface area for reaction [70,103–105]. Development of novel oxygen carriers and their support materials is expected to have great influence in future to commercialize the CLC technology.

Metal oxides play a dual role both as oxygen supplier and catalyst. The gasification efficiency of fuel is influenced by the presence of suitable metal oxides in the CLC process. Ni acts as a catalyst for steam gasification reaction [106] and it is reported that the rate of water gas shift reaction is higher in the case of Ni-based metal oxides during the CLC process. Cho et al. [107] found that Ni and Fe-based oxygen carriers act as catalysts for Boudouard reaction and progress gasification reactions at low temperatures. The conversion of solid fuel, char, volatiles, and gasified products in the CLC process depends on the choice of metal oxide and gasifying medium ($CO_2/H_2O$). The CuO as the metal oxide achieves a higher weight loss in the range of 30–40% of the reaction mixture in thermogravimetric analysis (TGA) [108]. This is due to the CLOU nature of the CuO, which can produce the gas phase oxygen. Whereas, the reactivity of other metal oxides shows a lower weight loss of ∼10.0% in TGA [109,110]. However, bauxite, exhibiting non-CLOU nature, achieved 37.5% solid conversion using lignite char while anthracite char lost only 8% of its total weight. This is due to the higher surface area of lignite char, compared to anthracite coal. The suitability of metal particles and its corresponding oxides in the CLC process are discussed by Adanez et al. [7] and Cho et al. [111]. It is reported in the literature that nickel, manganese, copper, iron, cobalt, etc. are the major oxygen carriers for the CLC operation. Nickel and cobalt-based oxygen carriers exhibit higher reactivity with fuels compared to other metal oxides [111]. However, these metal oxides own their disadvantages. Nickel exhibits a low oxidation rate in the air reactor, and furthermore, these metal oxides are toxic and expensive [7,111]. Cobalt and nickel-based oxygen carriers have thermodynamic limitations for the complete conversion of $H_2$ and CO [112]. Thus, low-cost and environmentally-friendly metal oxides are needed and should be identified for the economic operation of the CLC process.

The high ash coals need low cost metal oxides for the CLC operations as separation of coal ash and metal oxide particles is involved [71]. Table 2.2 shows the performance comparison of different studies available in the literature for various coal ash contents. It is observed that, low ash content (or high calorific value) coals have high overall efficiency and high ash content (or low calorific value) coals have low overall efficiency. The overall efficiency of CLC based power plant is also dependent on type of oxygen carrier used. To date, many researchers have been working on the development of low cost oxygen carriers to make CLC technology economically favourable. Some industrial wastes and natural ores are widely available for the CLC process. Hematite, pyrite cinder, perovskite, bauxite and natural iron ore are some low cost metal oxides with higher conversion rates with coals [13]. The iron based oxygen carriers have gas conversion efficiency of 79.00 to 98.00% with $CO_2$ yield 7 of 3.70 to 99.90% [71]. The $CO_2$ yield of hematite is found to be ~93.00% with bituminous coal [113]. Bauxite waste showed gas conversion efficiency of 87.00 to 98.00% with coal chars [114]. The ilmenite oxygen carrier has higher gas conversion efficiency and carbon capture efficiency compared to hematite and bauxite oxygen carriers [115]. Ilmenite also has high oxygen transport capacity and shows better performance during redox reactions [7].

The theoretical oxygen carrying capacity of different metal oxides used to carry out reduction-oxidation reactions is shown in Table 2.3. The oxygen carrying capacity is an important parameter to measure the effectiveness of CLC operations. A metal oxide with higher oxygen carrying capacity requires lower oxygen carrier circulation rate and smaller volume reactor.

Table 2.3 Oxygen carrying capacity for various metal oxides in their pure form [116].

| Initial state | Reduced state | Extent of conversion | Extent of maximum weight change |
|---|---|---|---|
| CuO | Cu | 100.00 | 20.11 |
| $Cu_2O$ | Cu | 50.00 | 10.06 |
| CuO | $Cu_2O$ | 50.00 | 10.06 |
| $Fe_2O_3$ | $Fe_3O_4$ | 11.11 | 3.34 |
| $Fe_2O_3$ | FeO | 33.33 | 10.02 |
| $Fe_3O_4$ | FeO | 22.22 | 6.68 |
| $Fe_3O_4$ | Fe | 88.89 | 26.72 |
| FeO | Fe | 66.67 | 20.04 |
| $Fe_2O_3$ | Fe | 100.00 | 30.06 |
| NiO | Ni | 100.00 | 21.42 |
| MnO | Mn | 50.00 | 18.40 |
| $MnO_2$ | MnO | 50.00 | 18.40 |
| $MnO_2$ | $Mn_2O_3$ | 25.00 | 9.20 |
| $MnO_2$ | $Mn_3O_4$ | 33.33 | 12.27 |
| $MnO_2$ | Mn | 100.00 | 36.81 |
| $Mn_2O_3$ | $Mn_3O_4$ | 8.33 | 3.07 |
| $Mn_2O_3$ | Mn | 75.00 | 27.61 |
| $Mn_2O_3$ | MnO | 25.00 | 9.20 |
| $Mn_3O_4$ | MnO | 16.67 | 6.13 |

| | | | |
|---|---|---|---|
| $Mn_3O_4$ | Mn | 66.67 | 24.54 |

Large quantity of iron ores are available in India [117]. The hematite oxygen carriers are low cost and environmentally compatible, hence, they are considered as an attractive option for the CLC applications, despite of having low conversion, weak redox characteristics and low oxygen transport capacity. On the other hand, Cu-based metal oxides have high oxygen transfer capacity and reaction rates with no thermodynamic restrictions to achieve 100% fuel conversion to $H_2O$ and $CO_2$. These oxygen carriers are costlier than iron-based, bauxite, perovskite and pyrite cinder but, they are cheaper than cobalt and nickel based oxygen carrier [13]. This makes Cu-based oxygen carriers more suitable for CLC applications than Fe-based oxygen carriers. Hence, addition of some fraction of Cu-based oxygen carrier in Fe-based oxygen carrier could improve carbon conversion, redox characteristics and overall performance of the plant. This work presents the effect of addition of CuO in $Fe_2O_3$ supported on $Al_2O_3$ on the overall performance of CLC based coal fired power plant.

Currently, the chemical looping concept has been used widely in different applications as summarized in Table 2.4. Some of the transition metal oxide characteristics that are not well compatible with the CLC process are beneficial in other applications. For example, the tendency of copper, cobalt and manganese oxides to decompose at low temperatures and lose their lattice oxygen is utilized in CLAS or CLOU [118]. CLAS aims to separate oxygen from air utilizing the decomposition trend of those metal oxides [119], while CLOU uses the separated oxygen to combust the solid hydrocarbon fuels to overcome the slow rate of the reaction between solids (fuel and oxygen carrier) [120]. In CLRG, the desired product is $H_2$ instead of heat as in CLC. Thus, oxygen concentration is kept low to prevent the full oxidation of glycerol to $H_2O$ [121]. The tendency of iron oxides to promote partial oxidation of methane to form syngas ($H_2$ and CO) can be utilized as an alternative method to produce syngas or $H_2$ and electricity [122]. Investigating the performance of metal oxides as oxygen carriers for CLC and their associated solid-state reduction mechanisms during CLC can provide new insights linking material properties and performance that not only are beneficial for CLC but also these other, analogous processes. Thus, beyond CLC, there are more applications of the chemical looping concept utilizing the oxygen carriers. However, the study presented in this thesis focuses only on integration of CLC with coal-fired power plants for power and hydrogen production with $CO_2$ capture and utilization.

Table 2.4 Applications derived from chemical looping concept.

| Technology | Approach | Typically used oxygen carriers | Source |
|---|---|---|---|
| Chemical Looping Air Separation (CLAS) | Separate $O_2$ from air by utilizing metal oxide decomposition | Ca, Cr, Mn, Co, Cu-based | [119] |
| Chemical Looping Reforming (CLR) | Generation $H_2$ from natural gas | Fe, Ni, Cu, Mn-based | [122] |
| Chemical Looping Gasification (CLG) | Convert biomass to syngas | Cu, Fe, Mn-based | [118] |
| Chemical Looping Oxygen Uncoupling (CLOU) | Combust solid fuels by utilizing metal oxide decomposition | Cu, Mn-based | [120] |
| Self-sufficient Chemical Looping Reforming of Glycerol (CLRG) | Generate $H_2$ rather than heat | Cu, Mn, Ni, Co-based | [121] |
| Syngas Chemical Looping gasification (SCL) | Generate $H_2$ and electricity from coal-derived syngas | Fe, Ni, Cu, Co-based | [123] |

## 2.5 Different plant configurations for power production

The low calorific value (or high-ash content) in Indian coal reduces the net efficiency of the power plant as compared to low ash content (or high calorific value) coals [5]. One way of increasing net plant efficiency is by integrating the power plant with CLC technology. The overall plant efficiency can further be increased by adapting advanced power plant technologies such as - supercritical (SupC) and ultra-supercritical (Ultra-SupC) plants.

The CLC based approach has been widely used for IGCC plants for subcritical (SubC) and supercritical steam parameters because of its higher overall plant efficiency and low $CO_2$ emissions compared to other coal-based conventional plants [13]. Some of the important contributions in the application of CLC for IGCC plants using coal are presented below. Erlach et al. [124] studied the effect of gas turbine inlet temperature on various configurations of CLC-IGCC plants at 127 bar (SubC) and 280 bar (SupC) steam parameters. Prabu [125] conducted a thermodynamic analysis of CLC based IGCC plant with SubC, SupC and Ultra-SupC boilers. An increase in net plant efficiency by 5.98% for Ultra-SupC CLC based IGCC plant when compared to a SubC CLC based IGCC plant was reported. Further, Spallina et al. [126] carried out a thermodynamic analysis of IGCC-CLC plant for Ultra-SupC boilers. With this Ultra-SupC steam boiler, the performance of the CLC based IGCC plant is improved by 2.91% compared to conventional IGCC plant. Mukherjee et al. [127] compared the performance of various oxygen carriers (copper, iron, cobalt, nickel and manganese oxides) for IGCC-CLC (350 to 500 MW) power plants with the supercritical boiler. The study revealed that, among five oxygen carriers, the iron oxide resulted in more efficient (net electric efficiency 34.3%) process. Shijaz et al. [24] evaluated a CLC integrated IGCC power plant against the conventional IGCC power plant with and without $CO_2$ capture based on energy and exergy analyses. The study showed 2.49% energy penalty for the IGCC-CLC plant compared to the conventional IGCC plant without $CO_2$ capture and 4.8% energy gain compared to the conventional IGCC plant with $CO_2$ capture, thus establishing the superiority of CLC technology.

In CLC based coal-fired power plants, coal is directly fed to the fuel reactor along with the oxygen carrier, eliminating the need for air separation unit and water gas shift reactor [49]. There are limited studies reported on CDCL or CLC based CFPP. He et al. [128] proposed a study on CDCL of a mixture of copper oxide and iron oxide oxygen carriers. The study reveals that a small amount of CuO in $Fe_2O_3$ increases the plant efficiency compared to $Fe_2O_3$ alone. Zeng et al. [129] analyzed the CDCL concept for moving bed reactors using iron oxide as an OC for a subcritical boiler. Ozcan and Dincer [79] developed CDCL plant for tri-generation of hydrogen, power, and heating for a subcritical boiler and found the overall plant energy and exergy efficiencies to be 56.9% and 45.05%, respectively. Cormos and Cormos [55] evaluated power and hydrogen co-generation of CDCL plant for subcritical boiler and achieved net efficiency of ~42% with zero $CO_2$ emissions. Performance comparison of CDCL plant with IGCC-CLC is conducted by Mukherjee et al. [49] for the supercritical boiler. An increase in net electric efficiency of CDCL plant by 4.67% compared to IGCC-CLC plant is observed. Fan et al. [72] conducted thermodynamic and environmental analyses for iG-CLC plant for the subcritical boiler. Their study achieved ~10% higher net plant efficiency for iG-CLC plant compared to a conventional plant. Most of these CLC integration studies in the literature are with subcritical steam parameters and supercritical steam parameters for low ash content coals. There are no studies available in the literature on CLC based CFPP for ultra-supercritical boilers. This is also identified as one of the gaps for the present study.

## 2.6 CLC for hydrogen generation

Hydrogen is one of the most promising source of renewable energy. It is an important feedstock to the ammonia synthesis and oil refining and is environmental friendly fuel for the transportation and power generation in the future [130]. The natural gas is the most frequently used source for the hydrogen synthesis through steam methane reforming technology [131,132]. However, the steam methane reforming process has some disadvantages such as: high energy requirement due to its endothermic nature, lower conversion, greenhouse gas emissions, relatively higher operational and maintenance costs [70]. Chemical-looping combustion (CLC) is another attractive technology for power and $H_2$ co-generation with the inherent $CO_2$ capture [133]. Nowadays, the CLC technology for multi-generation (i.e. power and hydrogen) using a gaseous fuel has been widely studied.

Due to the huge coal reserves and low price, more research needs to be focused on co-generation of power and $H_2$ using CLC based coal fired power plants. Basically, there are two approaches of CLC technology- two reactor system for power generation alone and three reactor system for co-generation of power and hydrogen [8]. The block diagram of these two approaches is shown in Figure 1.3 and the details of these two approaches are explained in *Chapter 1*.

So far most of the literature available is on the CLC integrated systems for co-generation of power and $H_2$ using mainly gaseous fuels [134–138]. The simulation of CLC based plant results confirmed the improvement in syngas production, $CO_2$ capture, energy utilization [137], and reduction in hydrogen production cost [138]. The performance of the CLC based power plants mainly depends on the strength, durability and reactivity of the oxygen carrier particles. A suitable combination of oxygen carrier with different compositions of the support is studied to check the performance of the CLC integrated steam methane reformer by Alam and Sumana [70]. Vos et al. [139] compared performance of CLC based plant with methane for $Fe_2O_3$ on $Al_2O_3$ and $MgFeAlO_x$ supports. The study showed that $Fe_2O_3$ with $MgFeAlO_x$ support is a promising material that can replace Ni-based metal oxides as it forms a sustainable green, stable and non-toxic alternative for $H_2$ generation by CLC.

The literature on the CLC based power plants with coal as the fuel such as CDCL combustion with power and $H_2$ co-generation is limited and a very less recent literature is found on the coal-based power plants for hydrogen co-generation. The advantage of solid fuel over gaseous fuel is the possibility of achieving more $H_2$ to $CO_2$ ratio with lower coal-feed. The CDCL offers promising route for the co-generation of high purity hydrogen along with power [140]. Wu et al. [141] presented calcium looping, chemical looping and syngas chemical looping combustions coupled with IGCC plant to produce high purity hydrogen. Their study reported that, the optimization algorithm corresponding to system efficiency, $CO_2$ emissions and economics are worth considering in the future. Various power plant configurations of CDCL system were proposed for 300 – 450 MW of net electricity generation with flexible hydrogen co-generation (i.e. 0-200 MW, based on lower heating value) [55]. Cormos et al. [142] presented CLC and calcium looping combustion integrated with decarbonised IGCC plant to produce 435 – 592 MW of electricity and up to 200 MW of hydrogen with more than 90% plant decarbonisation degree. Their study concluded that, the IGCC technology coupled with CLC technology was favorable to deliver higher carbon capture rate and was energy efficient and had better economic operational flexibility compared to the conventional technologies. Shi et al. [81] investigated process design and simulation of IGCC plant integrated with chemical looping $H_2$ generation, methanol synthesis and chemical looping air separation to evaluate net plant efficiencies, carbon emission rate, water saving ratio and energy saving ratio. Despite having the better carbon capture and multi-generation technology, the selection of oxygen carrier plays vital role in the hydrogen generation system [143]. He et al. [128] proposed to incorporate the copper oxide into the iron-based oxygen carrier to improve the conversion rate. The presence of copper oxide in the iron-based oxygen carrier does not take part in the reaction to produce the hydrogen, but enhances the overall performance of the power plant by improving the electrical efficiency [128]. Hence, in this work, an effort is made to propose the CLC based CFPP with flexible hydrogen generation along with electricity.

## 2.7 Carbon capture and utilization

Once the carbon dioxide is captured from the power plant, the next step is to utilize $CO_2$ to produce valuable products. These products can include methanol, methane, formic acid, dimethyl ether (DME), dimethyl carbonate, formaldehyde, etc. [15]. All these products need hydrogen and $CO_2$ as additional raw materials. Hence, coupling of CLC based CFPP with CDU plant not only provides the $CO_2$ but also provides hydrogen as raw material. Methanol is a single carbon compound that can be produced from biomass, natural gas, coal. Demirel et al. [18] presented review work on the CLC to help the researchers in the field of power sector to identify the sustainable energy and chemical technologies for the capture and conversion of

$CO_2$. The feasibility study of co-producing methanol in CFPP with entrained-flow coal-gasification system with 207.99 MT/day of methanol and 32.76 MWh of electric power production is assessed by Wang and Demirel [144]. Schakel et al. [145] explored techno-environmental performance of carbon dioxide utilization through methane reformation into syngas to produce DME. The techno-environmental performance of the plant was assessed by hybrid LCA. Bassano et al. [146] designed and built first moveable and modular plant to convert $CO_2$ to methane with 0.2-1 $Nm^3/h$ of methane production rate. Pan et al. [147] thermodynamically investigated municipal solid waste gasification integrated with solid oxide electrolyzer cell for efficient and environment friendly natural gas production. Fortes et al. [148] developed synthesis of formic acid from captured $CO_2$ and $H_2$ and compared with the conventional formic acid synthesis method. The overall performance of the synthesis plants was compared based on the techno-economic and environmental feasibility. The market analysis showed the annual demand of formic acid: 0.76 MT [148], methane: 439.71 MT [30], methanol: 78.09 MT [149] and DME: 6.91 MT [149].

## 2.8 Performance evaluation of power plants

### 2.8.1 Energy, exergy, ecological and economic analyses

Energy plays a key role to increase the modern economy for agriculture, transport, industry and household uses in any country. Fossil fuel based power plants contribute around 80% of power generation and rest is generated from other sources like geothermal, solar, nuclear and other energies [25]. Enough research is available on the optimization of these power plant cases based on energy analysis. In several developing countries, energy supply is less secure due to its costlier price. Hence, there was a need to reconsider the low-cost energy option. Therefore, from the energy point of view, the first law of thermodynamic analysis is found to be insufficient. Exergy analysis has its own importance in the thermodynamic analysis. Exergy is the maximum energy available for the conversion of heat into work. In last few decades, exergy analysis of power plant has been found as a valuable practice in the design, optimization, development and improvement of the power plants. The concept of term exergy was first developed by J. W. Gibbs in 1878 and further developed in 1957 by Z. Rant [25]. H. D. Baehr in 1965, termed the part of energy converted into all other forms of energy as exergy [23]. The exergy analysis assists in finding the location of actual losses taken place in the overall system and helps in taking essential actions to reduce the losses [19,150].

Evaluation of environmental impact and economic impact is essential in addition to energy and exergy analyses for a comprehensive techno-economic assessment of a power generation system [25]. However, to compare the environmental impact of different power plant and carbon dioxide utilization technologies on an equal footing, a cost should be assigned to the environmental degradation and cost of electricity or products obtained should be calculated. Hence, a 4-E i.e. energy, exergy, ecological and economic analyses of all the power plants and/or carbon dioxide utilization plants should be carried out to compare with each other and with the conventional power plant technologies.

Table 2.2 shows the performance evaluation basis for the CLC based power plants. Most of the literature is found on the performance evaluation based on the energy analysis followed by the exergy analysis. Few literatures is available on the ecological and economic performance evaluation. A comprehensive study involving energy, exergy, ecological and economic assessments is not available for direct comparison of the CLC based power plants. Such an analysis plays an important role in selecting the most suitable technology to increase the power capacity for the next generation.

### 2.8.2 Life cycle analysis

LCA is aimed to evaluate the environmental impact throughout the product's life cycle by taking into consideration of GHG emissions from construction and/or power plant operation to final decommissioning. Several life cycle analysis studies have been conducted for CCS process, but they are mainly on CFPP with $CO_2$ capture unit [151–154]. With increase in energy demand, a substantial decrease in GHG emissions is found for pre-combustion, post-combustion and oxy-combustion approaches [153]. Odeh and Cockerill [154] conducted life cycle analysis to evaluate GHG emissions from three different types of fossil fuel power plants with CO2 capture and without $CO_2$ capture unit. They found GHG emissions reduction by 75 to 84% 90% for 90% carbon capture efficiency.

Very less attention is given to the life cycle analysis of CLC based plant with hydrogen and power co-generation plants and CLC based plant coupled with $CO_2$ utilization process. The LCA of a power plant evaluates the environmental impact by identifying the energy flow and material flow [155]. Li et al [156] carried out life cycle GHG emission and primary fossil energy consumption (PFEC) analysis for a coal to $H_2$ process with and without $CO_2$ capture systems. Xiang et al. [157] conducted LCA of the GHG emission and energy consumption of olefin production from coal, oil and natural gas. Schakel et al. [145] explored techno-environmental performance of carbon dioxide utilization through methane reformation into syngas to produce DME. The techno-environmental performance of the plant was assessed by hybrid life cycle analysis. Navajas et al [158] presented environmental evaluation of natural gas fueled CLC process with iron, nickel and copper based oxygen based carriers on life cycle analysis. Their study showed nickel based metal oxides are most adequate to be used in CLC operations for natural gas combustion. Moreover, several analyses were performed to improve the well known metal oxides that can be used to replace the NiO oxygen carrier and they found $Fe_2O_3$ oxygen carrier was the best replacement over it. He et al. [159] presented LCA analysis of coal-driven synthetic natural gas and poly-generation system integrated with CLC technology to justify the environmental unsustainability. The results showed the lifetime of metal oxides is the main element in determining the sustainability of the CLC system and global warming impact is almost independent when lifetime of metal oxide exceeds 3000 h. Bareschino et al. [160] presented CLC based power plant with hydrogen production through water electrolysis by integrating it with polymer electrolysis membrane to produce methane. The environmental performance was evaluated using LCA analysis. Their study showed the production and disposal of metal oxides used in CLC operation represents the large source of environmental impact (around 90% of overall impact).

## 2.9 Research gaps identified from literature

From the review of the literature on the chosen field of study, following research gaps are identified to develop the chemical looping combustion based thermal power plants.

1. Limited literature is available on the thermodynamic and economic analyses of CFPPs based on high-ash coal and advanced steam boilers. Although few studies on energy and exergy analyses are available on the CLC based subcritical CFPPs as discussed above, a comprehensive study involving 4-E (energy, exergy, ecological and economic) assessments is not available for direct comparison of the CLC based CFPPs with different steam boiler parameters using coal. Such an analysis plays an important role in selecting

the most suitable technology to increase the power capacity for the next generation, especially in the developing countries where coal is the major energy source.

2. Many oxygen carriers have been reported in the literature with their own advantages and disadvantages. Hence, selection of oxygen carrier is a challenging task. According to U.S. Geological survey 2017, India ranks fourth in iron ore production [117]. Thus, iron oxide can be a potential oxygen carrier for CLC application in India. The copper oxide is more reactive and costly compared to the iron oxide, but addition of some fraction of copper oxide in the iron oxide can enhance the reactivity and should not add much in the overall operational cost. The energy, exergy, ecological and economic analyses of CLC based coal fired power plant using such mixed oxygen carriers is missing in the literature. Moreover, comparison of those plants with conventional coal fired power plant based on 4-E analyses is also not available in the literature.
3. Further, a comprehensive report on the CLC based coal fired power plant for power and $H_2$ co-generation with energy, exergy, ecological and economic analyses is not available in the literature. This comprehensive analysis is required for feasibility assessment and to make policy decisions on coming up with these environmental friendly co-generation power plants in future.
4. The reported literature is either on the CLC based power plant for hydrogen generation or on the $CO_2$ utilization to produce valuable products. Further, no study is found on the comprehensive analysis on the energy, exergy, ecological, economic analyses of CLC technology integrated with $CO_2$ utilisation.
5. Some studies are found in the literature that includes life cycle analysis of hydrogen generation from the power plant and also on the synthesis product obtained from carbon dioxide. However, no study has been reported in the literature that involves life cycle analysis of CLC based power plant integrated with the $CO_2$ utilization technology.

Above research gaps lead to the formulation of the following objectives of the present work.

## 2.10 Aim and objectives of the research work

**Aim:** The main aim of the research work is to study the feasibility of integrating chemical looping combustion and $CO_2$ utilization technologies in Indian coal based power plants theoretically.

**Objectives:** Accordingly, the following objectives have been formulated to conduct the research work in achieving the above goal.

Objective 1: 4-E (Energy, Exergy, Ecological and Economic) analyses of CLC based Indian coal fired power plant with subcritical, supercritical and ultra-supercritical steam boilers for efficient $CO_2$ capture.

Objective 2: 4-E analyses of CLC based coal fired power plant with different oxygen carriers.

Objective 3: 4-E analyses of CLC based coal fired power plant for hydrogen and power co-generation system.

Objective 4: 4-E and life cycle analysis on the integration of the $CO_2$ utilization plant (formic acid, methane, methanol and dimethyl ether) with CLC based power plant for hydrogen and power co-generation system.

# Chapter 3

# Modelling and Simulation Methodology

# Chapter 3

# *Modeling and Simulation Methodology*

Having identified the research objectives of the study, the aim of this chapter is to discuss about the detailed methodology adopted to achieve the objectives. This chapter starts with the classification of the various power plant configurations considered in the whole study and simulation assumptions, process simulation tools used followed by the common methodology adopted to develop the conventional and CLC based (power alone and power with hydrogen co-generation) power plants and utilization plants for the production of formic acid, methane, methanol and dimethyl ether synthesis (with $CO_2$ as a raw material) plants using Aspen plus. This chapter also presents the methodology and equations involved in the performance evaluation of these cases based on energy, exergy, ecological, economic and life cycle analyses.

This work includes construction of numerous flowsheet models of coal-fired power plants. Simulation environment, *aspenONE* v10.0, is used to develop plant layout, operating conditions (temperature, pressure, flow rates, fuel composition and unit efficiency) and key parameters. The conventional CFPP, CLC based CFPP and $CO_2$ utilization plants are simulated using the appropriate models and data from the published literature. The different plant types considered in the present study can be grouped in to the following four categories:

Category 1: Conventional CFPP with and without $CO_2$ capture.

Category 2: CLC based CFPP with power generation alone.

Category 3: CLC based CFPP with hydrogen and power co-generation.

Category 4: CLC based CFPP with hydrogen and power co-generation coupled with $CO_2$ utilization plant.

Each category involves different cases defined as per the need of the objective, which are discussed in the individual chapters. Steady-state simulations of all the cases of these categories are conducted with suitable models using Aspen plus v10.0. The description of these cases are detailed in the section 3.3.

## 3.1 Simulation assumptions

To enable direct comparison among the power plant configurations, common operating assumptions have been considered while simulating different configurations in this study. Table 3.1 shows the characteristics of high-ash Indian coal with higher heating value (HHV) of 15.83 MJ/kg, lower heating value (LHV) of 14.88 MJ/kg and exergy of 17.30 MJ/kg (based on HHV) & 16.20 MJ/kg (based on LHV) on dry basis. Note that, present work is not focused on the separation of ash particles from the oxygen carrier particles and interaction of coal-ash with the oxygen carriers. However, the composition of coal ash is used in the aspenONE software for the calculation of exergy of non-conventional ash. The ash in the coal is a non-conventional component in the aspenONE simulation software. The exergy flow rate of this non-conventional ash is calculated using conventional ash composition as given in Table 3.2.

Table 3.1. Characteristics of coal [5].

| Proximate analysis (wt.%) | | | Ultimate analysis (wt.%) | | | | | HHV (MJ/kg) | Exergy (MJ/kg) |
|---|---|---|---|---|---|---|---|---|---|
| VM | FC | Ash | C | H | N | S | O | | |
| 23.86 | 27.27 | 48.87 | 39.16 | 2.76 | 0.78 | 0.51 | 7.92 | 15.83 | 17.30 |

Table 3.2. Composition of ash [161].

| Component | $SiO_2$ | $Al_2O_3$ | $Fe_2O_3$ | CaO | $K_2O$ | $TiO_2$ | $Na_2O$ | MgO |
|---|---|---|---|---|---|---|---|---|
| Weight percentage (%) | 56.77 | 31.83 | 2.82 | 0.78 | 1.96 | 2.77 | 0.67 | 2.39 |

Table 3.3 specifies the key assumptions and parameters involved in this study and Table 3.4 gives the property methods, unit operation models, stream class, simulation strategy, etc. used in the present study while simulating different cases.

In this work, the stream class MIXED defines the conventional fluids and the stream class CIPSD and NCPSD defines the conventional and non-conventional solids, respectively. The HCOALGEN and DCOALIGT are used as enthalpy models to define non-conventional components (coal and ash). Peng Robinson and Boston Mathias (PR-BM), Soave Redlich Kwong (RKS), Electrolyte NRTL, Ideal gas, and STEAMNBS were used for the estimation of properties of solid, electrolytes components in the $CO_2$ capture process, air, flue gases, steam and water. ELECNRTL is used for formic acid, methanol and DME production plants [162]. Furthermore, the streams split ratio is assumed to be the same as the ratio used by Suresh et al. [5].

Table 3.3. Key assumptions and operating parameters used to develop the process flowsheet models [5,49,79,145,147,148,163,164].

| Unit | Operating conditions/assumptions |
|---|---|
| Air Compressor | Pressure: 1.04 bar (Case 1); 10.5 bar (Case 2); 15.75 bar (Case 3 and 4) |
| | Isentropic efficiency: 90% |
| Combustor (Case 1) | Excess air: 20% |
| | Temperature: 1782.7$^o$C |
| | Pressure: 1.01 bar |
| Fuel Reactor | Temperature: 840$^o$C (Case 2); 900$^o$C (Case 3 and 4) |
| | Pressure: 10 bar (Case 2); 15 bar (Case 3 and 4) |
| | Oxygen carrier: 10% CuO & 90% $Fe_2O_3$ (mass basis) |
| | $Fe_2O_3$.CuO to $Al_2O_3$: 70:30 (mass basis) |
| | No pressure drop |
| | Calculation Option: chemical and phase equilibrium |
| Steam Reactor | Temperature: 750$^o$C (Case 3 and 4) |
| | Pressure: 15 bar (Case 3 and 4) |
| | No pressure drop |
| | Calculation Option: chemical and phase equilibrium |
| Air Reactor | Temperature: 900$^o$C (Case 2); 1000$^o$C (Case 3 and 4) |
| | Pressure: 10 bar (Case 2); 15 bar (Case 3 and 4) |
| | No pressure drop |
| | Calculation Option: chemical and phase equilibrium |
| Gas Turbine | GT/expander number: 1 |
| | Inlet temperature of turbine: 900$^o$C (Case 2); 1000$^o$C (Case 3 and 4) |
| | Discharge pressure: 1.013 bar |
| | Outlet temperature of turbine: 415-420$^o$C |

| | |
|---|---|
| | Isentropic efficiency: 90% |
| HRSG & steam turbines | *(i) SubC:* Three level pressures (HP/IP/LP): 166.7 bar/39.7 bar/7.3 bar and steam temperature: 537$^{o}$C/537$^{o}$C/303.3$^{o}$C<br>Isentropic efficiencies (HPT/IPT/LPT): 89.0%/90.3%/85.1%<br>*(ii) SupC:* Three level pressures (HP/IP/LP): 242.2 bar/42 bar/2.9 bar and steam temperature: 537$^{o}$C/565$^{o}$C/215.6$^{o}$C<br>Isentropic efficiencies (HPT/IPT/LPT): 89.6%/91.7%/85.7%<br>*(iii)* Ultra-SupC*:* Three level pressures (HP/IP/LP): 350 bar/60 bar/5 bar and steam temperature: 700$^{o}$C/720$^{o}$C/338.2$^{o}$C<br>Isentropic efficiencies (HPT/IPT/LPT): 88.0%/91.5%/88.8% |
| Condenser | Condenser pressure: 0.103 bar<br>Temperature gain: 10$^{o}$C<br>No pressure drop |
| $CO_2$ Compressor | Delivery pressure (Case 1, 2 and 3): 110 bar<br>Delivery pressure (Case 4): 105 bar (formic acid plant); 78 bar (methanol plant); 78 bar (dimethyl ether plant)<br>Isentropic efficiency: 85% |
| $H_2$ compressor | Delivery pressure (Case 3): 60 bar<br>Delivery pressure (Case 4): 105 bar (formic acid plant); 78 bar (methanol plant); 78 bar (dimethyl ether plant)<br>Isentropic efficiency: 85% |
| Synthesis reactors (Case 4) | Temperature: 93$^{o}$C (formic acid reactor); 288$^{o}$C (methanol reactor); 296.8$^{o}$C (dimethyl ether reactor); 385$^{o}$C (methane reactor)<br>Pressure: 100 bar (formic acid reactor); 78 bar (methanol reactor); 15 bar (dimethyl ether reactor); 30 bar (methane reactor) |

Table 3.4. The aspenONE model setup.

| | |
|---|---|
| Stream class | MCINCPSD |
| Non-conventional solid components | Coal, ash |
| Conventional solid components | $Fe_2O_3$, $Fe_3O_4$, carbon |
| Solution strategy | Sequential modular approach |
| Property methods | PR-BM, STEAM-TA |

| | |
|---|---|
| Unit operations models | |
| Combustor | RGibbs |
| Air, fuel and steam reactors | RGibbs |
| Synthesis reactors | RGibbs |
| Mixers/splitters | Mixer/Fsplit |
| Separators | Sep/Flash2 |
| Pressure changers | Pumps/Compr/MCompr/Turbine |
| Heat exchangers | Heater/HeatX/MHeatX |
| Plant assumptions [5] | |
| Reference environment | T = 33°C and P = 1.013 bar. |
| Chemical composition of reference environment | 75.62% $N_2$, 20.3% $O_2$, 3.12% $H_2O$, 0.03% $SO_2$, 0.92% others |
| Temperature gain across the condenser | ≈ 10°C |
| Terminal temperature difference across FWHs | ≈ 3°C |
| Bottom to fly ash ratio | 20:80 |
| Auxiliary power consumption | SubC and SupC: 7.5% and Ultra-SupC: 9% of total steam turbine output |
| Efficiency of pumps | 85% |

## 3.2 Model description and approach

Individual units in each case is modelled and validated with the published data in the literature. All the flowsheets have been modelled with the assumptions given in the Table 3.1 to 3.4. The model description for Category 1 to Category 4 is given below.

### 3.2.1 Description of conventional coal fired power plant

In this work, the conventional CFPPs for three different steam parameters (subcritical, supercritical and ultra-supercritical) are considered as reference cases. Operational data from these plants [5] is used for validating the model developed in the present study. The block diagram of conventional CFPP with and without $CO_2$ capture is shown in Figure 3.1. A conventional CFPP without $CO_2$ capture (Figure 3.1(a)) consist of sizing & drying, combustor, heat recovery steam generation (HRSG), feed water heaters (FWHs), condenser and steam turbine units. A coal is fed to the combustor after crushing and drying in presence of air. Heat is recovered from the hot flue gas generated from combustor and steam is generated in the HRSG unit. A steam from HRSG unit is sent to the steam turbine unit (to generate the power) followed by condenser and FWH unit. The water from condenser is preheated in the FWH to achieve desired temperature and recycled back to the HRSG unit. A conventional CFPP with MEA based post combustion capture (Figure 3.1(b)) involves all the units in the Figure 3.1(a). In addition, the MEA based post combustion capture (PCC) and $CO_2$ compressor units are incorporated in the flowsheet. A flue gas from the HRSG unit after heat extraction is sent to the MEA based PCC unit to separate $CO_2$ from the other flue gases (mainly $N_2$). The separated $CO_2$ is passed through the compressor unit and stored. A brief overview of the subcritical, supercritical and ultra-supercritical steam based coal fired power plants is given in the *Chapter 4*.

### 3.2.2 Description of CLC based CFPP with power generation alone

A general block diagram of CLC based CFPP is represented in Figure 3.2. The main components involved in this plant are – sizing and drying unit, CLC reactor unit, heat recovery steam generation (HRSG) unit, steam and gas turbine unit, FWH and condenser unit and the $CO_2$ compressor and storage unit. The steam parameters (temperature and pressure) and the number of high-pressure and low-pressure FWHs for these plants are the same as that of the conventional CFPPs. The combustor of conventional CFPP is replaced by the air and fuel reactors in CLC based plants. In addition, the $CO_2$ separator and compressor unit are coupled with the CLC plant flowsheet.

The pulverized coal from sizing and drying unit along with the oxygen carrier is initially fed to the adiabatic fuel reactor for combustion of coal. The $N_2$-rich stream from CLC unit is first sent to the gas turbine and then sent to the HRSG unit to recover heat. The $CO_2$-rich stream from CLC unit is directly sent to the HRSG unit to recover heat. The flue gas leaving the HSRG is sent to a condenser unit to condense the steam and the separated pure $CO_2$ is compressed and stored.

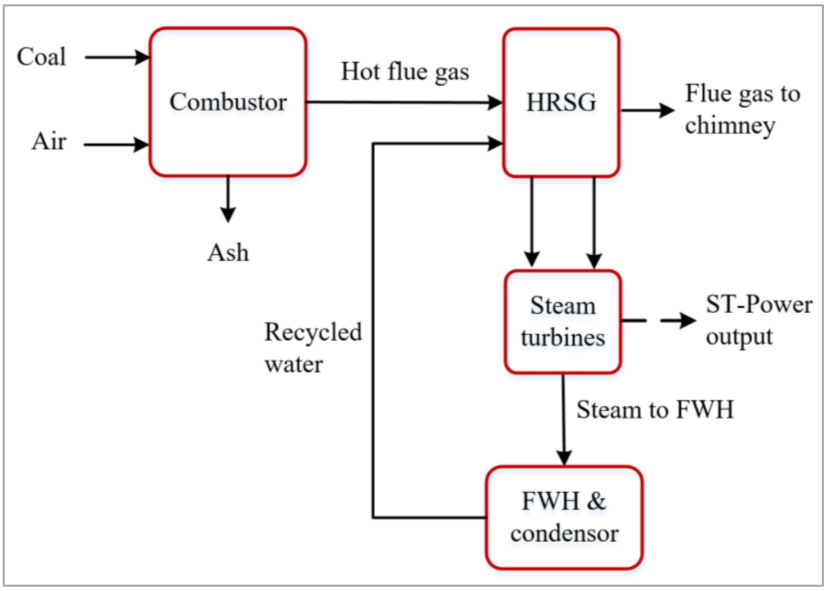

(a) Without CO2 capture.

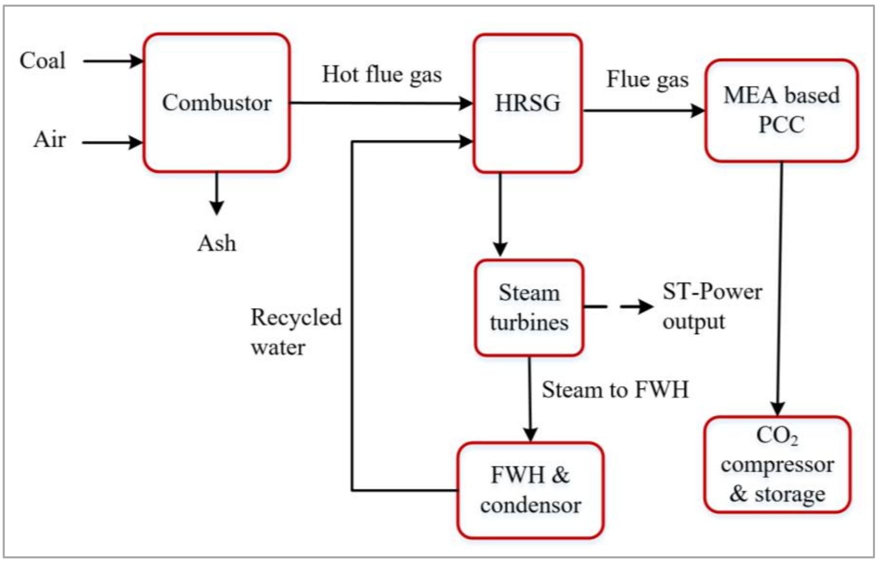

(b) With CO2 capture.

Figure 3.1 Block diagram of conventional CFPP.

A generalised description of the overall reaction in air and fuel reactors are expressed as given in Eq. (3.1) and (3.2).

$$(2n+m)M_yO_x + C_nH_{2m} \rightarrow (2n+m)M_yO_{x-1} + mH_2O + nCO_2 \qquad (3.1)$$

$$M_yO_{x-1} + {}^{1}\!/_{2}\, O_2 \rightarrow M_yO_x + N_2 + O_{2(unreacted)} \qquad (3.2)$$

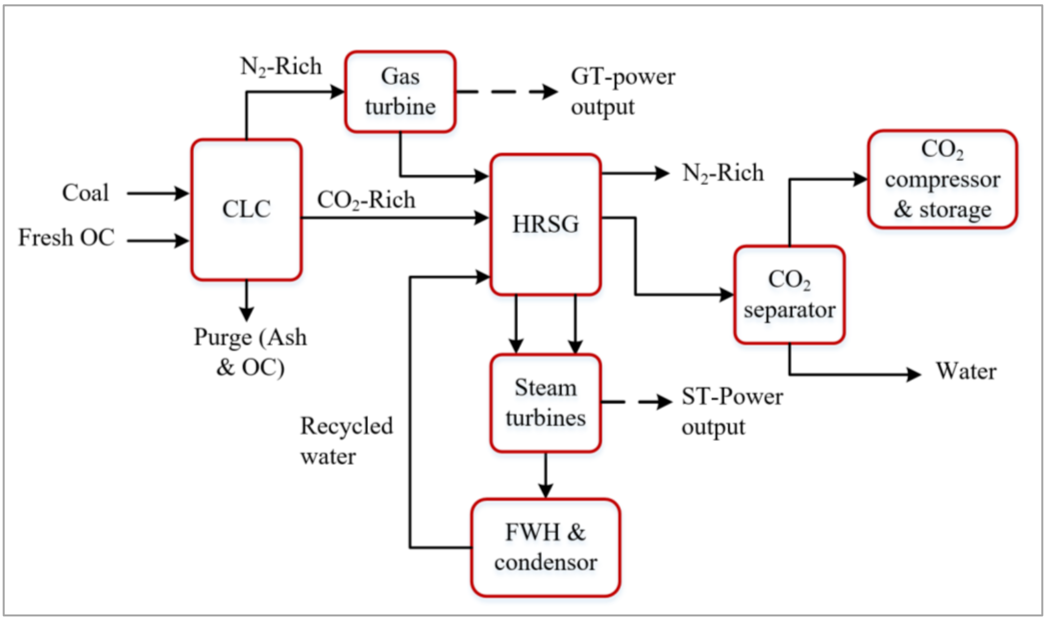

Figure 3.2 Block diagram of CLC based CFPP with power generation alone.

### 3.2.3 Description of CLC based CFPP with power and $H_2$ co-generation

A block diagram of CLC based CFPP plant for power and hydrogen co-generation is shown in Figure 3.3. This plant is composed of CLC reactors (air, steam and fuel reactors), air compressor, gas turbine unit, HRSG, $CO_2$ separator and compressor units, $H_2$ separator and compressor units, steam turbine, FWHs, de-aerator unit and condenser. Compared to the CLC based plant with power generation alone case, this plant involves additional $H_2$-rich stream from the CLC reactor block. This $H_2$-rich stream is also sent to the HRSG unit along with $CO_2$-rich stream for heat extraction and steam generation. The hydrogen is separated from steam in a $H_2$ separator unit and transported to the $H_2$ compressor unit. Other all the units follows the same path as given for CLC based power plant with power generation alone case. The chemical reactions involved in the air, fuel and steam reactors are given in Reaction (6.1) to (6.13).

### 3.2.4 Description of CLC based CFPP with power and $H_2$ co-generation coupled with $CO_2$ utilization plant

A simplified block diagram of CLC based CFPP with hydrogen and power co-generation coupled with carbon dioxide utilization plant is presented in Figure 3.4. This plant follows the same path as given for the CLC based power plant with power and hydrogen co-generation. In addition to this plant, this case includes the $CO_2$ utilization block. This $CO_2$ utilization plant is simulated for various synthesis products obtained from $CO_2$ such as – formic acid, methane, methanol and dimethyl ether. $CO_2$ and $H_2$ from the CLC based CFPP are compressed to desired pressure and sent to the $CO_2$ utilization plant. In $CO_2$ utilization plant, $CO_2$ and $H_2$ are reacted together to produce the synthesis products.

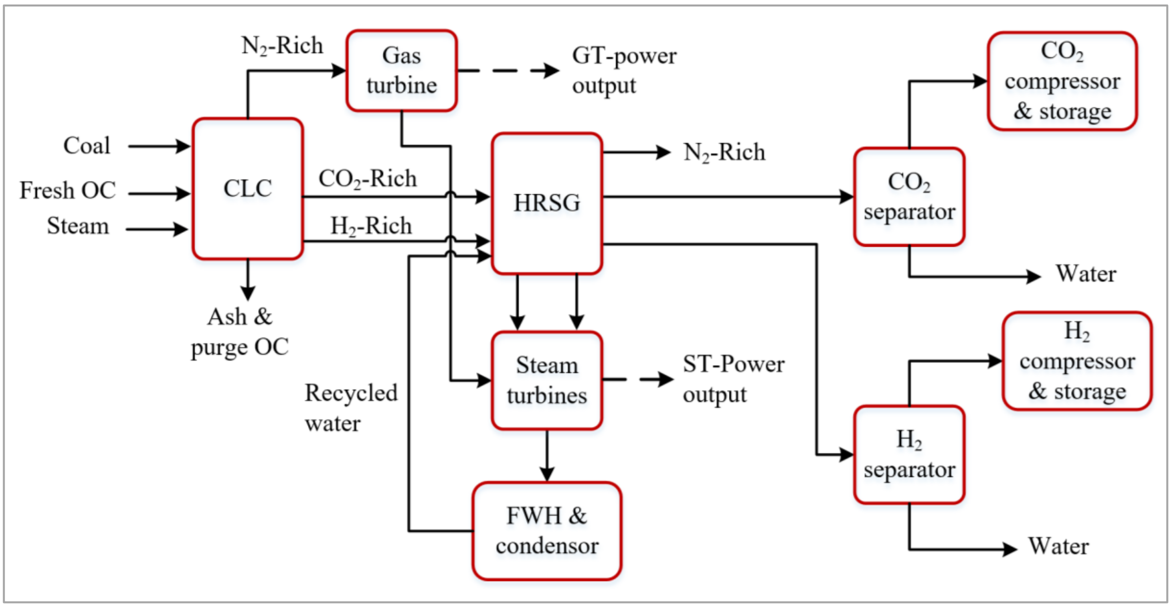

Figure 3.3 Simplified block diagrams of CLC based CFPP with power and hydrogen co-generation.

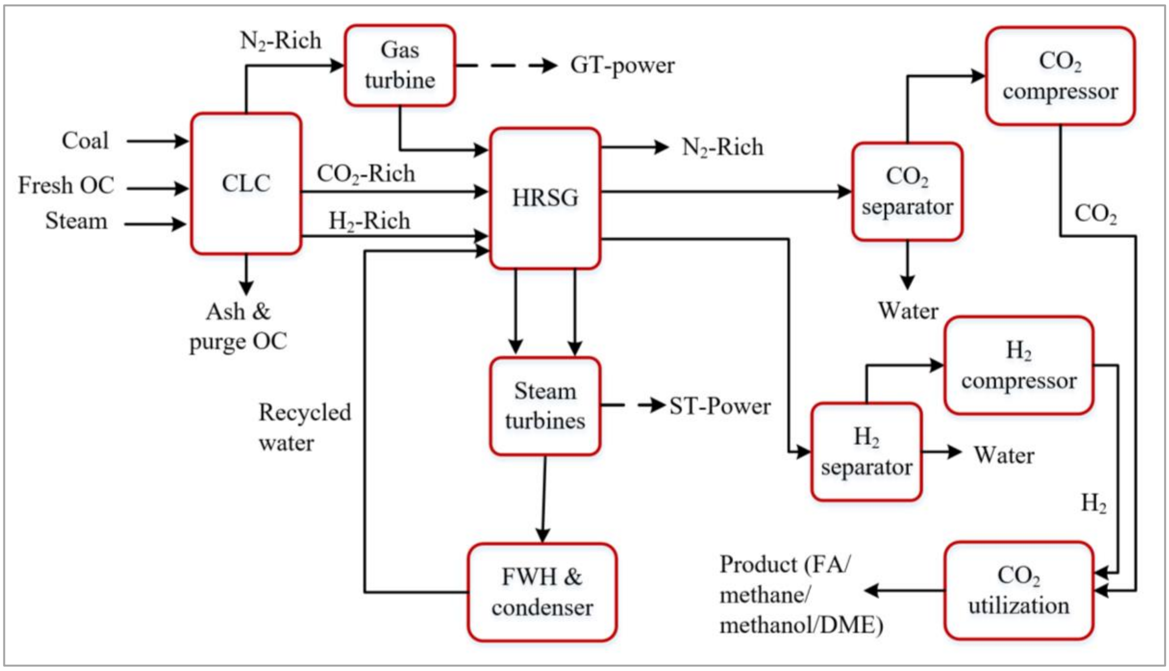

Figure 3.4 Block diagram of CLC based CFPP plant integrated with CDU plant.

## 3.3 Plant performance indicators

In addition to the thermodynamic analysis, by way of estimating energy and exergy efficiencies, evaluation of environmental impact and economic analysis is essential for a comprehensive techno-economic assessment of a power generation system [25]. The economics is the final and most important metric for comparison of various schemes, with the other three serving the purpose of providing better insights into the weak links of the process flow sheet. Hence, in the present study, the performance of all the cases is analyzed based on the 4-E (energy, exergy, environment, and economic) analyses. In addition, the life cycle analysis (LCA) is also carried out for the integrated plants of CLC based power plants coupled with $CO_2$ utilization plants to identify and evaluate the environmental impacts of individual and overall process. It also finds the ways to minimize those environmental impacts. The material and energy balances are used in the LCA analysis to quantify the GHG emissions and primary resource consumption in the processes. These results can be used to evaluate the environmental impacts of the individual process that can be focused to mitigate the possible effects.

The performance indicators for each of these analyses are presented below.

### 3.3.1 Energy analysis

In this study, the overall performance of each plant configuration is evaluated in terms of the overall energy efficiency. The gross energy efficiency ($\eta_{\mathrm{Gross}}$) and net energy efficiency ($\eta_{Net}$) are defined as the ratio of gross or net power output ($W_{Gross}$ *or* $W_{Net}$) to the energy input to the plant (*MW*):

$$\eta_{Gross} = \frac{W_{Gross}}{\dot{m}_{coal} \times HHV\ or\ LHV\ of\ \text{the}\ coal} \qquad (3.3)$$

$$\eta_{Net} = \frac{W_{Net}}{\dot{m}_{coal} \times HHV\ or\ LHV\ of\ \text{the}\ coal} \qquad (3.4)$$

The energy input to the plant is the product of coal mass flow rate ($\dot{m}_{coal}$) and HHV or LHV of the coal.

### 3.3.2 Exergy analysis

Exergy analysis also plays a key role in evaluating the real performance of power plants by identifying the energy and exergy loss. It provides the location of the highest energy losses in the system by estimating the exergy destruction in individual sections [24].

Initially, the exergy flow rate of each stream in the system including coal, ash, water, steam, and flue gases are calculated. In this study, the *EXERGYFL* property set is added in *aspenONE* to measure the exergy flow rate of individual streams [165]. The exergy of non-conventional coal [10] is calculated by using Eq. (3.5) and (3.6) and the non-conventional ash is considered as a conventional solid component with the composition of ash for Indian coal [161].

$$Ex_{ch,coal} = (CV + w \times \lambda) \times \varphi_{dry} + 9417 \times S \tag{3.5}$$

$$\varphi_{dry} = 0.1882\frac{H}{C} + 0.061\frac{O}{C} + 0.0404\frac{N}{C} + 1.0437 \tag{3.6}$$

where, $CV$ is the calorific value of the coal, $\lambda$ is the latent heat of vaporization of water, $w$ and $S$ are the moisture and sulphur content of the coal. The term, $\varphi_{dry}$ is calculated based on the ultimate analysis of the coal, where the hydrogen ($H$), carbon ($C$), nitrogen ($N$) and oxygen ($O$) are provided in mass fractions.

Finally, the exergy destruction ($Ex_d$) and exergy efficiency of the individual unit ($\varepsilon_{unit}$) are calculated from the exergy flow in ($Ex_{in}$) and exergy flow out ($Ex_{in}$) of the unit using Eq. (3.7) and (3.6), respectively [10].

$$Ex_d = \sum Ex_{in} - \sum Ex_{out} \tag{3.7}$$

$$\varepsilon_{unit} = \frac{\sum Ex_{out}}{\sum Ex_{in}} = 1 - \left(\frac{Ex_d}{\sum Ex_{in}}\right) \tag{3.8}$$

The maximum improvement possible in a unit is $Ex_d$. The concept of exergetic improvement potential is useful in analyzing different processes economically. The improvement potential ($\dot{IP}$) of a plant or individual unit in the plant is defined as [10].

$$\dot{IP} = (1 - \frac{\sum Ex_{out}}{\sum Ex_{in}}) \times Ex_d \tag{3.9}$$

The overall gross exergy efficiency ($\varepsilon_{Gross}$) and net exergy efficiency ($\varepsilon_{Net}$) are defined as [5]:

$$\varepsilon_{Gross} = \frac{W_{Gross}}{\dot{m}_{coal} \times Specific\ exergy\ of\ \text{the}\ coal} \tag{3.10}$$

$$\varepsilon_{Net} = \frac{W_{Net}}{\dot{m}_{coal} \times Specific\ exergy\ of\ \text{the}\ coal} \tag{3.11}$$

### 3.3.3 Ecological analysis

In this section, the environmental analysis is carried out to assess the effect of the $CO_2$ capture unit on CLC based CFPPs and/or CDU plants. However, it may be noted that the $CO_2$ footprint is the only ecology part that is considered in this work. An ecological analysis is carried out in this study to assess the environmental impact. The specific $CO_2$ emission rate ($E_{CO_2}$) [166] is expressed as shown in Eq. (3.12):

$$\mathrm{E}_{\mathrm{CO}_2} = \frac{\left(\dot{\mathrm{m}}_{\mathrm{CO}_2\ \mathrm{emit}}\right)}{\left(\mathrm{W}_{\mathrm{net}}\right)} \tag{3.12}$$

where, $\dot{m}_{CO_2\ emit}$ is the net $CO_2$ emitted into the atmosphere in (*kg/s*) and the net power output ($W_{net}$) from the plant in (MW). An annual $CO_2$ emission for 7000 operation hours per unit of fuel ($\varepsilon^{a}_{f\ CO_2}$) [166] is defined by Eq. (3.13).

$$\varepsilon^{a}_{f\ CO_2} = \frac{\left(\dot{m}^{a}_{CO_2\ emit}\right)}{\left(3.6 \times E^{a}_{chf}\right)} \tag{3.13}$$

Here, $E^{a}_{chf}$ is the annual energy input to the power plant in ($MW.h$) and $\dot{m}^{a}_{CO_2\ emit}$ is the annual $CO_2$ emission into the atmosphere from the power plant in (kg). The carbon capture efficiency of CFPP [5] is defined as Eq. (3.14):

$$CO_2\text{capture efficiency} = \frac{\left(\dot{\mathrm{m}}_{\mathrm{CO}_2\ \mathrm{captured}}\right)}{\left(\dot{\mathrm{m}}_{\mathrm{CO}_2\ \mathrm{prior\ to\ capture}}\right)} \times 100 \tag{3.14}$$

The term $\dot{m}_{CO_2\ captured}$ is the carbon dioxide captured in (*kg/s*).

### 3.3.4 Economic analysis

The capital cost and operation & maintenance (O&M) cost of all the plants considered in this study are estimated and compared. The economic assessment has been performed according to the NETL guidelines of techno-economic analysis for thermal power plants [26], which involves estimations of total capital cost (including equipment and installation costs), estimation of fixed O&M costs, and variable O&M costs [27]. However, the magnitudes of costs are not exact due to the following reasons:-

a) The costs associated with the minor equipment of the CFPP are not considered [28].
b) Uncertainties in the values of equipment cost data.
c) Uncertainties in the values of oxygen carriers/fuel/raw material prices which are market dependent.
d) Uncertainties in the value of the capacity factor.
e) Carbon tax is assumed to be zero [167].

Yet, the obtained results in the present study can be used to study the economic feasibility of CLC based technologies against conventional technologies.

The capital-cost estimation of equipment is made by using the capacity ratio exponent method based on the existing values. Eq. (3.15) gives the cost estimation correlation for the equipment/plant [71]. If $C_1$ is the cost of equipment for the capacity (plant size/mass or energy flow rate) of $q_1$, the cost of similar equipment, $C_2$ for the capacity $q_2$ can be calculated as:

$$C_2 = C_1(q_2/q_1)^n \tag{3.15}$$

where, $n$ is the scaling factor, which depends on the plant or equipment type.

In addition, the present cost of the equipment is calculated using the original cost by knowing the Chemical Engineering Plant Cost Index (CEPCI) for present and past years (see Eq. (3.16)). The values of CEPCI and scaling factors are taken from the literature [26].

$$Present\ cost = original\ cost \times \left(\frac{CEPCI\ at\ present}{CEPCI\ at\ the\ time\ of\ original\ cost}\right) \tag{3.16}$$

The exchange rate between the countries is calculated using the purchasing power parity index (PPPI), which is the ratio of currencies of corresponding purchasing power. The Eq. (3.17) gives the calculation of cost conversion between two countries. The details of PPPI and Power Capital Costs Index (PCCI) for the different countries are available in the literature [168].

$$C_{country} = C_{known\ country} \times \left(\frac{PCCI\ for\ current\ year}{PCCI\ for\ original\ year}\right) \times PPPI_{country} \tag{3.17}$$

In the present study, the fixed and variable O&M costs are considered as a fraction of the total capital cost of the plant. The operating costs associated with the OC and fuel consumption, and $CO_2$ transportation and storage are estimated based on the power plant simulation data (Table 3.5). The attrition rate of 0.09%/h and 0.04%/h is considered in this thesis for iron oxide and copper oxide supported on aluminium oxide, respecitvely. The life span of iron oxide and copper oxide supported on aluminium oxide are assumed to be 1100 h and 2500 h, respectively [169].

Table 3.5. Assumptions for economic analysis.

| Parameter | Unit | Value | Reference |
|---|---|---|---|
| Variable cost as a fraction of total capital cost | % | 2.00 | [167] |
| Fixed cost as a fraction of total capital cost | % | 1.00 | [167] |
| Carbon tax | €/t$CO_2$ | 0.00 | [167] |
| Raw iron oxide cost | €/t | 52.70 | [117] |
| Raw aluminium oxide cost | €/t | 1526.60 | [170] |
| Copper oxide cost | €/t | 3598.66 | [170] |
| $CO_2$ transport and storage cost | €/t$CO_2$ | 7.00 | [167] |
| Coal price | €/t | 9.35 | [171] |
| Expected lifetime of plant | years | 30 | [71] |
| Interest rate | % | 10 | [134] |
| Capacity factor | % | 80 | [167] |
| Attrition rate of $Fe_2O_3$ supported on $Al_2O_3$ | %/h | 0.09 | [169] |
| Attrition rate of CuO supported on $Al_2O_3$ | %/h | 0.04 | [169] |
| Lifetime of $Fe_2O_3$ supported on $Al_2O_3$ | h | 1100 | [169] |
| Lifetime of CuO supported on $Al_2O_3$ | h | 2500 | [169] |
| Social cost of carbon | €/t$CO_2$ | 60.46 | [172] |

To compare the environmental impact of different technologies on an equal footing, a cost should be assigned to the environmental benefit/degradation and hence levelised cost of electricity (LCOE) and levelised cost of product (LCOP) are defined and calculated.

The economic performance of the CLC based plants are compared with the corresponding conventional CFPPs without $CO_2$ capture unit in terms of the LCOE and the $CO_2$ avoided cost that are calculated from Eq. (3.18) and Eq. (3.19) [167], respectively.

$$LCOE = \frac{TCR \times FCF + FOM}{W_{net} \times CF \times 8760} + VOM + \frac{SFC}{\eta_{th}} \tag{3.18}$$

$$CO_2\ avoided\ cost = \frac{LCOE_{capture} - LCOE_{non-capture}}{E_{CO2,non-capture} - E_{CO2,capture}} \tag{3.19}$$

The parameters in the Eq. (3.18) correlates the thermodynamic performance of the plant such as - capacity factor (CF), net power output ($W_{net}$), net energy efficiency ($\eta_{th}$), and the specific $CO_2$ emissions, with the economic performance parameters such as – specific fuel cost (SFC), the total capital requirement (TCR), fixed O&M (FOM), variable O&M (VOM), and fixed charge factor (FCF). These parameters consider the project interest rate and plants lifetime. $E_{CO2}$ in Eq. (3.19) refers to specific $CO_2$ emission rate in tons of $CO_2$ per $MW.h$, which can be calculated using Eq. (3.20).

Climate change because of the increased $CO_2$ emissions causes devastating impacts such as rise in the sea level, extreme weather conditions like flooding and deadly storms, changes in agricultural yields and other disasters. These effects can cost families, businesses and governments through increased food prices, rising health care costs, property destruction, etc. The social cost of carbon (SCC) is a measure of the economic detriment from those impacts, expressed as the cost of the total damages resulting from one ton of $CO_2$ into the atmosphere [173]. Different estimates for SCC are reported in the literature and there is a variation in the methods of prediction of SCC [174]. Ricke et al. [40] estimated country-level contributions to the SCC using climate model projections, empirical climate-driven economic damage estimations and socio-economic projections. In the present work, economic analysis is carried out based on the social cost of carbon reported by Ricke et al. [172], which is \$86 per ton of $CO_2$ emitted for India. Taking this as a typical case study, the damage cost due to $CO_2$ emissions from the CFPP ($Ec_{CO_2}$) [173] is estimated as the product of specific $CO_2$ emission rate ($E_{CO_2}$) and SCC as given Eq. (3.20).

$$Ec_{CO_2} = \mathrm{E}_{\mathrm{CO}_2} \times SCC \tag{3.20}$$

$LCOE_{overall}$ is defined in this work as given below to incorporate the social cost of carbon.

$$LCOE_{overall} = LCOE + Ec_{CO_2} \tag{3.21}$$

Category 3 includes the production of hydrogen and Category 4 includes the production of synthesis products (formic acid, methane, methanol and dimethyl ether). The economic assessment of these plant cases are compared by determining the total cost to evaluate the production cost in €/kg. The levelised cost of product (LCOP) specifies a break-even cost for a unit product generation, often used to compare different product generation technologies from the economic perspective. The LCOP is calculated as given in Eq. (3.22) [175].

$$LCOP = \frac{ACC + O\&M\ cost}{Annual\ hydrogen\ production} \tag{3.22}$$

The annual capital cost (ACC) is a product of TCR and capital recovery factor (CRF) as given below:

$$ACC = TCR \times CRF \tag{3.23}$$

The CRF is calculated as the ratio of constant annuity to the present value with interest rate ($i$) at a period of time ($t$) as given below:

$$CRF = \frac{i(1+i)^t}{(1+i)^t - 1} \tag{3.24}$$

A payback period for all the integrated plant cases is also carried out to investigate the recovery time of initial investment. This is done by calculating total plant capital expenditure (CAPEX), annual plant operating expenditure (OPEX) and total plant revenues. In this study, the sources of annual plant revenues include cost of electricity and cost of product (hydrogen, formic acid, methane, methanol and DME). The payback period and annual plant profit is estimated as given below [176]:

$$Payback\ period = \frac{Total\ plant\ CAPEX}{\text{Annual plant profit}} \tag{3.25}$$

$$Annual\ plant\ profit = \text{Annual plant revenue} - \text{Annual plant OPEX} \tag{3.26}$$

### 3.3.5 Life cycle analysis

In addition to the above 4-E analyses, the LCA is also carried out for the CLC based plants coupled with $CO_2$ utilization. This is conducted to assess the GHG emissions and PFEC of the total system which contains CLC based CFPP with hydrogen and power generation by defining the stages and boundaries of the system and different functional units of the system. The cradle-to-grave analysis presented by Li et al. [29] has been carried out in this study. Figure 3.5 shows the boundary of LCA for the system, which involves seven stages – (i) coal mining & washing, (ii) coal transportation, (iii) CLC-CFPP plant, (iv) $CO_2$ compression, (v) $CO_2$ transportation, (vi) $H_2$ compression, (vii) $H_2$ transportation and (viii) $CO_2$ utilization plant. The primary energy input to the system includes coal, natural gas, electricity, gasoline, steam etc. and the GHG emissions from the system include $N_2O$, $CO_2$ and $CH_4$. These individual GHG emissions from each stage are estimated as the sum of possible GHG emissions (direct emissions (D) and indirect emissions (I)) from the suitable energy sources used in that stage. Indirect emissions indicate the emissions from the upstream stages and the direct emissions refer to the exhaust gas stream from the combustion process and the process energy use.

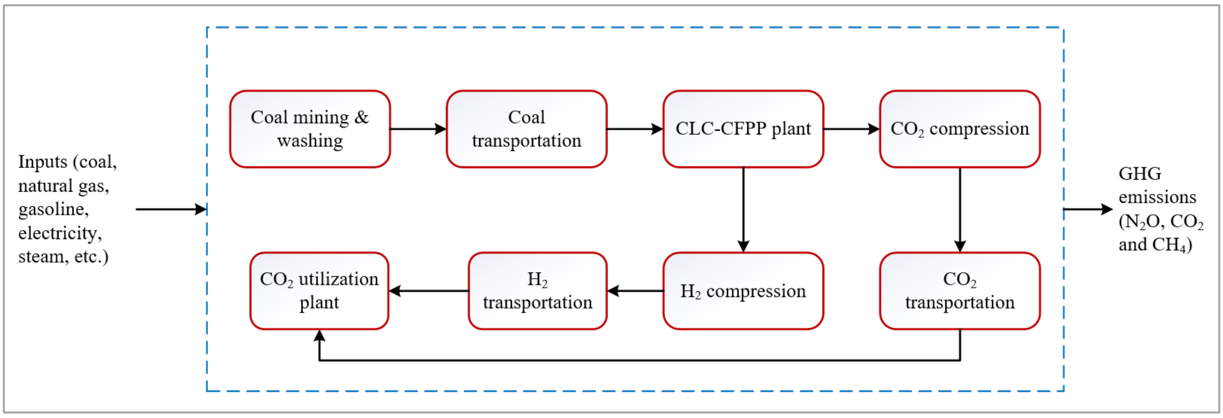

Figure 3.5 The boundary of LCA.

The total GHG emissions from the entire system are calculated as the sum of all the GHG emissions from each stage, estimated as the weighted sum of $N_2O$, $CO_2$ and $CH_4$ emissions. The PFEC and GHG emissions from the vehicles, infrastructure constructions and equipment manufacturing are not estimated in the present work.

The $CO_2$, $N_2O$ and $CH_4$ emissions are expressed as [29]:

$$CO_2 = CO_{2,direct} + CO_{2,indirect} = \sum_{m=1}^{7} \sum_{n=1}^{7/8} EC_{m,n}\left(D_{CO_2,n} + I_{CO_2,n}\right) \quad (3.27)$$

$$N_2O = N_2O_{direct} + N_2O_{indirect} = \sum_{m=1}^{7} \sum_{n=1}^{7/8} EC_{m,n}\left(D_{N_2O,n} + I_{N_2O,n}\right) \quad (3.28)$$

$$CH_4 = CH_{4,direct} + CH_{4,indirect} = \sum_{m=1}^{7} \sum_{n=1}^{7/8} EC_{m,n}\left(D_{CH_4,n} + I_{CH_4,n}\right) \quad (3.29)$$

$EC_{m,n}$ refers to the quantity of process energy (m) consumed in the stage (n). The total number of stages for the system without $CO_2$ utilization are 7 and with $CO_2$ utilization are 8. The necessary $EC_{m,n}$ values for coal mining & washing, coal transportation, $CO_2$ and $H_2$ transportation are taken from Li et al. [29]. The $EC_{m,n}$ used in coal mining & washing stage are 0.01 MJ/MJ of coal for electricity, 0.05 MJ/MJ of coal for raw coal and 0.001 MJ/MJ of coal for diesel, natural gas and gasoline. The process energy used in the CLC based CFPP stage is 1287 MW (based on HHV of coal) for Indian coal and 273.61 MW for the steam. The process energy used in $CO_2$ and $H_2$ compressor stages are calculated based on energy consumptions to compress them to 110 bar and 60 bar, respectively. for without CO2 utilization case, the $H_2$ and

$CO_2$ transportation distance of 300 km and 100 km by road is assumed with the energy intensity of 1.2 MJ/t.km and 1.36 MJ/t.km, respectively. The coal is transported by road and rail for a distance of 100 km and 500 km with 1.36 MJ/t.km energy intensity, respectively. A 68% diesel and 32% gasoline has been considered for these transportation modes.

The total GHG emission of the system is carbon dioxide equivalent emissions, as given below [29]:

$$GHG = CO_2 + 296 \cdot N_2O + 23 \cdot CH_4 \quad (3.30)$$

The PFEC of a system is sum of products of process energy consumed and primary fossil energy in each stage. The PFEC can be calculated as given below [29]:

$$PFEC = \sum_{m=1}^{7} \sum_{n=1}^{7/8} \sum_{p=1}^{3} \left( EC_n \times EF_{n,p} \right) \quad (3.31)$$

$EF_{n,p}$ refers to the primary fossil energy (suffix $p$ as coal, natural gas and oil) used to achieve unit process energy ($n$).

The values of $D_{CO_2}, D_{N_2O}, D_{CH_4}, I_{CO_2}, I_{N_2O}$ and $I_{CH_4}$ considered to calculate the GHG emissions, $EF_{n,p}$ to calculate PFEC of a system and the energy intensities for transportation modes (rail and road) are shown in Table 3.6 and 3.7.

Table 3.6. Direct and indirect emissions factors [29].

| Process Energy | $I_{N2O}$ (g/MJ) | $I_{CH4}$ (g/MJ) | $I_{CO2}$ (g/MJ) | $D_{N2O}$ (g/MJ) | $D_{CH4}$ (g/MJ) | $D_{CO2}$ (g/MJ) |
|---|---|---|---|---|---|---|
| Electricity | $6.20 \times 10^4$ | 2.16 | 248.02 | 0.00 | 0.00 | 0.00 |
| Diesel | $4.40 \times 10^4$ | $8 \times 10^2$ | 27.87 | $2.8 \times 10^5$ | $4.00 \times 10^3$ | 72.585 |
| Residual oil | $4.10 \times 10^4$ | $7 \times 10^2$ | 25.33 | 0.00 | $2.00 \times 10^3$ | 75.819 |
| Coal | $1.70 \times 10^4$ | 0.43 | 5.73 | $1.00 \times 10^6$ | $1.00 \times 10^3$ | 81.642 |
| Gasoline | $4.70 \times 10^4$ | $9 \times 10^2$ | 28.83 | $2.00 \times 10^6$ | $8.00 \times 10^2$ | 67.914 |
| Natural gas | $1.20 \times 10^4$ | $5 \times 10^2$ | 16.58 | $1.00 \times 10^6$ | $1.00 \times 10^3$ | 55.612 |
| Steam | $1.79 \times 10^3$ | 0.29 | 113.87 | 0.00 | 0.00 | 0.00 |

Table 3.7. Primary fossil energy used in the system to obtain unit process energy [29].

| Process Energy | Oil (MJ/MJ) | Natural gas (MJ/MJ) | Coal (MJ/MJ) |
|---|---|---|---|

| | | | |
|---|---|---|---|
| Natural gas | 0.05 | 1.04 | 0.11 |
| Gasoline | 1.12 | 0.03 | 0.18 |
| Coal | 0.11 | 0.00 | 1.06 |
| Diesel | 1.12 | 0.03 | 0.18 |
| Steam | 0.01 | 0.00 | 1.38 |
| Residual gas | 1.06 | 0.03 | 0.14 |
| Electricity | 0.37 | 0.03 | 2.86 |

## 3.4 Model validation

As there is no data available in the literature on the CLC based CFPPs on advanced steam boilers, the validation is carried out in three parts.

(i) Validation of the developed models for all three conventional plants (sub, super and ultra-super critical CFPPs).
(ii) Validation of the two-reactor CLC configuration used in objectives 1 and 2.
(iii) Validation of the three-reactor CLC configuration used in objectives 3 and 4.

Validation of the conventional plants is based on the data taken from operating plants [5]. Table 3.8 shows the comparison of model prediction of the key variables in conventional CFPPs with SubC, SupC, and Ultra-SupC steam boilers. The highest relative error (2.55%) is seen in the superheater and reheater steam flow rates. The gross steam turbine power output and overall efficiency of the plant is in good agreement with the literature data.

The models for two-reactor CLC system (i.e. air reactor and fuel reactors) are validated with data from Authier and Moullec [177]. A comparison of two-reactor CLC system with the model data is presented in Table 3.9. The deviation in the predicted flue gas flow rate from the air reactor is 3.57% and that from the fuel reactor is less than 1.2%.

Further, the three-reactor CLC system (air, fuel and steam reactors) is also validated with the study reported by He et al. [128]. Table 3.10 represents the validation of air, fuel and steam reactors of the CLC system. It can also be observed that the current simulation results of CLC reactors are in good agreement with the results given in He et al. [128].

After successful validation of the conventional CFPP, two-reactor CLC system and three-reactor CLC system, the present study involving the simulation of the overall CLC based CFPP with and without hydrogen generation have been carried out by replacing the conventional combustor in the CFPP with CLC reactors.

Table 3.8 Steady-state validation of SubC, SupC, and Ultra-SupC CFPP.

| Parameters | Unit | SubC CFPP | | SupC CFPP | | Ultra-SupC CFPP | |
|---|---|---|---|---|---|---|---|
| | | Suresh et al. [5] | Model | Suresh et al. [5] | Model | Suresh et al. [5] | Model |
| Coal mass flow | *kg/s* | 81.30 | 81.30 | 102.90 | 102.90 | 58.40 | 58.40 |
| Superheater steam flow | *kg/s* | 425.80 | 415.00 | 550.70 | 550.00 | 296.60 | 293.00 |
| Superheater steam out temp | $^{o}C$ | 537.00 | 537.00 | 537.00 | 537.00 | 700.00 | 700.00 |
| Superheater steam out pressure | *bar* | 166.70 | 166.70 | 242.20 | 242.20 | 350.00 | 350.00 |
| Feedwater temperature at economiser inlet | $^{o}C$ | 253.20 | 253.64 | 279.60 | 276.26 | 330.20 | 329.44 |
| Reheater steam inlet temp | $^{o}C$ | 339.40 | 339.77 | 288.70 | 282.14 | 429.70 | 422.51 |
| Reheater steam outlet temp | $^{o}C$ | 537.00 | 537.00 | 565.00 | 565.00 | 720.00 | 720.00 |
| Reheater steam flow | *kg/s* | 380.50 | 370.85 | 466.20 | 465.61 | 243.10 | 240.15 |
| Reheater outlet pressure | *bar* | 39.70 | 39.50 | 42.00 | 42.00 | 60.00 | 60.00 |
| Condenser outlet temperature | $^{o}C$ | 43.00 | 42.61 | 43.00 | 42.87 | 43.00 | 42.74 |
| Condenser mass flow rate of water | *kg/s* | 15614.70 | 15614.70 | 18992.80 | 18992.80 | 9852.80 | 9852.80 |
| Gross power output | *MW* | 500.00 | 499.21 | 660.00 | 657.79 | 430.00 | 428.11 |
| Auxiliary loss | *MW* | 37.50 | 37.44 | 49.50 | 49.33 | 38.70 | 38.53 |
| Overall plant efficiency | *%* | 35.90 | 35.88 | 37.50 | 37.35 | 42.30 | 42.14 |

Table 3.9 validation of two-reactor CLC system.

| Stream | Gas stream (ex. FR) | | Gas stream (ex. AR) | |
|---|---|---|---|---|
| | Authier and Moullec [177] | Simulation | Authier and Moullec [177] | Simulation |
| Pressure (bar) | 1.00 | 1.00 | 1.00 | 1.00 |
| Temperature ($^{o}$C) | 985.00 | 983.44 | 1000.00 | 1000.00 |
| Mass flow (kg/s) | 80.28 | 80.31 | 189.17 | 188.95 |
| $H_2O$ | 54.70 | 54.76 | 0.00 | 0.00 |
| $CO_2$ | 44.20 | 44.32 | 0.00 | 0.00 |

|  |  |  |  |  |
|---|---|---|---|---|
| $SO_2$ | 0.20 | 0.20 | 0.00 | 0.00 |
| $N_2$ | 0.50 | 0.51 | 94.40 | 94.60 |
| $O_2$ | 0.20 | 0.20 | 5.60 | 5.40 |

Table 3.10 Validation of three-reactor CLC system.

| Stream | Fuel reactor exit gas stream | | Steam reactor exit gas stream | | Air reactor exit gas stream | |
|---|---|---|---|---|---|---|
| | He et al. [128] | Simulation | He et al. [128] | Simulation | He et al. [128] | Simulation |
| Mass flow (kg/s) | 104.78 | 104.97 | 32.11 | 32.12 | 98.57 | 98.67 |
| Temperature (°C) | 900.00 | 900.00 | 750.00 | 750.00 | 1169.00 | 1155.00 |
| Pressure (bar) | 30.40 | 30.40 | 30.90 | 30.90 | 30.40 | 30.40 |
| $H_2O$ | 18.83 | 18.91 | 25.94 | 26.03 | 2.75 | 2.64 |
| $CO_2$ | 85.19 | 85.32 | 0.00 | 0.00 | 0.00 | 0.00 |
| $O_2$ | 0.00 | 0.00 | 0.00 | 0.00 | 1.31 | 1.35 |
| $N_2$ | 0.50 | 0.49 | 0.00 | 0.00 | 92.94 | 93.23 |
| $H_2$ | 0.00 | 0.00 | 6.17 | 6.09 | 0.00 | 0.00 |
| HCl | 0.11 | 0.11 | 0.00 | 0.00 | 0.00 | 0.00 |
| $SO_2$ | 0.00 | 0.00 | 0.00 | 0.00 | 1.56 | 1.44 |
| $SO_3$ | 0.00 | 0.00 | 0.00 | 0.00 | 0.01 | 0.00 |
| $H_2S$ | 0.14 | 0.14 | 0.00 | 0.00 | 0.00 | 0.00 |
| NO | 0.00 | 0.00 | 0.00 | 0.00 | 0.01 | 0.01 |

## 3.5 Summary

This chapter presented the common methodology that is used to develop the Aspen plus flowsheet models of all the processes/plants considered in *Chapters 4 to 7*. The details about the modelling of process flowsheets in Aspen plus and the properties and capabilities of inbuilt Aspen plus units, which were used in the flowsheets to represent a particular process such as gasification and compression are discussed. The chapter also covered the general methods used to evaluate and compare the performances of the developed flowsheet models. In particular, the definitions and equations for parameters such as net electrical efficiency, $CO_2$ capture rate and net energy and exergy efficiency, annual $CO_2$ emissions, levelised cost of electricity and synthesis products, which are the key aspects for comparison of different processes are provided. Finally, the validation process used for validating the simulation models with data reported in the literature are presented. The validation results showed that, the models developed in aspenONE v10.0 simulation software are in good agreement with the results reported in the literature. With the confidence gained from the validated models, further work is carried out with the developed flowsheets to address the four objectives in the coming Chapters 4 to 7.

# Chapter 4

# CLC based coal fired power plants with different steam generation approaches

# Chapter 4

# *CLC based coal fired power plants with different steam generation approaches*

---

The first objective of the present study is addressed in this chapter by conducting the performance evaluation and comparison of conventional and CLC based coal fired power plants with three different steam generation approaches (i.e. subcritical, supercritical and ultra-supercritical). The overall performance of these configurations are examined based on the energy, exergy, ecological and economic analyses. Various sensitivity analyses such as effects of operating temperature, pressure and OC-to-coal ratio on the overall performance of CLC based CFPPs are also presented in this chapter.

---

## 4.1 Motivation and objective

As explained in *Chapter 2*, limited literature is available on the thermodynamic and economic analyses of CFPPs based on high-ash coal and advanced steam boilers. Although few studies on energy and exergy analyses are available on the CLC based subcritical CFPPs as discussed above, a comprehensive study involving energy, exergy, ecological and economic assessments is not available for direct comparison of the CLC based CFPPs with different steam boiler parameters using coal. Such an analysis plays an important role in selecting the most suitable technology to increase the power capacity for the next generation, especially in the developing countries where coal is the major energy source. Keeping this in view, the objective of this study is set as to identify the effect of CLC integration on the performance of the CFPP for three different steam parameters (i.e., SubC, SupC, and Ultra-SupC) for high-ash content coals. In this study, high-ash coal (typically available in India) is considered as the fuel and the power plants are simulated for Indian climatic conditions. Further, a comparative assessment of these plants has been carried out based on 4-E (energy, exergy, ecological and economic) analyses. The study is further extended to the individual unit-wise exergy analysis in terms of exergy destruction and exergy efficiency to locate the maximum exergy losses. The oxygen carrier used for the current study is $Fe_2O_3$ supported on $Al_2O_3$. Effects of various parameters such as operating temperature, pressure and OC-to-coal ratio on the overall performance of all three CLC based CFPPs are analysed and optimized to reduce the exergy losses in the plant. The key outcome of the present study is to facilitate the configuration or layout of an energetically, exergetically, ecologically and economically efficient Chemical looping combustion based coal-fired power plant.

## 4.2 Model description and approach

In this chapter, steady-state models of CLC based CFPPs with SubC, SupC and Ultra-SupC steam boilers are developed using *aspenONE* v10.0 based on mass, momentum and energy balances. The present chapter focuses on evaluating the effect of CLC integration for three different steam parameters and comparison of the integrated plant with the conventional plant without capture. Accordingly, the steady-state simulations of six cases are performed in this study (which come under the groups of category-1 and category-2 as defined in *Chapter 3*):

Case 1: Conventional subcritical CFPP without $CO_2$ capture.
Case 2: CLC based subcritical CFPP with $CO_2$ capture.
Case 3: Conventional supercritical CFPP without $CO_2$ capture.
Case 4: CLC based supercritical CFPP with $CO_2$ capture.
Case 5: Conventional ultra-supercritical CFPP without $CO_2$ capture.
Case 6: CLC based ultra-supercritical CFPP with $CO_2$ capture.

### 4.2.1 Description of reference plants

In this study, the conventional CFPPs for three different steam parameters are considered as reference cases. The block diagram of conventional CFPP without $CO_2$ capture is shown in Figure 3.1(a) of *Chapter 3*. A brief overview of SubC, SupC, and Ultra-SupC CFPPs is given below:

#### *4.2.1.1 Conventional subcritical coal-fired power plant*

A 500 MW conventional CFPP with SubC steam boiler configuration for steam parameters of high-pressure (HP), intermediate-pressure (IP), and low-pressure (LP) of 166.7 bar/537$^o$C, 39.7 bar/537$^o$C, and 7.3 bar/303.3$^o$C, respectively and the final feed-water temperature of 253$^o$C [5] is considered. The coal input flow rate used is 81.3 kg/s, which corresponds to the 500 MW gross power output. This plant has two high pressure feed water heaters (FWHs) and three low pressure FWHs, which are used to preheat the water entering the evaporator.

#### *4.2.1.2 Conventional supercritical coal-fired power plant*

The first CFPP comprised of SupC steam boiler installed in India by National Thermal Power Corporation (NTPC) is for the gross power output of 660 MW [5]. The SupC CFPP is configured for the steam parameters of HP, IP, and LP of 242.2 bar/537$^{o}$C, 42.0 bar/565$^{o}$C, and 2.9 bar/215.6$^{o}$C, respectively and the final feed-water temperature of 280$^{o}$C. This plant consists of three high-pressure FWHs and four low-pressure FWHs.

#### *4.2.1.3 Conventional ultra-supercritical coal-fired power plant*

A 430 MW conventional CFPP with Ultra-SupC steam boiler configuration is considered. The plant involves steam parameters of HP, IP, and LP of 350 bar/700$^{o}$C, 60 bar/720$^{o}$C, and 5 bar/338.2$^{o}$C, respectively. The plant also consists of single stage reheating with a final feed-water temperature of 330$^{o}$C. The Ultra-SupC plant operates with three high-pressure FWHs and five low-pressure FWHs.

### 4.2.2 Description of chemical looping combustion based plants

A general block diagram of CLC based CFPP is represented in Figure 3.2. The process flow diagrams of SubC, SupC, and Ultra-SupC CFPP with CLC integration are shown in Figures 4.1 to 4.3. The steam parameters (temperature and pressure) and the number of high-pressure and low-pressure FWHs for these plants are the same as that of the conventional CFPPs. The combustor of conventional CFPP is replaced by the air and fuel reactors in CLC based plants. Also, the $CO_2$ capture and compressor unit are coupled with the CLC plant flowsheet.

The pulverized coal from sizing and drying unit along with the OC (70% iron oxide on 30% aluminium oxide; mass basis) is initially fed to the adiabatic fuel reactor for combustion of coal. The reduced OC (magnetite, $Fe_3O_4$) from the fuel reactor is transported to the isothermal air reactor, where the OC gets re-oxidized in the presence of pressurized air. The high temperature and pressure gas product from the air reactor (i.e., depleted air) is first sent to the gas turbine and then sent to the HRSG unit to recover heat. The flue gas from the fuel reactor ($CO_2$ and $H_2O$) is directly sent to the HRSG unit to recover heat. The sub-critical/super-critical/ultra-supercritical steam is generated in the HRSG unit according to the plant requirement to generate power using steam turbines. The flue gas leaving the HSRG comprising of $CO_2$ and steam is sent to a condenser to condense the steam and the separated pure $CO_2$ is compressed and stored.

The reactions involved in fuel and air reactor are given in Equation (4.1) to (4.5). A fuel reactor is assumed to be adiabatic reactor and air reactor is assumed as an isothermal reactor in the two-reactor CLC system. The reactions involved in fuel reactor are endothermic and solid stream from air reactor is at high temperature. The nature of reactions in air reactor are exothermic and excess heat is removed by supplying excess air to the air reactor. This is done by using calculator block in aspenONE simulation software. Mass flow rate of air in the air reactor has been fixed by considering a calculator block in the aspenONE to maintain the operating temperature of air reactor. For the same flow rate, the complete oxidation of reduced oxygen carrier is cross-checked.

$$C + H_2O \rightarrow CO + H_2 \tag{4.1}$$

$$C + CO_2 \rightarrow 2CO \tag{4.2}$$

$$CO + 3Fe_2O_3 \rightarrow 2Fe_3O_4 + CO_2 \tag{4.3}$$

$$H_2 + 3Fe_2O_3 \rightarrow 2Fe_3O_4 + H_2O \tag{4.4}$$

$$2Fe_3O_4 + {}^1\!/_2\, O_2 \rightarrow 3Fe_2O_3 \tag{4.5}$$

The iron oxide has several oxidation states. When considering the different reduction degrees, the $Fe_2O_3$ to $Fe_3O_4$ step is faster than the following steps of $Fe_3O_4$ to FeO and FeO to Fe. The oxygen transport capacity (Table 2.3) of iron oxide increases with the reduction degree of $Fe_2O_3$. In the fluidized bed fuel reactor for solid fuels, the oxygen transport capacity will be low (corresponding to the transformation from $Fe_2O_3$ to $Fe_3O_4$) due to the equilibrium limitation under the reaction atmosphere, where $CO_2$ and/or $H_2O$ are used as the fluidization medium and are also the combustion products [116].

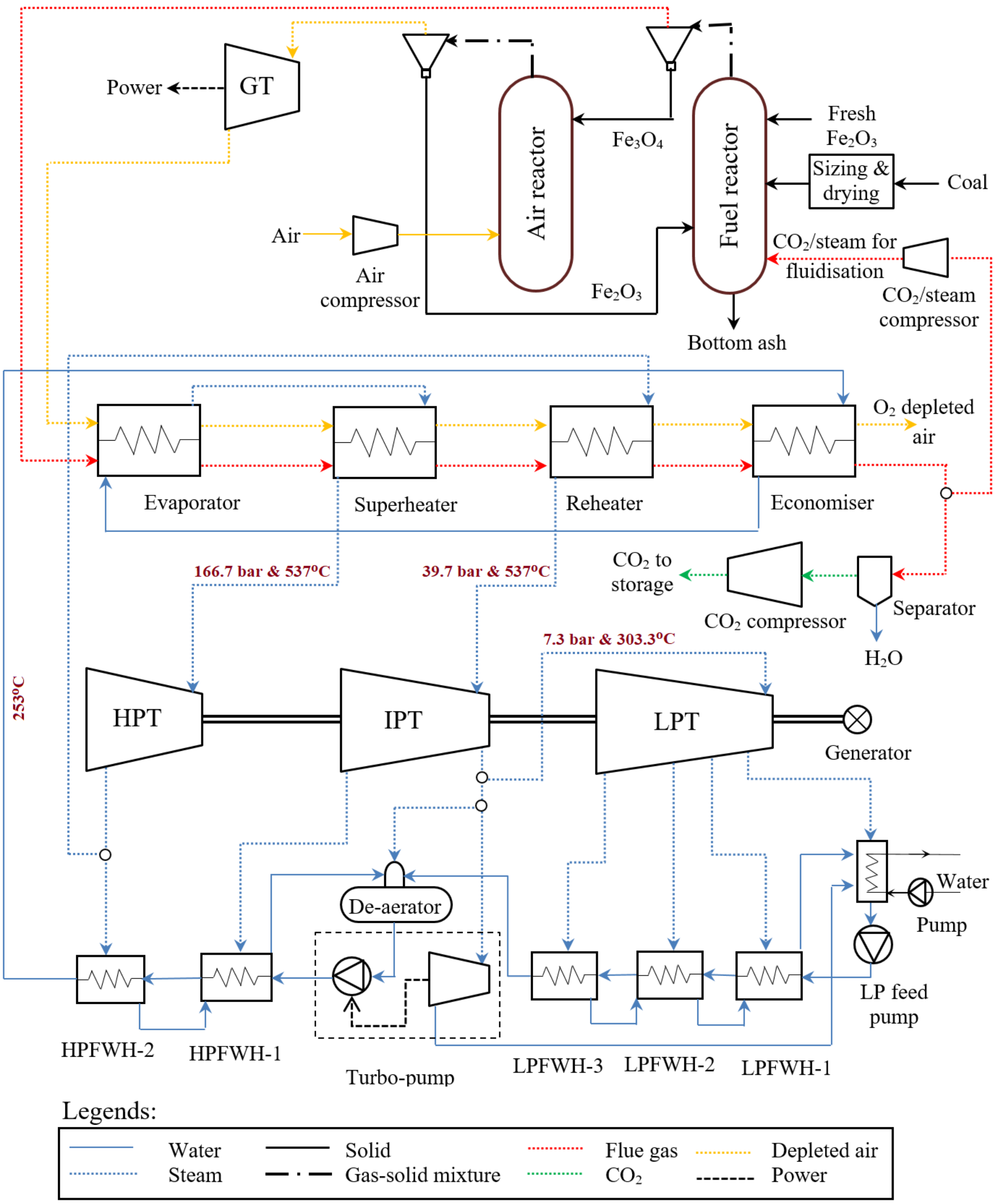

Figure 4.1 Schematic representation of CLC based SubC CFPP.

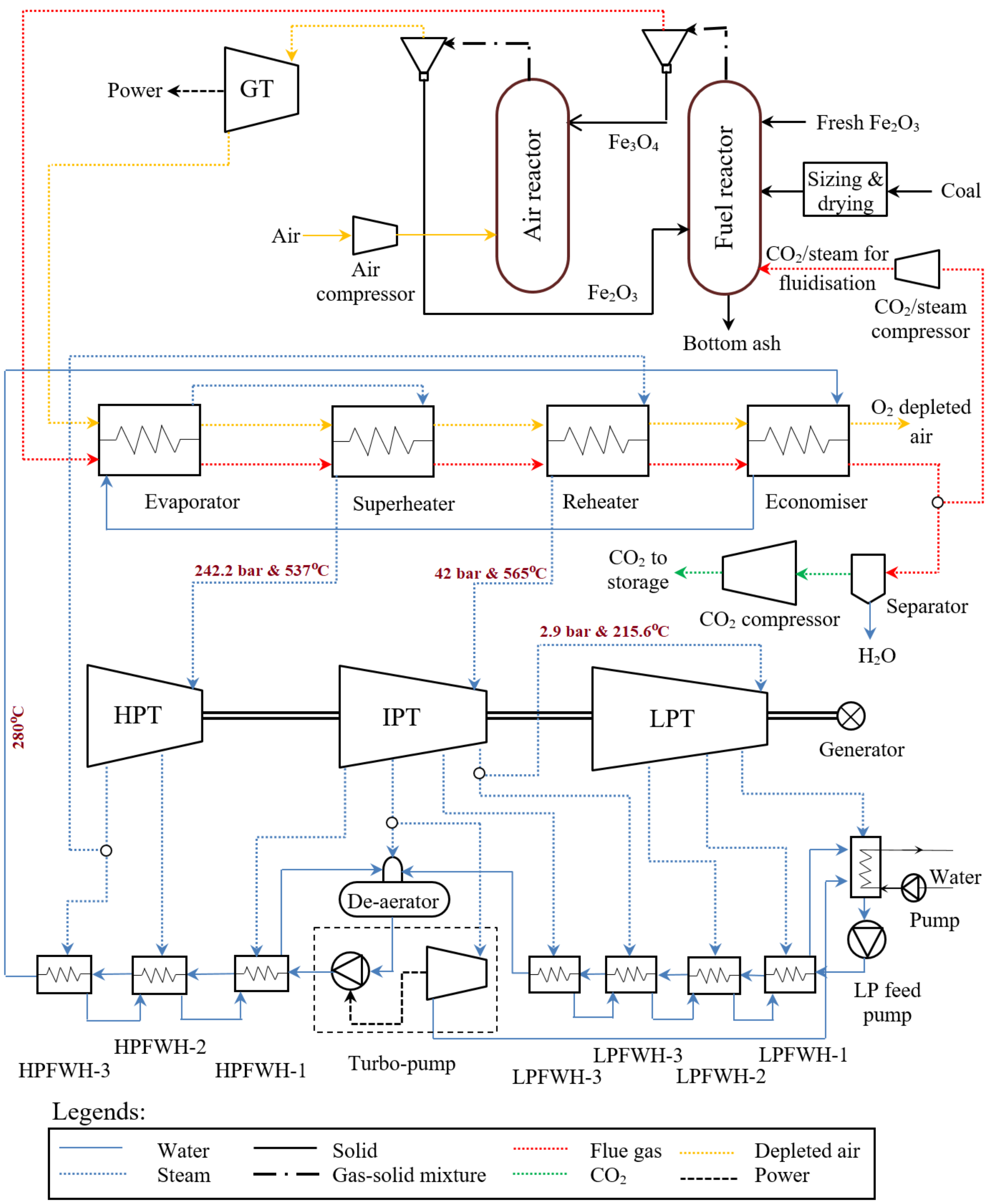

Figure 4.2 Schematic representation of CLC based SupC CFPP.

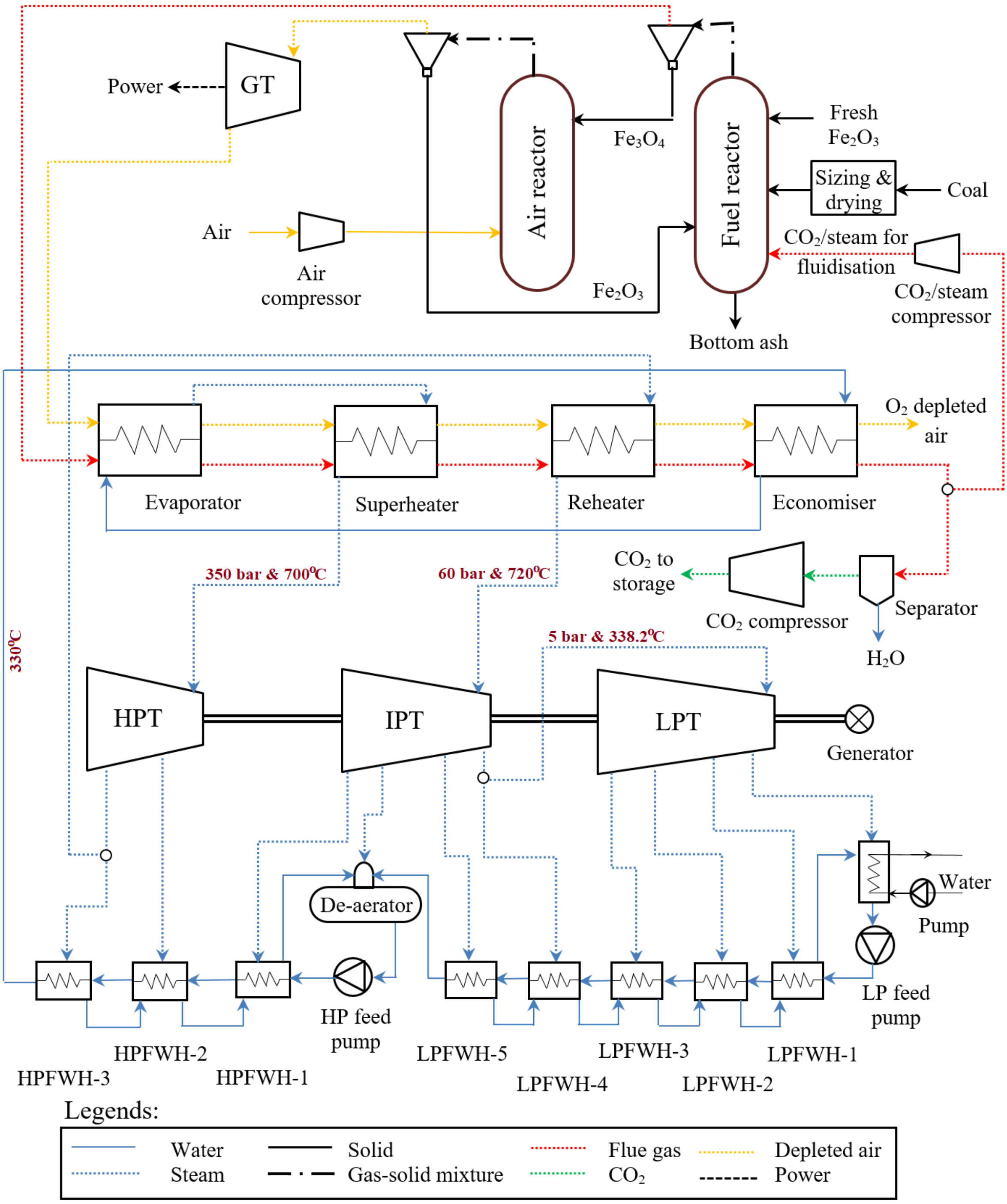

Figure 4.3 Schematic representation of CLC based Ultra-SupC CFPP.

As mentioned earlier, the number of HP and LP FWHs used in different configurations is different (see section 2.1) and thus the number of steam turbines is also different. A similar configuration of coupled steam turbines and FWHs as in conventional plants are considered for the case of CLC based plants as shown in the Figures 4.1 to 4.3. Apart from this, the de-aerator unit is installed after the low-pressure FWHs to remove dissolved gases and impurities in the feed water. A set of two boiler feed pumps are used before the low and high-pressure FWHs to supply the water.

## 4.3 Results and discussion

For carrying out a comparative study on the performance assessment, all the six configurations mentioned in *Section 4.2* have been simulated using the models used and validated in the present thesis. The energy input is uniformly considered for all the cases as 1287 MW (corresponding to coal input of 81.3 kg/s). This simulation facilitates the performance comparison of conventional CFPPs with the three steam parameters SubC, SupC and Ultra-SupC among themselves and also with CLC integration. The performance assessment is conducted based on energy, exergy, ecological and economic analyses.

The operating conditions of CLC reactors are first optimised by conducting parametric studies. These optimized conditions are considered for simulation of air and fuel reactors in CLC based plants.

### 4.3.1 Parametric analysis

The objective of the sensitivity/parametric studies is to analyse the effect of key operating parameters on the overall performance of CLC based plants. The key operating parameters examined are operating temperature, pressure and OC-to-coal ratio. A parametric study is conducted by varying one parameter by keeping all other parameters at fixed values.

#### *4.3.1.1. Effect of oxygen carrier to coal ratio*

Oxygen carrier is used as the source of oxygen for combustion of coal in the fuel reactor. Thus, OC-to-coal ratio (kg/kg) has a significant effect on the overall energy and exergy efficiencies of SubC, SupC and Ultra-SupC plants. Figure 4.4 shows the influence of OC-to-coal ratio on the energy and exergy efficiencies (as calculated using Equations 3.2 and 3.9 of chapter 3) of the CLC based plants. The variation trends for SubC, SupC and Ultra-SupC plants are similar. The air and steam side combined cycle is the principal contributor to the gross and net work output for all three plant configurations. The peak in the efficiencies for SubC, SupC and Ultra-SupC steam boilers have been observed at OC-to-coal ratio of 44.7 with the corresponding peak values of 34.96%, 36.03% and 38.39% for net energy efficiency and 32.15%, 33.13% and

35.31% for net exergy efficiency, respectively. As can be seen from Figure 4.5, the composition of carbon monoxide (CO) and $H_2$ decreased when the OC-to-coal ratio is increased from 40 to 44.7 and the composition of $CO_2$ and steam increased. At 44.7 of OC-to-coal ratio, complete combustion of coal occurs and there is no change in the composition of $CO_2$ and steam. The dip in efficiencies beyond 44.7 of OC-to-coal ratio is because of the additional energy/exergy loss in the fuel reactor because of the excess OC. Higher OC flow rate to the CLC cycle will also increase the costs. Thus, 44.7 has been selected as an optimal OC-to-coal ratio for further studies. The stoichiometric or theoretical requirement of the oxygen carrier to coal ratio based on ultimate analysis of coal given in Table 3.1 is 34.73. Hence, the obtained optimal value of oxygen carrier to coal ratio (44.70) has 28.71% excess oxygen carrier supplied to the plant.

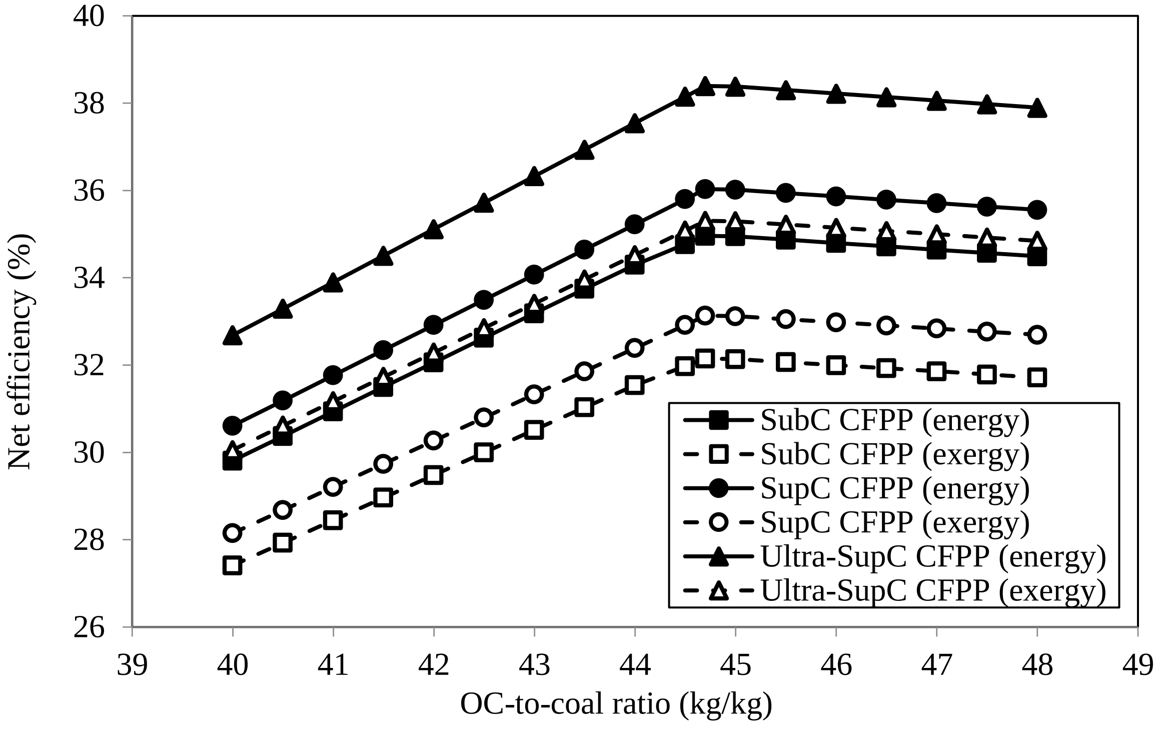

Figure 4.4 Variation of net energy and exergy efficiencies with OC-to-coal ratio.

#### *4.3.1.2. Effect of air reactor temperature*

Figure 4.6 shows the effect of increasing air reactor temperature on the net energy efficiency of CLC based SubC, SupC and Ultra-SupC CFPPs. As specified in the assumptions, the air reactor is assumed to be isothermal and fuel reactor as adiabatic in the current study. Since the fuel reactor is endothermic, heat is supplied to the reactor by means of solid particles from the air reactor [89]. The thermal efficiencies for all three plants have increased when air reactor temperature increased from 700°C to 900°C. With further increase in temperature, the efficiencies reduced gradually.

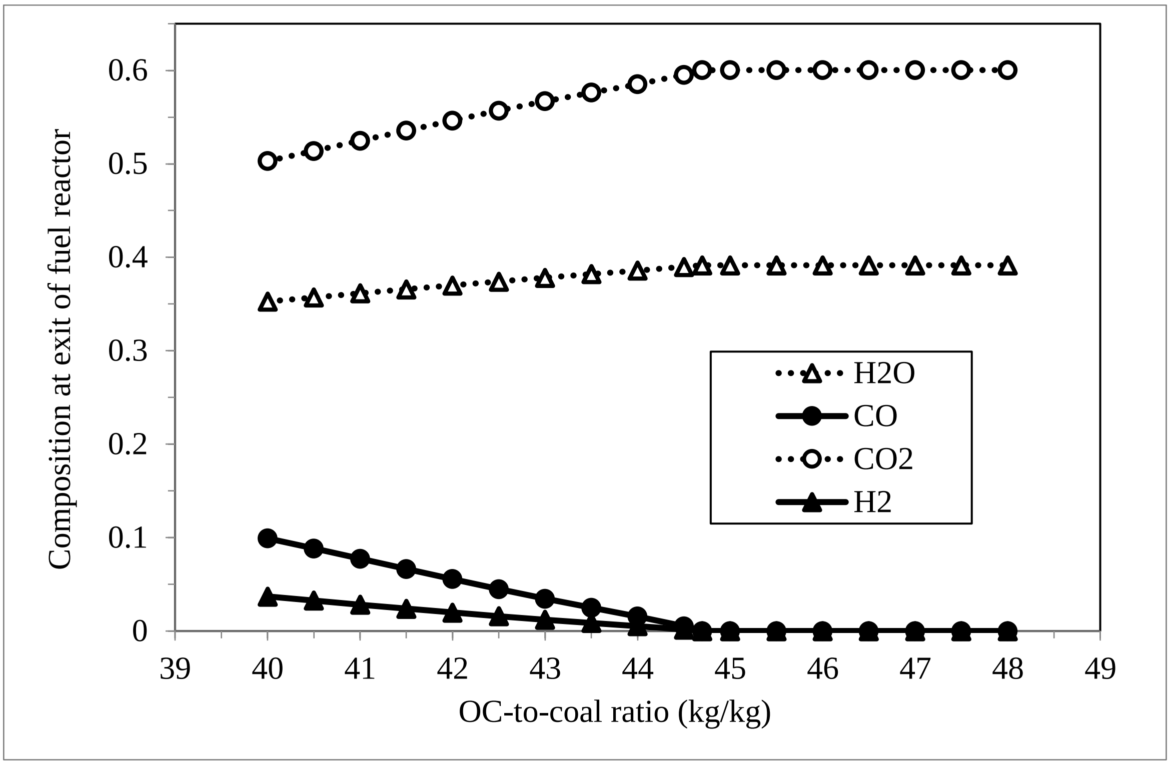

Figure 4.5 Variation of flue gas composition with OC-to-coal ratio.

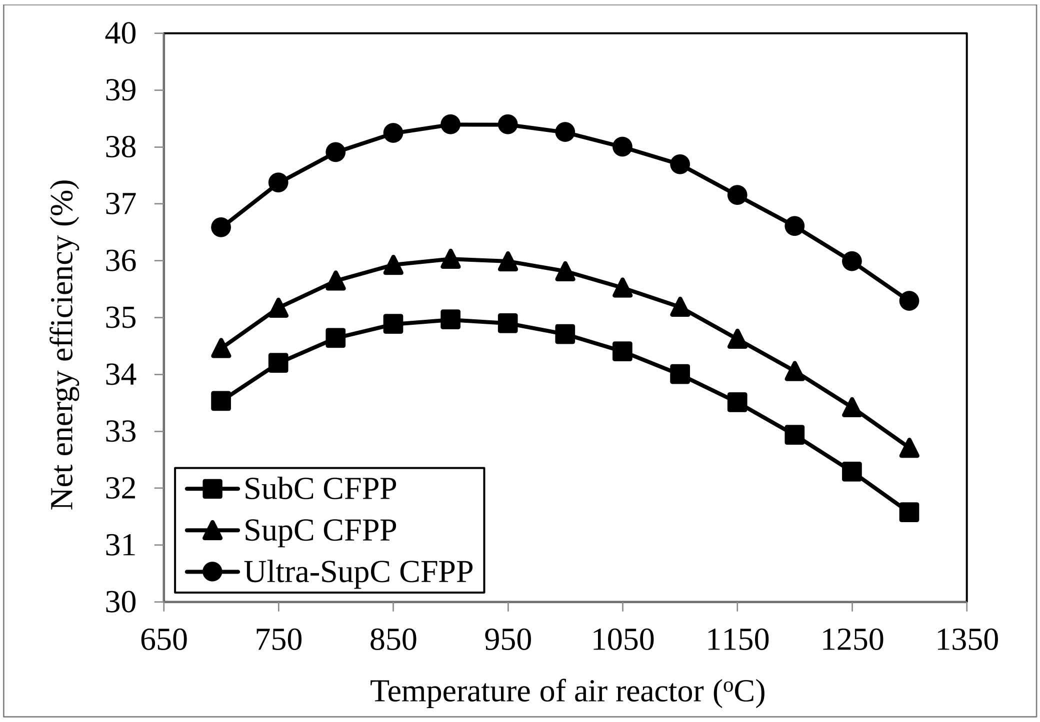

Figure 4.6 Variation of net energy efficiency with operating temperature of air reactor.

With the increase in operating temperature of air reactor, fuel reactor temperature also increases and the flue gas leaving at high temperature goes to HRSG and more amount of steam is generated, which ultimately increases steam turbine power output. On the other hand, the increase in air reactor temperature reduces the mass flow rate of excess air supplied, which is used to maintain the air reactor temperature. This results in reduction of gas turbine power output with an increase in air reactor temperature. Due to these two counteracting power outputs, there is a peak in the net power output and hence the net energy efficiency, which is observed at 900$^o$C. Experimental studies in literature also show that the char gasification in the fuel reactor is high at the higher temperatures which lead to greater char conversion. Thus, higher $CO_2$ capture efficiency can be obtained. However, the OC particles have the sintering/melting point limitation with the temperature [8]. During reduction process, $Fe_2O_3$ undergoes phase change (i.e. $Fe_3O_4$, FeO and Fe) and the molar volume decreases in sequence. This can influence the sintering behaviour of Fe-based oxygen carrier. The melting point temperatures of $Fe_2O_3$, $Fe_3O_4$, FeO and Fe are 1560$^o$C, 1538$^o$C, 1420$^o$C and 1275.5$^o$C, respectively, and these have a significant impact on the sintering properties of Fe-based oxygen carriers [8]. The temperature which is not in this range is always better to choose and hence the use of 900$^o$C air reactor operating temperature is the best choice for Fe-based oxygen carriers.

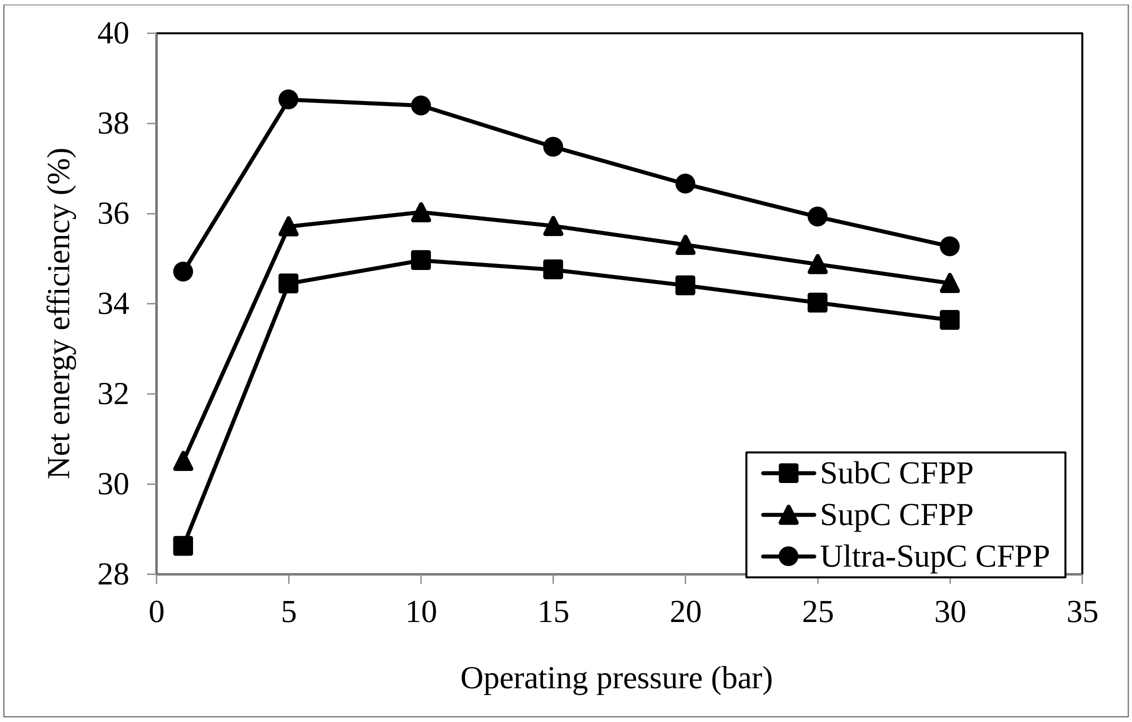

Figure 4.7 Variation of net energy efficiency with operating pressure of CLC reactors.

#### *4.3.1.3. Effect of operating pressure*

The operating pressure of air and fuel reactors has a considerable effect on the overall performance of CLC based SubC, SupC and Ultra-SupC CFPPs. It can be clearly seen from Figure 4.7 that the energy efficiency is increasing when operating pressure is varied from 1.013 bar (atmospheric pressure) to 5 bar. As the operating pressure increases, the gas turbine power output increases while the steam turbine power output decreases, hence there will be a peak in the net power output/efficiency. The peak for SubC, SupC and Ultra-SupC plant configurations occurred between 5 bar and 15 bar operating pressure. A similar trend was obtained by Iloeje et al. [178] for the combined CLC cycle. Based on the operating point of view, the power plant with the lower operating pressure of both air and fuel reactors seems to be most attractive. However, lower operating pressure involves higher volumetric gas flow rates and perhaps, higher cost. Hence, in this study, the optimal pressure of 10 bar is used as the operating pressure for both air and fuel reactors for further investigations.

## 4.3.2 4-E analyses of all the configurations

The operating parameters considered for CLC plants are: OC-to-coal ratio: 44.70 (mass basis), operating pressure of both air and fuel reactors: 10 bar, and operating temperature of air reactor: 900$^{o}$C, which are obtained from the parametric analysis as given in the previous section. 4-E analyses of all the six cases is presented here.

### *4.3.2.1 Energy analysis*

The conventional and CLC based CFPPs have been simulated for the constant fuel energy input of 1286.98 MW (based on HHV). The power production, power consumption, and plant efficiency (estimated using Equations 3.1 and 3.2) from all these plants are summarised in Table 4.1. Net electric efficiency is presented based on both HHV and LHV of the input fuel. However, further comparative analysis is done based on HHV instead of LHV as HHV is the generally used basis in the power plant industries and is used by several researchers for such an analysis [5,24,55]. HHV gives a conservative estimate of the energy efficiency, as presented in Table 4.1. As can be seen from Table 4.1, there is an increase of about 1.13% in net efficiency for conventional SupC CFPP and 5.48% for conventional Ultra-SupC CFPP compared to that of conventional SubC CFPP. These are in good agreement with the results presented by Suresh et al. [5] in their study for all three conventional CFPP configurations. The increase in net plant efficiency is due to the advanced steam parameters (T and P) at the exit of superheater and reheater.

Table 4.1 Plant performance of conventional and CLC based SubC, SupC, and Ultra-SupC CFPPs based on overall energy analysis.

| Plant data | Units | Sub-critical | | Super-critical | | Ultra-supercritical | |
|---|---|---|---|---|---|---|---|
| | | Conv. CFPP | CLC CFPP | Conv. CFPP | CLC CFPP | Conv. CFPP | CLC CFPP |
| Fuel input energy (HHV) | MW | 1286.98 | 1286.98 | 1286.98 | 1286.98 | 1286.98 | 1286.98 |
| Fuel input energy (LHV) | MW | 1209.74 | 1209.74 | 1209.74 | 1209.74 | 1209.74 | 1209.74 |
| GT output | MW | 0.00 | 232.88 | 0.00 | 233.02 | 0.00 | 233.02 |
| ST output | MW | 499.21 | 255.47 | 522.07 | 270.21 | 597.56 | 308.08 |
| Gross power output | MW | 499.21 | 488.35 | 522.07 | 503.22 | 597.56 | 541.09 |
| Power consumption in $CO_2$ capture and compression | MW | 0.00 | 19.25 | 0.00 | 19.25 | 0.00 | 19.25 |
| Auxiliary loss | MW | 37.44 | 19.16 | 39.16 | 20.27 | 53.78 | 27.73 |
| Net power consumption | MW | 37.44 | 38.41 | 39.16 | 39.51 | 53.78 | 46.97 |
| Net electric power output | MW | 461.77 | 449.94 | 482.91 | 463.71 | 543.78 | 494.12 |
| Gross electric efficiency | % | 38.79 | 37.95 | 40.57 | 39.10 | 46.43 | 42.04 |
| Net electric efficiency (based on HHV) | % | 35.88 | 34.96 | 37.52 | 36.03 | 42.25 | 38.39 |
| Net electric efficiency (based on LHV) | % | 38.17 | 37.19 | 39.92 | 38.33 | 44.95 | 40.85 |

As all the CLC based SubC, SupC, and Ultra-SupC CFPPs are operating under similar air and fuel reactor operating conditions, the same amount of net gas turbine output (around 233 MW) and power consumption by $CO_2$ compressor (19.25 MW) are obtained (Table 4.1). The steam turbine output increased from CLC based SubC to CLC based Ultra-SupC plant because of the advanced steam parameters compared to the SubC plant, which leads to an increase in the total power output. The total net power output obtained from the conventional SubC, SupC, and Ultra-SupC CFPPs without $CO_2$ capture is more than the respective CLC based CFPPs, resulting in the net energy penalty of 0.92%, 1.49%, and 3.86%, respectively. For the same high-ash Indian coal (as in the current study), Karmakar et al. [9] reported penalties in the energy efficiency of 10.8%, 8%, and 12.4%, respectively, for the conventional CFPPs with

SubC, SupC, and Ultra-SupC steam boilers, when a post-combustion $CO_2$ capture is integrated. These penalties are much high compared to the penalties obtained in the present study of CLC based CFPPs.

#### *4.3.2.2 Exergy analysis*

Figure 4.8 shows the comparative performance in terms of the overall exergy efficiency for conventional and CLC based power plants. The net exergy efficiencies of CFPPs with advanced steam boilers (SupC and Ultra-SupC) are found to be more compared to both the conventional type and CLC based SubC plant. The increase in energy and exergy efficiencies is due to the advanced steam parameters which are considered at the inlet of the high-pressure turbine and intermediate-pressure turbine. Similar to the energy efficiency, CLC based SubC, SupC and Ultra-SupC CFPPs have shown some penalty in the exergy efficiencies compared to the respective conventional plants. This exergy penalty in CLC based plants is because of the more exergy destruction in the boiler section (two reactors in CLC vs. single combustor in conventional CFPP), air compressor (10.5 bar in CLC vs. 1.04 bar in conventional CFPP) and $CO_2$ compressor (not present in conventional CFPP).

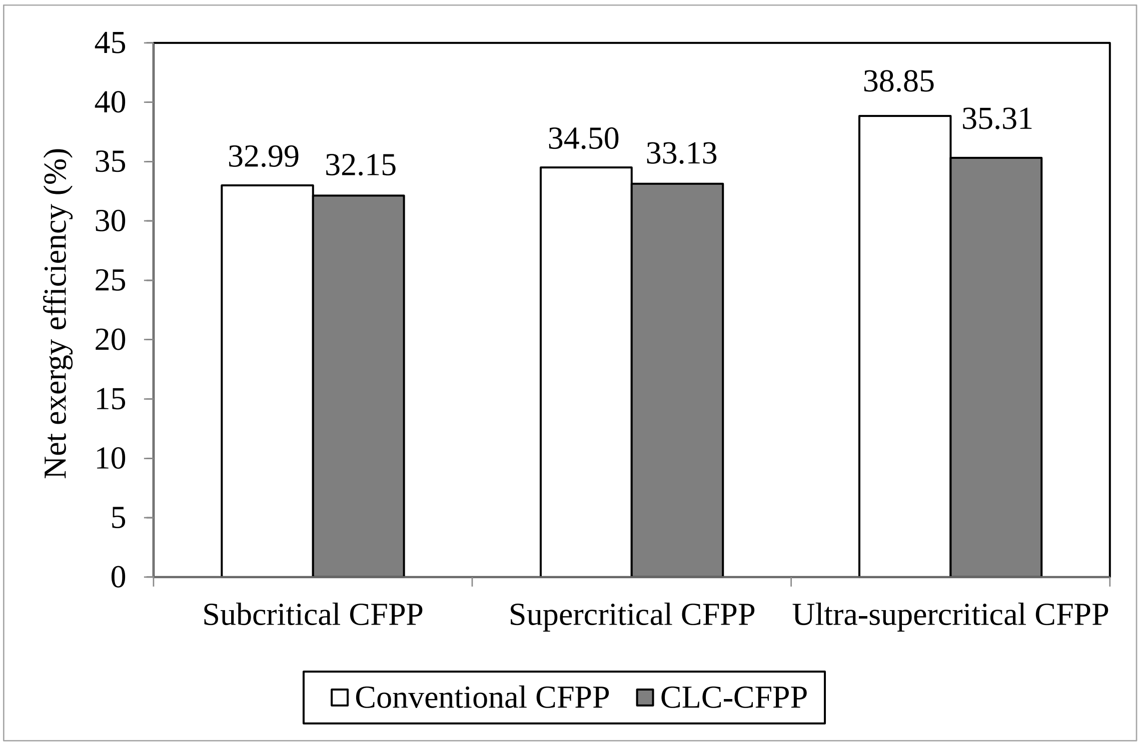

Figure 4.8 Comparison of conventional and CLC based CFPPs based on overall exergy efficiency.

In the proposed conventional and CLC based plants, the external input flows are: coal, air, makeup OC, and makeup water. Among them, air, makeup OC, and makeup water are entering at environmental conditions, thus the exergy of these flow streams are negligible. In order to identify the units, where the exergy loss/destruction is high, component-wise exergy analysis is conducted for all six cases of coal-fired power plant designs. The exergy destructions in individual process/components are estimated using the equations shown in section 3.2.2 of Chapter 3 in the same way as presented in Gao et al. [179]. Figure 4.9 shows the percentage contribution in exergy destruction by the important units of all the conventional and CLC based CFPPs. The boiler sections account for more exergy destruction among other units in all the cases due to the higher operating conditions (temperature and/or pressure) and the heat transfer processes. The exergy destruction is observed to be lower when the subcritical steam boiler is replaced with the supercritical or ultra-supercritical. Though the exergy destruction in steam boiler and its percentage contribution in the overall plant exergy destruction in case of CLC based power plants is more (0.77% to 2.25%) than the respective conventional power plants, the overall performance of the CLC based power plants is improved. The higher exergy destruction in the boiler section of CLC plants is because of higher flue gas and oxygen depleted air flow rates compared to the flue gas leaving conventional combustor. A similar observation was also reported in the literature [124]. It can also be observed that the advanced steam boiler plants offer less exergy destruction compared to the SubC steam boiler plant because of the better heat integration. The exergy destruction in the compressors is found to be high in case of CLC based plants compared to the conventional cases, because of high energy requirements for air compressor to compress the air to 10.5 bar pressure and for $CO_2$ compressor to compress the captured $CO_2$ to 110 bar pressure, which is absent in the conventional cases.

As a first step towards 4-E analysis, the first two factors viz, exergy and energy are compared for different units to locate the losses, as indicated in *Chapter 3* and scope for improving is presented in terms of improvement potential. In the second step, economic analysis is carried out taking all the costs including ecological consequences.

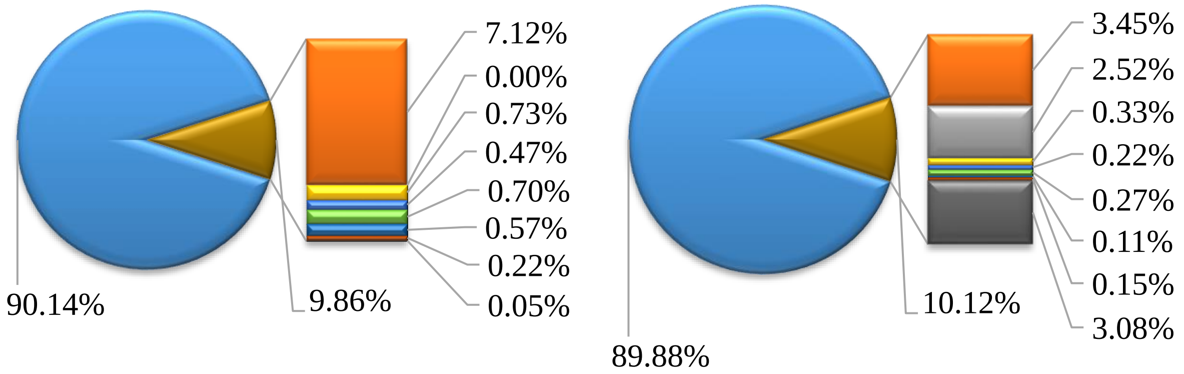

(a) Conventional SubC CFPP (b) CLC based SubC CFPP

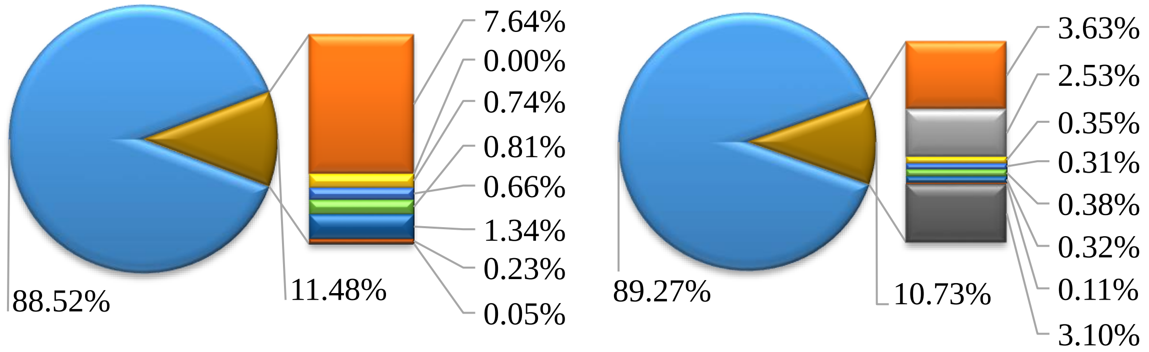

(c) Conventional SupC CFPP (d) CLC based SupC CFPP

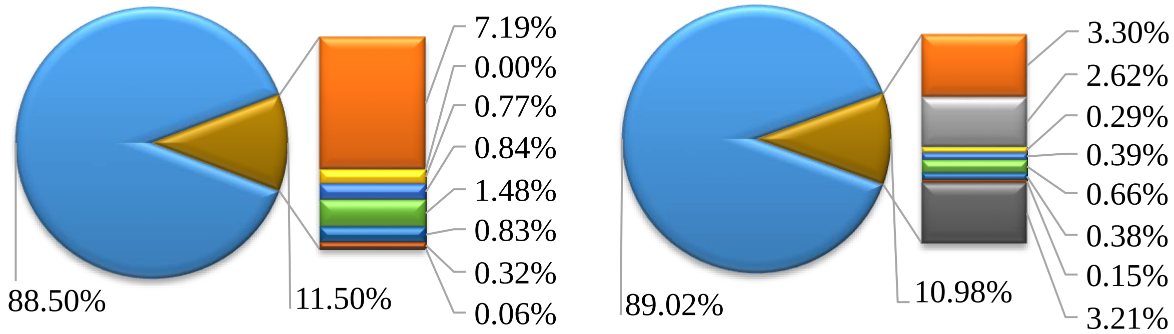

(e) Conventional Ultra-SupC CFPP (f) CLC based Ultra-SupC CFPP

Figure 4.9 Percentage contribution in exergy destruction by the important units of the conventional and CLC based CFPPs for different steam boilers.

The exergy and energy losses and improvement potential for the three different CLC based CFPPs are presented in Table 4.2. It can be noted that the primary source of the energy loss in all three power plants is the condenser, which contributes to around 41.16%, 36.84% and 29.67% of the total energy loss for the CLC based SubC, SupC and Ultra-SupC plants, respectively. On the contrary, the exergetic destruction contribution of the condenser is only around 0.3% of total exergy destruction for all the three plants. This is indicated by the low improvement potential of 0.92 to 6 MW. The second largest contributor in energy loss is the boiler unit, which accounts for 13% to 15.64% of total energy loss, while the exergetic destruction in the boiler unit accounts for around 89% of total plant exergy destruction. This is reflected in the high improvement potentials of 326.62 MW, 318.34 MW and 288.44 MW for the boilers.

Though large amounts of energy are lost in the condensers, the potential to utilize the waste heat energy as the useful work is less and hence the improvement of efficiencies is very low. On the other hand, boilers of all the three plants have high improvement potentials because of their higher exergy destructions. This inference is an important result of analysing exergy and energy together. Analysis of only energy would have been misleading to look for methods of improving the condenser efficiency. The improvement potential in the exergy destruction for all other units is very small. Having identified that the most inefficient unit of the power plant is the boiler, the next step is to look for methods of improvement of the boiler efficiency. Boiler in a CLC based power plant consists of fuel reactor, air reactor and HRSG, as stated earlier. The overall energy and exergy efficiencies can be improved by reducing steam boiler irreversibilities, by using other oxygen carriers such as copper oxide, nickel oxide, mixed carriers etc., and better heat integration strategies.

Table 4.2 Energy loss, exergy destruction and exergetic improvement potential for the CLC based SubC, SupC and Ultra-SupC CFPPs.

| Block | Unit | CLC based SubC | | | CLC based SupC | | | CLC based Ultra-SupC | | |
|---|---|---|---|---|---|---|---|---|---|---|
| | | Energy loss | $Ex_d$ | $\dot{IP}$ | Energy loss | $Ex_d$ | $\dot{IP}$ | Energy loss | $Ex_d$ | $\dot{IP}$ |
| Boiler | MW | 125.75 | 804.37 | 326.62 | 125.27 | 794.12 | 318.34 | 125.22 | 766.48 | 288.44 |
| ST | MW | 85.16 | 30.83 | 1.38 | 90.07 | 32.26 | 1.59 | 102.69 | 28.37 | 1.05 |
| GT | MW | 74.02 | 22.52 | 0.85 | 74.16 | 22.54 | 0.85 | 74.16 | 22.54 | 0.85 |
| Condenser | MW | 330.83 | 2.92 | 0.92 | 310.16 | 2.92 | 1.04 | 286.45 | 2.50 | 0.77 |

| | | | | | | | | | | |
|---|---|---|---|---|---|---|---|---|---|---|
| LPFWH | MW | 43.13 | 1.95 | 0.21 | 80.68 | 2.74 | 0.22 | 87.11 | 3.32 | 0.18 |
| HPFWH | MW | 76.55 | 2.42 | 0.05 | 92.02 | 3.38 | 0.07 | 117.72 | 5.67 | 0.13 |
| De-aerator | MW | 1.72 | 0.99 | 0.04 | 3.51 | 2.89 | 0.35 | 102.94 | 3.28 | 0.33 |
| Pumps | MW | 11.14 | 1.33 | 0.05 | 10.31 | 0.98 | 0.03 | 13.41 | 1.27 | 0.04 |
| Compressors | MW | 55.52 | 27.59 | 3.06 | 55.66 | 27.60 | 3.06 | 55.66 | 27.60 | 3.06 |

### *4.3.2.3 Ecological analysis*

In this section, the environmental analysis is carried out using equations described in section 3.2.3 of Chapter 3 to assess the effect of the $CO_2$ capture unit on CLC based CFPPs. Comparison based on ecological analysis with various environmental parameters is summarized in Table 4.3. As the conventional plants in the present study are not equipped with a capture unit, they emit around 102 kg/s of carbon dioxide into the environment. On the contrary, the CLC based CFPPs with all three steam boilers capture nearly all the $CO_2$ from the flue gas leaving fuel reactor. The conventional CFPPs release $2.57 \times 10^9$ kg of $CO_2$ annually, whereas for CLC case, almost zero $CO_2$ emissions are attained. Accordingly, annual $CO_2$ avoided per fuel consumption is found to be 62.96 kg of $CO_2$/GJ for CLC cases.

Table 4.3 Comparison of conventional and CLC based plants based on ecological assessment.

| Parameters | Unit | Sub-critical | | Super-critical | | Ultra-supercritical | |
|---|---|---|---|---|---|---|---|
| | | Conv. CFPP | CLC CFPP | Conv. CFPP | CLC CFPP | Conv. CFPP | CLC CFPP |
| $CO_2$ emission | kg/s | 101.79 | ~0.00 | 101.82 | ~0.00 | 101.64 | ~0.00 |
| $CO_2$ captured | kg/s | 0.00 | 102.55 | 0.00 | 102.55 | 0.00 | 102.57 |
| $CO_2$ capture efficiency | % | 0.00 | ~100.00 | 0.00 | ~100.00 | 0.00 | ~100.00 |
| Specific $CO_2$ emission | kg/MW.h | 793.56 | ~0.00 | 759.03 | ~0.00 | 672.88 | ~0.00 |
| Annual $CO_2$ emission | kg | $2.57{\times}10^9$ | ~0.00 | $2.57{\times}10^9$ | ~0.00 | $2.56{\times}10^9$ | ~0.00 |
| Average annual emission rate aggravating per unit fuel | kg.$CO_2$/GJ | 62.49 | ~0.00 | 62.51 | ~0.00 | 62.40 | ~0.00 |
| Annual $CO_2$ avoided emission per unit fuel | kg.$CO_2$/GJ | 0.00 | 62.96 | 0.00 | 62.96 | 0.00 | 62.97 |
| Net electric output per kg of $CO_2$ captured | MW/kg | - | 4.39 | - | 4.52 | - | 4.82 |

#### *4.3.2.4 Economic analysis*

Having proven the technical feasibility of the CLC and advanced steam generation technologies, it is essential to compare the economic feasibility of the plants. Table 4.4 shows the economic performance indicators estimated as explained in section 3.2.4 for the above-studied conditions for all the conventional and CLC based plants. The specific capital cost in terms of €/kW$_{gross}$ for the conventional SupC and Ultra-SupC CFPPs is lower than that of the conventional SubC plant by 1.47% and 5.76%, respectively. This is due to the high gross power production in SupC and Ultra-SupC cases compared to SubC case. These figures are in good agreement with the estimated range given in the literature [167,180]. The specific capital costs of CLC based plants are estimated to be 1039.04 €/kW$_{gross}$ (for CLC-SubC), 1039.84 €/kW$_{gross}$ (for CLC-SupC) and 1038.91 €/kW$_{gross}$ (for CLC-Ultra-SupC). The results indicate that the specific capital cost is lower for the CLC based CFPP compared to the conventional CFPP by 19.14% for subcritical, 17.87% for supercritical and 14.20% for the ultra-supercritical. This is because of the lower ratio of total capital cost to the plant power output in case of CLC based CFPP. The total capital cost, FOM cost, VOM cost and specific fuel cost are calculated as explained in section 2.4.4. The magnitudes of cost $C_1$ and respective capacity $q_1$ given in Eq. (3.15) are taken from [26,181–184] for all the plants. However, the cost of the materials of construction for all the plants is not accounted in these calculations due to unavailability of sufficient data for Ultra-SupC plant.

The LCOE associated with the CLC plants for SubC, SupC, and Ultra-SupC are estimated to be 93.72 €/MW.h, 89.05, and 87.83 €/MW.h, respectively. The magnitudes of these costs of electricity are in the range of the values given in the literature for IGCC-CLC plants [71]. The cost of $CO_2$ avoided per ton of $CO_2$ is found to be lower for the CLC based SupC CFPP (39.77 €/t$CO_2$) compared to the CLC based SubC and Ultra-SupC plants because of the lower LCOE difference between CLC based and conventional CFPPs. This shows that the CLC based CFPP with supercritical steam generation technology would be economically favoured option compared to conventional and other CLC based CFPPs.

Table 4.4 Economic performance indicators under initial design conditions.

| Parameters | Unit | Sub-critical | | Super-critical | | Ultra-supercritical | |
|---|---|---|---|---|---|---|---|
| | | Conv. CFPP | CLC CFPP | Conv. CFPP | CLC CFPP | Conv. CFPP | CLC CFPP |

|  |  |  |  |  |  |  |  |
|---|---|---|---|---|---|---|---|
| Specific capital cost | €/kW$_{\mathrm{gross}}$ | 1284.94 | 1039.04 | 1266.10 | 1039.84 | 1210.90 | 1038.91 |
| LCOE | €/MW.h | 58.96 | 93.72 | 58.87 | 89.05 | 55.84 | 87.83 |
| $CO_2$ avoided cost | €/t$CO_2$ | - | 43.80 | - | 39.77 | - | 47.53 |
| $\mathrm{LCOE}_{\mathrm{overall}}$ | €/MW.h | 106.94 | 93.72 | 104.76 | 89.05 | 96.53 | 87.83 |

As all the CLC based CFPPs are resulting in zero emission, LCOE and $\mathrm{LCOE}_{\mathrm{overall}}$ are similar for these plants. As can be observed from the Table 4.4, CLC based CFPPs have better $\mathrm{LCOE}_{\mathrm{overall}}$ compared to their conventional counterparts. It can also be seen that the CLC based SupC and Ultra-SupC plants are competitive with respect to economics. However, as explained earlier, the material costs have not been taken into account in this analysis and these costs may well decide the most economic option.

### 4.3.3 Comparison of CLC based CFPPs with conventional subcritical CFPP

As per the report by Caldecott et al. [185], the sub-critical steam-based power plants contribute around 75% of the global capacity. Thus, a comparative analysis of the three CLC based power plants with reference to the conventional SubC CFPP will be useful while deciding the configuration of the upcoming power plants in the future. Figure 4.10 shows the comparison of CLC based SubC, SupC, and Ultra-SupC CFPPs with conventional SubC CFPP on the basis of energy, exergy, ecological and economic analyses. The CLC based SubC CFPP displays penalty in the energy and exergy efficiency, while CLC based SupC and Ultra-SupC CFPPs show gain in the energy and exergy efficiencies compared to the conventional SubC CFPP. There is a significant increase in net electric efficiency by 1.07% and 3.43% for CLC based SupC and Ultra-SupC CFPPs compared to that of SubC CFPP with CLC integration. The gain in energy and exergy efficiency for CLC based Ultra-SupC CFPP is more compared to the CLC based SupC CFPP by 2.36% and 2.17%, respectively. Since no $CO_2$ capture unit is involved in the conventional SubC CFPP, the annual $CO_2$ emission is 62.49 kg of carbon dioxide per GJ of coal input rate. CLC based all three plants capture nearly 100% by avoiding all $CO_2$ emissions. The economic analysis shows 106.92 €/MW.h of overall LCOE for the conventional SubC CFPP, whereas all the three CLC based CFPPs result in lower overall LCOE than the conventional SubC CFPP. Thus based on the 4-E analyses, the choice of CLC based SupC and Ultra-SupC CFPPs are the promising options for the growing countries, where coal is a primary source of energy. The materials of construction for the steam generators and turbines in Ultra-

SupC plants that can withhold the high temperature and pressure are still under research stage [186]. If they are available commercially, this advanced steam boiler plant with CLC integration would be a favourable technological option for clean power production.

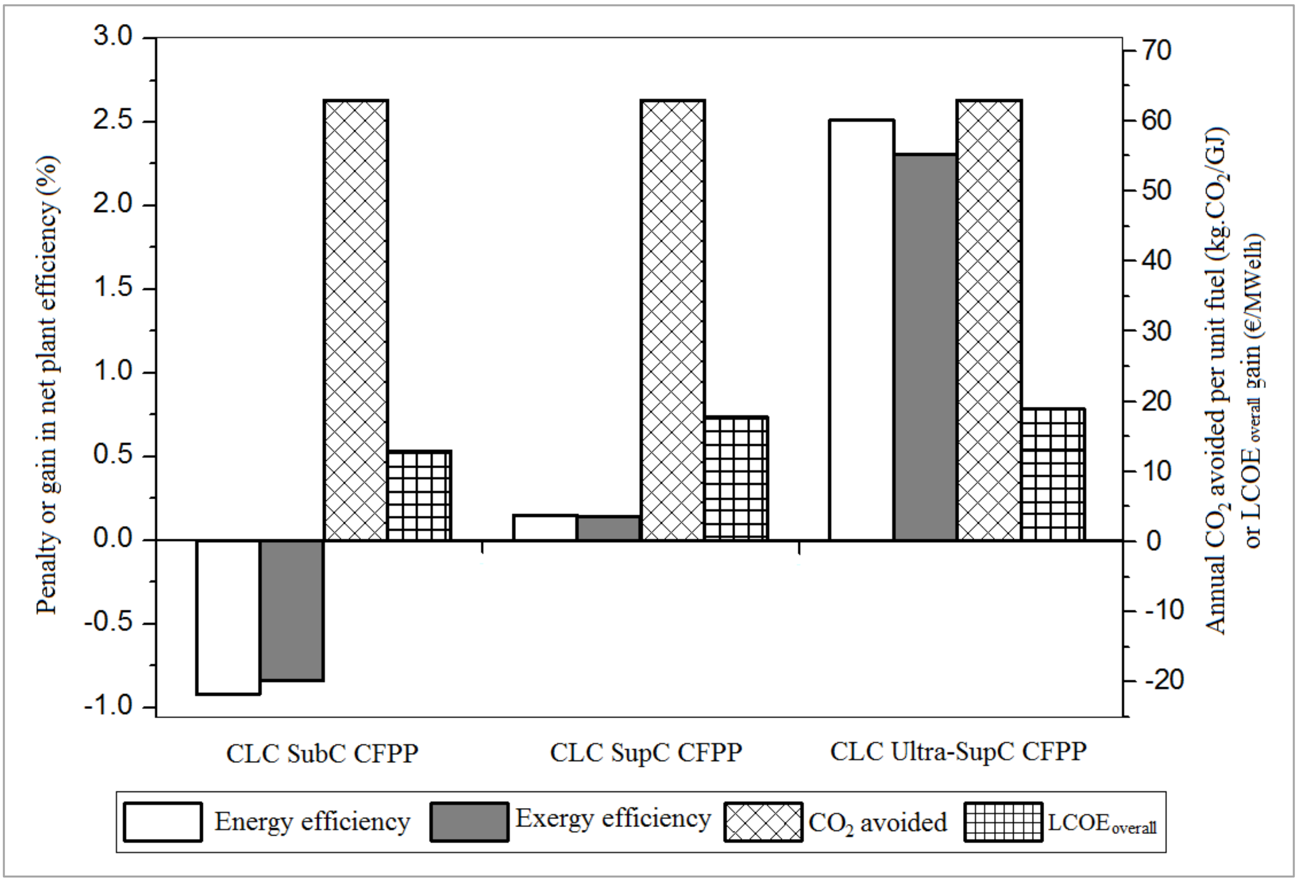

Figure 4.10 Comparison of CLC based SubC, SupC, and Ultra-SupC CFPPs with conventional SubC CFPP.

## 4.4 Summary

The present study is intended to demonstrate the feasibility of a CLC based power plants for zero $CO_2$ emissions based on 4-E (i.e. energy, exergy, ecological, and economic) analyses. The conventional CFPPs without $CO_2$ capture (SubC, SupC, and Ultra-SupC) and the advanced CLC based CFPPs using iron ore as the metal oxide are simulated and compared. Following are the conclusions that can be drawn from the present study:

- The energy analysis has shown that the CLC based SubC, SupC, and Ultra-SupC plants have net energy efficiency penalty of 0.92%, 1.49%, and 3.86%, compared to their respective conventional plants. This penalty is very low as compared to the reported values of 7-10% for other $CO_2$ capture technologies such as: pre-combustion, post-combustion and oxy-combustion [9,49].

- The exergy analysis showed that the net exergy efficiency penalty of 0.84%, 1.37%, and 3.55% for CLC based plants for SubC, SupC, and Ultra-SupC CFPPs, respectively compared to their conventional cases. Further, the unit wise exergy analysis showed that the highest exergetic losses are in the boiler section.
- Integration of CLC to CFPPs brings down the annual $CO_2$ release of $2.57 \times 10^9$ kg to zero.
- The economic analysis revealed that the overall LCOE of CLC based SupC and Ultra-SupC CFPPs are comparatively less than the conventional CFPPs and also CLC based SubC CFPP.

# Chapter 5

# CLC based SupC coal fired power plant with different oxygen carriers

# Chapter 5

# *CLC based SupC coal fired power plant with different oxygen carriers*

---

In this chapter, the best suitable CLC based power plant configuration obtained from *Chapter 4* is selected for further study. Further, three different oxygen carriers are considered, which are iron oxide, copper oxide and mixture of iron and copper oxides. In addition to CLC based power plant, a MEA based $CO_2$ capture technology coupled with the conventional power plant is also simulated. The overall performance of CLC based CFPP using different oxygen carriers is compared among themselves and with the conventional CFPP with $CO_2$ capture. The energy, exergy, ecological and economic analyses are considered to compare the overall performance of these plants.

---

## 5.1 Background and motivation

*Chapter 4* concludes that the CLC based CFPP with supercritical steam boiler is energetically, exergetically, ecologically and economically favourable plant. Hence, this chapter considers the supercritical steam based power plant configuration for further study. As mentioned in *Chapter 2,* many oxygen carriers are reported in literature with their own advantages and disadvantages. Hence, the choice of oxygen carrier in CLC has substantial weight on overall plant efficiency. According to U.S. Geological survey 2017, India ranks fourth in iron ore production in the world [117]. Thus in this study, iron oxide is considered as a main oxygen carrier. The copper oxide is more reactive and costly compared to the iron oxide, but addition of some fraction of copper oxide in the iron oxide can enhance the reactivity and does not add much in the overall operational cost. Although the CLC based process is energy efficient and environment friendly, the activity of $Fe_2O_3$ as oxygen carrier is relatively low, especially for coal conversion [8,128]. The experimental and simulation work of He et al. [73] presented the feasibility of copper oxide and its oxygen uncoupling properties to improve the iron oxide-coal reaction rates. Their study showed that, the bimetallic oxygen carrier consisting small amount of CuO (5 wt. % in $Fe_2O_3$) is more effective for char conversion compared to the $Fe_2O_3$ alone as oxygen carrier. As explained in *Chapter 1* and *2*, copper oxide has more reactivity and more oxygen carrying capacity compared to the iron oxide. It is also found from the literature that, the net energy efficiency of plant is more for CuO-based CLC plant compared to the $Fe_2O_3$-based CLC plant. Hence, it is proposed to use CuO along with $Fe_2O_3$ to increase the overall plant efficiency compared to that obtained with $Fe_2O_3$ alone. Thus in the present work, the bimetallic oxygen carrier (mixture of iron and copper oxide) is considered for the CLC based plant.

Therefore, this study is intended to:

1. Establish a CLC based CFPP configuration using different oxygen carriers ($Fe_2O_3$, CuO, and mixture of $Fe_2O_3$ and CuO) for Indian climatic conditions.
2. Conduct a detailed exergy, energy, ecological and economic analyses of the conventional supercritical CFPP and CLC based supercritical CFPP and compare.
3. Carry out further, a comparative analysis with a MEA based post-combustion capture (PCC) simulated model.

The outcome of this study would be helpful to understand the possible feasibility of CLC integration with Indian SupC CFPP using different oxygen carriers that offer quite competent plant performance.

## 5.2 Model description and approach

A supercritical steam based conventional and CLC based CFPPs are considered in this chapter and are simulated with the assumptions and performance evaluation given in *Chapter 3*. The process flow diagram of the CLC based CFPP with supercritical steam generation is shown in Figure 4.2 (*Chapter 4*). Table 5.1 shows the description of the different cases used in this chapter. These also belong to the categories 1 and 2 as defined in *Chapter 3*.

Table 5.1 Description of different cases used in this study.

| Case no. | Technology used | Oxidising agent |
|---|---|---|
| Case 1 | Conventional SupC CFPP without $CO_2$ capture | Air |
| Case 2 | Conventional SupC CFPP with post-combustion $CO_2$ capture | Air |

|  |  |  |
|---|---|---|
| Case 3 | CLC based SupC CFPP | $Fe_2O_3$ |
|  | CLC based SupC CFPP | CuO |
|  | CLC based SupC CFPP | $Fe_2O_3$ & CuO |

### 5.2.1 Plant wide simulation of conventional SupC CFPP with MEA based PCC

The MEA based post-combustion capture plant is integrated with the conventional SupC CFPP as given in *Chapter 4*. The simplified block diagram of this case is shown in Figure 3.1(b). The model was initially developed and validated on the pilot plant scale using the data available in literature [187]. The scale up of model parameters were handled using Chemical Engineering design and principles [188]. The preliminary design calculation results and process specifications for the plant are given in Table 5.2. Table 5.3 shows the aspenONE input specifications for the absorber and stripper sections of scaled-up MEA based post combustion capture.

Table 5.2 Assumptions in preliminary design calculation and results for $CO_2$ separation using MEA at first stage.

| Description | Unit | Value |
|---|---|---|
| Flow rate of flue gas entering the absorber | kg/s | 544.24 |
| Flow rate of $CO_2$ entering the absorber | kg/s | 101.79 |
| Mass fraction of $CO_2$ in the flue gas | -- | 0.19 |
| Required MEA flow rate | kg/s | 405.19 |
| $CO_2$/MEA ratio | -- | 0.255 |
| Required lean solution flow rate | kg/s | 1832.21 |
| Rich solution flow rate | kg/s | 1956.75 |
| Condenser Heat Duty | MW | 398.76 |
| Reboiler Heat Duty | MW | 473.1 |

Table 5.3 aspenONE input specification for the full-scale MEA based PCC absorber and stripper.

| Parameter | Absorber | Stripper |
|---|---|---|
| Column number | 1 | 1 |

| | | |
|---|---|---|
| Calculation type | Rate-based | Rate-based |
| Number of equilibrium stages | 30 | 40 |
| Condenser | None | Partial-vapour |
| Reboiler | None | Kettle |
| Operating pressure (bar) | 1.013 | 1.62 |
| Type of packing | IMTP - NORTON | FLEXIPAC - KOCH |
| Total height of packing (m) | 40 | 50 |
| Diameter of column (m) | 10 | 18 |

Figure 5.1 shows the concept of standard regenerative absorption-desorption system. The exhaust flue gas leaving from the HRSG unit of the conventional CFPP is directly sent to direct contact cooler (DCC), where it is cooled from $125^0$C to $40^0$C before entering into the absorber. The aqueous absorbent (MEA) solution enters the absorber counter-currently with the flue gas, where MEA reacts chemically with $CO_2$. Chemically bonded MEA and $CO_2$ pumped to the stripper after passing through the heat exchanger, where it is heated to the temperature close to operating temperature of stripper. The MEA solvent is regenerated in stripper at the temperature and pressure higher than the atmosphere. A large quantity of steam (about 50% to 60% of total steam at LP inlet in base plant) is required in the reboiler to regenerate MEA. Low quality steam is usually preferred in the reboiler to avoid significant drop in the plant energy efficiency and, hence, extraction of steam in general is assumed to be carried out from IPT-LPT crossover pipe to meet the huge energy demand in the reboiler.

During the absorption and stripping processes, the equilibrium and kinetic reactions that take place are presented below:

$$H_2O + MEAH^+ \leftrightarrow MEA + H_3O^+ \quad (5.1)$$

$$2H_2O \leftrightarrow H_3O^+ \; OH^- \quad (5.2)$$

$$CO_2 + 2H_2O \leftrightarrow H_3O+ + HCO_3^- \quad (5.3)$$

$$HCO3^- + H_2O \leftrightarrow CO_3^{--} + H3O^+ \quad (5.4)$$

$$CO_2 + OH^- \rightarrow HCO_3^- \quad (5.5)$$

$$HCO_3^- \rightarrow CO_2 + OH^- \quad (5.6)$$

$$MEA + CO_2 + H_2O \rightarrow MEACOO^- + H_3O^+ \quad (5.7)$$

$MEACOO^- + H_3O^+ \rightarrow MEA + H_2O + CO_2$ (5.8)

The equilibrium constants for the reactions (5.1) to (5.4) were calculated from the standard Gibbs free energy change (DGAQFM). DHAQFM and CPAQ0 of $MEAH^+$ and $MEACOO^-$, to calculate the standard $MEAH^+$ and $MEACOO^-$ Gibbs free energy [187]. The kinetic parameters and power law expressions used for the rate-controlled reactions (5.5) to (5.8) [189] are listed in Table 5.4.

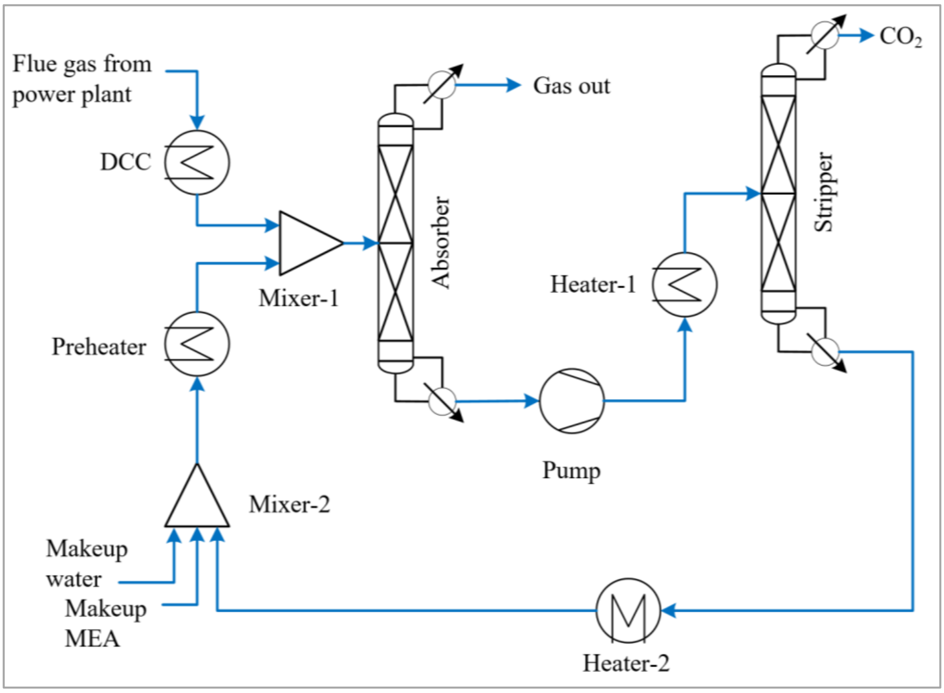

Figure 5.1 Flowsheet of MEA based PCC unit simulated in Aspen Plus.

Table 5.4 Parameters of $k_0$ and E for the kinetic reactions [189].

| Reaction | $k_0$ | E (cal/mol) |
|---|---|---|
| (5.5) | $4.32\times10^{13}$ | 13249 |
| (5.6) | $2.38\times10^{17}$ | 29451 |
| (5.7) | $9.77\times10^{10}$ | 9855.8 |
| (5.8) | $3.23\times10^{19}$ | 15655 |

### 5.2.2 Plant wide simulation of CLC based SupC CFPP for different oxygen carriers

In this section, CLC based CFPP with supercritical steam boiler as discussed in *section 4.2.2* of *Chapter 4* has been considered. In addition to iron oxide oxygen carrier, two more oxygen carriers such as – copper oxide and mixture of 10% copper oxide in iron oxide are used. The general reduction-oxidation reactions of $Fe_2O_3$ oxygen carrier are given in equations (4.1) to (4.4), respectively. The possible reduction-oxidation reaction of coal with copper oxide in the fuel (Equation (5.9) to (5.12)) and air (Equation (5.13) and (5.14)) reactors are given below.

$$4CuO \rightarrow 2Cu_2O + O_2 \tag{5.9}$$

$$C + O_2 \rightarrow CO_2 \tag{5.10}$$

$$CuO + CO \rightarrow Cu + CO_2 \tag{5.11}$$

$$CuO + H_2 \rightarrow Cu + H_2O \tag{5.12}$$

$$Cu_2O + O_2 \rightarrow 2CuO \tag{5.13}$$

$$Cu + 1/2\, O_2 \rightarrow CuO \tag{5.14}$$

## 5.3 Results and discussion

The overall performance of conventional and CLC based SupC CFPPs for all three cases are evaluated in this study. The energy input is uniformly considered for all the cases as 1287 MW (corresponding to coal input of 81.3 kg/s). The performance assessment is conducted based on energy, exergy, ecological and economic analyses.

### 5.3.1 Energy analysis

#### *5.3.1.1 Performance Comparison of plants: CFPP without $CO_2$ capture vs CFPP with conventional MEA capture vs CLC based CFPP for $CO_2$ capture*

In this section, the performance of conventional SupC CFPP without $CO_2$ capture (Case 1), SupC CFPP with $CO_2$ capture using MEA process (Case 2) and CLC based CFPP using $Fe_2O_3$ oxygen carrier (Case 3) are compared. The fuel input energy to the plant, individual unit power production and power consumption are given in the Table 5.5 for all three cases. Table 5.6 compares the overall performance of both the cases based on energy and exergy efficiencies.

In the current scenario, the $CO_2$ capture unit is mandatory to capture the $CO_2$ produced from CFPPs in order to reduce GHG emissions. It can be clearly observed from the comparison of conventional with and without $CO_2$ capture CFPP (case 1 and 2) that this additional $CO_2$ capture unit reduces the net energy and exergy efficiency of conventional SupC CFPP from 37.52% to 28.51% and 33.13% to 26.22%, respectively. The reduction in energy efficiency is due to requirement of large quantity of steam (about 50% to 60% of total steam at LP inlet in base plant) in the reboiler to regenerate MEA. Low quality steam was usually preferred in the reboiler to avoid any significant drop in the plant energy efficiency. This additional power consumption cannot be avoided in other $CO_2$ capture technologies such as oxy-combustion and pre-combustion.

Table 5.5 Energy analysis and $CO_2$ emission for with and without $CO_2$ capture processes.

| Plant Data | Unit | Conv. CFPP without $CO_2$ capture | Conv. CFPP with $CO_2$ capture | CLC-CFPP using $Fe_2O_3$ |
|---|---|---|---|---|
| Fuel input energy | MW | 1286.98 | 1286.98 | 1286.98 |
| Net GT output | MW | 0.00 | 0.00 | 233.02 |
| HPT | MW | 162.88 | 162.88 | 81.68 |
| IPT | MW | 233.03 | 233.03 | 125.27 |
| LPT | MW | 126.16 | 47.94 | 63.26 |
| ST output | MW | 522.07 | 443.85 | 270.21 |
| Gross turbine power output | MW | 522.07 | 443.85 | 503.22 |
| Power consumption in $CO_2$ compression | MW | 0.00 | 43.62 | 19.25 |
| Auxiliary loss | MW | 39.16 | 33.29 | 20.27 |
| Net power consumption | MW | 39.16 | 76.91 | 39.51 |
| Net electric power output | MW | 482.91 | 366.94 | 463.71 |

The competitiveness of post-combustion (MEA based) with CLC technology has also been analysed on the basis of net energy and exergy efficiencies. The results indicates that, the gross energy and exergy efficiency of conventional SupC CFPP with $CO_2$ capture are 34.49% and 31.71% while the gross energy and exergy efficiency of CLC based SupC CFPP using $Fe_2O_3$ OC are 39.10% and 35.96%, respectively (Table 5.6). The higher gross efficiency in CLC based SupC CFPP is due to the additional power produced in the gas turbine. Similar results were observed by Mukherjee et al. [80] and Cormos and Cormos [190] for gas and steam turbines. Although the energy consumed by air compressor of CLC plant is more than the conventional SupC CFPP with $CO_2$ capture, the net energy efficiency of CLC based SupC CFPP is higher than the conventional CFPP with PCC. This is due to the condensation and separation technology of CLC based plant that consumes less amount of energy as compared with the conventional plant. In the case of CLC based CFPP, the flue gas consists mainly $CO_2$ and steam. This enables the system to capture almost 100% $CO_2$ by means of condensation and separation.

Table 5.6 Performance comparison of SupC CFPP for with and without $CO_2$ capture processes.

| Parameter | Unit | Conv. CFPP without $CO_2$ capture | Conv. CFPP with $CO_2$ capture | CLC-CFPP using $Fe_2O_3$ |
|---|---|---|---|---|
| Fuel exergy | MW | 1399.57 | 1399.57 | 1399.57 |
| Gross electric efficiency | % | 40.57 | 34.49 | 39.10 |
| Net electric efficiency | % | 37.52 | 28.51 | 36.03 |
| Gross exergy efficiency | % | 37.30 | 31.71 | 35.96 |
| Net exergy efficiency | % | 34.50 | 26.22 | 33.13 |

#### *5.3.1.2 Comparison CLC-CFPP plant performance for different oxygen carriers*

In this section, the CLC integration of SupC CFPP using $Fe_2O_3$, CuO and bimetallic (mixture of 90% $Fe_2O_3$ and 10% CuO, mass basis) as oxygen carriers are considered as part of Case 3 and the performances are compared. The overall heat produced in the CLC system depends on the type of oxygen carrier used for CLC reactors [127]. In all the three cases of CLC plant, the total heat produced is in the two separate reactors (i.e. air and fuel reactors). Thus, the heat available for the steam generation is the difference between the total heat available from both CLC reactors and heat energy of depleted air available at the exit of gas turbine. Table 5.7 represents the comparison of CLC-CFPP using different oxygen carriers based on energy analysis and Table 5.8 shows the overall performance of these cases. The net energy efficiency of CLC-CFPP using $Fe_2O_3$, CuO and bimetallic oxygen carriers are found to be 36.03%, 41.72% and 38.39%, respectively. The net power production for CLC plant using $Fe_2O_3$, CuO and bimetallic OC are found to be 463.71 MW, 536.93 MW, and 494.07 MW, respectively. It is observed that, the CuO oxygen carrier in CLC based CFPP has higher net power production than the $Fe_2O_3$ oxygen carrier. The higher net power generation or net energy efficiency for CLC plant with CuO is because of its higher oxygen carrying capacity when CuO is reduced to Cu and which led to the use of lower oxygen carrier to coal ratio. In addition, the reaction mechanism of the CuO is different from Fe2O3 as it releases oxygen, which directly reacts with carbon present in the solid coal particles. This also contributes to the improvement in the performance in reality. The addition of 10% CuO in $Fe_2O_3$ improved the overall plant performance by 2.36% net energy efficiency and 2.17% net exergy efficiency when compared with the $Fe_2O_3$ alone.

Table 5.7 Energy analysis of CLC-CFPPs using different oxygen carriers.

| Plant Data | Unit | CLC-CFPP using $Fe_2O_3$ | CLC-CFPP using CuO | CLC-CFPP using bimetallic OC |
|---|---|---|---|---|
| Fuel input energy | MW | 1286.98 | 1286.98 | 1286.98 |
| Net GT output | MW | 233.02 | 256.92 | 249.70 |
| HPT | MW | 81.68 | 97.79 | 86.14 |
| IPT | MW | 125.27 | 149.98 | 132.11 |
| LPT | MW | 63.26 | 75.75 | 66.72 |
| ST output | MW | 270.21 | 323.52 | 284.97 |
| Gross turbine power output | MW | 503.22 | 580.44 | 534.67 |
| Power consumption in $CO_2$ compression | MW | 19.25 | 19.25 | 19.23 |
| Auxiliary loss | MW | 20.27 | 24.26 | 21.37 |
| Net power consumption | MW | 39.51 | 43.51 | 40.60 |
| Ne electric power output | MW | 463.71 | 536.93 | 494.07 |

Table 5.8 Comparison of performance factor of CLC-CFPP's using different oxygen carriers.

| Parameter | Unit | CLC-CFPP using $Fe_2O_3$ | CLC-CFPP using CuO | CLC-CFPP using bimetallic OC |
|---|---|---|---|---|
| Fuel exergy | MW | 1399.57 | 1399.57 | 1399.57 |
| Gross electric efficiency | % | 39.10 | 45.10 | 41.54 |
| Net electric efficiency | % | 36.03 | 41.72 | 38.39 |
| Gross exergy efficiency | % | 35.96 | 41.47 | 38.20 |
| Net exergy efficiency | % | 33.13 | 38.36 | 35.30 |

### 5.3.2 Exergy analysis

The concept of exergy destruction is used to determine the term that is dependent of both energy flow and environmental parameters. The net exergy destruction of the main components of conventional and CLC based CFPPs is given in the Figure 5.2. Table 5.9 shows the unit wise exergy efficiency of conventional and CLC based CFPPs. As mentioned in *Chapter 4*, the term boiler includes a combustor (in conventional SupC CFPP) or CLC unit (in CLC based SupC CFPP), economizer, evaporator, superheater and a reheater.

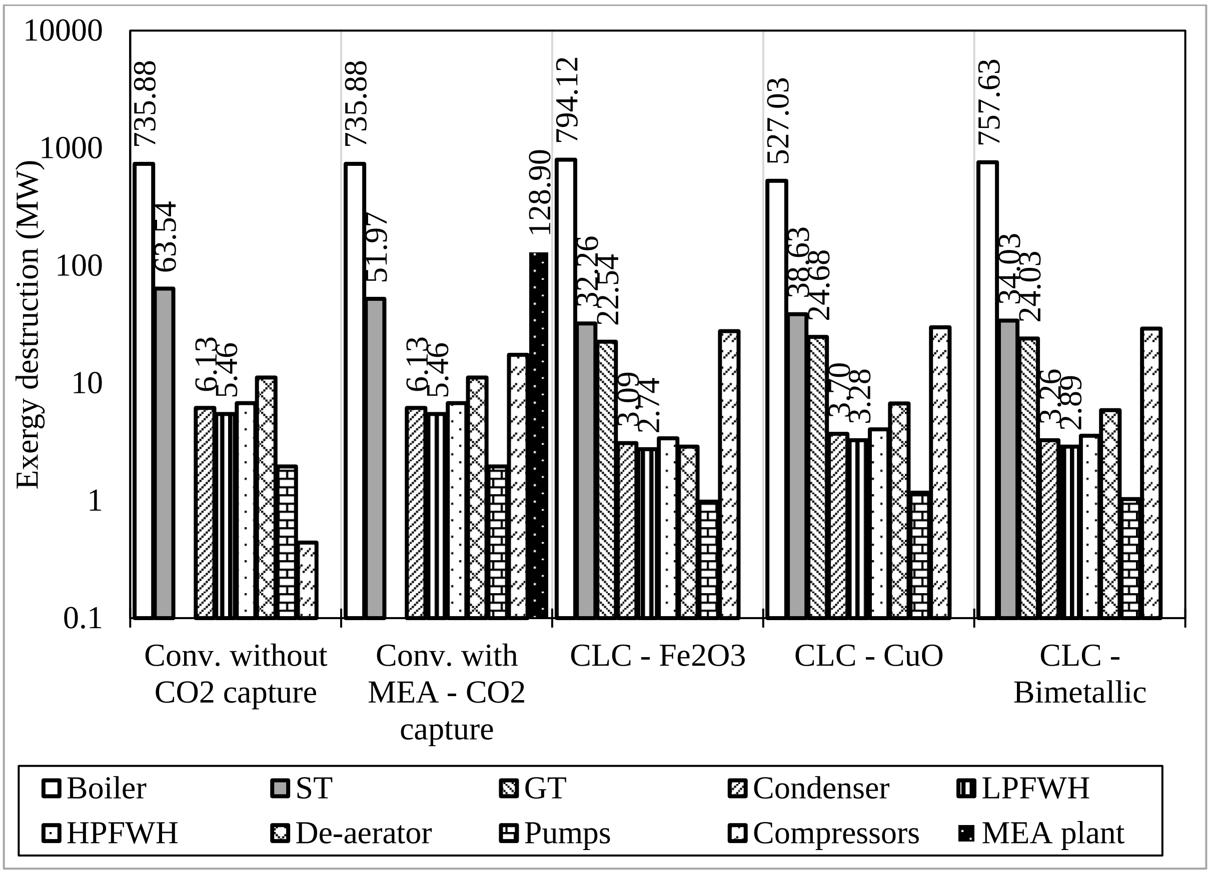

Figure 5.2 Exergy destruction of the main components of conventional and CLC based SupC CFPP.

Based on exergy balances, the highest magnitude of exergy destruction is observed in the boiler section of all the cases. This is mainly due to the higher operating conditions, heat transfer processes and mass flow rates of gas and solid streams. For the case of CLC based plant with CuO oxygen carrier, the required mass flow rate of solids is lower than the CLC based plant with $Fe_2O_3$ oxygen carrier. This is due to their oxygen carrying capacity. This results lower exergy destruction in the boiler for the case of CLC based CFPP using CuO. The exergy destruction rates are found to be 794.12 MW, 527.03 MW and 757.63 MW for CLC-CFPP with $Fe_2O_3$, CuO, and bimetallic oxygen carriers, respectively. The corresponding exergy efficiencies of boilers of CLC based CFPPs using $Fe_2O_3$, CuO, and mixture of $Fe_2O_3$ and CuO were 59.91%, 72.02%, and 62.41%, respectively. It was found that the exergy efficiency of boiler unit in CuO case is high as compared to other cases due to the lower exergy destruction in it.

Table 5.9 Individual exergy efficiency (%) of conventional and CLC based CFPPs.

| Block | Conv. CFPP without $CO_2$ capture | Conv. CFPP with $CO_2$ capture | CLC-CFPP using $Fe_2O_3$ | CLC-CFPP using CuO | CLC-CFPP using bimetallic |
|---|---|---|---|---|---|
| Boiler | 62.39 | 62.39 | 59.91 | 72.02 | 62.41 |
| HPT | 96.67 | 96.67 | 96.67 | 96.67 | 96.67 |
| IPT | 95.29 | 95.29 | 95.13 | 95.13 | 95.13 |
| LPT | 89.33 | 89.33 | 89.33 | 89.33 | 89.33 |
| GT | 0.00 | 0.00 | 96.24 | 96.24 | 96.24 |
| Condenser | 66.35 | 66.35 | 66.22 | 66.22 | 66.22 |
| Condenser Pump | 95.31 | 95.31 | 95.31 | 95.31 | 95.31 |
| LPF Pump | 93.97 | 93.97 | 93.97 | 93.97 | 93.97 |
| HPF Pump | 96.95 | 96.95 | 96.95 | 96.95 | 96.95 |
| LPFWH 1 | 80.85 | 80.85 | 80.85 | 80.85 | 80.85 |
| LPFWH 2 | 91.29 | 91.29 | 91.29 | 91.29 | 91.29 |
| LPFWH 3 | 87.63 | 87.63 | 87.63 | 87.63 | 87.63 |
| LPFWH 4 | 96.33 | 96.33 | 96.33 | 96.33 | 96.33 |
| HPFWH 1 | 97.78 | 97.78 | 97.78 | 97.78 | 97.78 |
| HPFWH 2 | 97.13 | 97.13 | 97.13 | 97.13 | 97.13 |
| HPFWH 3 | 98.79 | 98.79 | 98.79 | 98.79 | 98.79 |
| De-aerator | 79.07 | 79.07 | 87.99 | 79.07 | 79.07 |
| CO2 Compressor | 0.00 | 61.25 | 94.60 | 94.60 | 94.60 |
| Air Compressor | 72.14 | 72.14 | 88.06 | 88.06 | 88.06 |
| MEA | 0.00 | 46.43 | 0.00 | 0.00 | 0.00 |

Higher energy is required for the air compressor to maintain the pressure of feed air into the air reactor. This causes higher exergy destruction in air compressors for all CLC based CFPPs compared to conventional CFPP. In addition, higher energy is required to compress the $CO_2$ from 1.013 bar to 110 bar (conventional CFPP with $CO_2$ capture) than compressing $CO_2$ from 10 bar to 110 bar (CLC integrated CFPP). This ultimately results in higher exergy destruction in $CO_2$ capture unit in conventional CFPP as compared to that of CLC based CFPP.

Furthermore, the MEA based PCC in the conventional CFPP has about 128.90 MW of exergy destruction with 46.43% exergy efficiency due to the large amount of energy loss in the absorber and stripper. Apart from these units, the exergy destruction and exergy efficiency of all other units were similar in all the cases except the gas turbine.

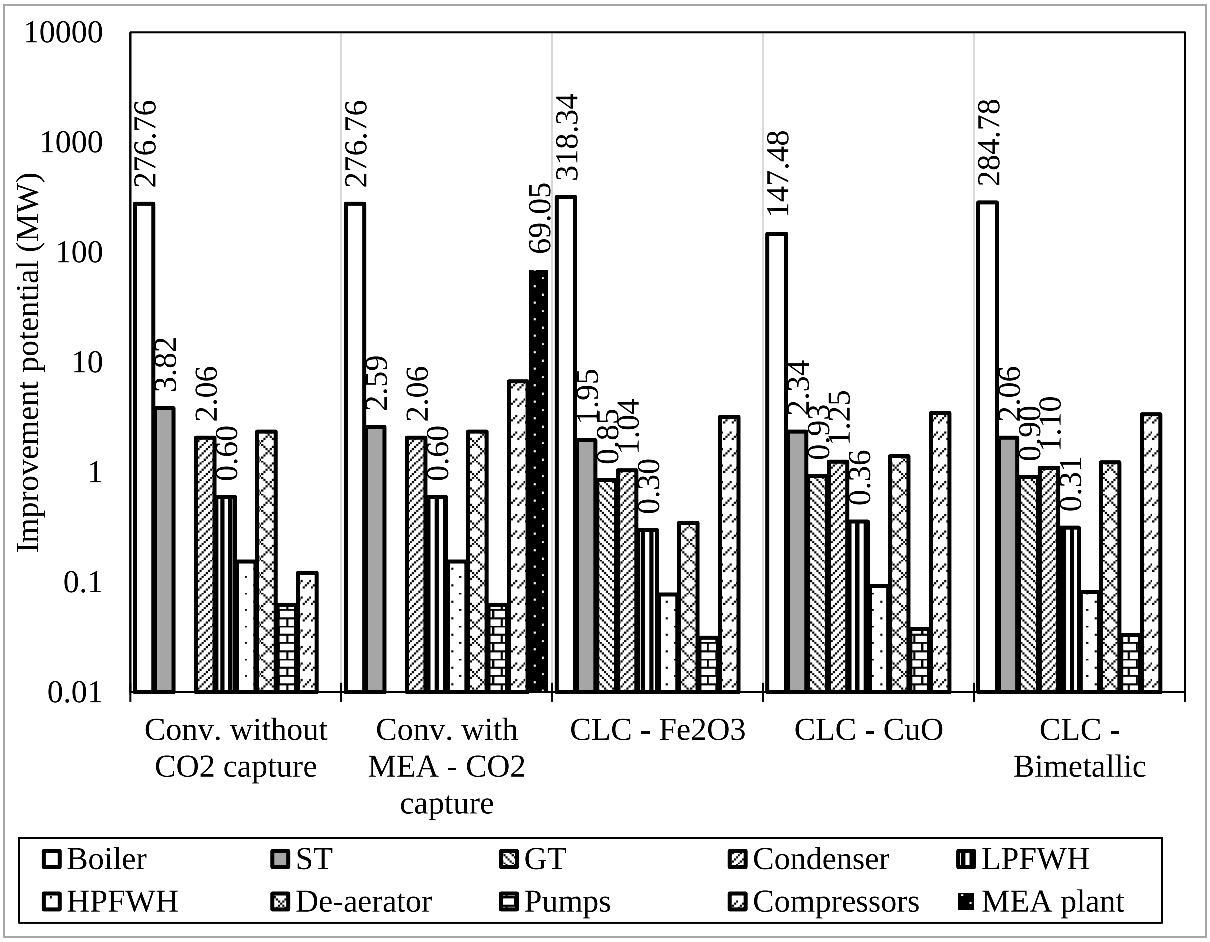

Figure 5.3 Improvement potential of the main components of conventional and CLC based SupC CFPP.

The exergy destruction of boiler (76.21% - 89.27%) dominates the overall exergy destruction, followed by the exergy destruction of steam turbines (3.95% - 7.64%). In addition, the MEA PCC consumes about 13.35% of overall exergy destruction for conventional plant with $CO_2$ capture. In summary, the boiler proves to be a highly energy sensitive unit in the plant, and reduces the overall exergy efficiency of the plant significantly. The exergetic improvement potential of main units for all the cases is given in Figure 5.3. The highest exergy destruction in the boiler unit reflects the higher improvement potential of 276.76 MW, 276.76 MW, 318.34 MW, 147.48 MW and 284.78 MW for the conventional plant without CO2 capture, conventional plant with $CO_2$ capture, CLC-CFPP using $Fe_2O_3$, CuO and bimetallic oxygen carriers, respectively. The possible improvement potential in other units of the all cases is found to be low except the MEA plant for the Case 2, which has improvement potential of about 69.05 MW.

### 5.3.3 Ecological analysis

In this chapter, the ecological analysis is carried out to assess the effect of the $CO_2$ capture unit on conventional and CLC based CFPPs. Comparison based on ecological analysis with various environmental parameters is summarized in Table 5.10. As the conventional plant without $CO_2$ capture (Case 1) in the present study are not equipped with a capture unit, they emit around 101.82 kg/s of carbon dioxide into the environment. Integration of MEA based $CO_2$ capture process in the same plant reduces $CO_2$ emissions from 102.82 kg/s to 4.87 kg/s. On the contrary, the CLC based CFPPs with all three oxygen carriers capture nearly all the CO2 from the flue gas leaving fuel reactor. The conventional CFPP without $CO_2$ capture release $2.57 \times 10^9$ kg of $CO_2$ annually. The same plant with MEA based $CO_2$ capture results in reduction of $2.447 \times 10^9$ kg of $CO_2$, whereas for all the CLC cases, zero $CO_2$ emissions are attained. Accordingly, annual $CO_2$ avoided per fuel consumption is found to be 62.96 kg of $CO_2$/GJ for CLC cases. These annual $CO_2$ avoided per unit fuel consumption values are same as given in the Chapter 4 for the different steam boiler configurations using CLC technology.

Table 5.10. Comparison of conventional and CLC based plants based on ecological assessment.

| Parameter | Unit | Conv. CFPP without $CO_2$ capture | Conv. CFPP with $CO_2$ capture | CLC-CFPP using $Fe_2O_3$ | CLC-CFPP using CuO | CLC-CFPP using bimetallic |
|---|---|---|---|---|---|---|
| $CO_2$ emission | kg/s | 101.82 | 4.87 | 0.00 | 0.00 | 0.00 |
| $CO_2$ captured | kg/s | 0.00 | 96.92 | 102.55 | 102.55 | 102.57 |
| $CO_2$ capture efficiency | % | 0.00 | 95.22 | 100.00 | 100.00 | 100.00 |
| Specific $CO_2$ emission | kg/MWh | 759.03 | 47.75 | 0.00 | 0.00 | 0.00 |
| Annual $CO_2$ emission | kg | $2.57 \times 10^9$ | $0.123 \times 10^9$ | 0.00 | 0.00 | 0.00 |
| Average annual emission rate | kg.$CO_2$/GJ | 62.51 | 2.99 | 0.00 | 0.00 | 0.00 |

| | | | | | | |
|---|---|---|---|---|---|---|
| aggravating per unit of fuel | | | | | | |
| Annual $CO_2$ avoided emission per unit fuel | kg.$CO_2$/GJ | 0.00 | 59.50 | 62.96 | 62.96 | 62.96 |
| Net electric output per kg of $CO_2$ captured | MW/kg | - | 3.79 | 4.52 | 5.24 | 4.82 |

### 5.3.4 Economic analysis

Having proven the technical feasibility of the CLC, it is essential to compare the economic feasibility of the plants to check the feasibility of all three oxygen carriers. Table 5.11 shows the economic performance indicators for the above-studied conditions for all the conventional and CLC based plants. The specific cost of the conventional CFPP with $CO_2$ capture is found to be more by 385.87 €/kW$_{gross}$ than the conventional CFPP without $CO_2$ capture, due to the additional capital cost of MEA based capture process. Moreover, a part of steam from the low pressure turbine is used to compensate the energy requirement in the MEA based capture process which results in lower steam turbine power output compared to that without $CO_2$ capture plant. These figures are in good agreement with the estimated range given in the literature [167,180]. The specific capital costs of CLC based plants are estimated to be 1039.84 €/kW$_{gross}$ (for CLC using $Fe_2O_3$), 1004.51 €/kW$_{gross}$ (for CLC using CuO) and 1017.09 €/kW$_{gross}$ (for CLC using bimetallic OC). The results indicate that the specific capital cost is lower for the CLC based CFPP using CuO compared to all other cases. This is because of the lower ratio of total capital cost to the plant power output in case of CLC based CFPP.

The LCOE associated with the CLC plants using $Fe_2O_3$, CuO and bimetallic OC are estimated to be 89.05 €/MW.h, 98.25, and 91.95 €/MW.h, respectively. The magnitudes of these costs of electricity are in the range as explained in the *Chapter 4*. Though the net power generation for CuO case is high, the operating cost due to use of copper oxide results in higher LCOE.

The cost of $CO_2$ avoided per ton of $CO_2$ is found to be lower for the conventional CFPP with $CO_2$ capture (36.91 €/t$CO_2$) compared to other all cases. This is because of the lower LCOE difference between the plant with $CO_2$ capture and without $CO_2$ capture. The conventional plant with PCC has lowest LCOE$_{overall}$ of 85.48 €/MW.h. Though the MEA based conventional CFPP has lowest LCOE$_{overall}$, the plant capture only 95.22% of $CO_2$ emitted from CFPP. This shows that the CLC based CFPP with supercritical steam generation technology would be economically favoured option compared to conventional and other CLC based CFPPs.

As all the CLC based CFPPs are resulting in zero emission, LCOE and $LCOE_{overall}$ are similar for these plants. The CLC based CFPPs have better $LCOE_{overall}$ compared to the conventional plant without $CO_2$ capture. It can also be seen that, addition of 10% CuO in the $Fe_2O_3$ in the CLC based plant increased overall LCOE by 2.90 €/MW.h only.

Table 5.11. Economic performance indicators under initial design conditions.

| Parameter | Unit | Conv. CFPP without $CO_2$ capture | Conv. CFPP with $CO_2$ capture | CLC-CFPP using $Fe_2O_3$ | CLC-CFPP using CuO | CLC-CFPP using bimetallic |
|---|---|---|---|---|---|---|
| Specific capital cost | €/$kW_{gross}$ | 1266.10 | 1651.96 | 1039.84 | 1004.51 | 1017.09 |
| LCOE | €/MW.h | 56.34 | 82.59 | 89.05 | 98.25 | 91.95 |
| $CO_2$ avoided cost | €/$tCO_2$ | - | 36.91 | 43.10 | 55.21 | 46.92 |
| $\mathrm{LCOE}_{\mathrm{overall}}$ | €/MW.h | 102.23 | 85.48 | 89.05 | 98.25 | 91.95 |

Thus based on the 4-E analyses as given above, the choice of CLC based SupC CFPP using bimetallic oxygen carrier is the promising option for the growing countries, where coal is a primary source of energy and iron ores are available at lower cost compared to copper ores [117,191]. Keeping all this in view, the mixture of $Fe_2O_3$ and CuO is preferable option as compared to CuO and $Fe_2O_3$ alone.

## 5.4 Summary

In this chapter, steady state simulations of CLC based SupC CFPP using different oxygen carriers along with the conventional SupC CFPP with and without $CO_2$ capture are carried out using aspenONE v10.0. The conventional technology with and without $CO_2$ capture and the advanced CLC technologies for Indian coal were compared in terms of 4-E (energy, exergy, ecological and economic) analyses. It is observed from this study that, the MEA based post-combustion $CO_2$ capture technology contributes about 7.52% net energy penalty and 6.91% exergy penalty in the overall plant performance with 95.22% $CO_2$ capture efficiency. The integration of CLC technology using $Fe_2O_3$ as oxygen carrier improved the net energy efficiency by 7.52% compared to the conventional CFPP with $CO_2$ capture for approximately

100% $CO_2$ capture efficiency. Highest net energy efficiency of 41.72% was observed for CLC SupC CFPP using CuO as oxygen carrier; however, addition of 10% CuO in $Fe_2O_3$ improved the net energy efficiency by 2.36% compared to $Fe_2O_3$ alone. The $CO_2$ avoided cost and LCOE are found to be lower for the conventional CFPP with 95.22% $CO_2$ capture. The overall LCOE of CLC based CFPP using $Fe_2O_3$, CuO and bimetallic OC are found to be 89.05 €/MW.h, 98.25 €/MW.h and 91.95 €/MW.h, respectively. Based on the 4-E analyses, the study recommends bimetallic oxygen carrier (i.e. mixture of $Fe_2O_3$ and CuO) to be preferable option as compared to CuO and $Fe_2O_3$ alone.

# *Chapter 6*

# CLC based coal fired power plant for hydrogen and power co-generation

# Chapter 6

# *CLC based coal fired power plant for hydrogen and power co-generation*

The best configuration from *Chapter 4* and *Chapter 5 is utilized for further investigation of hydrogen generation* from CLC technology in this chapter to address the third objective of the thesis work. A three-reactor CLC based supercritical coal fired power plant for hydrogen and power co-generation using iron oxide and bimetallic oxygen carrier is presented in this chapter. Further, a sensitivity analysis is conducted on three-reactor CLC system. The overall performance of this hydrogen and electricity co-generation power plant is compared based on energy, exergy, ecological and economic analyses.

## 6.1 Background and motivation

Hydrogen is an important feedstock to the formic acid synthesis, methanol synthesis, ammonia synthesis and oil refining. It is also an environmental friendly renewable energy source for the transportation and power generation in the future [130]. Chemical-looping combustion is an attractive technology for power and $H_2$ co-generation with the inherent $CO_2$ capture [133]. The three-reactor CLC system is used for the production of hydrogen as given in *Chapter 3*.

The literature on the coal based CLC based power plants with power and hydrogen co-generation is limited and a very less recent literature is found on the coal-based power plants for hydrogen co-generation. The studies available on the CLC based CFPP for $H_2$ and power co-generation are mainly focused on the evaluation of electrical efficiency, energy efficiency and environmental parameters. Limited studies are found in the literature that provides comprehensive analysis from the energetic and exergetic analyses in co-generation plants. In addition to the energy and exergy analyses, the economic analysis and environmental impact is necessary for a comprehensive technoeconomic analysis of the power production system [25]. A comprehensive report on the CLC based CFPP for power and $H_2$ co-generation comprising of these four metrics is not available in the literature. This kind of a comprehensive analysis is required for feasibility assessment and to make policy decisions on establishing the environmental friendly co-generation power plants in future. This part of the work attempts to fill this gap by adapting a comprehensive assessment, by using all the above four aspects on integration of three-reactor coal-direct chemical looping combustion plant for flexible hydrogen generation along with electricity. The objective of this work is to propose CLC based CFPP configuration with the flexible electric power (462 MW to 157 MW) and hydrogen (0 MW to 900 MW) co-generation. The plant configurations, simulation of these plants, assumptions, assessment techniques and validation of the three reactor configuration are detailed in the Chapter 3. Sensitivity analysis of the CLC based power plant and the performance analysis and comparison of these flexible output configurations among themselves and against conventional supercritical power plant without $CO_2$ capture based on the 4-E analyses are discussed in detail in results and discussion section. Finally, the major findings of the study are concluded in the summary.

## 6.2 Model description and plant configuration

In this study, three cases of plant configurations - conventional SupC CFPP for power generation without $CO_2$ capture (see *Chapter 4*), CLC based SupC CFPP for power generation only (see *Chapter 5*) and SupC CLC based CFPP for power and hydrogen co-generation layouts as listed in Table 6.1 are considered and simulated. These three cases belong to Categories 1 to 3 respectively as defined in *Chapter 3* and the simplified block diagrams of these plants are shown in Figure 3.1, 3.2 and 3.3, respectively. The process models of these plant flowsheets are developed at supercritical steam generation conditions using aspenONE v10.0 from Aspen Technology, Inc., USA.

Table 6.1 The description of conventional and CLC cases used in present study.

| Case | Plant | $CO_2$ capture | Power and/or $H_2$ co-generation |
|---|---|---|---|
| 1 | Conventional SupC CFPP | No | Power only |
| 2 | SupC CLC based CFPP | Yes | Power only |
| 3 | SupC CLC basedCFPP | Yes | Power & Hydrogen |

For the direct comparison of all the cases, common assumptions are considered. The operating parameters, reference environment conditions and the key assumptions are given in Table 3.3 and 3.4 of *Chapter 3*.

A process flow diagram of SupC CLC based coal-fired power plant for power and hydrogen co-generation is shown in Figure 6.1. The CLC system is mainly composed of three reactors (air, steam and fuel reactors), air compressor, gas turbine unit, heat recovery steam generation (HRSG), $CO_2$ separator and compressor units, steam turbine, feed water heaters (FWHs), de-aerator unit and condenser.

In this study, a bimetallic oxygen carrier (mixture of 90% $Fe_2O_3$ and 10% CuO) supported on $Al_2O_3$ is used as solid metal oxides and circulated in the CLC loop to improve the overall plant efficiency. Though CuO doesn't take part in the generation of hydrogen, the overall plant performance can be improved [128]. The coal is combusted in the fuel reactor in presence of CuO and $Fe_2O_3$ to reduce them to Cu and Fe/FeO. The reduced Fe/FeO are partially oxidized to FeO/$Fe_3O_4$ in the steam reactor (multi-stage moving bed RGibbs reactor) in presence of steam. These partially oxidized iron oxide particles (FeO/$Fe_3O_4$) and Cu are oxidised back to their original form (CuO/$Fe_2O_3$) in an air reactor (single stage RGibbs reactor) of the three-reactor CLC system. The reactions involved in individual reactors [11,73] are given below:

***Fuel Reactor:***

$$4CuO \rightarrow 2Cu_2O + O_2 \tag{6.1}$$

$$Cu_2O + C \rightarrow Cu + CO_2 \tag{6.2}$$

$$C + O_2 \rightarrow CO_2 \tag{6.3}$$

$$CO_2 + C \rightarrow 2CO \tag{6.4}$$

$$3Fe_2O_3 + CO \rightarrow 2Fe_3O_4 + CO_2 \tag{6.5}$$

$$Fe_3O_4 + CO \rightarrow 3FeO + CO_2 \tag{6.6}$$

$$FeO + C \rightarrow Fe + CO \tag{6.7}$$

***Steam Reactor:***

$$Fe + H_2O \rightarrow FeO + H_2 \tag{6.8}$$

$$3FeO + H_2O \rightarrow Fe_3O_4 + H_2 \tag{6.9}$$

***Air Reactor:***

$$4FeO + O_2 \rightarrow 2Fe_2O_3 \tag{6.10}$$

$$4Fe_3O_4 + O_2 \rightarrow 6Fe_2O_3 \tag{6.11}$$

$$2Cu + O_2 \rightarrow 2CuO \tag{6.12}$$

$$2Cu_2O + O_2 \rightarrow 4CuO \tag{6.13}$$

The gaseous streams leaving the fuel, steam and air reactors are $CO_2$-rich, $H_2$-rich and $N_2$-rich, respectively. The $N_2$-rich gas stream is sent to the gas expander/turbine to generate the power. A part of power generated in the gas turbine unit is provided to compress the air to the 15.75 bar pressure. The $N_2$-rich stream leaving gas turbine still carries heat, which is recovered in the HRSG unit. The $CO_2$-rich, $H_2$-rich and $N_2$-rich gases are passed through the evaporator, superheater, reheater and economiser of the HRSG unit to generate the high pressure steam (242.2 bar and 537°C) and intermediate pressure steam (42 bar and 565°C). The $H_2$-rich stream is comprised of steam and hydrogen, hence, steam is condensed and hydrogen is separated, compressed and stored. The $CO_2$-rich stream is comprised of $CO_2$, steam and other gases in the flue gas. The steam is condensed to separated gases. The cold gas stream is further sent to the selexol based acid gas removal (AGR) unit, where 99.99% $H_2S$ is removed from the $CO_2$.

These steams are expanded in the series of steam turbines to generate the power. A part of steam leaving these steam turbines is utilised in the FWHs to preheat the feed-water entering evaporator of HRSG unit. The three high-pressure FWHs, one deaerator and four low-pressure FWHs have been considered for the SupC power plants. The split ratios of the streams leaving the steam turbines is reported by Suresh et al. [5] and is considered constant for all the cases.

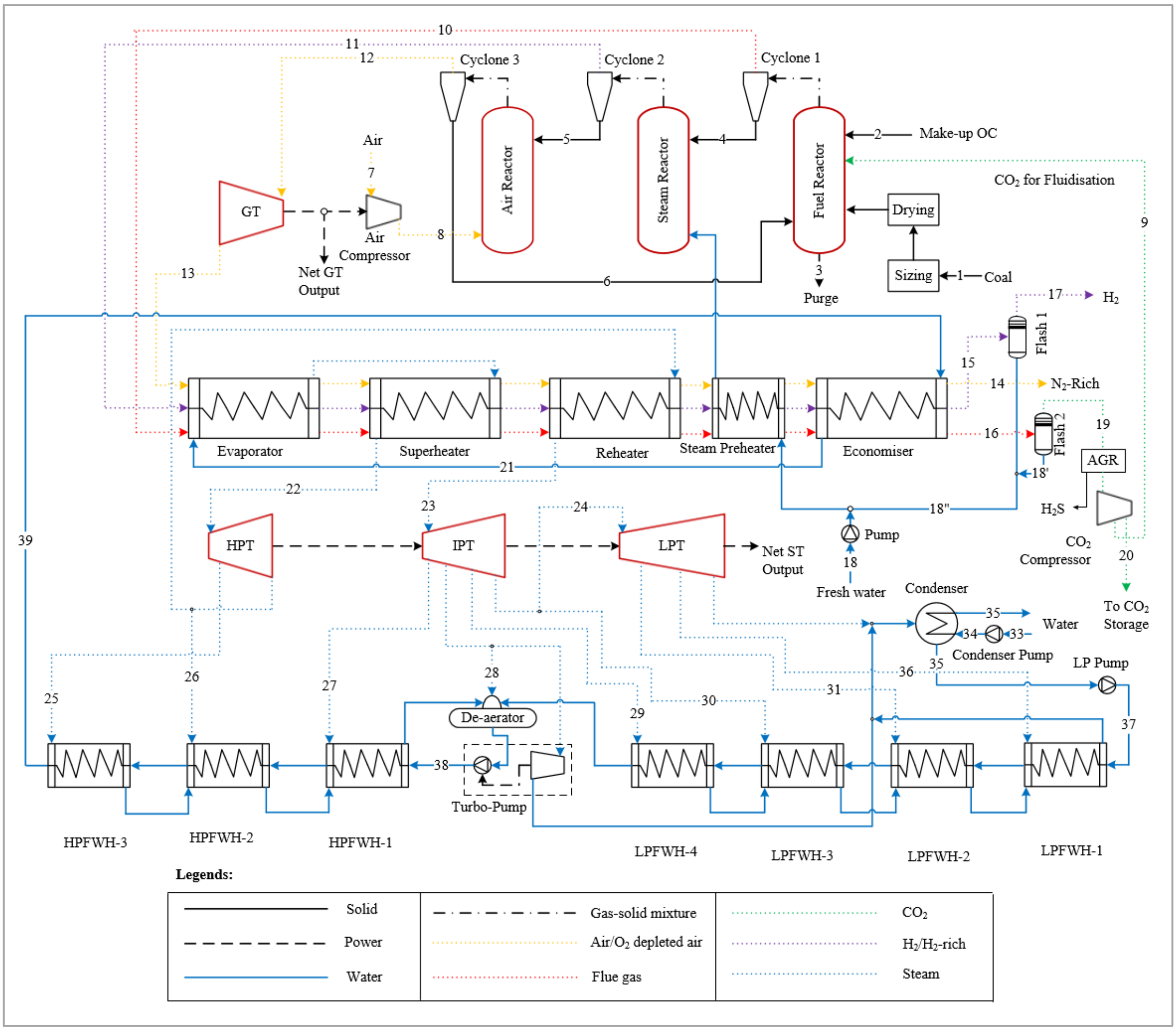

Figure 6.1 Process flow diagram of supercritical CLC based CFPP for power and hydrogen co-generation.

## 6.3 Results and discussion

In this section, comprehensive 4-E (energy, exergy, ecological and economic) analyses are carried out for SupC CLC based co-generation plant. The results of CLC based CFPP with $H_2$ co-generation plant are compared with the conventional SupC CFPP and CLC based CFPP without hydrogen generation. In this comparison, the CLC based CFPP is considered for 50% hydrogen and 50% power co-generation. A sensitivity analysis of several sensitive parameters of three-reactor CLC system is carried out to optimise the overall performance of power plant. Further, a comparison among the CLC based CFPP with different ratios of $H_2$ and power generation has been presented as a parametric study.

A constant energy input of 1287 MW (based on HHV of coal) to all the power plant cases has been considered for a fair comparison among all the cases. The operating conditions used in conventional and CLC based CFPP are given in *Section 3.1* of *Chapter 3*.

## 6.3.1 Sensitivity analysis

Sensitivity analysis for the key operating parameters of the three-reactors system of CLC based CFPP for $H_2$ co-generation such as operating pressure and operating temperatures of the reactors has been conducted. It is carried out by estimating the effect of these parameters on the overall energy and exergy efficiency of the plant by varying one parameter at a time while fixing the other parameters. The values of the parameters reported by He et al. [128] are taken as the base values for this sensitivity study. The sensitivity analysis is also carried for the constant hydrogen generation of 500 MW. The optimal values of these sensitive parameters obtained from this analysis have been used for further study. A comparison of the plant efficiencies obtained with the optimal values of the parameters against those obtained with the values reported by He et al. [128] is also presented.

### *6.3.1.1 Effect of operating pressure*

To study the effect of operating pressure of the three reactors system on the $H_2$ co-generation plant efficiency, the operating temperatures of air, steam and fuel reactors are fixed at 1169$^oC$, 750$^oC$ and 900$^oC$, respectively as reported in He et al. [128]. The performance of the plant is simulated by varying the operation pressure of the reactor system in the range of atmospheric pressure (i.e. 1.013 bar) to 40 bar. Figure 6.2 shows the variation in net electric energy and exergy efficiency with CLC reactors system operating pressure. Both efficiencies are found to be the lowest at atmospheric pressure and increased with increase in operating pressure. The increase in these efficiencies is reduced beyond 15 bar pressure, which can be noticed from the minimal change in the efficiencies. This is mainly due to increase in the net gas turbine power output and decrease in the steam turbine power output. Similar trends are reported for CLC based CFPP with power generation only case in the literature [178]. Hence operating air, steam and fuel reactors above 15 bar pressure is not much energy efficient.

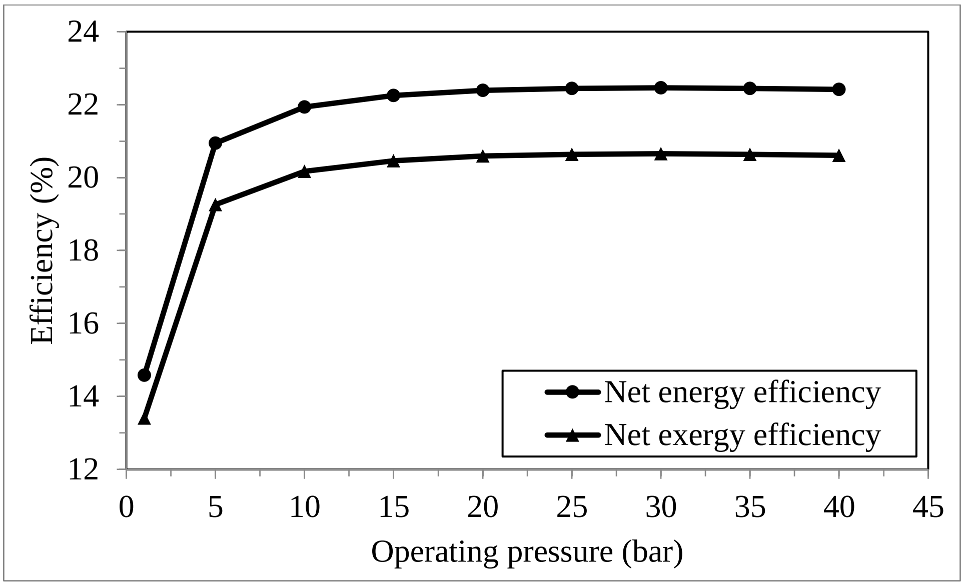

Figure 6.2 Effect of operating pressure on overall energy and exergy efficiencies.

### *6.3.1.2 Effect of operating temperatures of the three reactors*

The effect of operating temperatures of air, fuel and steam reactors on the overall plant performance is studied for the optimal operating pressure of 15 bar. The operating temperatures of three reactors is studied individually by varying one reactor temperature while keeping the temperatures of other two reactors fixed.

The effect of fuel reactor temperature is studied for constant air reactor and steam reactor temperatures of 1169°C and 750°C, respectively. Figure 6.3(a) shows the effect of fuel reactor temperature on the net electric energy and exergy efficiencies. The net electric energy and exergy efficiencies are found to be increasing with increase in the fuel reactor temperature from 600°C to 900°C and decreasing with further increase in the fuel reactor temperature. The endothermic nature of the fuel reactor necessitates supply of heat to the fuel reactor via solid oxygen carrier particles from air reactor. The peak in the efficiencies is observed at 900°C as maintaining fuel reactor temperature beyond 900°C requires more amount of heat to be supplied, resulting in the reduction of the heat availability in the HRSG section, which ultimately results in the reduction of the overall plant performance.

Copper oxide has gained a great attention in CLC system as it has some advantageous characteristics of high oxygen carrying/transport capacity, high reactivity, moderate cost, being exothermic during fuel combustion and having suitable equilibrium partial pressure of $O_2$ at 800 to 1000°C [89,192]. However, pure copper oxide oxygen carrier suffers from a tendency towards agglomeration and sintering upon full reduction to *Cu* with low melting temperature about 1083°C. This limits fuel reactor to operate at lower temperature (i.e. 800 to 850°C) which is advantageous for defluidisation, agglomeration and sintering but disadvantageous for achieving fast reaction kinetics and high energy utilization efficiency [193]. The active component CuO supported on $Al_2O_3$ can withstand high temperature such as 900 to 1000°C [194]. Moreover, present work does not use copper oxide directly; instead a bimetallic oxygen carrier supported on aluminium oxide (i.e. 7% CuO, 63% $Fe_2O_3$ and 30% $Al_2O_3$ on mass basis) is used. Hence, this bimetallic oxygen carrier does not result in partial melting and sintering of copper-based oxygen carrier at 900°C.

The optimal value of fuel reactor temperature of 900°C and air reactor temperature of 1169°C are considered to study the effect of steam reactor temperature on the plant performance. Figure 6.3(b) shows the effect of steam reactor temperature on overall performance of CLC based plant. The net electric energy and exergy efficiencies are found to increase with increase in steam reactor temperature up to 750°C. The reactions in steam reactor are both endothermic and exothermic as oxygen carrier is partially oxidised in it. This results in the reduction in steam turbine power output above 750°C. Hence, these efficiencies reduced with further increase of the steam reactor temperature.

The optimal values of both fuel and steam reactor temperatures, 900°C and 750°C respectively are considered to study the effect of air reactor temperature on the overall performance of the CLC based plant for $H_2$ co-generation. The net electric energy and exergy efficiencies are increased up to 1000°C and decreased with further increase in air reactor temperature as shown in Figure 6.3(c). The air reactor is an exothermic reactor and releases some amount of excess heat at lower temperature. This increases steam turbine power output with increase of air reactor temperature up to 1000°C. The excess heat from the air reactor starts reducing beyond 1000°C resulting lower steam turbine power output. Moreover, the net gas turbine power output increases with increase of air reactor temperature due to availability of higher temperature at the gas turbine inlet. Hence, the peak in the net power output or net electric efficiency is observed at 1000°C.

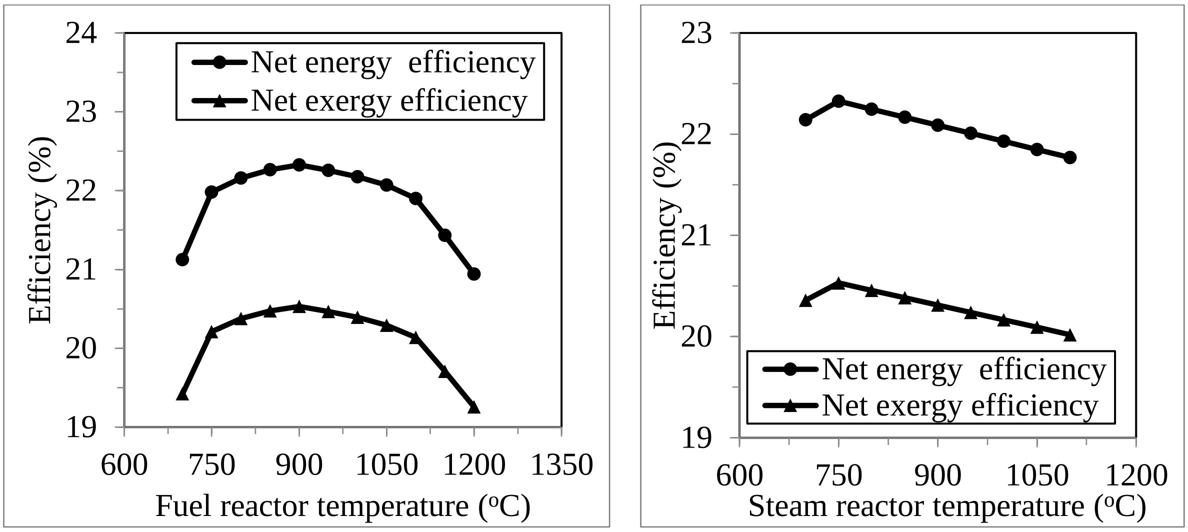

(a) Effect of fuel reactor temperature

(b) Effect of steam reactor temperature

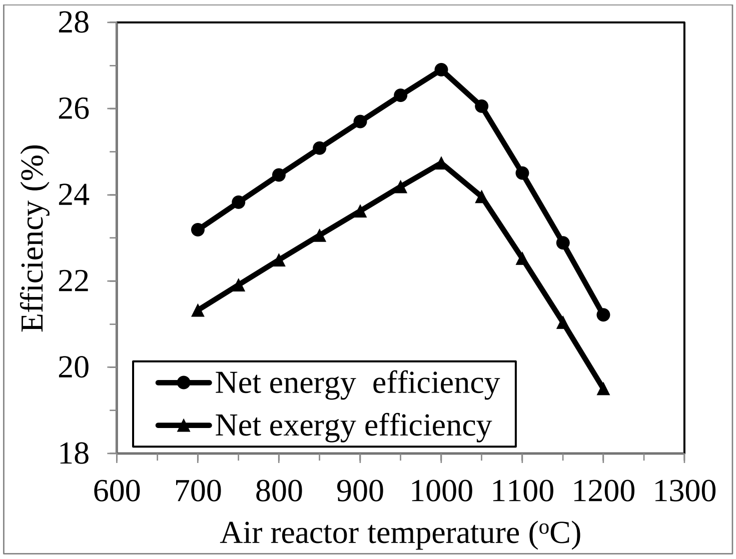

(c) Effect of air reactor temperature

Figure 6.3 Effect of air, steam and fuel reactor temperatures on overall energy and exergy efficiencies.

Table 6.2 shows the comparison of the energy and exergy efficiencies of the CLC based CFPP for $H_2$ cogeneration obtained with the optimal values of the operating pressure and temperatures of the three reactor system after sensitivity study against those obtained with the conditions given in He et al. [128]. It can be observed that the conditions finalized after sensitivity analysis (operating pressure of three reactors: 15 bar, fuel reactor operating temperature: 900°C, steam reactor operating temperature: 750°C and air reactor operating temperature: 1000°C) resulted in improvement in the performance of the plant. Hence, these conditions have been used in the further analysis carried out as presented below. The conversion of oxygen carriers (both Cu and Fe) in air and steam reactors are achieved 100% by providing excess air and steam. The 100% CuO conversion in fuel reactor is obtained as it is more reactive than $Fe_2O_3$. The $Fe_2O_3$ to Fe/FeO conversion in fuel reactor is found to be 56.30%.

Table 6.2 Comparison of CLC based plant performance for 500 MW of hydrogen production with Operating conditions of He et al. [128] vs operating conditions obtained after sensitivity analysis.

| Performance indicator | Obtained with operating conditions of He et al. [128] | Obtained with operating conditions after sensitivity analysis in the present study |
|---|---|---|
| Net electric energy efficiency, % | 22.47 | 26.90 |
| Net energy efficiency, % | 61.33 | 65.75 |
| Exergy destruction in Boiler, MW | 491.99 | 415.46 |
| Exergetic improvement potential, MW | 66.31 | 94.65 |

## 6.3.2 4-E analyses

4-E analyses for all the three plant configurations have been carried out and presented here. In this section, a CLC based CFPP with 50% hydrogen and 50% power co-generation (i.e. 382.50 MW) is assumed for the comparison of results with conventional and CLC based CFPPs with power generation alone.

### *6.3.2.1 Energy analysis*

This section focuses on the analysis of energy balance for the conventional CFPP, CLC based CFPP for power generation only and CLC based CFPP for power and $H_2$ co-generation. The simulation results based on energy analysis are presented in Figure 6.4. Since the gas turbine is not involved in the conventional CFPP, the gross turbine power output for the first case is equal to the steam turbine power output. While, both gas and steam turbines contribute to gross turbine power output in case of CLC based plant with and without $H_2$ co-generation. In this study, part of work from the gas turbine is supplied to compensate the energy requirement to the air compressor and hence the net gas turbine output is calculated by subtracting the power consumed by air compressor from the power generated by gas turbine.

Since the reduced oxygen (Fe/FeO) carrier is partially oxidised ($FeO/Fe_3O_4$) in the steam reactor of CLC based plant with hydrogen co-generation, the air requirement for the complete oxidation of $FeO/Fe_3O_4$ in air reactor is lower than the air requirement for the CLC based plant without $H_2$ co-generation. This results in the lower net gas turbine power generation for CLC based plant. A conventional SupC CFPP generates about 522 MW from steam turbine, whereas steam turbine of CLC based CFPP with power only and CLC based CFPP with 50% $H_2$ and 50% power co-generation plants generate 395.00 MW and 344.66 MW, respectively. Though the steam turbine generates lower power for CLC based plant with power only case than the conventional CFPP, the net electric power is only slightly lower by 3.11 MW due to the contribution of gas turbine. The obtained net electric power output from CLC based plant with power only case is observed to be more than the net electric power output is due to the use of bimetallic oxygen carrier. Because of hydrogen production in co-generation plant, the net electrical output is reduced compared to CLC based plant with power only case. The net electric efficiency of co-generation plant is less by 7.56% compared to the CLC based CFPP with power only. However, the net overall energy output including electrical energy and hydrogen energy in case of co-generation plant is found to be high. Hence, the net overall energy efficiency for CLC based plant with $H_2$ cogeneration is increased by 22.16% compared to CLC based plant without $H_2$ co-generation (refer Figure 6.5).

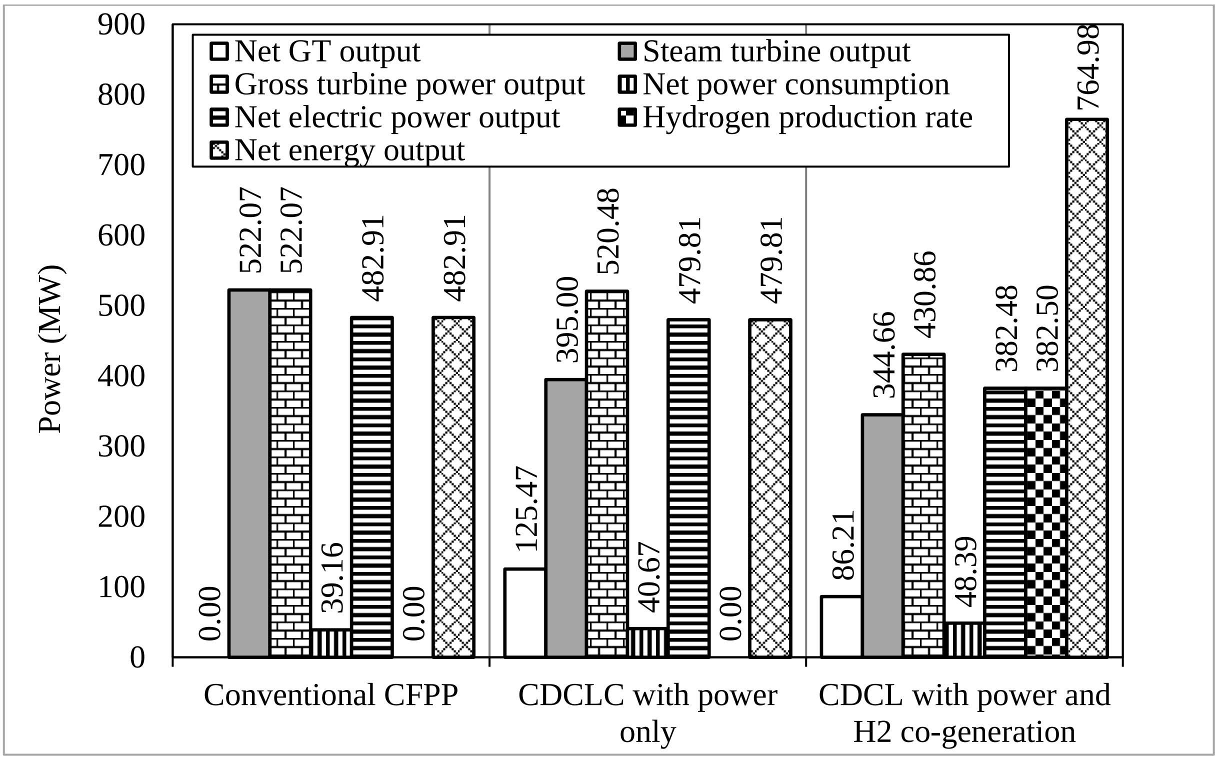

Figure 6.4 Overall performance comparison based on energy analysis.

#### *6.3.2.2 Exergy analysis*

In this section, exergy is determined for each material stream and the exergy destruction rates have been calculated for individual blocks as well as for overall power plant. Figure 6.5 shows the exergy flow diagrams of main units in conventional and CLC based CFPP without and with hydrogen co-generation plants. The exergy destruction rates in individual unit is calculated as presented in our previous study [179].

In this study, a combustor along with HRSG is termed as boiler unit of conventional SupC CFPP, air and fuel reactors coupled with HRSG are termed as boiler unit of CLC based CFPP for power generation only and the air, fuel and steam reactors along with HRSG are termed as boiler unit of CLC based CFPP for co-generation plant. Highest exergy destruction rate is found in the boiler section compared to any other unit in all the power plant cases, as can be observed in Figure 6.5. The highest exergy destruction rate in boiler is because of higher operating conditions such as pressure, temperature and mass flow rates and heat transfer processes [10]. Higher exergy losses/destructions in the boiler unit of the thermal power plants was also observed in the previous studies [24,49]. The boiler unit of CLC based CFPP for hydrogen co-generation plant has lower exergy destruction rate compared to the conventional CFPP and CLC based plant with power generation alone. The lower exergy destruction rate in boiler unit of CLC based plant co-generation plant is due to the additional exergy flow of hydrogen stream leaving the steam reactor. Hydrogen leaving steam reactor has HHV of 141.90 MJ/kg [129]. In addition, the exergy destruction in the boiler section of CLC based co-generation plant is reduced to 490.92 MW by using the optimal operating conditions of the three reactors obtained after sensitivity analysis, when compared to 544.11 MW noted with the conditions given by He et al. [128] for the generation of 382.5 MW of hydrogen.

The net energy and exergy efficiencies of all three cases are presented in Figure 6.6. The CLC based plant with power only case is found to be slightly less efficient in terms of energy and exergy compared to the conventional CFPP without $CO_2$ capture. The integration of hydrogen co-generation in the CLC based plant results in the additional energy output in the form of hydrogen energy. Thus, the net energy and exergy efficiencies for the CLC based plant with hydrogen co-generation are more compared to the CLC based plantwith power only and conventional CFPP. The CLC based technology, with or without hydrogen co-generation is both energetically and exergetically efficient technology.

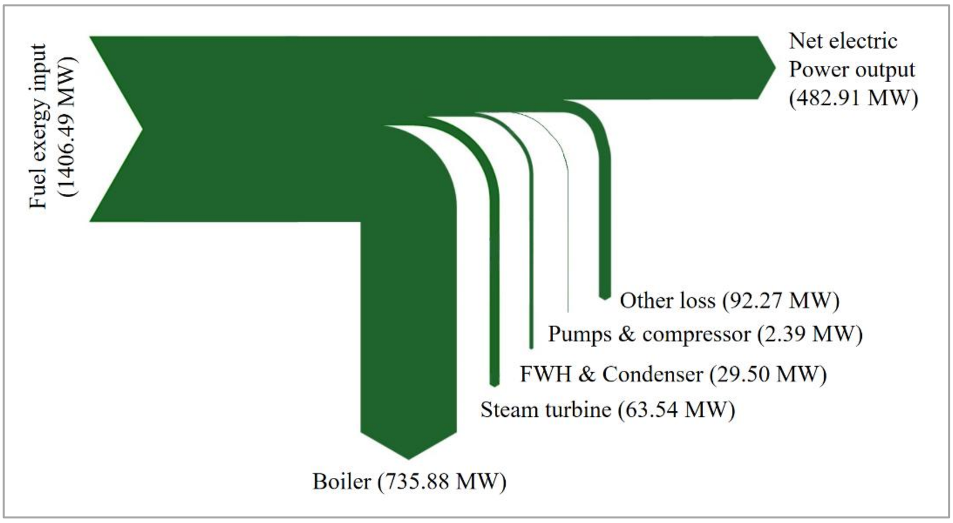

(a) Conventional CFPP.

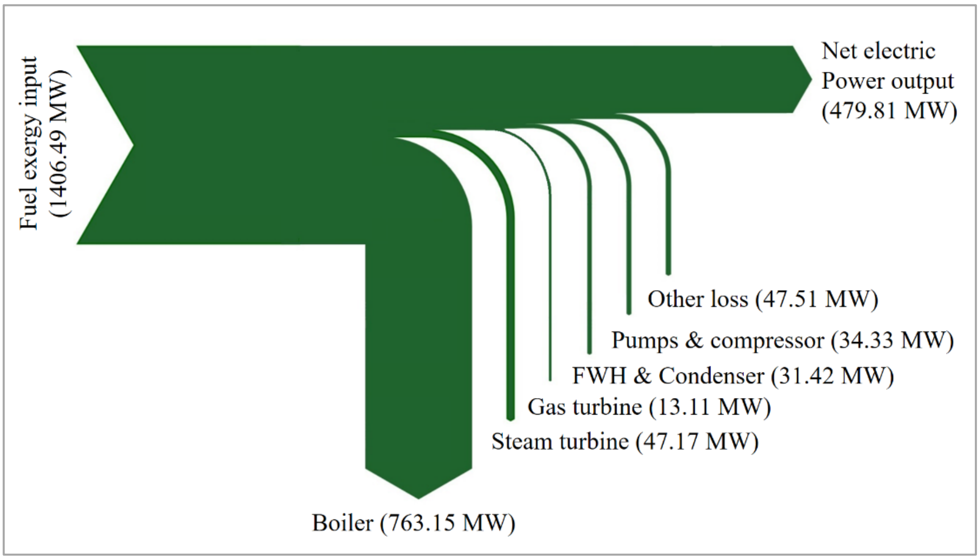

(b) CLC based plant with power only.

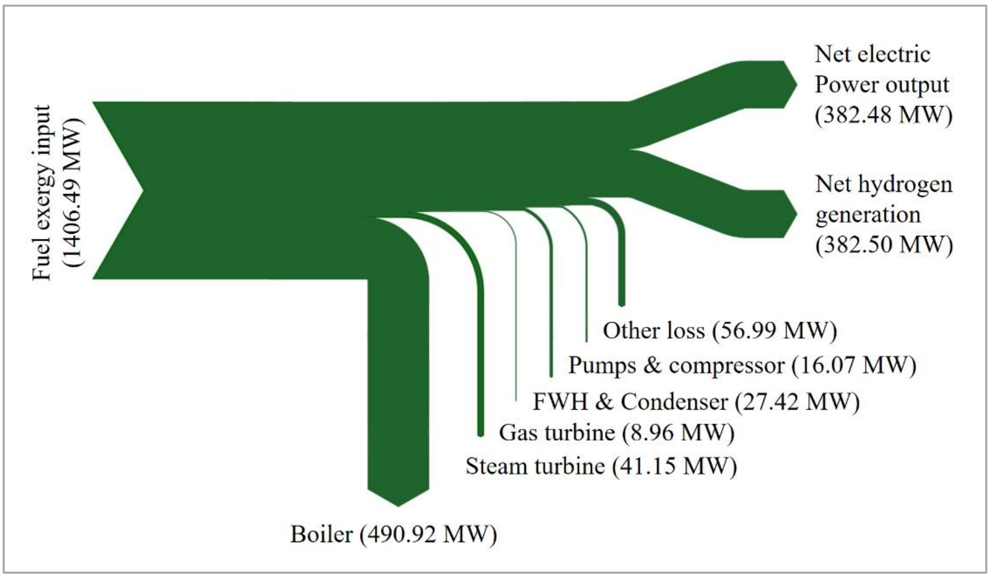

(c) CLC based plant with power and hydrogen.

Figure 6.5 Exergy flow diagrams for the three cases.

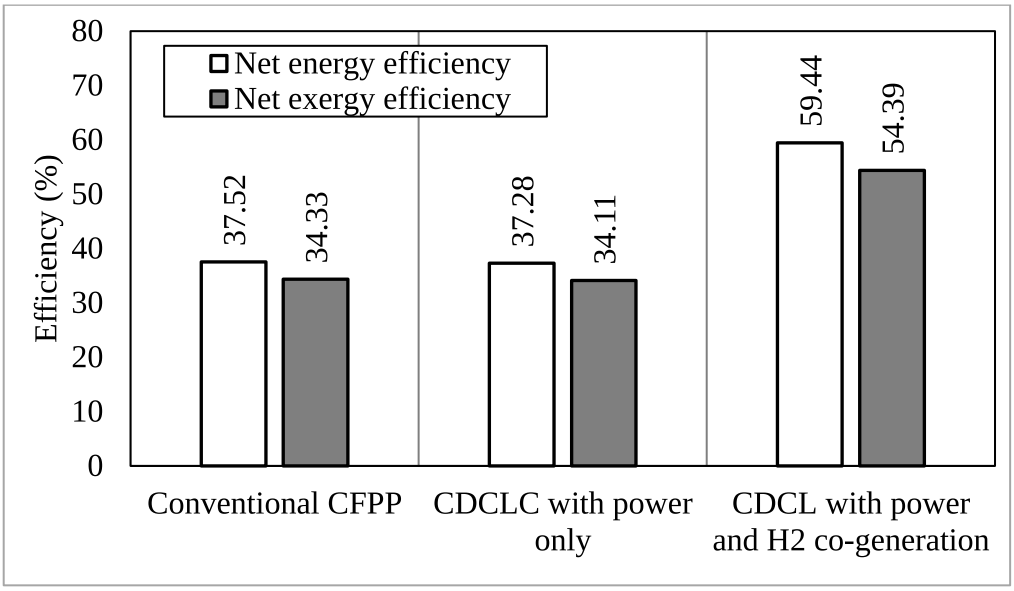

Figure 6.6 Performance comparison based on energy and exergy efficiencies.

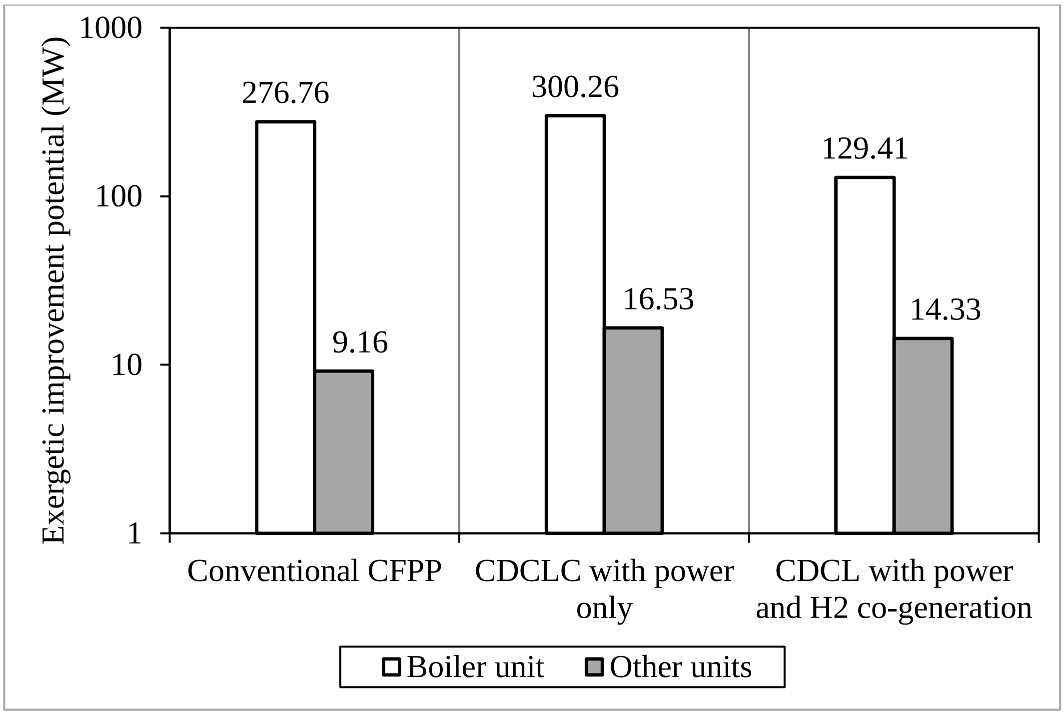

Figure 6.7 Exergetic improvement potential for three cases.

Figure 6.7 shows the exergetic improvement potential of the boiler in comparison with other units for all the three plants. The boilers are having higher exergy destruction rates, hence maximum possible improvement potential is observed in the boiler unit compared to other units. The reduction of exergy destruction rates can enhance the net energy and exergy efficiencies of the power plants. The exergy destruction rates in the boiler can be reduced by conducting several parametric analysis, replacing the coal combustion technology, selecting higher calorific value coals, etc. In the present study, the coal combustion technology has been selected as CLC technology for CLC based CFPPcase. Moreover, the CLC based plant with hydrogen co-generation plant has been optimised by conducting parametric analysis (*see section 6.3.1*). Hence, the lower exergy destruction and exergetic improvement potential are noticed when compared to those obtained with conditions of Uysal et al. [195].

#### *6.3.2.3 Ecological analysis*

The role of CLC technology is to evade the carbon dioxide emissions. An environmental analysis is carried out and performance of the three plants is assessed in terms of $CO_2$ emissions and $CO_2$ avoided. The ecological assessment is carried out based on ecological indicators as given in Table 6.3. The annual emission rate is evaluated for 8760 working hours per year. An annual $CO_2$ emission of $32.11 \times 10^8$ kg can be avoided with nearly 100% $CO_2$ capture efficiency for the CLC based plant with or without for $H_2$ co-generation compared to the conventional SupC CFPP. The net electric power output per unit carbon dioxide captured is observed more for CLC based plant with power generation only case compared to the CLC based plant with co-generation due to higher net electrical power output from CLC based with power only case. However, the co-generation plant results in higher net energy output per unit $CO_2$ captured compared to the CLC based plant with power only case.

Table 6.3 Ecological analysis for three plant cases.

| Parameter | Conventional CFPP | CLC based CFPP with power only | CLC based CFPP with power and $H_2$ |
|---|---|---|---|
| $CO_2$ emission $(kg/s)$ | 101.82 | 0.00 | 0.00 |
| $CO_2$ captured $(kg/s)$ | 0.00 | 101.99 | 101.99 |
| $CO_2$ capture efficiency (%) | 0.000 | 100.00 | 100.00 |
| Specific $CO_2$ emission $(kg/MWh)$ | 759.03 | 0.000 | 0.000 |
| Annual $CO_2$ emission $(kg)$ | $32.11 \times 10^8$ | 0.00 | 0.00 |
| Annual emission rate per unit of fuel $(kgCO_2/GJ)$ | 79.11 | 0.000 | 0.000 |
| Annual $CO_2$ avoided per unit fuel $(kgCO_2/GJ)$ | 0.00 | 79.25 | 79.25 |

| | | | |
|---|---|---|---|
| Net electric output per unit $CO_2$ captured ($MW/kg$) | - | 4.70 | 3.75 |
| Net energy output per unit $CO_2$ captured ($MW/kg$) | - | 4.70 | 7.50 |

### *6.3.2.4 Economic analysis*

The total capital requirement (TCR), annual capital cost (ACC), total operating cost (TOC), LCOE and LCOH for CLC based plant with hydrogen co-generation are estimated and the results are presented in Table 6.4. Since hydrogen is not co-generated in the conventional SupC CFPP and CLC based plant without hydrogen co-generation cases, only LCOE is estimated as LCOH is not applicable.

Table 6.4 Estimation of TCR, ACC and LCOH for CLC based processes.

| Plant | Conventional CFPP | CLC based CFPP with power only | CLC based CFPP with power and $H_2$ |
|---|---|---|---|
| TCR (M€) | 660.99 | 606.12 | 551.60 |
| ACC (M€/y) | 70.12 | 64.30 | 58.51 |
| TOC (M€/y) | 50.22 | 108.83 | 106.07 |
| LCOE (€/MW.h) | 56.34 | 68.98 | 83.64 |
| $H_2$ production (kg/y) | 0 | 0 | $8.50 \times 10^7$ |
| LCOH (€/kg) | - | - | 1.94 |

For the case of CLC based plant with hydrogen co-generation, lower cost of equipment is required for the HRSG, turbines, FWH and condenser units due to lower steam flow rates. But, as large amount of steam needs to be handled in the steam reactor, the cost of steam reactor is higher. However, the required overall capital investment for the CLC based plant with hydrogen co-generation is found to be lower. The TCR of CLC based plant with $H_2$ co-generation (551.60 M€) is lower than the conventional SupC CFPP without $CO_2$ capture (661 M€) and CLC based plant for power generation only (606.12 M€). The capital cost would be even more than 661 M€ for the conventional plant, if a post-combustion $CO_2$ capture unit is installed. Hence, the lower value of TCR for CLC based plant reveals that CLC based configuration is capable of co-generating $H_2$ with power in the most economical way. The annual capital cost and total operating costs estimated for the three cases followed similar trends as TCR. The annual capital cost is estimated for the interest rate of 10% and 30 years plant lifetime [134].

The economic performance of all three cases is compared in terms of cost of electricity of the power plant. The LCOE of conventional CFPP is found to be lowest (56.34 €/MW.h) compared to that of the CLC based power plants. This LCOE for conventional CFPP would be high if either the social cost of carbon [134] to account for the damage caused by the release of $CO_2$ into the atmosphere is considered or post-combustion capture installation is considered. The hydrogen co-generation in CLC based plant resulted in higher LCOE than CLC based without hydrogen generation plant by 14.66 34 €/MW.h.

Based on the estimation of TCR, ACC and TOC, the LCOH (i.e. LCOE) of CLC based process is estimated according to the Equation (3.20). The cost of hydrogen of CLC based plant with 50% hydrogen - 50% power co-generation is found to be 1.94 €/kg. The cost of hydrogen obtained from different technologies by various researchers is given in Table 6.5. The cost of hydrogen obtained from the CLC based plant for the co-generation is in the order of the cost of hydrogen obtained from other processes reported in literature.

Table 6.5 Cost of hydrogen from various processes.

| Plant/process | Cost of hydrogen | Unit | Reference |
|---|---|---|---|
| SMR | 3.28 | €/kg | [175] |
| SMR-CLC | 3.24 | €/kg | [175] |
| ICLWS | 1.14 | €/kg | [134] |
| SMR | 1.15 | €/kg | [134] |
| TRCLR | 1.18 | €/kg | [138] |
| Akkuyu NPP | 1.62 | €/kg | [196] |
| Sinop NPP | 1.73 | €/kg | [196] |
| wind-powered hydrogen supply | 6.26 | €/kg | [197] |
| CLC based CFPP 50-50% | 1.94 | €/kg | Present study |

### 6.3.3 Comparison among different ratios of $H_2$ and power in CLC based co-generation plant

The 4-E analyses of CLC based plant conducted for 50% hydrogen and 50% power has been extended to study the hydrogen co-generation flexibility by varying hydrogen and power production ratios. The variation of CLC based CFPP performance indicators for various hydrogen outputs (100 to 900 MW) are given in Table 6.6. The CLC based CFPP with flexible hydrogen co-generation is denoted by CLC followed by the amount of hydrogen co-generated. For example, CLC-100 indicates the 100 MW of $H_2$ in the co-generation plant. The performance indicators are compared with the CLC based plant without hydrogen co-generation (i.e. 0 MW of hydrogen co-generation). These performance indicators reflect positive influence of hydrogen co-generation flexibility.

*Energy analysis*: It is observed that, both steam and gas turbine power output is reduced with increase in hydrogen production from CLC based power plant. A part of energy is utilised to produce the hydrogen in steam reactor, which causes reduction in the electrical power generation. Although the net electrical efficiency is decreasing with increase in hydrogen production, the net energy efficiency of CLC based plant is increased due to increase of hydrogen efficiency.

*Exergy analysis*: The exergy destruction rate in the boiler unit is found to be highest for the CLC based CFPP without hydrogen generation and lowest for the CLC based plant case with 900 MW of $H_2$ co-generation. For higher hydrogen production, higher steam flow rate is required to the steam reactor. The water stream to the steam reactor is being supplied at 191$^{o}$C and 15.75 bar after preheating the liquid water leaving the HRSG (where, steam from the $CO_2$ rich and $H_2$ rich streams is condensed and separated as shown in Figure 6.1). Moreover, hydrogen leaving steam reactor itself has HHV of 141.90 MW/kg of hydrogen produced [129]. Hence, exergy flow leaving the steam reactor is more for higher hydrogen production case. This results lower exergetic destruction rate for higher hydrogen production case. The improvement potential in the lower hydrogen co-generation cases is also found to be low, which implies that there is scope for better heat integration.

*Ecological analysis*: As the CLC technology captures almost 100% $CO_2$ released from the plant, the annual $CO_2$ avoided is constant for all the hydrogen co-generation cases. But, the net electrical output per unit $CO_2$ captured is observed more for CLC based plant without hydrogen co-generation. The net electric power output per unit $CO_2$ captured decreased when the amount of hydrogen co-generation is increased. This is due to the lower turbine output for the higher hydrogen co-generation cases. However, the net overall energy output including hydrogen power per unit $CO_2$ captured is more for the higher hydrogen co-generation cases.

*Economic analysis*: The TCR of all the CLC based plant with $H_2$ co-generation cases is lower than the CLC based plant without $H_2$ co-generation. Further, the CLC based plant with higher hydrogen co-generation generates the hydrogen with lower levelised cost of $H_2$. The LCOH of 100 and 900 MW hydrogen co-generation is 7.81 and 0.65 €/kg, respectively. For increased hydrogen co-generation, large amount of steam is required. But, the design of piping system and reactors for the large amount of steam flows is practically very difficult. Steam used in steam reactor for 700 and 900 MW of hydrogen co-generation is very high compared to that for 100 to 600 MW of hydrogen co-generation. The LCOH for this plant is also seen to be decreasing with increase in hydrogen co-generation. However, the difference between the successive LCOH values is found to be decreasing with increase of hydrogen co-generation. The decrease in LCOH after 600 MW is small compared to that up to 600 MW of hydrogen production. The LCOE of the CLC based plant without hydrogen generation is found to be lowest and its magnitude is increased with increase of hydrogen generation. This is due to the lower electricity generation with increase of hydrogen generation in the plant.

From the above analysis, it may observed that although the increase in hydrogen production increases the performance indicators of the CLC based plant for cogeneration, the improvement in the indicators after 600 MW of hydrogen generation is less compared to the cases up to 600 MW. Hence, from the practical application point of view, the cogeneration plant with 600 MW of hydrogen generation may be considered as the better case. However, further detailed economic analysis may be required to provide better justification towards this.

The comparative results presented in the entire study are based on several assumptions and sizes/dimensions of individual units are not considered. Hence, the obtained results are the preliminary estimates and are used for the comparison of CLC based plant for flexible hydrogen co-generation against conventional and CLC based CFPPs on a common basis. The comprehensive 4-E analysis plays an important role in evaluating the most suitable technology for the power and hydrogen co-generation, especially in the coal rich developing countries.

Table 6.6 Comparison of CLC based plant with flexible hydrogen co-generation.

| Parameter | CLC-0 | CLC-100 | CLC-200 | CLC-300 | CLC-400 | CLC-500 | CLC-600 | CLC-700 | CLC-800 | CLC-900 |
|---|---|---|---|---|---|---|---|---|---|---|
| Energy analysis | | | | | | | | | | |
| Net electric efficiency (%) | 37.28 | 35.92 | 33.79 | 31.67 | 29.60 | 26.90 | 23.98 | 20.35 | 16.66 | 12.20 |
| Hydrogen efficiency (%) | 0.00 | 7.77 | 15.54 | 23.31 | 31.08 | 38.85 | 46.62 | 54.39 | 62.16 | 69.93 |
| Net energy efficiency (%) | 37.28 | 43.69 | 49.33 | 54.98 | 60.68 | 65.75 | 70.60 | 74.74 | 78.82 | 82.13 |
| Exergy analysis | | | | | | | | | | |
| Net exergy efficiency (%) | 34.11 | 32.87 | 30.92 | 28.98 | 27.08 | 24.62 | 21.95 | 18.62 | 15.24 | 11.17 |
| Exergy destruction rate in boiler unit (MW) | 763.15 | 681.42 | 612.63 | 543.78 | 474.32 | 414.38 | 358.35 | 313.38 | 269.37 | 237.32 |
| Improvement potential of boiler unit (MW) | 300.26 | 238.41 | 195.69 | 156.57 | 120.97 | 94.21 | 72.05 | 56.69 | 43.15 | 34.75 |
| Ecological analysis | | | | | | | | | | |

| | | | | | | | | | | |
|---|---|---|---|---|---|---|---|---|---|---|
| Annual $CO_2$ avoided emission per unit fuel (kg.$CO_2$ /GJ) | 79.25 | 79.25 | 79.25 | 79.25 | 79.25 | 79.25 | 79.25 | 79.25 | 79.25 | 79.25 |
| Net electric output per kg of CO2 captured (MW/kg) | 4.70 | 4.53 | 4.26 | 4.00 | 3.73 | 3.39 | 3.03 | 2.57 | 2.10 | 1.54 |
| Net energy output per kg of $CO_2$ captured (MW/kg) | 4.70 | 5.51 | 6.22 | 6.94 | 7.66 | 8.30 | 8.91 | 9.43 | 9.95 | 10.36 |
| Economic analysis | | | | | | | | | | |
| TCR (M€) | 606.12 | 612.39 | 598.63 | 571.15 | 550.30 | 523.52 | 487.52 | 441.89 | 393.22 | 327.84 |
| ACC (M€/yr) | 64.30 | 64.96 | 63.50 | 60.59 | 58.37 | 55.53 | 51.72 | 46.87 | 41.71 | 34.78 |
| LCOE | 68.98 | 71.72 | 75.63 | 79.40 | 83.91 | 90.82 | 99.64 | 114.05 | 134.86 | 175.60 |
| $H_2$ production (kg/s) | 0.00 | 0.70 | 1.41 | 2.11 | 2.82 | 3.52 | 4.23 | 4.93 | 5.64 | 6.34 |
| LCOH (€/kg) | - | 7.81 | 3.86 | 2.51 | 1.85 | 1.44 | 1.16 | 0.95 | 0.79 | 0.65 |

## 6.4 Summary

A CLC based plant configuration for power and hydrogen co-generation with zero emissions using high-ash Indian coal and iron based bimetallic oxygen carrier has been proposed as a part of Objective -3 of the current study in this chapter. The overall performance of the CLC based plant for power and $H_2$ co-generation is compared with the conventional and CLC based CFPP with power generation only cases based on 4-E (energy, exergy, ecological and economic) analyses. Following are the useful points observed from the study:

- The optimal operating conditions from sensitivity analysis are – operating pressure of CLC reactors is 15 bar, operating temperature of fuel reactor is $900^oC$, operating temperature of steam reactor is $750^oC$ and operating temperature of air reactor is $1000^oC$.
- Energy analysis has shown that the CLC based plant with $H_2$ co-generation is more energy efficient compared to the conventional CFPP and CLC based plant with power generation only cases. The net energy efficiency of CLC based plant for 50% hydrogen and 50% power co-generation is higher than conventional CFPP and CLC based plant with power generation alone by 21.92 and 22.16%, respectively.
- Exergy analysis revealed that the highest exergy destruction rate was in the boiler unit of all the CLC based plant cases compared to the other units. The exergy destruction rate is found to be decreasing with increase in hydrogen generation from the CLC based plant.
- All the CLC based power plant cases are environmentally feasible. The net energy output per unit $CO_2$ captured is found to be high for higher hydrogen co-generation cases.
- The CLC based plant with 50% hydrogen and 50% power co-generation has LCOH of 1.94 €/kg of hydrogen, which is in the marginal range reported in literature.

Based on the 4-E analyses, it can be concluded that the CLC based CFPP plant with hydrogen co-generation is energetically, exergetically, environmentally and economically feasible and efficient. Moreover, it is highly promising plant for the developing nations for hydrogen and electricity production with coal as a prime source of energy.

# Chapter 7

# CLC based coal fired power plant integrated with carbon dioxide utilization

# Chapter 7

# *CLC based coal fired power plant integrated with carbon dioxide utilization*

The final objective of the study is presented in this chapter. The performance analysis of CLC based CFPP with hydrogen and power co-generation integrated with carbon dioxide utilization (CDU) plant is discussed in this chapter. Various CDU plants have been considered such as – formic acid, methane, methanol and dimethyl ether synthesis from capture $CO_2$ and $H_2$. The overall performance of these coupled plants is compared based on energy, exergy, ecological and economic (4-E) analyses. In addition to 4-E analyses, this chapter also compares the overall performance based on life cycle analysis.

## 7.1 Background and motivation

Chemical looping combustion (CLC) is an inherent $CO_2$ capture and separation technology that can capture almost 100% $CO_2$ emitted from power plants [13]. The carbon capture and sequestration (CCS) plays a key role in curbing the carbon dioxide emissions and mitigating the climate change. The major concerns associated with the $CO_2$ sequestration are safety of geological and ocean storages [14]. Although underground storage is the fastest and largescale solution in a linear economy, a link to a circular carbon economy [14], is represented by $CO_2$ use and conversion into materials, chemicals and energy products. Hence, carbon dioxide utilization (CDU) is a viable option to provide renewable energy source as it produces numerous valuable products. $CO_2$ utilization is expected to overcome the known challenges associated with carbon capture and sequestration such as high cost, long-term uncertainty and public acceptance. Additionally, it makes $CO_2$ capture worthy and can be substituted partially for fossil fuels as the main source of energy [18].

As mentioned in *Chapter 2*, the reported literature is either on the CLC based power plant with power and hydrogen co-generation or on the $CO_2$ utilization to produce valuable products. Till date, no study is found on the comprehensive analysis based on the energy, exergy, ecological, economic and life cycle (4-E&L) analyses for the integrated plant of CLC based power plant for co-generation system coupled with $CO_2$ utilization. The study presented in this chapter aims to fill this gap in the literature. The 4-E analyses of CLC based CFPP for power generation alone and CLC based CFPP with power and hydrogen co-generation are presented in *Chapters 4* and 6, respectively. The final objective of the thesis work which is to develop the CLC based plant for hydrogen and power co-generation coupled with the CDU plant and analyse the integrated plant performance using 4-E&L analyses, is presented in this chapter. The formic acid, methane, methanol and dimethyl ether (DME) synthesis using captured $CO_2$ and $H_2$ are considered as utilization product case studies. The selection of these chemicals is based on their high global market annual demand, for e.g. 0.76 MT of formic acid [148], 439.71 MT of methane [30], 78.09 MT of methanol [149] and 6.91 MT of DME [149].

## 7.2 Description of CDU plants

In this chapter, flowsheets of integrated plants of CLC based CFPP for hydrogen and power co-generation with $CO_2$ utilization for different end products are synthesized. These are modelled and simulated using aspenONE V10.0. Different cases considered in the present study are listed in Table 7.1. The cases 2 to 5 are part of the Category-4, while case 1 is part of Category-3 as defined in *Chapter 3*.

Table 7.1 Different cases used in present study.

| Case | Plant | End product |
|---|---|---|
| 1 | CLC based CFPP with hydrogen and power co-generation | Hydrogen |
| 2 | CLC based CFPP with hydrogen and power co-generation | Formic acid |
| 3 | CLC based CFPP with hydrogen and power co-generation | Methane |
| 4 | CLC based CFPP with hydrogen and power co-generation | Methanol |
| 5 | CLC based CFPP with hydrogen and power co-generation | Dimethyl ether |

The CLC based CFPPs with hydrogen and power co-generation are modelled for the supercritical steam boilers as given in *Chapter 6*. A block diagram of CLC based plant integrated with CDU is shown in Figure 3.4. A bimetallic oxygen carrier, which is mixture of

90% $Fe_2O_3$ and 10% CuO, supported on 30% $Al_2O_3$ (weight basis) oxygen carrier has been considered for the indirect supply of oxygen for the combustion of coal for all the cases.

A high-ash Indian coal, principal energy input to all the power plant cases is assumed as given in the Table 3.1. Air is used in the CLC based plant to oxidise reduced oxygen carrier and water is another input to the CLC based plant for steam generation and also used in CDU plants. The net output from the overall system is power (electric power output is from the gas and steam turbines), hydrogen, synthesis product (formic acid, methane, methanol and DME). Another significant effect is the captured carbon dioxide. A part of captured $CO_2$ is utilized in the synthesis of the chosen valuable end product (depending on the synthesis requirement in CDU plant) and the rest is compressed and sequestrated.

The process flow diagram of CLC based CFPP for hydrogen and power co-generation is shown in Figure 6.1 of the previous chapter. The $CO_2$ captured from the CLC based plant is utilized in this section to produce valuable products such as formic acid, methane, methanol and dimethyl ether. The operating conditions of the main units of these plants are given in Table 3.3 of *Chapter 3* (see also *Chapter 6* for more details). Following subsections show the plant descriptions of these synthesis products.

### 7.2.1 Description formic acid synthesis plant

The process flow diagram of production of formic acid from captured $CO_2$ and $H_2$ is shown in Figure 7.1. The homogeneous chemical catalysis has been performed for the formation of formic acid from captured $H_2$ and $CO_2$ from the CLC based plant. This follows the process described by Fortes et al [148]. The formic acid synthesis process is mainly divided in to five stages – compression stage, reaction stage, catalyst recovery stage, stripping for methanol recovery stage and reactive distillation stage.

*Compression stage*: As the catalytic reactor is operated at higher pressure (100 bar), the gaseous streams need to be liquefied and compressed to higher pressure than the reactor operating pressure. Hence, $CO_2$ and $H_2$ are compressed to 105 bar and cooled to 33$^{o}$C temperature.

*Reaction stage*: In the catalytic reactor, the amines of formic acid or formic acid adduct is formed from the liquid reaction of $H_2$ and $CO_2$ in the presence of a phosphino- and ruthenium based catalysts. This reaction is given below:

$$CO_2 + H_2 + C_{18}H_{39}N \leftrightharpoons C_{18}H_{39}N - HCOOH \quad (7.1)$$

A stoichiometric amount of hydrogen and carbon dioxide, captured/produced from the CLC plant is fed to the reactor along with the amine ($C_{18}H_{39}N$). The reactor is operated at 93°C isothermally. Although the reaction is exothermic, a small amount of heat is required to maintain the 93°C operating temperature, which is compensated by supplying steam from the HRSG unit of CLC plant. The unreacted gases leaving the reactor are recycled back to the reactor and 1% (mass basis) of purge stream is assumed to avoid accumulations. Fortes et al. [148] produced 25.6 kg of formic acid per kg of $H_2$ with 98.00% conversion efficiency of $CO_2$ to formic acid. For the same amount of formic acid production, 98.48% conversion efficiency is observed from aspenONE simulation of the present work. This shows that the aspenONE model flowsheet developed for the formic acid synthesis plant is in good agreement with the results reported in the literature [148].

*Catalyst recovery stage*: The catalysts need to be recovered and recycled as phosphino- and ruthenium based catalysts are expensive [148]. Hence, two decanters, operated at 130 bar and 70 bar have been used to achieve maximum possible recovery. In the present work, almost 100% catalyst recovery is considered.

*Stripping stage*: The methanol solvent is recovered in this section with the use of equilibrium based stripper at 3 bar. The gaseous products from the main stream are separated using flash vessel before the stripping column. The methanol along with water and dissolved gases are recovered from the top and adduct is collected at the bottom of the stripper. The purity of adduct is adjusted to achieve 85% (mass basis) final formic acid product purity from the next stage.

*Reactive distillation stage*: A rate based reactive distillation column has been used in this section. The dissociation of adduct to formic acid and amine is initiated by reducing the operating pressure to 0.25 bar and increasing temperature to 180°C. In this stage, the dissociation reaction and separation of products is attained in the reactive distillation column. This can also be done with the use of reactor followed by distillation column in an Aspen plus. The dissociation reaction is given below:

$$C_{18}H_{39}N - HCOOH \leftrightharpoons C_{18}H_{39}N + HCOOH \quad (7.2)$$

The dissociation of adduct to formic acid and amine is an endothermic reaction, thus leads to the reduction of operating temperature. The extra heat energy required to the reboiler to maintain columns bottom temperature to 180°C is provided from the steam coming from the

HRSG unit of CLC based plant. The amine separated from this stage is recycled back to the reaction stage after purification and formic acid from the top product is collected and cooled.

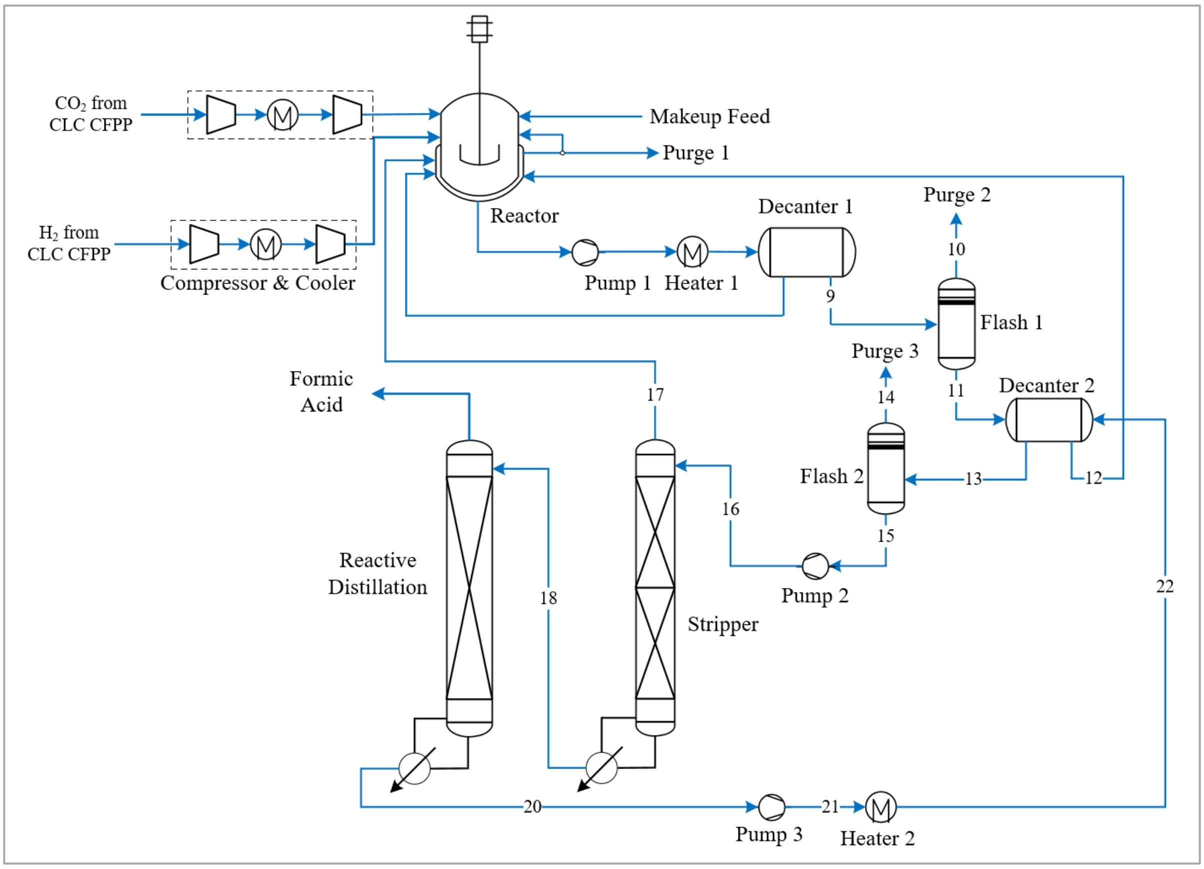

Figure 7.1 Process flow diagram for the formic acid synthesis from $CO_2$ and $H_2$.

### 7.2.2 Description of methane synthesis plant

Process flow diagram of methane synthesis using captured $CO_2$ and $H_2$ is shown in Figure 7.2. It consists of methanation reactor and separator. Carbon dioxide and hydrogen from the CLC based CFPP are available at 15 bar and at 50$^{o}$C temperature. These reactants are first compressed to 30 bar and then fed to the methanation reactor. This methanation reaction is catalytic hydrogenation reaction (also called Sabatier reaction) and Pan et al. [147] proved that there is less than 2% deviation in the kinetic solution and equilibrium based solution, if catalyst is in sufficient quantity. Methane synthesis from $CO_2$ is investigated using catalytic metals (Rh, Ru) supported on metal oxides ($TiO_2$, $Al_2O_3$, $SiO_2$, $ZrO_2$, $CeO_2$), but the supported Ni-based catalyst has been most widely used [198]. In this study, the methanation reaction is simulated by RGibbs model in Aspen plus using Ni/$MgAl_2O_4$ catalyst for the reactions given below [198]:

$$CO_2 + 4H_2 \rightarrow CH_4 + 2H_2O \ (\Delta H_{298\,K} = -252.95\, kJ/mol) \qquad (7.3)$$

Methanation is an exothermic reaction and the reactor temperature is achieved without any external heat input. The exit stream leaving methanation reactor is comprised of mainly methane and steam. Methane from this stream is separated by condensing the steam. Flash 2 model palette is used to condense steam and separate methane in Aspen plus.

The carbon conversion of 98% has been found in the study of Pan et al. [198], whereas the $CO_2$ conversion of 98.34% has been achieved in this work. This shows that the aspenONE model flowsheet developed for the methane synthesis is in good agreement with the results reported in the literature [198].

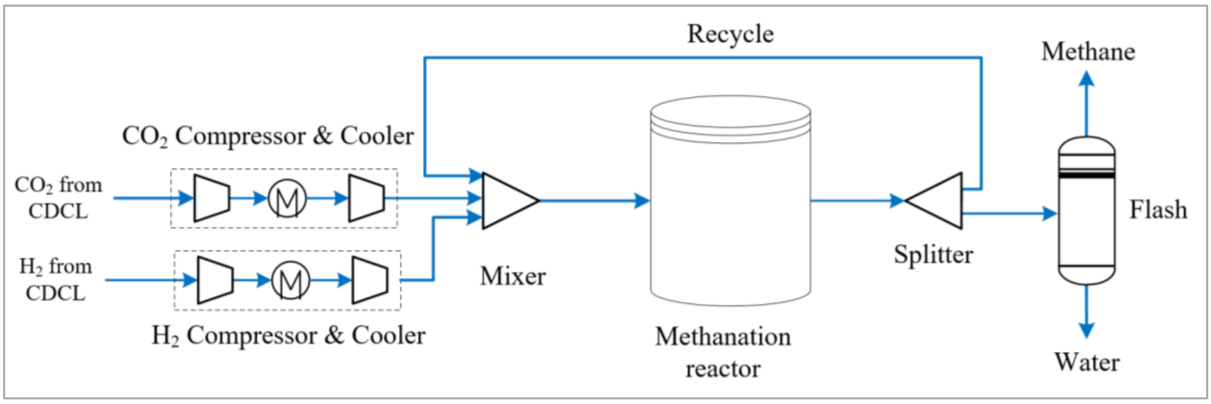

Figure 7.2 Process flow diagram of methane synthesis from captured $CO_2$ and $H_2$.

### 7.2.3 Description of methanol synthesis plant

The process flow diagram of methanol synthesis from captured $CO_2$ and $H_2$ is shown in Figure 7.3. The methanol synthesis process is divided in to three stages such as: compression stage, reaction stage and separation stage.

$CO_2$ and $H_2$ available at 15 bar pressure from CLC plant are used in stoichiometric ratio with $Cu/ZnO/Al_2O_3$ catalyst. $CO_2$ and $H_2$ are first compressed to 78 bar in compressor and cooler. The $CO_2$ and $H_2$ streams are mixed and preheated to 210°C temperature before feeding to the reactor. An ideal adiabatic plug flow reactor with 40 $m^3$ volume is modelled according to the following reactions.

$$CO_2 + 3H_2 \rightarrow CH_3OH + H_2O \qquad (7.4)$$

$$CO_2 + H_2 \rightarrow CO + H_2O \qquad (7.5)$$

Reaction (7.4) produces methanol, which is a desired reaction and reaction (7.5) is undesired reaction. The kinetics for the above given reactions are taken from Van-Dal and Bouallou [199]. The selectivity of the above reactions is pushed towards the methanol formation by recycling the gaseous stream in two flash units. The gaseous stream leaves the reactor at 290°C temperature and 78 bar pressure. To achieve the reaction temperature, a part of the heat from HRSG unit of CLC based plant is used to preheat the feed stream to the reactor. The conversion of $CO_2$ into methanol is found to be 22.10% and about 0.42% of $CO_2$ is converted into CO due to reaction (7.5) in the methanol reactor, while the total amount of $CO_2$ converted in the overall process is found to be 94.65%. Fortes et al. [164] found 22.00% $CO_2$ conversion into methanol and 0.40% $CO_2$ conversion into CO in methanol reactor with 95.00% overall $CO_2$ conversion in the process. This shows that the aspenONE model flowsheet developed for the methanol synthesis is in good agreement with the results reported in the literature.

A liquid stream leaving the second flash is the mixture of methanol and water with methanol concentration approximately 63% (weight basis). This mixture, after preheating, is sent to the distillation column to separate methanol from water. The distillation column is modelled to achieve 99.95% (weight basis) methanol purity at top product. Finally, liquid methanol is collected after removing off-gases in the flash unit.

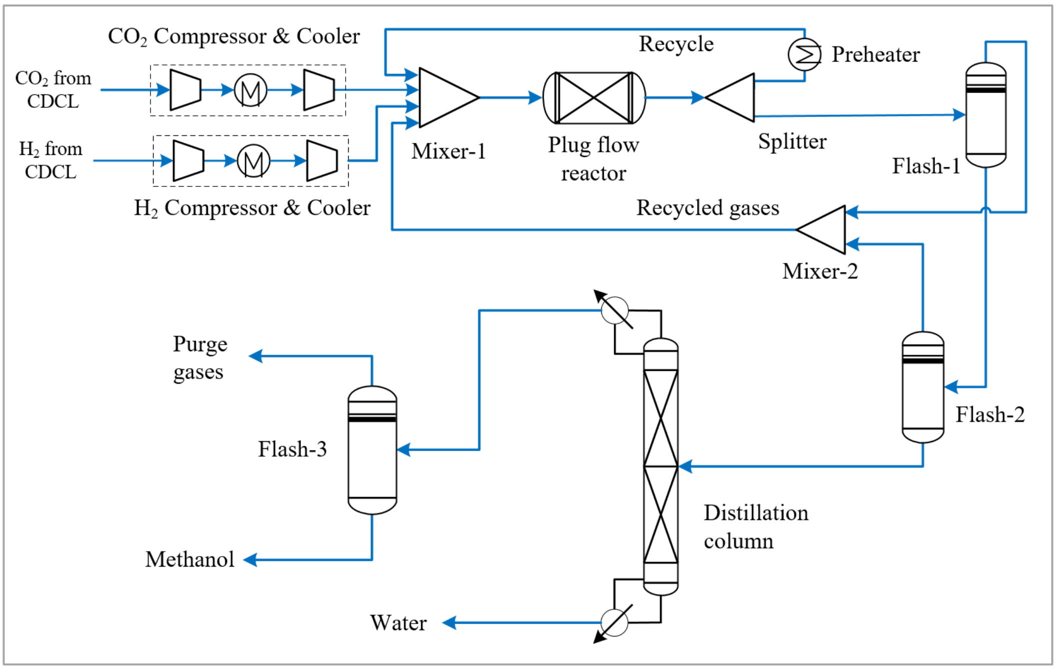

Figure 7.3 Process flow diagram of methanol synthesis from captured $CO_2$ and $H_2$.

### 7.2.4 Description of dimethyl ether synthesis plant

Figure 7.4 shows the process flow diagram of DME synthesis from the captured $CO_2$ and $H_2$. The process flow diagram up to the formation and separation of methanol is same as given in Figure 7.3 (see *section 7.2.3*). Liquid methanol is first pumped to 15 bar and mixed with the recycled methanol. This stream is then preheated to 160°C in heater-1 and fed to the adiabatic RGibbs DME reactor. In DME reactor, methanol is converted to dimethyl ether and water as per the reaction given below:

$$CH_3OH \rightarrow CH_3OCH_3 + H_2O \tag{7.6}$$

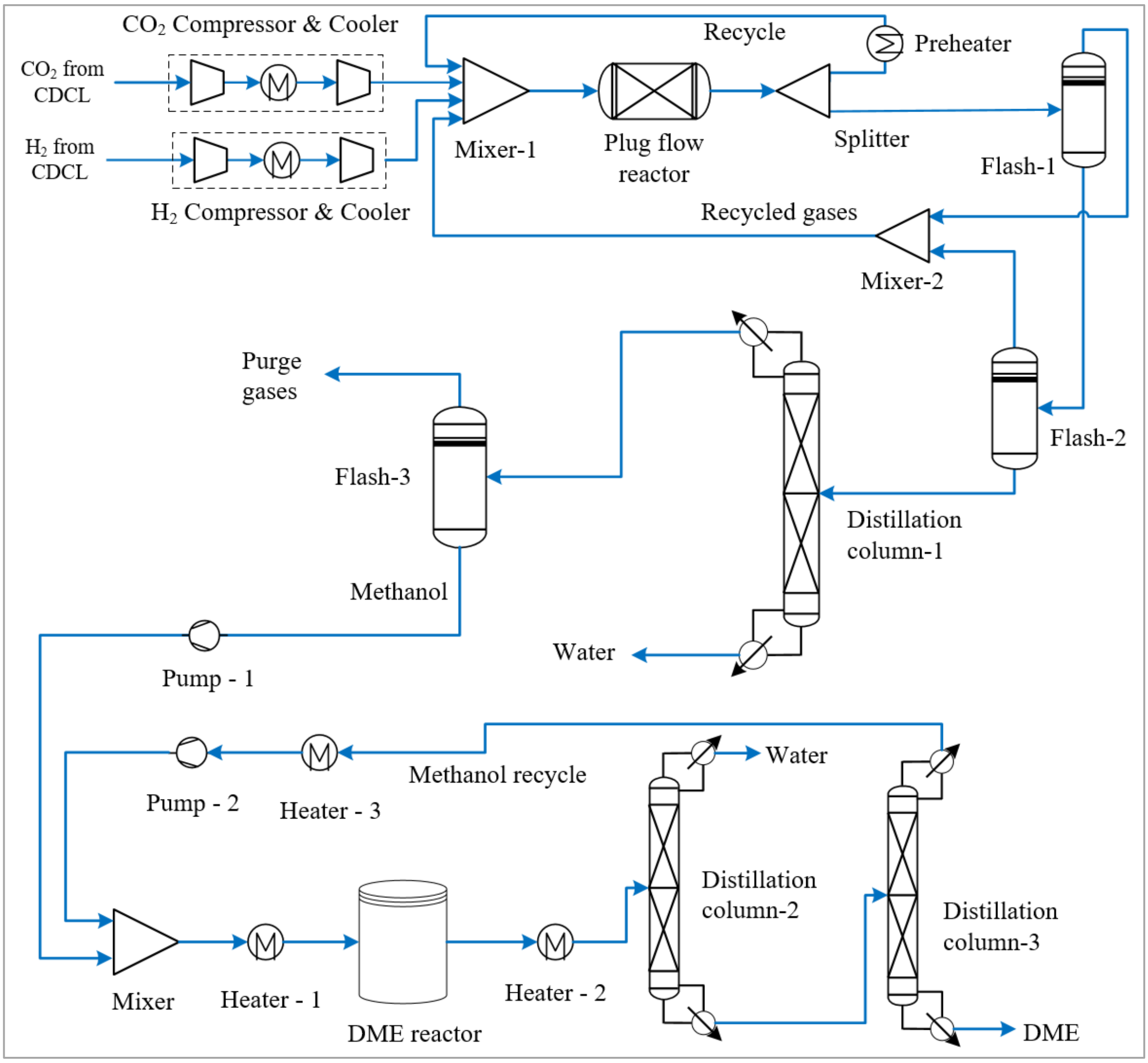

Figure 7.4 Process flow diagram of dimethyl ether synthesis from captured $CO_2$ and $H_2$.

The mixture of DME and water is cooled down to 50°C in heater-2 before entering into the distillation column-1. In column-1, DME is separated from water and the unconverted methanol is collected as the top product. Methanol is separated from the water in column-2 and water is purged. This methanol is recycled back to the DME reactor after preheating to the desired temperature. The heat required to the heaters is compensated from HRSG unit of CLC based plant.

The syngas conversion of Schakel et al. [145] is found to be 99.50% at 220°C DME reactor temperature, whereas $CO_2$ conversion of 98.56% is observed in present work at 220°C DME reactor temperature. This shows that the aspenONE model flowsheet developed for the dimethyl ether synthesis is in good agreement with the results reported in the literature [145].

## 7.3 Results and discussion

A comparative performance analysis has been carried out based on energy, exergy, ecological, economic and life cycle analyses of the CLC based plant integrated with different carbon dioxide utilization plants. A constant energy input of 1287 MW is considered for the all cases.

### 7.3.1 4-E & Life cycle analyses

The amount of hydrogen required for the production of formic acid, methane, methanol and dimethyl ether is kept equivalent to the hydrogen required for complete utilization of $CO_2$ to produce formic acid. Utilization of captured $CO_2$ from the CLC based power plant to form different chemical products is explored and in the following subsections, CLC based plant integrated with various CDU plants is compared based on the 4-E&L analyses. These results are also compared with the results of conventional coal based power plant without $CO_2$ capture and CLC based coal-fired power plant without hydrogen production (which are given in *Chapter 4* and *Chapter 5*).

#### *7.3.1.1 Energy analysis*

The comparative energy analysis of CLC based plant integrated with various CDU plants is summarised in Table 7.2. A constant energy input to the plant is assumed for all the cases and the energy requirement in CDU is being supplied from the HRSG unit of CLC based plant. Hence, the power generation in gas turbine and the energy consumption by air compressor are not affected and are same for all cases. A constant net gas turbine power output of 64.95 MW is found for all the five cases. As steam turbine power output depends on the steam generation in the HRSG unit and as some of energy is supplied to the CDU plants, the steam turbine power output is different for different cases. The net steam turbine power output is lower than the CLC based plant without CDU by 32.61 MW, 12.46 MW and 32.00 MW for CLC based plant with formic acid, methanol and DME synthesis, respectively. The CLC based plant with methane synthesis has the same steam turbine power output as that of CLC based plant without CDU case. This is because there are no energy-consuming units that require energy from HRSG of CLC based plant.

The total power consumption of the integrated plant is considered to have two contributions – power consumption in CLC based plant and power consumption in CDU plant. Major power consuming units in CLC based plant and CDU plant are auxiliary units of the plant, $CO_2$ compressor and $H_2$ compressor present in each plant. For the case of CLC based plant without CDU, hydrogen and $CO_2$ are compressed in CLC based plant to 110 bar and 60 bar respectively resulting in net power consumption of 47.34 MW. As all hydrogen and $CO_2$ are utilised in the case of CLC based plant with formic acid synthesis, the power consumption in CLC based plant is equal to the auxiliary losses in the CLC based plant. However, the net power consumption is higher by 9.58 MW in CLC based with formic acid synthesis compared to the CLC based without CDU. This is due to the higher power consumption by the hydrogen compressor to 105 bar as required in formic acid synthesis plant.

A constant hydrogen output rate of 663 MW is considered in all the cases, which is equivalent to complete utilization of $CO_2$ in formic acid synthesis case. The stoichiometric ratio of $H_2$ to $CO_2$ is 1:1, 4:1, 3:1 and 3:1 for the CLC based with formic acid, methane, methanol and DME, respectively. Hence, the amount of $CO_2$ utilised for methane, methanol and DME plants is lower than the amount of $CO_2$ utilised in formic acid plant. Thus, the remaining $CO_2$ of these cases is compressed in the CLC based plant and considered for sequestration. However, the $CO_2$ and $H_2$ compression operating conditions and energy input to the CDU plants is different for different synthesis cases. This resulted in the net energy consumption of 56.92 MW, 41.10 MW, 56.16 and 54.75 MW for CLC based plant with FA, methane, methanol and DME synthesis, respectively.

Table 7.2 Comparison of CLC based plant with and without CDU based on energy input, output and consumption (MW).

| Plant Data | CLC based plant without CDU | CLC based plant with FA | CLC based plant with $CH_4$ | CLC based plant with MeOH | CLC based plant with DME |
|---|---|---|---|---|---|
| Fuel input energy | 1286.98 | 1286.98 | 1286.98 | 1286.98 | 1286.98 |
| Air Compressor | 64.95 | 64.95 | 64.95 | 64.95 | 64.95 |
| Gas turbine | 126.32 | 126.32 | 126.32 | 126.32 | 126.32 |
| Net GT output | 61.37 | 61.37 | 61.37 | 61.37 | 61.37 |
| Steam turbine output | 264.19 | 231.58 | 264.09 | 251.73 | 232.19 |
| Gross turbine power output | 325.56 | 292.95 | 325.46 | 313.10 | 293.56 |
| Auxiliary loss | 19.81 | 17.37 | 19.81 | 18.88 | 17.41 |
| Power consumption in CLC plant | 47.34 | 17.37 | 19.81 | 18.88 | 17.41 |
| Power consumption in CDU plant | 0.00 | 39.55 | 21.29 | 37.28 | 37.34 |
| Net power consumption | 47.34 | 56.92 | 41.10 | 56.16 | 54.75 |
| Net electric power output | 278.22 | 236.03 | 284.37 | 256.94 | 238.80 |
| Net hydrogen output | 663.00 | 663.00 | 663.00 | 663.00 | 663.00 |
| Net energy output | 941.22 | 236.03 | 284.37 | 256.94 | 238.80 |

The net electric output is found to be lower by 42.20 MW, 21.28 MW and 39.42 MW for CLC based plant with FA, methanol and DME synthesis, respectively, compared to the net electric output of CLC based plant without CDU case. While, the CLC based plant with methane synthesis plant resulted in higher net electric power output by 6.23 MW compared to the CLC based plant without CDU. This is due to the lower energy consumption in the methane synthesis case, since, it does not include $CO_2$ and $H_2$ compressors (Figure 7.2). As, all hydrogen generated in CLC based plant is utilised for the production of synthesis products in all CDU cases, it is not considered as energy output. This results in the net energy output of 941.22 MW, 236.03 MW, 284.46 MW, 256.94 MW and 238.80 MW for CLC based plant without CDU, with FA synthesis, with methane synthesis, with methanol synthesis and with DME synthesis, respectively. High net electric power output from the CLC based plant with methane synthesis results in high net electric efficiency.  It can be observed from Figure 7.5 that the net electric efficiency of CLC based plant without CDU is 21.62% while the same for the CLC based plants with FA, methanol and DME synthesis is less by 3.28%, 1.65% and 3.06%, respectively and more by 0.48% for CLC based plant with methane synthesis.

### *7.3.1.2 Exergy analysis*

A comparative performance of the CLC based plant without CDU and with CDU in terms of overall exergy efficiencies is shown in Figure 7.6 for different cases. The net exergy efficiency of the CLC based plant without CDU is found to be 71.30%, while the CLC based plant with FA, methane, MeOH, and DME are found to be 16.78%, 20.22%, 18.27% and 16.98%, respectively. The net energy and exergy efficiencies of CLC plant without CDU are higher than CLC plant with CDUs, because of higher energy output (which includes both electricity and hydrogen) from the CLC plant without CDU, while all the hydrogen (having high exergy) co-generated in the CLC plant is utilized in the CDU plants.

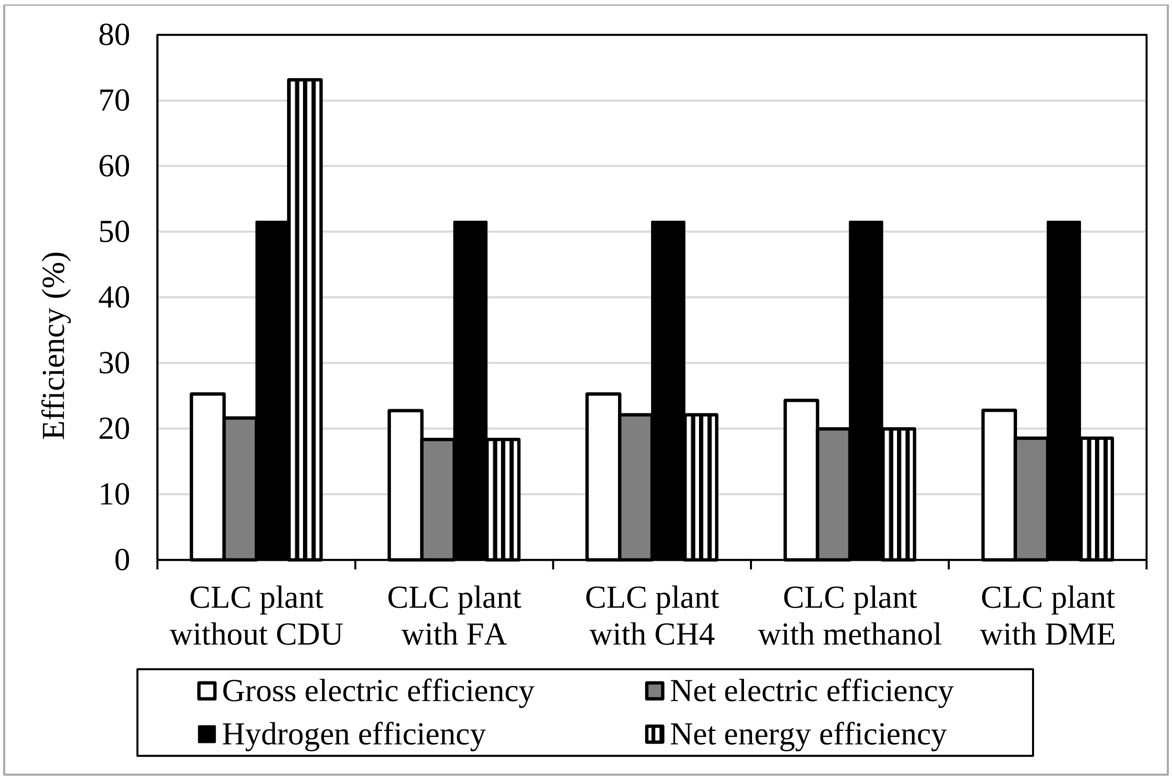

Figure 7.5 Overall performance comparison of CLC based plant with and without CDU plants based on energy analysis.

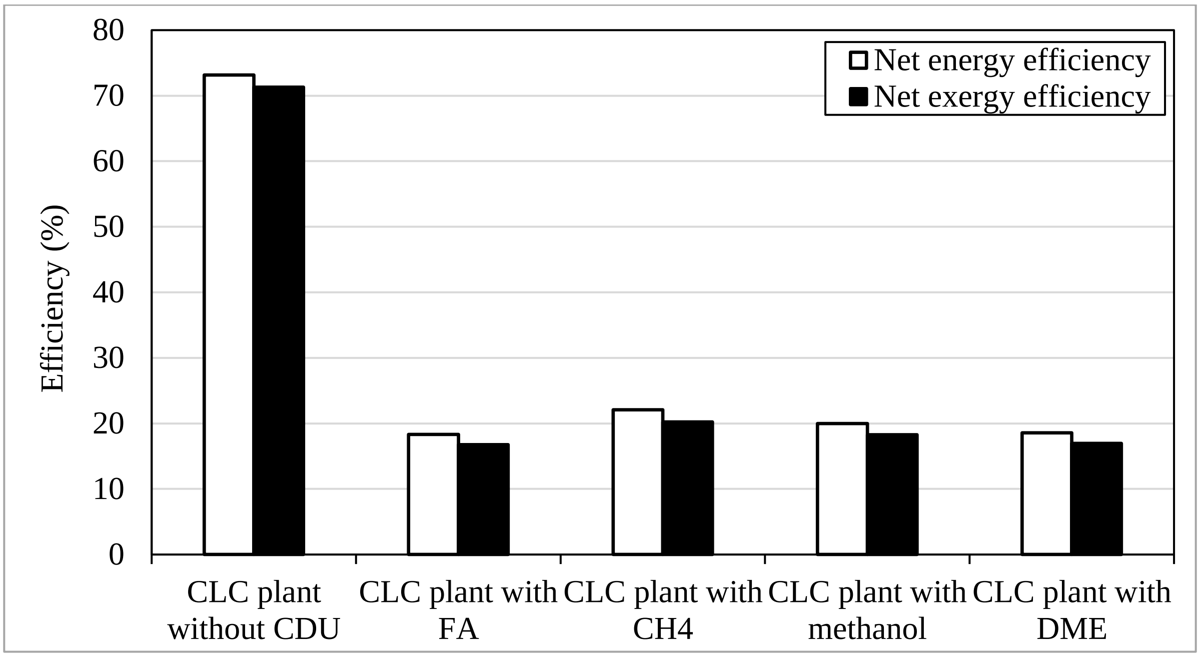

Figure 7.6 Overall performance comparison of CLC based plant with and without CDU plants based on exergy analysis.

A unit-wise exergy analysis is carried out for all considered plants as per the procedure described in *Section 3.3.2* in *Chapter 3*. Figure 7.7 shows the comparative analysis of exergy destruction rates of main units in the CLC based plant with and without CDU. The highest exergy destruction rate is found in the boiler unit for all the five cases. The boiler unit accounts for 81.69%, 68.82%, 78.42%, 75.30% and 75.81% of total exergy destruction rate for the CLC based plant without CDU, with FA, with methane, with MeOH and with DME synthesis, respectively. The highest exergy destruction rate in boiler is also found in other studies reported in literature [10,24]. The second highest contributor of exergy destruction rate is the CDU plant followed by steam turbine, compressor and gas turbine units.

The maximum possible improvement potential rate of main units of CLC based plant integrated with various CDU plants is shown in Figure 7.8. The highest contributor of the improvement potential rate is found in the boiler unit due it its higher exergy destruction rate. The next highest improvement potential rate is for CDU plant. This concludes that further studies including several parametric analyses on the boiler unit and CDU plant could help in improving the overall energy and exergy efficiencies of the integrated plants.

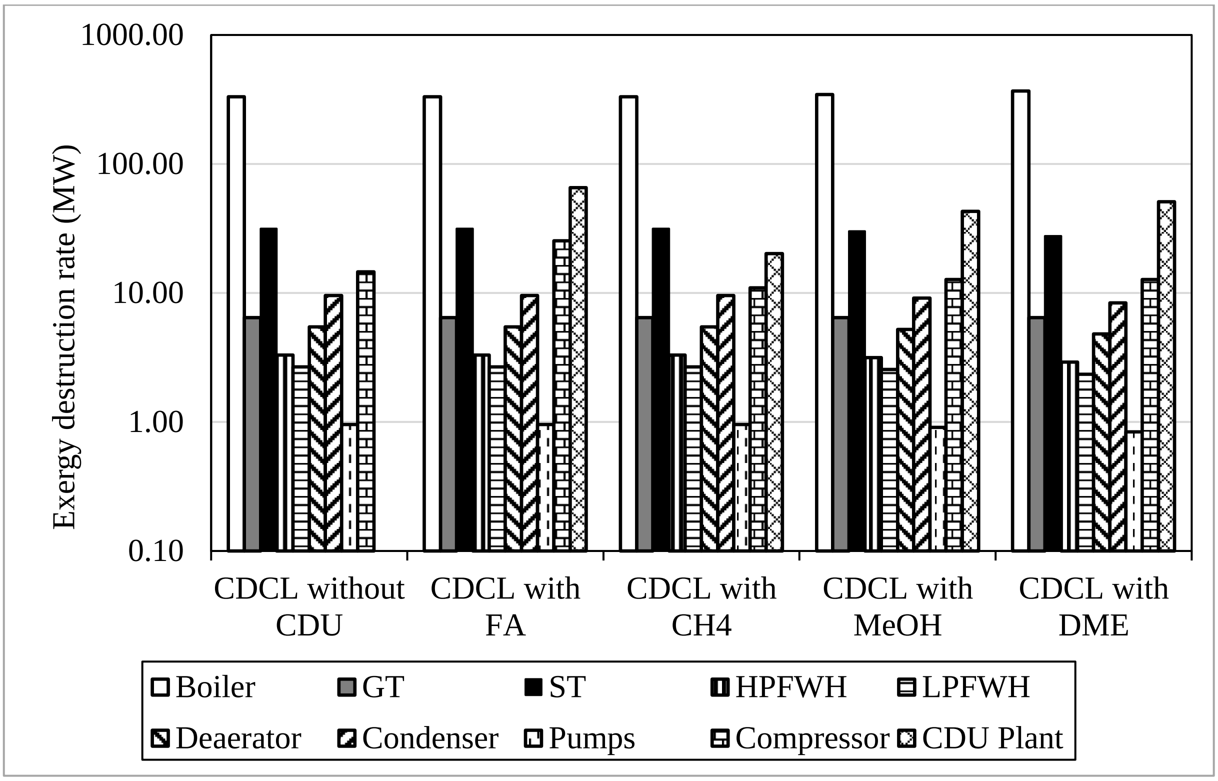

Figure 7.7 Comparison of exergy destruction rate of main units of CLC based plant integrated with various CDU plants.

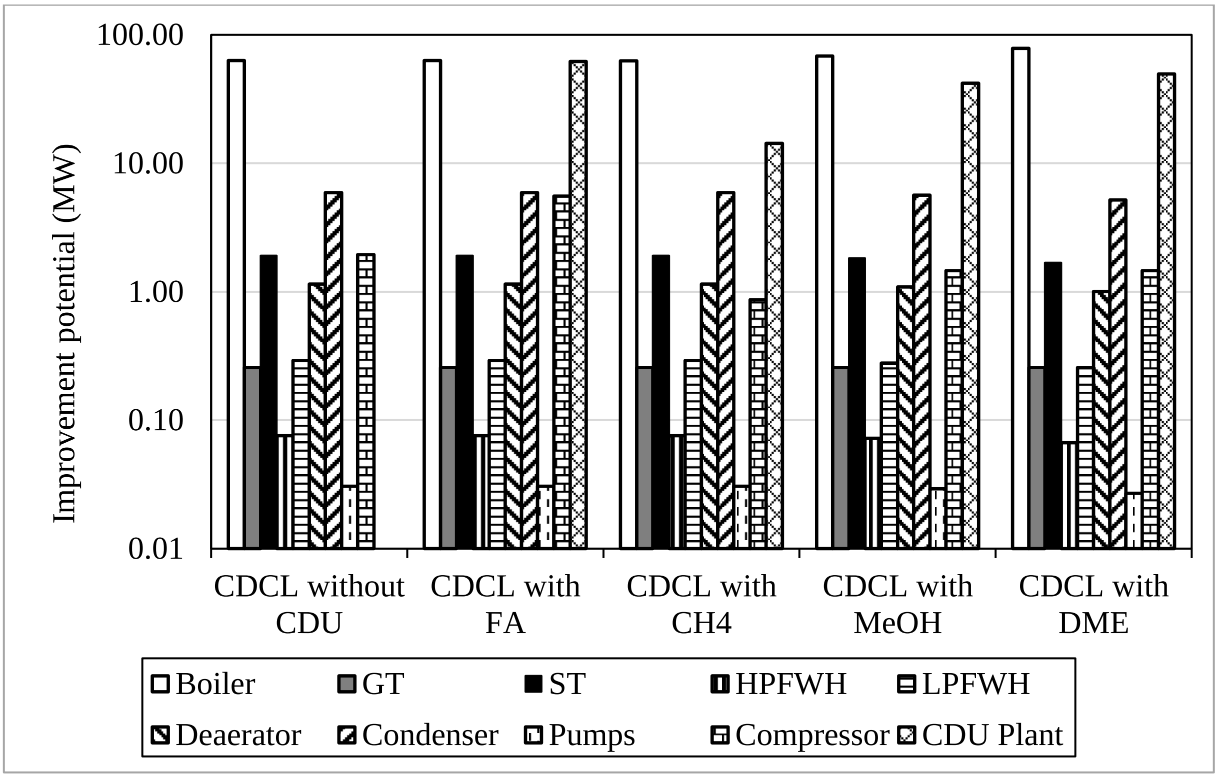

Figure 7.8 Comparison of improvement potential rate of main units of CLC based plant integrated with various CDU plants.

### *7.3.1.3 Ecological analysis*

The role of chemical looping combustion technology is to avoid $CO_2$ emissions. Hence, the ecological analysis has been carried out in this study and performance of CLC based plant with and without CDU is assessed in terms of overall $CO_2$ emission, annual $CO_2$ avoided, net energy output per amount of $CO_2$ captured, $CO_2$ capture efficiency and net energy output per amount of $CO_2$ utilized. Table 7.3 shows the comparison of CLC based plant integrated with various CDU plants based on ecological analysis. As CLC based technology has tendency to capture all $CO_2$ emitted from the power plant, the specific $CO_2$ emissions and annual $CO_2$ emission rate is almost zero with 100% $CO_2$ capture efficiency for all five cases up to hydrogen production stage. However, in the CDU plants, the overall conversion of $CO_2$ into the formic acid, methane, methanol and dimethyl ether is not 100% and remaining $CO_2$ (coming along with purge gases, as shown in the CDU flowsheets) is released in to the atmosphere. Hence, the plant emits 0.26 kg/s, 0.15 kg/s, 0.18 kg/s and 0.27 kg/s of $CO_2$ for CLC plant integrated with formic acid, methane, methanol and DME, respectively. These values are very low compared to the $CO_2$ emissions of 101.82 kg/s from a conventional CFPP without capture (as can be seen from Table 4.3). Annual $CO_2$ avoided emission per unit fuel is 79.25 kg.$CO_2$/GJ of coal input to the plant for CLC without $CO_2$ utilisation case. However, because of low $CO_2$ emissions in CDU cases, small reduction in annual $CO_2$ avoided emission per unit fuel is observed. The net energy output per $CO_2$ captured is found to be 9.23, 2.32, 2.79, 2.52 and 2.35 MW/kg for CLC based plant without CDU, with FA synthesis, with methane synthesis, with MeOH synthesis and with DME synthesis, respectively. The utilization of $CO_2$ in the various CDU plants resulted in the net energy output per $CO_2$ utilized as 2.31, 11.16, 7.56 and 7.02 MJ/kg for CLC plant with FA, methane, methanol and DME synthesis, respectively.

The synthesis products considered in this work (i.e. formic acid, methane, methanol and dimethyl ether) are used in various sectors, which can be again used as fuel and emits $CO_2$ in to the atmosphere. The amount of $CO_2$ released during the use of these synthesis products mainly depends on the type of their application. Hence, it would be difficult to draw generalization on this aspect and hence could not be included in this study.

### *7.3.1.4 Economic analysis*

The total capital cost, annual capital cost, total O&M cost and levelized cost of product are estimated as per the procedure described in *section 3.3.4* of *Chapter 3* and their results are shown in Table 7.4. In the case of CLC based plant without CDU, the end product is hydrogen and for rest of the cases, hydrogen is utilised to produce the products (FA, methane, methanol and DME). Hence, LCOP of CLC based plant without CDU, with FA, with methane, with methanol and with DME are estimated in terms of hydrogen, formic acid, methane, methanol and DME, respectively.

Table 7.3 Comparison of CLC based plant integrated with various CDU plants based on ecological analysis.

| Unit | Unit | CLC based plant without CDU | CLC based plant with FA | CLC based plant with $CH_4$ | CLC based plant with methanol | CLC based plant with DME |
|---|---|---|---|---|---|---|
| Overall $CO_2$ emission | kg/s | 0.00 | 0.26 | 0.15 | 0.18 | 0.27 |
| $CO_2$ capture efficiency | % | 100.00 | 94.53 | 98.51 | 94.78 | 93.05 |
| Specific $CO_2$ emission | kg/MWh | 0.00 | 99.75 | 99.86 | 99.82 | 99.74 |
| Average annual emission | kg | 0.00 | $6.48 \times 10^6$ | $3.71 \times 10^6$ | $4.63 \times 10^6$ | $6.79 \times 10^6$ |
| Annual $CO_2$ avoided emission per unit fuel | kg.$CO_2$/GJ | 79.25 | 79.05 | 79.13 | 79.10 | 79.04 |
| Net energy output per kg of $CO_2$ captured | MW/kg | 9.23 | 2.32 | 2.79 | 2.52 | 2.35 |
| Net energy output per kg of $CO_2$ utilized | MW/kg | - | 2.31 | 11.16 | 7.56 | 7.02 |

Total capital cost of CLC based plant with different CDUs is not much significant compared to CLC based plant without CDU. Highest TCC is observed for the CLC based plant with methane synthesis due to higher steam turbine power output, which results in higher cost of turbines, HRSG, FWH and condenser unit. Similar trends have been observed for the annual capital cost and total O&M cost. The LOCP of CLC based plant with hydrogen, formic acid, methane, methanol and DME is found to be 1.0265 €/kg, 0.0416 €/kg, 0.5433 €/kg, 0.1930 €/kg and 0.2914 €/kg, respectively. The cost of hydrogen found in the present study is lower by 0.1635 €/kg than the reported in literature for three reactor chemical looping reforming by Khan and Shamim [138]. Highest annual product production (3.20 Mt/year) is observed in the case of CLC based plant with formic acid synthesis compared to other cases, because of utilization of all the $CO_2$ produced in the power plant. This results in the lower LCOP for formic acid case. This estimated cost of formic acid is very low compared to that reported in literature. Amount of methane production is very low; hence, the cost of methane is high in present study. The CLC based plant integrated with methane synthesis may not be a better choice due to its higher cost of product compared to the cost reported in literature. Other than methane, all other cases resulted in the lower levelized cost of products compared to the values reported in literature as can be seen in the last but one column of the Table 7.4. The observed lower cost of formic acid, methanol and methane than their costs reported in literature is due to the higher annual product production compared to the literature. Moreover, the required hydrogen is produced from the CLC plant instead of purchasing it from some other source. The values of LCOP when hydrogen is produced from some other source than CLC plant are calculated and discussed in *Section 7.3.3*.

Table 7.4 Comparison of CLC based plant integrated with various CDU plants based on economic analysis.

| Plant | TCC (M€) | ACC (M€) | Total O&M (M€/yr) | Annual Product production (Mt/year) | LCOP (€/kg) | Cost of product from literature (€/kg) | Payback period (year) |
|---|---|---|---|---|---|---|---|
| CLC plant without CDU (with $H_2$) | 461.58 | 48.96 | 102.28 | 0.15 | 1.03 | 5.90 [200] | 1.47 |
| CLC plant with FA | 428.19 | 45.42 | 87.50 | 3.20 | 0.04 | 0.65 [148] | 1.47 |
| CLC plant with $CH_4$ | 466.92 | 49.53 | 97.44 | 0.27 | 0.54 | 0.12 [201] | 1.50 |
| CLC plant with MeOH | 448.84 | 47.61 | 93.28 | 0.73 | 0.19 | 0.35 [148] | 1.49 |
| CLC plant with DME | 427.76 | 45.38 | 92.41 | 0.47 | 0.29 | 0.38 [202] | 1.44 |

Electricity and products are considered as revenue from the plants. The LCOP are calculated based on no profit – no loss basis. Hence, the selling costs of products will be bit higher than those obtained in this study. The payback period is also estimated for all these plants with the obtained LCOPs in the present work and are listed in the last column of the Table 7.4. It can be noted that the payback period is less than or equal to one and half years for all the cases, which concludes that all the cases are economically favourable with formic acid case being most favourable option.

### *7.3.1.4 Life cycle analysis*

The goal of conducting life cycle analysis is to assess the GHG emissions and PFEC of CLC based plant with hydrogen, formic acid, methane, methanol and DME as end products. Figure 7.9 and 7.10 show amount of GHG emissions and PFEC at individual stages of overall system.

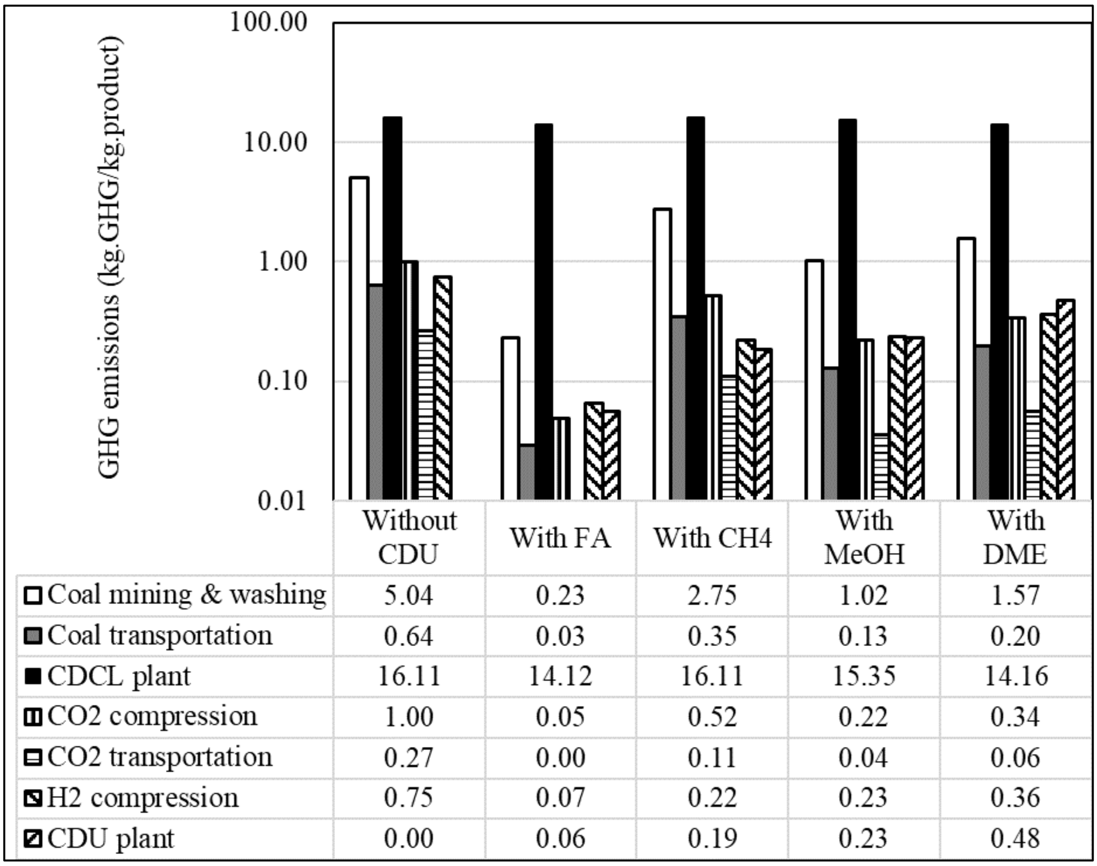

| | Without CDU | With FA | With CH4 | With MeOH | With DME |
|---|---|---|---|---|---|
| □ Coal mining & washing | 5.04 | 0.23 | 2.75 | 1.02 | 1.57 |
| ▩ Coal transportation | 0.64 | 0.03 | 0.35 | 0.13 | 0.20 |
| ■ CDCL plant | 16.11 | 14.12 | 16.11 | 15.35 | 14.16 |
| ▥ CO2 compression | 1.00 | 0.05 | 0.52 | 0.22 | 0.34 |
| ▤ CO2 transportation | 0.27 | 0.00 | 0.11 | 0.04 | 0.06 |
| ▧ H2 compression | 0.75 | 0.07 | 0.22 | 0.23 | 0.36 |
| ▨ CDU plant | 0.00 | 0.06 | 0.19 | 0.23 | 0.48 |

Figure 7.9 GHG emissions for CLC based plant integrated with various CDU plants.

The total GHG emissions from the CLC based plant with hydrogen, formic acid, methane, methanol and DME as end products are 16.11 kg/kg of hydrogen, 14.12 kg/kg of FA, 16.11 kg/kg of methane, 15.35 kg/kg of MeOH and 14.16 kg/kg of DME, respectively. The highest total GHG emissions are observed for CLC based plant without CDU because of the lower kg of product generation and the lowest total GHG emissions are noted for CLC based plant with FA synthesis because of the higher kg of product production compared to other cases. The contribution of CLC based plant stage in GHG emissions for all five cases is the highest. This is due to the large quantity of steam generation [29]. The second largest contributor of total GHG emissions is the coal mining & washing stage due to large amount of $CH_4$ and $CO_2$ emissions [29]. The CDU plant also contributes to the total GHG emissions due to fraction of $CO_2$ emissions from the plant. All other stages emit very low GHG emissions compared to these two stages. The total PFEC for the CLC based plant with hydrogen, formic acid, methane, methanol and DME as end products is also estimated and are found to be 507.26 MJ/kg of hydrogen, 177.00 MJ/kg of FA, 360.46 MJ/kg of methane, 241.32 MJ/kg of MeOH and 262.99 MJ/kg of DME, respectively as shown in Figure 7.10. Similar to GHG emissions, PFEC is observed to be high for CLC based plant without CDU case and low for CLC based plant with formic acid synthesis case. The contribution of CLC based plant stage in total PFEC is the highest (90.02% - 98.43%) for all five cases. Rest of the stages have very low PFEC contribution compared to the CLC based plant stage.

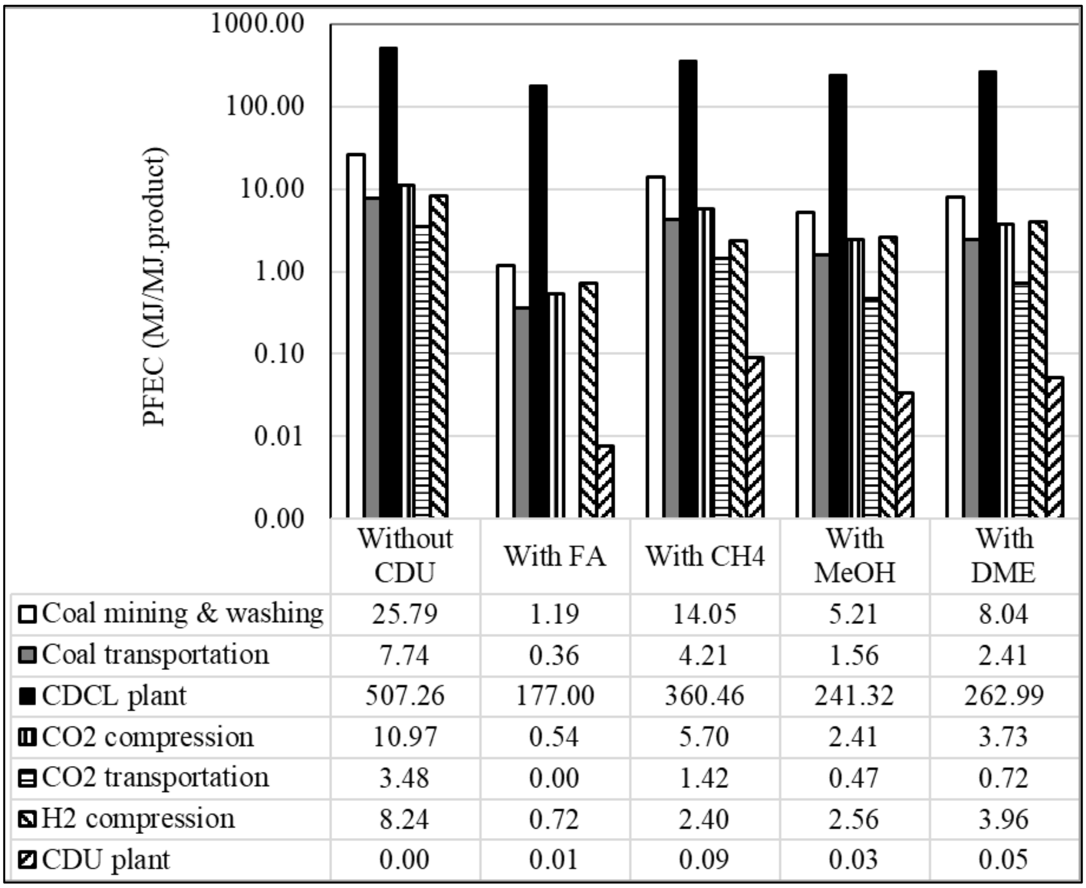

| | Without CDU | With FA | With CH4 | With MeOH | With DME |
|---|---|---|---|---|---|
| □ Coal mining & washing | 25.79 | 1.19 | 14.05 | 5.21 | 8.04 |
| ▩ Coal transportation | 7.74 | 0.36 | 4.21 | 1.56 | 2.41 |
| ■ CDCL plant | 507.26 | 177.00 | 360.46 | 241.32 | 262.99 |
| ◫ CO2 compression | 10.97 | 0.54 | 5.70 | 2.41 | 3.73 |
| ⊟ CO2 transportation | 3.48 | 0.00 | 1.42 | 0.47 | 0.72 |
| ▧ H2 compression | 8.24 | 0.72 | 2.40 | 2.56 | 3.96 |
| ▨ CDU plant | 0.00 | 0.01 | 0.09 | 0.03 | 0.05 |

Figure 7.10 PFEC for CLC based plant integrated with various CDU plants.

### 7.3.2 Comparison of 4-E& Life cycle analyses

This section presents comparative 4-E&L analyses of CLC based plant with and without CDU cases against the conventional CFPP and CLC based CFPP with power generation alone cases as given in *Chapter 4 and 5* (Table 7.5). The synthesis of useful chemical products from the captured $CO_2$ and $H_2$ culminates in the net electric efficiency penalty of 15.66%, 18.94%, 15.18%, 17.32% and 18.73% for the CLC based plant without CDU (cogeneration with $H_2$), with FA, methane, methanol and DME synthesis, respectively, compared to the CLC based CFPP with power alone. However, due to hydrogen generation, the net energy efficiency is higher for CLC based plant without CDU (co-generation) than both conventional and CLC based CFPPs with CDU. In this study, hydrogen energy output is not considered for CLC based plant with CDU cases as all the formed hydrogen is utilised in the CDU plant. Exergy analysis showed lower total exergy destruction rate and total exergetic improvement potential for CLC based plant with and without CDU compared to both conventional and CLC based CFPPs for power production alone. This is due to the hydrogen generation in the CLC reactors, which accounts for 663 MW of energy output stream from the boiler unit. The improvement potential rate follows similar trends as that of exergy destruction rate.

Based on the ecological analysis, the CLC plant without CDU case avoids 2.57 x $10^9$ kg of $CO_2$ emission annually. However due to $CO_2$ emissions from the CDU plant, the annual $CO_2$ emissions of 6.48x$10^6$, 3.71x$10^6$, 4.63x$10^6$ and 6.79x$10^6$ kg are observed for CLC plant with formic acid, methane, methanol and DME production, respectively. $CO_2$ utilisation efficiency of CLC based plant with formic acid, methane, methanol and DME is 100%, 25%, 33.33% and 33.33% with net energy output per product formation of 2.31 MW/kg, 11.16 MW/kg, 7.56 MW/kg and 7.02 MW/kg, respectively. The total GHG emissions and PFEC from the CLC based plants with hydrogen, formic acid, methane, methanol and DME as end products are 23.81, 14.50, 20.06, 16.99 and 16.69 kg/kg of product and 563.48, 179.82, 388.33, 253.57 and 281.90 MJ/kg of product, respectively.

Economic analysis indicates that all CLC based plants with/without CDU require around 3/4th of the total capital cost of the conventional and CLC based CFPPs. Although, the electricity generation from conventional and CLC based CFPPs is high (approximately 1.7 to 2 times), the utilization chemical products can be obtained with approximately 3/4th capital investment. Based on these results, cost of the products are obtained to be 1.0265, 0.0416, 0.5433, 0.1930 and 0.2914 €/kg of product for CLC plant with hydrogen, FA, methane, methanol and DME, respectively. The payback period for conventional and CLC based CFPPs is 3.51 years and 3.35 years, whereas it is less by around 2 years for CLC based plant with and without CDU plants.

Based on the comparative 4-E analyses, the CLC based plants with CDU compared to the conventional and CLC based CFPP cases are energetically, exergetically, ecologically and economically favourable cases with CLC based plant with formic acid synthesis being the most favourable choice.

Table 7.5 4-E&L analyses of CLC based plant integrated with hydrogen, FA, methane, methanol and DME.

| Case | Unit | CLC plant without CDU | CLC plant with FA | CLC plant with $CH_4$ | CLC plant with MeOH | CLC plant with DME | Conventional SupC CFPP | SupC CLC-CFPP |
|---|---|---|---|---|---|---|---|---|
| Electrical efficiency | % | 21.62 | 18.34 | 22.10 | 19.96 | 18.56 | 37.52 | 37.28 |
| Hydrogen efficiency | % | 51.52 | 51.52 | 51.52 | 51.52 | 51.52 | 0.00 | 0.00 |
| Energy efficiency | % | 73.13 | 18.34 | 22.10 | 19.96 | 18.56 | 37.52 | 37.28 |
| Total exergy destruction rate | MW | 407.06 | 483.22 | 422.19 | 458.27 | 484.39 | 831.31 | 889.60 |
| Total exergetic improvement potential | MW | 74.70 | 140.27 | 87.44 | 121.26 | 138.08 | 285.92 | 326.12 |
| Annual $CO_2$ emissions | kg | 0.00 | $6.48x10^6$ | $3.71x10^6$ | $4.63x10^6$ | $6.79x10^6$ | $2.57 \times 10^9$ | 0.00 |
| $CO_2$ utilization efficiency | % | 0.00 | 100.00 | 25.00 | 33.33 | 33.33 | 0.00 | 0.00 |
| Net energy output per kg of product | MW/kg | - | 2.31 | 11.16 | 7.56 | 7.02 | - | - |
| GHG emissions | kg GHG/kg product | 23.81 | 14.50 | 20.06 | 16.99 | 16.69 | - | - |
| PFEC | MJ/MJ product | 563.48 | 179.82 | 388.33 | 253.57 | 281.90 | - | - |
| TCC | M€ | 461.58 | 428.19 | 466.92 | 448.84 | 427.76 | 660.99 | 606.48 |
| COP | €/kg | 1.0265 | 0.0416 | 0.5433 | 0.1930 | 0.2914 | 0.00 | 0.00 |
| Payback period | years | 1.47 | 1.47 | 1.50 | 1.49 | 1.44 | 3.51 | 3.35 |

### 7.3.3 LCOP comparison for different approaches

In the preceding analysis, the hydrogen used in all the four CDU cases is assumed to be equivalent to that required for 100% $CO_2$ utilization to produce formic acid. As mole ratio of $CO_2$ to $H_2$ is 1:4, 1:3 and 1:3 for methane, methanol and DME synthesis plants respectively, the corresponding $CO_2$ utilization efficiencies are observed to be 25%, 33.33% and 33.33%. In this section, two other approaches are considered and evaluated with respect to the supply of hydrogen required for complete utilization of $CO_2$ captured from the proposed power plant based on CLC. These are compared with the results of the first approach. Following is the description of the three approaches for CDU compared with respect to the levelised cost of the end product.

Approach-1: CLC with 663 MW of hydrogen generation and CDU plant.

Approach-2: CLC based plant with 663 MW of hydrogen and remaining hydrogen considered from solid Oxide Electrolysis Cell (SOEC) [200].

Approach-3: CLC based CFPP (without hydrogen) with all the hydrogen considered from SOEC [200].

Table 7.6 shows the performance comparison of the CLC based plant with different CDU approaches. The cost of hydrogen from SOEC integrated with parabolic dish is considered as 5.9 €/kg of hydrogen as reported by Mastropasqua et al. [200].

Formic acid does not need any extra hydrogen for approach-2 as all $CO_2$ captured in CLC plant is utilized with the generated hydrogen as in approach-1. Thus, the LCOP, net electric efficiency and annual formic acid production are same for both approaches 1 and 2. The CLC based power plant with power generation alone is considered as third approach; hence, the net electrical energy efficiency is high compared to the first two approaches. However, the net electrical energy efficiency is reduced from 37.28% to 34.14% because of the increased power consumption in CDU plant. Hence, the LCOP of formic acid for third approach is higher by 0.259 €/kg than approach-1, but it is still around half of the cost of formic acid reported by Fortes et al. [148].

In case of synthesis of other products – methane, methanol and DME, additional hydrogen is required for approach-2 to utilize the captured $CO_2$ completely from the CLC based power plant. As mentioned earlier, the cost of methane reported in literature is low compared to the cost of methane obtained in CLC with 663 MW of hydrogen coupled with CDU plant. Moreover, the LCOP of methane plant is observed to be 4.5 times more for approach-2 compared to approach-1 with lower net electrical energy efficiency. Methane production for approach-3 has high net electrical energy efficiency compared to all other cases, but the LCOP of methane is very high (more than 6 times that of approach-1).

Methanol and DME synthesis plants have $CO_2$ utilization efficiency of 33.33% for approach-1. The additional hydrogen from SOEC to achieve 100% $CO_2$ utilization increases the cost of methanol and DME by 0.639 €/kg and 0.852 €/kg with net energy penalty of 6.98% and 6.60%, respectively. These costs of products for approach-2 are higher than those reported in literature (*see section 7.3.1*). The LCOP from approach-3 is found to be even higher compared to first two approaches (as can be seen from Table 7.6).

Table 7.6 Comparison of CLC based plant with different CDU approaches.

| Product | Plant | Net electric efficiency (%) | LCOP (€/kg) | Annual Product production (Mt/year) |
|---|---|---|---|---|
| Formic acid | Approach – 1 | 18.34 | 0.042 | 3.20 |
| | Approach – 2 | 18.34 | 0.042 | 3.20 |
| | Approach – 3 | 34.14 | 0.301 | 3.20 |
| Methane | Approach – 1 | 22.10 | 0.543 | 0.27 |
| | Approach – 2 | 17.42 | 2.455 | 1.08 |
| | Approach – 3 | 38.23 | 3.318 | 1.08 |
| Methanol | Approach – 1 | 19.96 | 0.193 | 0.73 |
| | Approach – 2 | 12.98 | 0.832 | 2.16 |
| | Approach – 3 | 32.22 | 1.249 | 2.16 |
| Dimethyl ether | Approach – 1 | 18.56 | 0.291 | 0.47 |
| | Approach – 2 | 11.96 | 1.143 | 1.57 |
| | Approach – 3 | 30.08 | 1.710 | 1.57 |

The CLC based plant with 663 MW of hydrogen generation coupled with CDU plant (approach-1) offers the lowest LCOP for all synthesis products. The results of approach-3 shows that, CLC based CFPP (without hydrogen generation) coupled with SOEC would result in higher cost of products compared to approach-1 and approach-2. Thus on comparison, it may be concluded that the CLC based plant integrated with CDU with hydrogen generation based on the demand of final synthesis product is the most favourable option.

## 7.4 Summary

Present work proposed a CLC based plant coupled with different $CO_2$ utilization plants to produce valuable chemical products – formic acid, methane, methanol and dimethyl ether. These cases are compared with the CLC based plant without $CO_2$ utilization based on 4-E&L analyses. Following are the key outcome of the present study:

- Based on energy analysis, the net electric efficiency of CLC based plant without CDU is found to be 21.62 % while the net electric efficiency for the CLC based plant with FA, methanol and DME synthesis is observed to be lesser by 3.28%, 1.65% and 3.06%, respectively and higher by 0.48% for CLC based plant with methane synthesis.
- Based on exergy analysis, the boiler unit accounts for 81.69%, 68.82%, 78.42, 75.30% and 75.81% of total exergy destruction rate for the CLC based plant without CDU, with FA, with methane, with MeOH and with DME synthesis with an improvement potential rate of 63.14 MW, 63.14 MW, 62.65 MW, 68.53 MW and 78.46 MW, respectively.
- Ecological analysis showed that all the CLC based CFPP plants integrated with CDU cases are environmentally feasible and avoids annual $CO_2$ emission of $2.57 \times 10^9$ kg and 79.25 kg of $CO_2$ per GJ of fuel input with $CO_2$ utilization % ranging from 25 to 100
- The LOCP values of CLC based plant with hydrogen, formic acid, methane, methanol and DME are found to be 1.0265 €/kg, 0.0416 €/kg, 0.5433 €/kg, 0.1930 €/kg and 0.2914 €/kg, respectively, with payback period of 1.47 years, 1.47 years, 1.50 years, 1.49 years and 1.44 years. The CLC based plant integrated with methane synthesis has not been turned out to be a better choice due to its higher cost of product compared to the cost reported in literature. All other cases resulted in lower cost of product compared to those reported in literature.
- The LCA showed that CLC plant stage contributes highest GHG emissions and PFEC compared to other all stages.

CLC based plant integrated with CDU with hydrogen generation based on the demand of chosen synthesis product may be a potential configuration to be considered for the upcoming power plants to be designed to completely capture and utilize the $CO_2$.

# Chapter 8

# Overall conclusions and scope for future work

# Chapter 8

# *Overall conclusions and scope for future work*

## 8.1 Overall conclusions

This thesis is intended to demonstrate the feasibility of integrating chemical looping combustion and carbon dioxide utilization technologies in Indian coal fired power plants for zero $CO_2$ emissions. The overall performance of these plants is assessed based on 4-E (i.e. energy, exergy, ecological and economic) analyses. The study is first conducted to check the feasibility of CLC based CFPP for three steam boilers such as – subcritical, supercritical and ultra-supercritical as presented in *Chapter 4*. Most feasible steam boiler from *Chapter 4* is considered to check the feasibility of different oxygen carriers in *Chapter 5*. The oxygen carrier with better overall performance is used to co-generate hydrogen along with power in CLC based SupC power plant in *Chapter 6*. This hydrogen co-generation CLC plant is then coupled with different carbon dioxide utilization plants to utilise the captured $CO_2$ from the CLC plant in *Chapter 7*.

Steady state simulations of all the CLC integrated plants are carried out using aspenONE v10.0. The conventional subcritical, supercritical and ultra-supercritical CFPPs are validated with the reported data in the literature. Moreover, the two- and three-reactor CLC systems are also validated with the literature data. All the validation results showed that, the simulation results obtained in the present work are in good agreement with the literature. A detailed parametric analysis of CLC integrated coal-fired power plant is carried out to check the effect of various CLC operating conditions on the overall performance of the plant. This parametric analysis is carried out for both two- and three-reactor CLC based CFPPs.

The key findings of the whole study presented in the previous chapters are summarized as follows:

- **Parametric analysis:**
    - The optimal operating parameters obtained for two-reactor CLC based CFPP are – oxygen carrier to coal ratio: 44.70 (mass basis), operating pressure of both air and fuel reactors: 10 bar, and operating temperature of air reactor: 900°C.

- The optimal operating parameters for three-reactor CLC based power plant for hydrogen and power co-generation are – operating pressure of air, fuel and steam reactors: 15 bar, fuel reactor operating temperature: 900$^o$C, steam reactor operating temperature: 750$^o$C and air reactor operating temperature: 1000$^o$C.

➢ **Energy analysis:**

- The energy analysis has shown that the CLC based SubC, SupC, and Ultra-SupC plants have net energy efficiency penalty of 0.92%, 1.49%, and 3.86%, compared to their respective conventional plants.
- This penalty is very low as compared to the conventional SupC CFPP with MEA based PCC.
- For a CLC based SupC CFPP, addition of 10% CuO in $Fe_2O_3$ (i.e. bimetallic oxygen carrier) improved the net energy efficiency by 2.36% compared to $Fe_2O_3$ alone.
- The CLC based power plant for hydrogen and power co-generation with bimetallic oxygen carrier has low net electrical efficiency but the net energy efficiency is high compared to the conventional and CLC based CFPP with power alone case.
- The net electric efficiency of CLC plant without CDU is found to be 21.62 % and these values for the CLC based plant with FA, methanol and DME synthesis are lower by 3.28%, 1.65% and 3.06%, respectively and higher by 0.48% for CLC based plant with methane synthesis.

➢ **Exergy analysis:**

- Exergy analysis revealed the highest exergy destruction rate and improvement potentials in the boiler unit of all the CLC based cases compared to all other units in the plant.
- The exergy destruction rate is reduced when the two-reactor CLC plant is modified to three-reactor CLC plant.
- Moreover, the exergy destruction rate is found to be decreasing with increase in hydrogen generation from the CLC plant.
- The boiler unit accounts for 81.69%, 68.82%, 78.42, 75.30% and 75.81% of total exergy destruction rate for the CLC based plant without CDU, with FA, with methane, with MeOH and with DME synthesis with an improvement potential rate of 63.14 MW, 63.14 MW, 62.65 MW, 68.53 MW and 78.46 MW, respectively.

➢ **Ecological analysis:**

- Both two- and three-reactor CLC based plants are environmentally feasible.

  - Integration of CLC to CFPPs brings down the annual $CO_2$ release of $2.57 \times 10^9$ kg to zero and avoids annual $CO_2$ emission of $2.57 \times 10^9$ kg from a 500 MW power plant (based on coal input) and 79.25 kg of $CO_2$ per GJ of fuel input.

- **Economic analysis:**
  - The economic analysis revealed that the overall LCOE of CLC based SupC and Ultra-SupC CFPPs are comparatively less than the conventional CFPPs without $CO_2$ capture and also CLC based SubC CFPP.
  - The $CO_2$ avoided cost and LCOE are found lowest for the conventional CFPP with MEA based $CO_2$ capture.
  - The overall LCOE of CLC based CFPP using $Fe_2O_3$, CuO and bimetallic oxygen carrier are found to be 89.05 €/MW.h, 98.25 €/MW.h and 91.95 €/MW.h, respectively.
  - The economic analysis is also evaluated based on the cost of product. The CLC based plant with 50% hydrogen and 50% power co-generation has LCOH of 1.94 €/kg of hydrogen, which is in the range reported in literature.
  - The LOCP of CLC based plant (for 663 MW of $H_2$ generation) with hydrogen, formic acid, methane, methanol and DME is found to be 1.0265 €/kg, 0.0416 €/kg, 0.5433 €/kg, 0.1930 €/kg and 0.2914 €/kg, respectively, with payback periods of 1.47 years, 1.47 years, 1.50 years, 1.49 years and 1.44 years.
- **Life cycle analysis:**
  - The LCA showed that CLC plant stage contributes highest GHG emissions and PFEC compared to all other stages.
  - The CLC plant with higher hydrogen production results in reduced GHG emissions and PFEC of overall system.
  - The total GHG emissions and PFEC from the CLC based plant with hydrogen, formic acid, methane, methanol and DME as end product are 23.81, 14.50, 20.06, 16.99 and 16.69 kg/kg of product and 563.48, 179.82, 388.33, 253.57 and 281.90 MJ/kg of product, respectively.

Based on the above extensive 4-E analyses study, it can be concluded that the CLC based SupC and Ultra-SupC CFPPs are energetically, exergetically, ecologically and economically efficient. The bimetallic oxygen carrier (with 90% $Fe_2O_3$ and 10% CuO) is preferable option as compared to CuO and $Fe_2O_3$ alone. Based on the 4-E and life cycle analyses, it can be concluded that the three-reactor CLC plant with hydrogen co-generation is energetically, exergetically, environmentally and economically feasible and efficient. Moreover, it is highly promising plant for the developing nations for hydrogen and electricity production with coal as a prime source of energy.

The CLC based plant integrated with methane synthesis may not be a better choice due to its higher cost of product compared to the cost reported in literature. Other than methane case, all other $CO_2$ utilization cases resulted in lower cost of product compared to those reported in literature. Based on the 4-E and life cycle analyses, it can be concluded that the three-reactor CLC plant with formic acid synthesis is the most favourable option with 100% $CO_2$ utilization efficiency. Moreover, based on the demand of product, the choice of multiple synthesis product by combining methanol and/or DME plants with formic acid plant could become the most favourable choice in future.

## 8.2 Scope for future work

In the present work, steady state simulations of CLC based coal fired power plants coupled with the $CO_2$ utilization plant are developed and analysed based on energy, exergy, ecological, economic and life cycle analyses. However, the work can be further continued, as there is a good scope for the future work as following:

- Equilibrium based Gibbs reactors are used in the CLC and CDU plants. These reactors may be replaced with the designed reactors with appropriate chemistries and kinetics to get better estimates. Hence, a detailed analysis involving design and simulation of the CLC based plants by considering rigorous models and size/dimensions of the individual units will be interesting to get a more realistic picture.
- Only four synthesis products (Formic acid, Methane, Methanol and DME) are considered in the CDU integration in the present study. The study can be extended to explore the feasibility of more synthesis products for better utilization of the captured $CO_2$ from the plant.
- The effect of ash in the coal on the performance of the oxygen carriers and the reactors is not considered. Hence, an experimental evaluation of the mixed oxygen carriers for CLC of high ash coal, study the effect of ash on the performance and developing the

models by incorporating the ash interaction effects would be a great effort in continuing this work.

- Development of pilot scale plant for CLC integrated CFPP and all the $CO_2$ utilization plants separately and coupled with each other as presented in the current study can be conducted.

# *List of Publications*

## INTERNATIONAL JOURNALS:

### (i) Based on the thesis:

1. **Surywanshi GD**, Pillai BBK, Patnaikuni VS, Vooradi R, Anne SB, 4-E analysis of chemical looping combustion based subcritical, supercritical and ultra-supercritical coal-fired power plants, *Energy Conversion and Management*, 200, 112050, 2019. https://doi.org/10.1016/j.enconman.2019.112050. (SCI impact factor: 8.208).

2. **Surywanshi GD**, Pillai BBK, Patnaikuni VS, Vooradi R, Anne SB, Energy and exergy analyses of Performance analysis of chemical looping combustion based 660 MWe supercritical coal fired power plant, *International Journal of Exergy*, 31 (1), 14-33, 2020. https://doi.org/10.1504/IJEX.2020.10024695. (SCI impact factor: 0.958).

3. **Surywanshi GD**, Pillai BBK, Patnaikuni VS, Vooradi R, Anne SB, Formic acid synthesis – A case study of $CO_2$ utilization from coal direct chemical looping combustion power plant, *Energy Sources Part-A: Recovery, Utilization, and Environmental Effects,* 2019. https://doi.org/10.1080/15567036.2019.1649325. (SCI impact factor: 1.184).

4. **Surywanshi GD**, Patnaikuni VS, Vooradi R, Anne SB, 4-E and life cycle analyses of a supercritical coal direct chemical looping combustion power plant with hydrogen and power co-generation, *Energy*, 217, 119418, 2021. https://doi.org/10.1016/j.energy.2020.119418. (SCI impact factor: 6.082).

5. **Surywanshi GD**, Patnaikuni VS, Coal fired power plant with chemical looping combustion, *Proceedings of Engineering and Technology Innovation*, 6, 2-16, 2017. ISSN 2518-833X.

6. **Surywanshi GD**, Patnaikuni VS, Vooradi R, Anne SB, CO2 capture and utilization from supercritical coal direct chemical looping combustion power plant – Comprehensive analysis of different case studies, *Applied Energy*, ***First Revision Submitted***. (SCI impact factor: 8.848).

7. **Surywanshi GD**, Pillai BBK, Patnaikuni VS, Vooradi R, Anne SB, Review on Chemical and calcium looping based coal fired power plants coupled with $CO_2$ utilization, ***Under preparation.***

**(ii) Other/co-authored publications:**

1. Sikarwar SS, **Surywanshi GD**, Patnaikuni VS, Kakunuri M, Vooradi R, Chemical looping combustion integrated organic Rankine cycled biomass fired power plant – energy and exergy analyses, Renewable Energy, 155, 931-949, 2020. https://doi.org/10.1016/j.renene.2020.03.114. (SCI impact factor: 6.274).
2. Pillai BBK, **Surywanshi GD**, Patnaikuni VS, Anne SB, Vooradi R, Performance analysis of a double calcium looping-integrated biomass-fired power plant: exploring a carbon reduction opportunity. International Journal of Energy Research, 43(10), 5301–5318, 2019. https://doi.org/10.1002/er.4520. (SCI impact factor: 3.741).

## INTERNATIONAL / NATIONAL CONFERENCES:

**(i) Based on the thesis:**

1. **Surywanshi GD**, Patnaikuni VS, Coal Fired Power Plant with Chemical Looping Combustion, International Conference on Advanced Technology Innovation (ICATI 2017), Samui, Thailand, 25-28 Jun 2017.
2. **Surywanshi GD**, Pillai BBK, Patnaikuni VS, Vooradi R, Anne SB, Energy and Exergy Analysis of Supercritical Coal Fired Power Plant Integrated with Chemical Looping Combustion, 10th International Energy, Exergy and Environment Symposium (IEEES-10), Katowice, Poland, July 1-4, 2018.
3. **Surywanshi GD**, Pillai BBK, Maheshwari M, Venkatesh K, Patnaikuni VS, Vooradi R, Anne SB, Synthesis of Formic Acid – A Case Study of $CO_2$ Utilization from Coal Direct Chemical Looping Combustion Power Plant, International Conference on Advances and Challenges for Sustainable Ecosystems (ICACSE 2018), NIT Tiruchirappalli, India, 6-8 December, 2018.
4. **Surywanshi GD**, Pillai BBK, Patnaikuni VS, Vooradi R, Anne SB, Chemical Looping Combustion based Advanced Ultra-Supercritical Coal Fired Power Plant, 2nd International Conference on New Frontiers in Chemical, Energy and Environmental Engineering (INCEEE- 2019), NIT Warangal, India, 15-16 February, 2019.
5. **Surywanshi GD**, Pillai BBK, Patnaikuni VS, Vooradi R, Anne SB, Analysis of Chemical Looping and Calcium Looping Combustion Integrated Power Plant for Hydrogen and

Power Co-generation, 11th International Exergy, Energy and Environment Symposium (IEEES-11), Chennai, India, 14-18 July 2019.

6. **Surywanshi GD**, Pillai BBK, Patnaikuni VS, Vooradi R, Anne SB, Energetic and exergetic analysis of chemical looping combustion integrated coal-fired power plant using different oxygen carriers, International Conference on Sustainable Energy and Green Technology 2019 (SEGT 2019), Millennium Hilton Bangkok, Bangkok, Thailand, 11-14 December 2019.

**(ii) Other/co-authored conferences:**

1. Pillai BBK, **Surywanshi GD**, Patnaikuni VS, Anne SB, Vooradi R, Energy analysis of sugarcane bagasse based biomass power plant integrated with calcium looping technology, 10th International Energy, Exergy and Environment Symposium (IEEES-10), Katowice, Poland, July 1-4, 2018.
2. Sikarwar SS, **Surywanshi GD**, Pillai BBK, Patnaikuni VS, Anne SB, Vooradi R, Thermodynamic Analysis of Chemical Looping Combustion Integrated Sugarcane Bagasse based Biomass Power Plant, International Conference on Advances and Challenges for Sustainable Ecosystems (ICACSE 2018), NIT Tiruchirappalli, India, 6-8 December, 2018.
3. Sharma DK, **Surywanshi GD**, Patnaikuni VS, Computational Modelling of Ash Slagging In Chemical Looping Combustion of High-Ash Indian Coal, 2nd International Conference on New Frontiers in Chemical, Energy and Environmental Engineering (INCEEE- 2019), NIT Warangal, India, 15-16 February, 2019.
4. Sikarwar SS, **Surywanshi GD**, Pillai BBK, Patnaikuni VS, Anne SB, Vooradi R, Heat Integration of Chemical Looping Combustion based Biomass-Fired Power Plant, 2nd International Conference on New Frontiers in Chemical, Energy and Environmental Engineering (INCEEE- 2019), NIT Warangal, India, 15-16 February, 2019.
5. Pillai BBK, **Surywanshi GD**, Patnaikuni VS, Anne SB, Vooradi R, Energy and Exergy Analysis of a Natural Gas Fired Combined Cycle Power Plant Integrated with Calcium Looping for CO2 Capture in Indian Climatic Conditions, 2nd International Conference on New Frontiers in Chemical, Energy and Environmental Engineering (INCEEE- 2019), NIT Warangal, India, 15-16 February, 2019.
6. Pillai BBK, Aband M, **Surywanshi GD**, Patnaikuni VS, Anne SB, Vooradi R, Integration of NGCC power plant with dry reforming of natural gas for dimethyl ether production:

$CO_2$ utilization approach, 11th International Exergy, Energy and Environment Symposium (IEEES-11), Chennai, India, 14-18 July 2019.

7. Sikarwar SS, **Surywanshi GD**, Pillai BBK, Patnaikuni VS, Anne SB, Vooradi R, Interaction between Coal-Ash and Iron-Ore in Chemical Looping Combustion, International Conference on Sustainable Energy and Green Technology 2019 (SEGT 2019), Millennium Hilton Bangkok, Bangkok, Thailand, 11-14 December 2019.
8. Sharma DK, **Surywanshi GD**, Patnaikuni VS, Computational modeling of ash slagging in oxy-coal combustion of low rank coal, A Two-Day National Conference on Dynamics of Interfaces in Multiphase Systems, NIT Warangal, India, December 15-16, 2018.

# *References*

[1] Muntean M, Guizzardi D, Schaaf E, Crippa M, Solazzo E, Olivier JGJ, et al. Fossil CO2 emissions of all world countries - 2018 report. Eur 29433 En 2018:1–7. https://doi.org/10.2760/30158.

[2] CO2 Emissions, Global Carbon Atlas - fossil fuels emissions 2018 2019. http://www.globalcarbonatlas.org/en/CO2-emissions (accessed May 11, 2020).

[3] Location wise regional summary of all India installed capacity (in MW) of utility power stations as on 31-03-2018" 2018:65546. https://npp.gov.in/public-reports/cea/monthly/installcap/2018/MAR/capacity1-2018-03.pdf.

[4] Energy. BP Statistical Review of World Energy - June 2017 2017. https://www.bp.com/en/global/corporate/energy-economics/statistical-review-of-world-energy.html (accessed December 12, 2018).

[5] Suresh MVJJ, Reddy KS, Kolar AK. 3-E analysis of advanced power plants based on high ash coal. Int J Energy Res 2010;34:716–35. https://doi.org/10.1002/er.1593.

[6] Katzer A. The Future of Coal. 2007.

[7] Adanez J, Abad A, Garcia-Labiano F, Gayan P, De Diego LF. Progress in chemical-looping combustion and reforming technologies. Prog Energy Combust Sci 2012;38:215–82. https://doi.org/10.1016/j.pecs.2011.09.001.

[8] Fan L. Chemical Looping Systems for Fossil Energy Conversion. American Institute of Chemical Engineers; 2010.

[9] Karmakar S, Suresh MVJJ, Kolar AK. The effect of advanced steam parameter-based coal-fired power plants with CO2capture on the Indian energy scenario. Int J Green Energy 2013;10:1011–25. https://doi.org/10.1080/15435075.2012.729171.

[10] Mukherjee S, Kumar P, Yang A, Fennell P. Energy and exergy analysis of chemical looping combustion technology and comparison with pre-combustion and oxy-fuel combustion technologies for CO<inf>2</inf> capture. J Environ Chem Eng 2015;3:2104–14. https://doi.org/10.1016/j.jece.2015.07.018.

[11] Zeng L, He F, Li F, Fan LS. Coal-direct chemical looping gasification for hydrogen production: Reactor modeling and process simulation. Energy and Fuels 2012;26:3680–90. https://doi.org/10.1021/ef3003685.

[12] Xiang D, Liu S, Xiang J, Cao Y. A novel path toward methanol and olefins production fueled by syngas via a coupling of coke-oven gas reforming with pulverized coke chemical looping combustion. Energy Convers Manag 2017;152:239–49. https://doi.org/10.1016/j.enconman.2017.09.053.

[13] Adánez J, Abad A, Mendiara T, Gayán P, de Diego LF, García-Labiano F. Chemical looping combustion of solid fuels. Prog Energy Combust Sci 2018;65:6–66. https://doi.org/10.1016/j.pecs.2017.07.005.

[14] Pérez-Fortes M, Schöneberger JC, Boulamanti A, Harrison G, Tzimas E. Formic acid synthesis using CO2 as raw material: Techno-economic and environmental evaluation and market potential. Int J Hydrogen Energy 2016;41:16444–62. https://doi.org/10.1016/j.ijhydene.2016.05.199.

[15] Alper E, Orhan OY. CO2 utilization: Developments in conversion processes. Petroleum 2017;3:109–26. https://doi.org/10.1016/j.petlm.2016.11.003.

[16] Koytsoumpa EI, Bergins C, Kakaras E. The CO2 economy : Review of CO2 capture and reuse technologies. J Supercrit Fluids 2018;132:3–16. https://doi.org/10.1016/j.supflu.2017.07.029.

[17] Chauvy R, Meunier N, Thomas D, De Weireld G. Selecting emerging CO2 utilization products for short to mid-term deployment. Appl Energy 2018;236:662–80. https://doi.org/10.1016/j.apenergy.2018.11.096.

[18] Demirel Y, Matzen M, Winters C, Gao X. Capturing and using CO2 as feedstock with chemical looping and hydrothermal technologies. Int J Energy Res 2014;39:1011–47. https://doi.org/10.1002/er.3277.

[19] Ibrahim Dincer, Cengel YA. Energy, Entropy and Exergy Concepts and Their Roles in Thermal Engineering. Entropy 2001;3:116–49. https://doi.org/10.3390/e3030116.

[20] Dincer I, Rosen MA. Exergy Energy, Environment And Sustainable Development. Elsevier; 2013.

[21] Panwar NL, Kaushik SC, Kothari S. A review on energy and exergy analysis of solar dying systems. Renew Sustain Energy Rev 2012;16:2812–9. https://doi.org/10.1016/j.rser.2012.02.053.

[22] Rosen MA. Energy- and exergy-based comparison of coal-fired and nuclear steam power plants. Exergy, An Int J 2001;1:180–92. https://doi.org/10.1016/s1164-0235(01)00024-3.

[23] Ibrahim Dincer, Marc A. Rosen. Exergy Analysis of Heating, Refrigerating, and Air Conditioning: Methods and Applications. 2015. https://doi.org/10.1016/C2013-0-06800-4.

[24] Shijaz H, Attada Y, Patnaikuni VS, Vooradi R, Anne SB. Analysis of integrated gasification combined cycle power plant incorporating chemical looping combustion for environment-friendly utilization of Indian coal. Energy Convers Manag 2017;151:414–25. https://doi.org/10.1016/j.enconman.2017.08.075.

[25] Kumar R. A critical review on energy, exergy, exergoeconomic and economic (4-E) analysis of thermal power plants. Eng Sci Technol an Int J 2017;20:283–92. https://doi.org/10.1016/j.jestch.2016.08.018.

[26] NETL. Quality guidelines for energy system studies performing a techno-economic analysis for power generation plants. 2015.

[27] NETL. Cost Estimation Methodology for NETL Assessments of Power Plant Performance. 2011.

[28] Warren D. Seider, J. D. Seader, Daniel R. Lewin SW. Product and Process Design Principles: Synthesis, Analysis and Evaluation. John Wiley & Sons; 2018.

[29] Li G, Liu F, Liu T, Yu Z, Liu Z, Fang Y. Life cycle assessment of coal direct chemical looping hydrogen generation with Fe2O3 oxygen carrier. J Clean Prod 2019;239:118118. https://doi.org/10.1016/j.jclepro.2019.118118.

[30] IEA. World Energy Outlook 2019, IEA, Paris 2019. https://www.iea.org/reports/world-energy-outlook-2019.

[31] IEA. Energy technology perspectives 2010: scenarios & strategies to 2050, OECD/IEA,

Paris. 2010.
[32] IEA. World Energy Outlook 2017, Paris, France. 2017.
[33] IEA. Carbon capture and storage: progress and next steps, IEA/CSLF report to the Muskoka 2010 G8 Summit, OECD/IEA, Paris. 2010. https://doi.org/10.1021/es903626u.
[34] Li MJ, Tao WQ. Review of methodologies and polices for evaluation of energy efficiency in high energy-consuming industry. Appl Energy 2017;187:203–15. https://doi.org/10.1016/j.apenergy.2016.11.039.
[35] Xu Y, Ren Q, Zheng ZJ, He YL. Evaluation and optimization of melting performance for a latent heat thermal energy storage unit partially filled with porous media. Appl Energy 2017;193:84–95. https://doi.org/10.1016/j.apenergy.2017.02.019.
[36] Nandy A, Loha C, Gu S, Sarkar P, Karmakar MK, Chatterjee PK. Present status and overview of Chemical Looping Combustion technology. Renew Sustain Energy Rev 2016;59:597–619. https://doi.org/10.1016/j.rser.2016.01.003.
[37] CCS. Carbon Capture and Storage Association n.d. http://www.ccsassociation.org/ (accessed October 10, 2020).
[38] Hossain MM, Lasa HI De. Chemical-looping combustion ( CLC ) for inherent CO2 separations — a review. Chem Eng Sci 2008;63:4433–51. https://doi.org/10.1016/j.ces.2008.05.028.
[39] Mondal MK, Balsora HK, Varshney P. Progress and trends in CO2 capture / separation technologies : A review. Energy 2012;46:431–41. https://doi.org/10.1016/j.energy.2012.08.006.
[40] Guan G. Clean coal technologies in Japan: A review Guoqing. Chinese J Chem Eng 2017;25:689–97. https://doi.org/10.1016/j.cjche.2016.12.008.
[41] Song C, Liu Q, Ji N, Deng S, Zhao J, Li Y, et al. Alternative pathways for efficient CO2 capture by hybrid processes—A review. Renew Sustain Energy Rev 2018;82:215–31. https://doi.org/10.1016/j.rser.2017.09.040.
[42] Berstad D, Anantharaman R, Blom R, Jordal K, Arstad B. International Journal of Greenhouse Gas Control NGCC post-combustion CO2 capture with Ca / carbonate looping : Efficiency dependency on sorbent properties , capture unit performance and process configuration. Int J Greenh Gas Control 2014;24:43–53. https://doi.org/10.1016/j.ijggc.2014.02.015.
[43] El SAN, Nelson T, Kataria A, Abu-zahra MRM. International Journal of Greenhouse Gas Control Benchmarking of a novel solid sorbent CO2 capture process for NGCC power generation. Int J Greenh Gas Control 2015;42:583–92. https://doi.org/10.1016/j.ijggc.2015.09.014.
[44] Merkel TC, Wei X, He Z, White LS, Wijmans JG, Baker RW. Selective Exhaust Gas Recycle with Membranes for CO2 Capture from Natural Gas Combined Cycle Power Plants. Ind Eng Chem Res 2013;52:1150–9.
[45] Hetland J, Marie H, Haugen G, Major F, Kårstad V, Tjellander G. Integrating a full carbon capture scheme onto a 450 MW e NGCC electric power generation hub for offshore operations : Presenting the Sevan GTW concept. Appl Energy 2009;86:2298–307. https://doi.org/10.1016/j.apenergy.2009.03.019.
[46] Spek M Van Der, Ramirez A, Faaij A. Challenges and uncertainties of ex ante techno-

economic analysis of low TRL CO2 capture technology : Lessons from a case study of an NGCC with exhaust gas recycle and electric swing adsorption. Appl Energy 2017;208:920–34. https://doi.org/10.1016/j.apenergy.2017.09.058.

[47] Lillia S, Bonalumi D, Grande C, Manzolini G. A comprehensive modeling of the hybrid temperature electric swing adsorption process for CO2 capture. Int J Greenh Gas Control 2018;74:155–73. https://doi.org/10.1016/j.ijggc.2018.04.012.

[48] Scholes CA, Ho MT, Wiley DE, Stevens GW, Kentish SE. International Journal of Greenhouse Gas Control Cost competitive membrane-cryogenic post-combustion carbon capture. Int J Greenh Gas Control 2013;17:341–8. https://doi.org/10.1016/j.ijggc.2013.05.017.

[49] Mukherjee S, Kumar P, Yang A, Fennell P. Energy and exergy analysis of chemical looping combustion technology and comparison with pre-combustion and oxy-fuel combustion technologies for CO2 capture. J Environ Chem Eng 2015;3:2104–14. https://doi.org/10.1016/j.jece.2015.07.018.

[50] Chiesa P, Consonni S, Kreutz T, Williams R. Co-production of hydrogen , electricity and CO2 from coal with commercially ready technology. PartA: Performance and emissions. Int J Hydrogen Energy 2005;30:747–67. https://doi.org/10.1016/j.ijhydene.2004.08.002.

[51] Franz J, Maas P, Scherer V. Economic evaluation of pre-combustion CO2 -capture in IGCC power plants by porous ceramic membranes. Appl Energy 2014:1–11. https://doi.org/10.1016/j.apenergy.2014.02.021.

[52] Rezvani S, Huang Y, Mcilveen-wright D, Hewitt N, Mondol JD. Comparative assessment of coal fired IGCC systems with CO2 capture using physical absorption , membrane reactors and chemical looping. Fuel 2009;88:2463–72. https://doi.org/10.1016/j.fuel.2009.04.021.

[53] Kunze C, Spliethoff H. Assessment of oxy-fuel, pre- and post-combustion-based carbon capture for future IGCC plants. Appl Energy 2012;94:109–16. https://doi.org/10.1016/j.apenergy.2012.01.013.

[54] Kunze C, Spliethoff H. Assessment of different solvent-based capture technologies within an IGCC-CCS power plant. Appl Energy 2012;94:109–16. https://doi.org/10.1016/j.apenergy.2012.01.013.

[55] Cormos AM, Cormos CC. Investigation of hydrogen and power co-generation based on direct coal chemical looping systems. Int J Hydrogen Energy 2014;39:2067–77. https://doi.org/10.1016/j.ijhydene.2013.11.123.

[56] Moioli S, Giuffrida A, Gamba S, Romano MC, Pellegrini L, Lozza G. Pre-combustion CO2 capture by MDEA process in IGCC based on air-blown gasification. Energy Procedia 2014;63:2045–53. https://doi.org/10.1016/j.egypro.2014.11.220.

[57] Petrescu L, Cormos CC. Environmental assessment of IGCC power plants with pre-combustion CO2 capture by chemical & calcium looping methods. J Clean Prod 2017;158:233–44. https://doi.org/10.1016/j.jclepro.2017.05.011.

[58] Wu Y, Chen X, Ma J, Wu Y, Liu D, Mi J, et al. System integration for coal-fired power plant with post combustion CO2 capture: Comparative study for different solid dry sorbents. Fuel 2020;280:118561. https://doi.org/10.1016/j.fuel.2020.118561.

[59] Wu X, Wang M, Shen J, Li Y, Lawal A, Lee KY. International Journal of Greenhouse

Gas Control Flexible operation of coal fired power plant integrated with post combustion CO2 capture using model predictive control. Int J Greenh Gas Control 2019;82:138–51. https://doi.org/10.1016/j.ijggc.2018.12.004.

[60] Wang J, Zhao J, Deng S, Sun T, Du Y, Li K, et al. Integrated assessment for solar-assisted carbon capture and storage power plant by adopting resilience thinking on energy system. J Clean Prod 2019;208:1009–21. https://doi.org/10.1016/j.jclepro.2018.10.090.

[61] Wang J, Sun T, Zhao J, Deng S, Li K, Xu Y, et al. Thermodynamic considerations on MEA absorption: Whether thermodynamic cycle could be used as a tool for energy efficiency analysis. Energy 2019;168:380–92. https://doi.org/10.1016/j.energy.2018.11.084.

[62] Wang J, Zhao J, Wang Y, Deng S, Sun T, Li K. Application potential of solar-assisted post-combustion carbon capture and storage (CCS) in China: A life cycle approach. J Clean Prod 2017;154:541–52. https://doi.org/10.1016/j.jclepro.2017.04.021.

[63] Oh S, Yun S, Kim J. Process integration and design for maximizing energy efficiency of a coal-fired power plant integrated with amine-based CO2 capture process. Appl Energy 2018;216:311–22. https://doi.org/10.1016/j.apenergy.2018.02.100.

[64] Mores PL, Manassaldi JI, Scenna NJ, Caballero JA, Mussati MC, Mussati SF. Optimization of the design, operating conditions, and coupling configuration of combined cycle power plants and CO2 capture processes by minimizing the mitigation cost. Chem Eng J 2018;331:870–94. https://doi.org/10.1016/j.cej.2017.08.111.

[65] He Z, Ricardez-sandoval LA. International Journal of Greenhouse Gas Control Dynamic modelling of a commercial-scale CO2 capture plant integrated with a natural gas combined cycle (NGCC) power plant. Int J Greenh Gas Control 2016;55:23–35. https://doi.org/10.1016/j.ijggc.2016.11.001.

[66] Shi Y, Liu Q, Shao Y, Zhong W. Energy and exergy analysis of oxy-fuel combustion based on circulating fluidized bed power plant firing coal, lignite and biomass. Fuel 2020;269:117424. https://doi.org/10.1016/j.fuel.2020.117424.

[67] Chen S, Yu R, Soomro A, Xiang W. Thermodynamic assessment and optimization of a pressurized fluidized bed oxy-fuel combustion power plant with CO2 capture. Energy 2019;175:445–55. https://doi.org/10.1016/j.energy.2019.03.090.

[68] Qing M, Jin B, Ma J, Zou X, Wang X, Zheng C, et al. Thermodynamic and economic performance of oxy-combustion power plants integrating chemical looping air separation. Energy 2020;206:118136. https://doi.org/10.1016/j.energy.2020.118136.

[69] Xin T, Xu C, Liu W, Xu G, Yang Y. Thermodynamic analysis of a novel oxy-combustion supercritical carbon dioxide power cycle integrating solar-driven coal gasification. Energy Procedia 2019;158:1962–7. https://doi.org/10.1016/j.egypro.2019.01.452.

[70] Alam S, Sumana C. Thermodynamic analysis of plant-wide CLC-SESMR scheme for H 2 production: Studying the effect of oxygen carrier supports. Int J Hydrogen Energy 2019;44:3250–63. https://doi.org/10.1016/j.ijhydene.2018.12.017.

[71] Mishra N, Bhui B, Vairakannu P. Comparative evaluation of performance of high and low ash coal fuelled chemical looping combustion integrated combined cycle power generating systems. Energy 2019;169:305–18. https://doi.org/10.1016/j.energy.2018.12.043.

[72] Fan J, Zhu L, Hong H, Jiang Q, Jin H. A thermodynamic and environmental performance of in-situ gasification of chemical looping combustion for power generation using ilmenite with different coals and comparison with other coal driven power technologies for CO2 capture. Energy 2017;119:1171–80. https://doi.org/10.1016/j.energy.2016.11.072.

[73] He F, Galinsky N, Li F. Chemical looping gasification of solid fuels using bimetallic oxygen carrier particles - Feasibility assessment and process simulations. Int J Hydrogen Energy 2013;38:7839–54. https://doi.org/10.1016/j.ijhydene.2013.04.054.

[74] Fan J, Hong H, Zhu L, Wang Z, Jin H. Thermodynamic evaluation of chemical looping combustion for combined cooling heating and power production driven by coal. Energy Convers Manag 2017;135:200–11. https://doi.org/10.1016/j.enconman.2016.12.022.

[75] Zeng L, He F, Li F, Fan L. Coal-Direct Chemical Looping Gasification for Hydrogen Production : Reactor Modeling and Process Simulation. Energy & Fuels 2012;26:3680–90. https://doi.org/10.1021/ef3003685.

[76] Lagtah NMA Al, Onaizi SA, Albadarin AB, Ghaith FA, Nour MI. Techno-economic analysis of the effects of heat integration and different carbon capture technologies on the performance of coal-based IGCC power plants. J Environ Chem Eng 2019;7:103471. https://doi.org/10.1016/j.jece.2019.103471.

[77] Li F, Kang J, Song Y, Feng J, Li W. Thermodynamic feasibility for molybdenum-based gaseous oxides assisted looping coal gasification and its derived power plant. Energy 2020;194:116830. https://doi.org/10.1016/j.energy.2019.116830.

[78] Xiang W, Chen S, Xue Z, Sun X. Investigation of coal gasification hydrogen and electricity co-production plant with three-reactors chemical looping process. Int J Hydrogen Energy 2010;35:8580–91. https://doi.org/10.1016/j.ijhydene.2010.04.167.

[79] Ozcan H, Dincer I. Thermodynamic analysis of a combined chemical looping-based trigeneration system. Energy Convers Manag 2014;85:477–87. https://doi.org/10.1016/j.enconman.2014.06.011.

[80] Mukherjee S, Kumar P, Yang A, Fennell P. Energy and exergy analysis of chemical looping combustion technology and comparison with pre-combustion and oxy-fuel combustion technologies for CO2 capture. J Environ Chem Eng 2015;3:2104–14. https://doi.org/10.1016/j.jece.2015.07.018.

[81] Shi B, Wen F, Wu W. Performance evaluation of air-blown IGCC polygeneration plants using chemical looping hydrogen generation and methanol synthesis loop. Energy 2020;200:117564. https://doi.org/10.1016/j.energy.2020.117564.

[82] Fan J, Hong H, Jin H. Biomass and coal co-feed power and SNG polygeneration with chemical looping combustion to reduce carbon footprint for sustainable energy development : Process simulation and thermodynamic assessment. Renew Energy 2018;125:260–9. https://doi.org/10.1016/j.renene.2018.02.116.

[83] Shen Z, Huang Z. High-efficiency and pollution-controlling in-situ gasification chemical looping combustion system by using CO2 instead of steam as gasification agent. Chinese J Chem Eng 2018;26:2368–76. https://doi.org/10.1016/j.cjche.2018.03.016.

[84] Lewis WK, Gilliland ER. Production of pure carbon dioxide. US2665972A, 1954.

[85] Richter HJ, Knoche KF. Reversibility of combustion process. In: Gaggioli RA, editor.

Efficiency and costing, second law analysis of process. vol. 235. 1983. https://doi.org/10.1021/bk-1983-0235.ch003.

[86] Ishida M, Zheng D, Akehata T. Evaluation of a chemical-looping-combustion power-generation system by graphic exergy analysis. Energy 1987;12:147–54. https://doi.org/10.1016/0360-5442(87)90119-8.

[87] Ishida M, Jin H. A new advanced power-generation system using chemical-looping combustion. Energy 1994;19:415–22. https://doi.org/10.1016/0360-5442(94)90120-1.

[88] Ishida M, Jin H. A Novel Combustor Based on Chemical-Looping Reactions and Its Reaction Kinetics. J Chem Eng Japan 1994;27:296–301. https://doi.org/10.1252/jcej.27.296.

[89] Adanez J, Abad A, Garcia-Labiano F, Gayan P, De Diego LF. Progress in chemical-looping combustion and reforming technologies. Prog Energy Combust Sci 2012;38:215–82. https://doi.org/10.1016/j.pecs.2011.09.001.

[90] Fennell P. Calcium and Chemical Looping Technology for Power Generation and Carbon Dioxide (CO2) Capture. Woodhead Publishing Series in Energy; 2015. https://doi.org/10.1016/B978-0-85709-243-4.00001-X.

[91] Boot-Handford ME, Abanades JC, Anthony EJ, Blunt MJ, Brandani S, Mac Dowell N, et al. Carbon capture and storage update. Energy Environ Sci 2014;7:130–89. https://doi.org/10.1039/c3ee42350f.

[92] Adánez J, De Diego LF, García-Labiano F, Gayán P, Abad A, Palacios JM. Selection of oxygen carriers for chemical-looping combustion. Energy and Fuels 2004;18:371–7. https://doi.org/10.1021/ef0301452.

[93] Arjmand M, Leion H, Mattisson T, Lyngfelt A. Investigation of different manganese ores as oxygen carriers in chemical-looping combustion (CLC) for solid fuels. Appl Energy 2014;113:1883–94. https://doi.org/10.1016/j.apenergy.2013.06.015.

[94] Bhavsar S, Najera M, Solunke R, Veser G. Chemical looping: To combustion and beyond. Catal Today 2014;228:96–105. https://doi.org/10.1016/j.cattod.2013.12.025.

[95] Mukherjee S, Kumar P, Yang A, Fennell P. A systematic investigation of the performance of copper-, cobalt-, iron-, manganese-and nickel-based oxygen carriers for chemical looping combustion technology through simulation models 2015;130:79–91. https://doi.org/10.1016/j.ces.2015.03.009.

[96] Bhui B, Vairakannu P. Prospects and issues of integration of co-combustion of solid fuels (coal and biomass) in chemical looping technology. J Environ Manage 2019;231:1241–56. https://doi.org/10.1016/j.jenvman.2018.10.092.

[97] Cabello A, Abad A, García-Labiano F, Gayán P, de Diego LF, Adánez J. Kinetic determination of a highly reactive impregnated Fe2O3/Al2O3 oxygen carrier for use in gas-fueled Chemical Looping Combustion. Chem Eng J 2014;258:265–80. https://doi.org/10.1016/j.cej.2014.07.083.

[98] Fan Y, Siriwardane R. Novel new oxygen carriers for chemical looping combustion of solid fuels. Energy and Fuels 2014;28:2248–57. https://doi.org/10.1021/ef402528g.

[99] Fang H, Haibin L, Zengli Z. Advancements in development of chemical-looping combustion: A review. Int J Chem Eng 2009;2009. https://doi.org/10.1155/2009/710515.

[100] Mattisson T, Lyngfelt A, Leion H. Chemical-looping with oxygen uncoupling for combustion of solid fuels 2009;3:11–9. https://doi.org/10.1016/j.ijggc.2008.06.002.

[101] Leion H, Jerndal E, Steenari B, Hermansson S, Israelsson M, Jansson E, et al. Solid fuels in chemical-looping combustion using oxide scale and unprocessed iron ore as oxygen carriers. Fuel 2009;88:1945–54. https://doi.org/10.1016/j.fuel.2009.03.033.

[102] Rubel A, Liu K, Neathery J, Taulbee D. Oxygen carriers for chemical looping combustion of solid fuels. Fuel 2009;88:876–84. https://doi.org/10.1016/j.fuel.2008.11.006.

[103] Miller DD, Smith M, Shekhawat D. Interaction of manganese with aluminosilicate support during high temperature (1100°C ) chemical looping combustion of the Fe-Mn-based oxygen carrier. Fuel 2020;263:116738. https://doi.org/10.1016/j.fuel.2019.116738.

[104] Kuang C, Wang S, Luo M, Cai J, Zhao J. Investigation of CuO-based oxygen carriers modified by three different ores in chemical looping combustion with solid fuels. Renew Energy 2020;154:937–48. https://doi.org/10.1016/j.renene.2020.03.027.

[105] Ma Z, Zhang S, Xiao R. Insights into the relationship between microstructural evolution and deactivation of Al2O3 supported Fe2O3 oxygen carrier in chemical looping combustion. Energy Convers Manag 2019;188:429–37. https://doi.org/10.1016/j.enconman.2019.03.073.

[106] Tetsuya Haga, Nishiyama Y. Influence of structural parameters on coal char gasification: 2. Ni-catalysed steam gasification. Fuel 1988;67:748–52. https://doi.org/10.1016/0016-2361(88)90144-5.

[107] Cho P, Mattisson T, Lyngfelt A. Carbon formation on nickel and iron oxide-containing oxygen carriers for chemical-looping combustion. Ind Eng Chem Res 2005;44:668–76. https://doi.org/10.1021/ie049420d.

[108] Cao Y, Casenas B, Pan WP. Investigation of chemical looping combustion by solid fuels. 2. Redox reaction kinetics and product characterization with coal, biomass, and solid waste as solid fuels and CuO as an oxygen carrier. Energy and Fuels 2006;20:1845–54. https://doi.org/10.1021/ef050424k.

[109] Wang B, Gao C, Wang W, Kong F, Zheng C. TGA-FTIR investigation of chemical looping combustion by coal with CoFe2O4 combined oxygen carrier. J Anal Appl Pyrolysis 2014;105:369–78. https://doi.org/10.1016/j.jaap.2013.12.002.

[110] Chen C, Han L, Bollas GM. Dynamic Simulation of Fixed-Bed Chemical-Looping Combustion Reactors Integrated in Combined Cycle Power Plants. Energy Technol 2016;4:1209–20. https://doi.org/10.1002/ente.201600079.

[111] Cho P, Mattisson T, Lyngfelt A. Comparison of iron-, nickel-, copper- and manganese-based oxygen carriers for chemical-looping combustion. Fuel 2004;83:1215–25. https://doi.org/10.1016/j.fuel.2003.11.013.

[112] Pröll T, Mayer K, Bolhàr-Nordenkampf J, Kolbitsch P, Mattisson T, Lyngfelt A, et al. Natural minerals as oxygen carriers for chemical looping combustion in a dual circulating fluidized bed system. Energy Procedia 2009;1:27–34. https://doi.org/10.1016/j.egypro.2009.01.006.

[113] Song T, Shen T, Shen L, Xiao J, Gu H, Zhang S. Evaluation of hematite oxygen carrier

in chemical-looping combustion of coal. Fuel 2013;104:244–52. https://doi.org/10.1016/j.fuel.2012.09.030.

[114] Mendiara T, Gayán P, Abad A, Diego LF De, Adánez J. Evaluation of the use of different coals in Chemical Looping Combustion using a bauxite waste as oxygen carrier. Fuel 2013;106:814–26. https://doi.org/10.1016/j.fuel.2012.11.047.

[115] Pérez-vega R, Abad A, García-labiano F, Gayán P, Diego LF De, Adánez J. International Journal of Greenhouse Gas Control Coal combustion in a 50 kW th Chemical Looping Combustion unit : Seeking operating conditions to maximize CO2 capture and combustion efficiency. Int J Greenh Gas Control 2016;50:80–92. https://doi.org/10.1016/j.ijggc.2016.04.006.

[116] Yu Z, Yang Y, Yang S, Zhang Q, Zhao J, Fang Y. Iron-based oxygen carriers in chemical looping conversions: A review. Carbon Resour Convers 2019;2:23–34. https://doi.org/10.1016/j.crcon.2018.11.004.

[117] U.S. Geological Survey. Mineral Commodity Summaries. Iron Ore 2017;1:2016–7. https://minerals.usgs.gov/minerals/pubs/commodity/iron_ore/mcs-2017-feore.pdf.

[118] Aghabararnejad M, Patience GS, Chaouki J. TGA and Kinetic Modelling of Co, Mn and Cu Oxides for Chemical Looping Gasification (CLG). Can J Chem Eng 2014;92:1903–10. https://doi.org/10.1002/cjce.22046.

[119] Wang W, Zhang B, Wang G, Li Y. O2 Release of Mn-Based Oxygen Carrier for Chemical Looping Air Separation (CLAS): An Insight into Kinetic Studies. Taiwan Assoc Aerosol Res 2016;16:453–63. https://doi.org/10.4209/aaqr.2014.07.0140.

[120] Skulimowska A, Di L, Kami N, Celi A, Mariola P, Krauz M, et al. Chemical looping with oxygen uncoupling (CLOU) and chemical looping combustion (CLC) using copper-enriched oxygen carriers supported on fly ash. Fuel Process Technol 2017;168:123–30. https://doi.org/10.1016/j.fuproc.2017.08.035.

[121] Wang W. Thermodynamic investigation on hydrogen production via self-sufficient chemical looping reforming of glycerol (CLRG) using metal oxide oxygen carriers. J Energy Inst 2014;87:152–62. https://doi.org/10.1016/j.joei.2014.03.006.

[122] Li F, Zeng L, Velazquez-vargas LG, Yoscovits Z, Fan L. Syngas Chemical Looping Gasification Process : Bench-Scale Studies and Reactor Simulations. Environ Energy Eng 2010;56:2186–99. https://doi.org/10.1002/aic.

[123] Salkuyeh YK, Saville BA, Maclean HL. Techno-economic analysis and life cycle assessment of hydrogen production from natural gas using current and emerging technologies. Int J Hydrogen Energy 2017;42:18894–909. https://doi.org/10.1016/j.ijhydene.2017.05.219.

[124] Erlach B, Schmidt M, Tsatsaronis G. Comparison of carbon capture IGCC with pre-combustion decarbonisation and with chemical-looping combustion. Energy 2011;36:3804–15. https://doi.org/10.1016/j.energy.2010.08.038.

[125] Prabu V. Integration of in - situ CO 2 -oxy coal gasification with advanced power generating systems performing in a chemical looping approach of clean combustion. Appl Energy 2015;140:1–13. https://doi.org/10.1016/j.apenergy.2014.11.056.

[126] Spallina V, Romano MC, Chiesa P, Gallucci F, van Sint Annaland M, Lozza G. Integration of coal gasification and packed bed CLC for high efficiency and near-zero

emission power generation. Energy Procedia 2014;27:662–70. https://doi.org/doi: 10.1016/j.egypro.2013.05.154.

[127] Mukherjee S, Kumar P, Yang A, Fennell P. A systematic investigation of the performance of copper-, cobalt-, iron-, manganese- and nickel-based oxygen carriers for chemical looping combustion technology through simulation models. Chem Eng Sci 2015;130:79–91. https://doi.org/10.1016/j.ces.2015.03.009.

[128] He F, Galinsky N, Li. F. Chemical looping gasification of solid fuels using bimetallic oxygen carrier particles-Feasibility assessment and process simulations. Int J Hydrog Technol 2013;8:7839–54. https://doi.org/http://dx.doi.org/10.1016/j.ijhydene.2013.04.054.

[129] Liang Zeng, Feng He, Fanxing Li L-SF. Coal-Direct Chemical Looping Gasification for Hydrogen Production : Reactor Modeling and Process Simulation. Energy & Fuels 2012;26:3680–90. https://doi.org/10.1021/ef3003685.

[130] Elam CC, Padró CEG, Sandrock G, Luzzi A, Lindblad P, Hagen EF. Realizing the hydrogen future: The International Energy Agency's efforts to advance hydrogen energy technologies. Int J Hydrogen Energy 2003;28:601–7. https://doi.org/10.1016/S0360-3199(02)00147-7.

[131] Balat M, Balat M. Political, economic and environmental impacts of biomass-based hydrogen. Int J Hydrogen Energy 2009;34:3589–603. https://doi.org/10.1016/j.ijhydene.2009.02.067.

[132] Konieczny A, Mondal K, Wiltowski T, Dydo P. Catalyst development for thermocatalytic decomposition of methane to hydrogen. Int J Hydrogen Energy 2008;33:264–72. https://doi.org/10.1016/j.ijhydene.2007.07.054.

[133] Luo M, Yi Y, Wang S, Wang Z, Du M, Pan J, et al. Review of hydrogen production using chemical-looping technology. Renew Sustain Energy Rev 2018;81:3186–214. https://doi.org/10.1016/j.rser.2017.07.007.

[134] Bahzad H, Shah N, Dowell N Mac, Boot-Handford M, Soltani SM, Ho M, et al. Development and techno-economic analyses of a novel hydrogen production process via chemical looping. Int J Hydrogen Energy 2019;44:21251–63. https://doi.org/10.1016/j.ijhydene.2019.05.202.

[135] Sanfilippo D. One-step hydrogen through water splitting with intrinsic CO2 capture in chemical looping. Catal Today 2016;272:58–68. https://doi.org/10.1016/j.cattod.2016.02.021.

[136] Edrisi A, Mansoori Z, Dabir B. Urea synthesis using chemical looping process - Techno-economic evaluation of a novel plant configuration for a green production. Int J Greenh Gas Control 2016;44:42–51. https://doi.org/10.1016/j.ijggc.2015.10.020.

[137] Kathe M V., Empfield A, Na J, Blair E, Fan LS. Hydrogen production from natural gas using an iron-based chemical looping technology: Thermodynamic simulations and process system analysis. Appl Energy 2016;165:183–201. https://doi.org/10.1016/j.apenergy.2015.11.047.

[138] Khan MN, Shamim T. Techno-economic assessment of a plant based on a three reactor chemical looping reforming system. Int J Hydrogen Energy 2016;41:22677–88. https://doi.org/10.1016/j.ijhydene.2016.09.016.

[139] Vos Y De, Jacobs M, Voort P Van Der, Driessche I, FransSnijkers, Verberckmoes A. Sustainable iron-based oxygen carriers for Chemical Looping for Hydrogen Generation. Int J Hydrogen Energy 2019;44:1374–91. https://doi.org/10.1016/j.ijhydene.2018.11.099.

[140] Liu T, Yu Z, Mei Y, Feng R, Yang S, Wang Z, et al. Potassium migration and transformation during the deep reduction of oxygen carrier (OC) by char in coal-direct chemical looping hydrogen generation using potassium-modified Fe2O3/Al2O3 OC. Fuel 2019;256:115883. https://doi.org/10.1016/j.fuel.2019.115883.

[141] Wu W, Wen F, Chen J, Kuo P, Shi B. Comparisons of a class of IGCC polygeneration/power plants using calcium/chemical looping combinations. J Taiwan Inst Chem Eng 2019;96:193–204. https://doi.org/10.1016/j.jtice.2018.11.010.

[142] Cormos A, Sandu V, Cormos C. Assessment of main energy integration elements for decarbonized gasification plants based on thermo-chemical looping cycles. J Clean Prod 2020;259:120834. https://doi.org/10.1016/j.jclepro.2020.120834.

[143] Rajabi M, Mehrpooya M, Haibo Z, Huang Z. Chemical looping technology in CHP (combined heat and power) and CCHP (combined cooling heating and power) systems : A critical review Organic Rankine cycle. Appl Energy 2019;253:113544. https://doi.org/10.1016/j.apenergy.2019.113544.

[144] Wang X, Demirel Y. Feasibility of Power and Methanol Production by an Entrained-Flow Coal Gasification System. Energy and Fuels 2018;32:7595–610. https://doi.org/10.1021/acs.energyfuels.7b03958.

[145] Schakel W, Oreggioni G, Singh B, Strømman A, Ramírez A. Assessing the techno-environmental performance of CO2 utilization via dry reforming of methane for the production of dimethyl ether. J CO2 Util 2016;16:138–49. https://doi.org/10.1016/j.jcou.2016.06.005.

[146] Bassano C, Deiana P, Lietti L, Visconti CG. P2G movable modular plant operation on synthetic methane production from CO2 and hydrogen from renewables sources. Fuel 2019;253:1071–9. https://doi.org/10.1016/j.fuel.2019.05.074.

[147] Pan Z, Chan WP, Veksha A, Giannis A, Dou X, Wang H, et al. Thermodynamic analyses of synthetic natural gas production via municipal solid waste gasification, high-temperature water electrolysis and methanation. Energy Convers Manag 2019;202:112160. https://doi.org/10.1016/j.enconman.2019.112160.

[148] Pérez-Fortes M, Schöneberger JC, Boulamanti A, Tzimas E. Formic acid synthesis using CO2 as raw material: Techno-economic and environmental assessment and market potential. Int J Hydrogen Energy 2016;41:16444–62. https://doi.org/10.1016/j.apenergy.2015.07.067.

[149] Saraswat VK, Bansal R. National Institution for Transforming India (NITI), India’s Leapfrog to Methanol Economy. 2017.

[150] Rosen MA, Bulucea CA. Using Exergy to Understand and Improve the Efficiency of Electrical Power Technologies. Entropy 2009;11:820–35. https://doi.org/10.3390/e11040820.

[151] Khoo H, Tan RBH. Life Cycle Investigation of CO2 Recovery and Sequestration. Environ Sci Technol 2006;40:4016–24.

[152] Schreiber A, Zapp P. Environmental assessment of German electricity generation from coal-fired power plants with amine-based carbon capture. Int J Life Cycle Assess 2009;14:547–59. https://doi.org/10.1007/s11367-009-0102-8.

[153] Pehnt M, Henkel J. Life cycle assessment of carbon dioxide capture and storage from lignite power plants. Int J Greenh Gas Control 2009;3:49–66. https://doi.org/10.1016/j.ijggc.2008.07.001.

[154] Ã NAO, Cockerill TT. Life cycle GHG assessment of fossil fuel power plants with carbon capture and storage. Energy Policy 2008;36:367–80. https://doi.org/10.1016/j.enpol.2007.09.026.

[155] Liu Y, Wang Y, Li D, Feng F, Yu Q, Xue S. Identification of the potential for carbon dioxide emissions reduction from highway maintenance projects using life cycle assessment: A case in China. J Clean Prod 2019;219:743–52. https://doi.org/10.1016/j.jclepro.2019.02.081.

[156] Li G, Zhang K, Yang B, Liu F, Weng Y, Liu Z, et al. Life cycle analysis of a coal to hydrogen process based on ash agglomerating fluidized bed gasification. Energy 2019;174:638–46. https://doi.org/10.1016/j.energy.2019.03.023.

[157] Xiang D, Yang S, Li X, Qian Y. Life cycle assessment of energy consumption and GHG emissions of olefins production from alternative resources in China. Energy Convers Manag 2015;90:12–20. https://doi.org/10.1016/j.enconman.2014.11.007.

[158] Navajas A, Mendiara T, Goñi V, Jiménez A, Gandía LM, Abad A, et al. Life cycle assessment of natural gas fuelled power plants based on chemical looping combustion technology. Energy Convers Manag 2019;198:111856. https://doi.org/10.1016/j.enconman.2019.111856.

[159] He Y, Zhu L, Li L, Rao D. Life-cycle assessment of SNG and power generation: The role of implement of chemical looping combustion for carbon capture. Energy 2019;172:777–86. https://doi.org/10.1016/j.energy.2019.02.037.

[160] Bareschino P, Mancusi E, Urciuolo M, Paulillo A, Chirone R, Pepe F. Life cycle assessment and feasibility analysis of a combined chemical looping combustion and power-to-methane system for CO 2 capture and utilization. Renew Sustain Energy Rev 2020;130:109962. https://doi.org/10.1016/j.rser.2020.109962.

[161] Menon KG, Patnaikuni VS. CFD simulation of fuel reactor for chemical looping combustion of Indian coal. Fuel 2017;203:90–101. https://doi.org/10.1016/j.fuel.2017.04.084.

[162] Aspen Tech. Aspen Physical Property System: Physical Property Methods. Methods 2009:1–234.

[163] Zhu L, Xie N, Jiang P, Li L, Chen H. Double-stage chemical looping combustion combined with sorption enhanced natural gas steam reforming process for hydrogen and power cogeneration: Thermodynamic investigation. Chem Eng Res Des 2016;114:247–57. https://doi.org/10.1016/j.cherd.2016.08.024.

[164] Pérez-Fortes M, Schöneberger JC, Boulamanti A, Tzimas E. Methanol synthesis using captured CO2as raw material: Techno-economic and environmental assessment. Appl Energy 2016;161:718–32. https://doi.org/10.1016/j.apenergy.2015.07.067.

[165] Olaleye AK, Wang M, Kelsall G. Steady state simulation and exergy analysis of

supercritical coal-fired power plant with CO2capture. Fuel 2015;151:57–72. https://doi.org/10.1016/j.fuel.2015.01.013.

[166] Skorek-Osikowska A, Bartela Ł, Kotowicz J. Thermodynamic and ecological assessment of selected coal-fired power plants integrated with carbon dioxide capture. Appl Energy 2017;200:73–88. https://doi.org/10.1016/j.apenergy.2017.05.055.

[167] Hanak DP, Manovic V. Calcium looping combustion for high-efficiency low-emission power generation. J Clean Prod 2017;161:245–55. https://doi.org/10.1016/j.jclepro.2017.05.080.

[168] Thomas A. Adams, Hoseinzade L, Madabhushi PB, Okeke IJ. Comparison of CO2 Capture Approaches for Fossil-Based Power Generation: Review and Meta-Study. Processes 2017;5:44. https://doi.org/10.3390/pr5030044.

[169] Cabello A, Gayán P, Diego LF De, Abad A, Adánez J. On the attrition evaluation of oxygen carriers in Chemical Looping Combustion. Fuel Process Technol 2016;148:188–97. https://doi.org/10.1016/j.fuproc.2016.03.004.

[170] Cash prices, market data center, wall street journal 2018:2–7. http://www.wsj.com/mdc/public/page/2_3023-cashprices.html (accessed May 25, 2018).

[171] CIL. Coal price notification, Coal India Limited 2019. https://www.coalindia.in/DesktopModules/DocumentList/documents/Price_Notification_dated_08.01.2018_effective_from_0000_Hrs_of_09.01.2018_09012018.pdf (accessed January 3, 2020).

[172] Ricke K, Drouet L, Caldeira K, Tavoni M. Country-level social cost of carbon. Nat Clim Chang 2018;8:895–900. https://doi.org/10.1038/s41558-018-0282-y.

[173] Rahil A, Gammon R, Brown N, Udie J, Mazhar MU. Potential economic benefits of carbon dioxide (CO2) reduction due to renewable energy and electrolytic hydrogen fuel deployment under current and long term forecasting of the Social Carbon Cost (SCC). Energy Reports 2019;5:602–18. https://doi.org/10.1016/j.egyr.2019.05.003.

[174] Zhen Z, Tian L, Ye Q. A simple estimate for the social cost of carbon. Energy Procedia 2018;152:768–73. https://doi.org/10.1016/j.egypro.2018.09.243.

[175] Fan J, Zhu L, Jiang P, Li L, Liu H. Comparative exergy analysis of chemical looping combustion thermally coupled and conventional steam methane reforming for hydrogen production. J Clean Prod 2016;131:247–58. https://doi.org/10.1016/j.jclepro.2016.05.040.

[176] Ogidiama OV, Abu-Zahra MRM, Shamim T. Techno-economic analysis of a poly-generation solar-assisted chemical looping combustion power plant. Appl Energy 2018;228:724–35. https://doi.org/10.1016/j.apenergy.2018.06.091.

[177] Authier O, Le Moullec Y. Coal chemical-looping combustion for electricity generation: Investigation for a 250 MWe power plant. Energy Procedia 2013;37:588–97. https://doi.org/10.1016/j.egypro.2013.05.146.

[178] Iloeje C, Zhao Z, Ghoniem AF. Efficient cycles for carbon capture CLC power plants based on thermally balanced redox reactors. Int J Greenh Gas Control 2015;41:302–15. https://doi.org/10.1016/j.ijggc.2015.07.023.

[179] Gao J, Zhang Q, Wang X, Song D, Liu W, Liu W. Exergy and exergoeconomic analyses

with modeling for CO2 allocation of coal-fired CHP plants. Energy 2018;152:562–75. https://doi.org/10.1016/j.energy.2018.03.171.

[180] NETL. 2012 Technology Readiness Assessment - Overview. Pathway for Readying the Next Generation of Affordable Clean Energy Technology - Carbon Capture, Utilization, and Storage (CCUS) FutureGen Alliance. National Energy Technology Laboratory, Pittsburgh, PA, US. 2012.

[181] NETL. Cost and Performance Baseline for Fossil Energy Plants Volume 1a: Bituminous Coal (PC) and Natural Gas to Electricity Revision 3. 2015. https://doi.org/DOE/NETL-2015/1723.

[182] NETL. Quality Guidelines for Energy System Studies Capital Cost Scaling Methodology. 2013. https://doi.org/DE-FE0004001 National.

[183] NETL. Guidance for NETL's oxycombustion R&D program: chemical looping combustion reference plant designs and sensitivity studies. 2014. https://doi.org/DE-FE0004001.

[184] NETL. Process Equipment Cost Estimation Final Report. 2002. https://doi.org/DOE/NETL-2002/1169.

[185] Caldecott B, Dericks G, Mitchell J. Stranded assets and subcritical coal - The risk to companies and investors. 2015.

[186] Purgert R, Phillips J, Hendrix H, Shingledecker J, Tanzosh J. Materials for Advanced Ultra-supercritical (A-USC) Steam Turbines-A-USC Component Demonstration Pre-FEED Final Technical Report. 2016.

[187] Aspen Technology. Rate-Based Model of the CO2 Capture Process by MEA using Aspen Plus 2013:1–25.

[188] Towler G, Sinnott R. Chemial Engineering Design Principles, Practice and Economics of Plant and Process Design. Elsevier; 2008. https://doi.org/10.1016/B978-0-08-096659-5.00022-5.

[189] Hikita H, Asai S, Ishikawa H, Honda M. The kinetics of reactions of carbon dioxide with monoethanolamine, diethanolamine and triethanolamine by a rapid mixing method. Chem Eng J 1977;13:7–12. https://doi.org/10.1016/0300-9467(77)80002-6.

[190] Cormos AM, Cormos CC. Investigation of hydrogen and power co-generation based on direct coal chemical looping systems. Int J Hydrogen Energy 2014;39:2067–77. https://doi.org/10.1016/j.ijhydene.2013.11.123.

[191] Abad A, Adánez J, García-Labiano F, de Diego LF, Gayán P, Celaya J. Mapping of the range of operational conditions for Cu-, Fe-, and Ni-based oxygen carriers in chemical-looping combustion. Chem Eng Sci 2007;62:533–49. https://doi.org/10.1016/j.ces.2006.09.019.

[192] Goldstein EA, Mitchell RE. Chemical kinetics of copper oxide reduction with carbon monoxide. Proc Combust Inst 2011;33:2803–10. https://doi.org/10.1016/j.proci.2010.06.080.

[193] Wang P, Means N, Howard BH, Shekhawat D, Berry D. The reactivity of CuO oxygen carrier and coal in Chemical-Looping with Oxygen Uncoupled (CLOU) and In-situ Gasification Chemical-Looping Combustion (iG-CLC). Fuel 2018;217:642–9. https://doi.org/10.1016/j.fuel.2017.12.102.

[194] Chuang SY, Dennis JS, Hayhurst AN, Scott SA. Development and performance of Cu-based oxygen carriers for chemical-looping combustion. Combust Flame 2008;154:109–21. https://doi.org/10.1016/j.combustflame.2007.10.005.

[195] Uysal C, Kurt H, Kwak H. International Journal of Thermal Sciences Exergetic and thermoeconomic analyses of a coal-fired power plant. Int J Therm Sci 2017;117:106–20. https://doi.org/10.1016/j.ijthermalsci.2017.03.010.

[196] Sorgulu F, Dincer I. Cost evaluation of two potential nuclear power plants for hydrogen production. Int J Hydrogen Energy 2018;43:10522–9. https://doi.org/10.1016/j.ijhydene.2017.10.165.

[197] Kim M, Kim J. An integrated decision support model for design and operation of a wind-based hydrogen supply system. Int J Hydrogen Energy 2017;42:3899–915. https://doi.org/10.1016/j.ijhydene.2016.10.129.

[198] Wang W, Gong J. Methanation of carbon dioxide: An overview. Front Chem Eng China 2011;5:2–10. https://doi.org/10.1007/s11705-010-0528-3.

[199] Van-dal ÉS, Bouallou C. Design and simulation of a methanol production plant from CO2 hydrogenation. J Clean Prod 2013;57:38–45. https://doi.org/10.1016/j.jclepro.2013.06.008.

[200] Mastropasqua L, Pecenati I, Giostri A, Campanari S. Solar hydrogen production : Techno-economic analysis of a parabolic dish- supported high-temperature electrolysis system. Appl Energy 2020;261:114392. https://doi.org/10.1016/j.apenergy.2019.114392.

[201] Domestic Natural gas price for the period October, 2019 - March, 2020 2019. https://www.ppac.gov.in/content/155_1_GasPrices.aspx (accessed April 22, 2020).

[202] Lopes G de F, Bonfim-Rocha L, Jorge LM de M, Paraíso PR. Dimethyl Ether Production from Sugarcane Vinasse : Modeling and Simulation for a Techno-economic Assessment. BioEnergy Res 2020. https://doi.org/10.1007/s12155-020-10089-9.

# *Resume*

**Name:** **Surywanshi Gajanan Dattarao**

**Gender:** Male

**Nationality:** Indian

**Academic profile:**

- Pursuing **Ph.D.** from Department of Chemical Engineering at National Institute of Technology, Warangal, Telangana, India.
- **M.Tech:** Computer Aided Process and Equipment Design (CAPED) drom Department of Chemical Engineering, National Institute of Technology, Warangal, Telangana, India (2015).
- **B.Tech:** Chemical Engineering from Dr. Babasaheb Ambedkar Marathwada University, Aurangabad, Maharashtra, India.

**Awards and Honors:**

- Secured first position in the “Badminton” Intramural Competitions, NIT Warangal, India, during the academic year 2019-2020.
- Awarded best paper presentation award at 2nd International Conference on New Frontiers in Chemical, Energy and Environmental Engineering (INCEEE- 2019), NIT Warangal, India, 15-16th February, 2019.
- Secured first position in the “Badminton” Intramural Competitions, NIT Warangal, India, during the academic year 2018-2019.
- Secured third position in “Badminton (boys)” competitions organized by Chemical Engineering Association (ChEA), NIT Warangal, India, during the academic year 2018-2019.
- Awarded second best paper presentation award at National Level Technical Symposium “KRATOS-2K13”, MPGI Group of Institutions, Nanded, India, 6-7 April 2013.
- Secured second position in the “Robo-Race” event of AWUT 2012, A National level Extravaganza, JNEC Aurangabad, India, 23-25 March 2012.